



# RESEARCH REPORT

---

---

## EVALUATION OF PREFABRICATED COMPOSITE STEEL BOX GIRDER SYSTEMS FOR RAPID BRIDGE CONSTRUCTION

by

Rigoberto Burgueño

Benjamin S. Pavlich

Report No. CEE-RR – 2008/01

February 2008

Research Report for MDOT under Contract No. 2002-0532 –  
Authorization 12, MSU APP 90038  
RC-1507

---

**Department of Civil and Environmental Engineering  
Michigan State University  
East Lansing, Michigan**

1. Research Report RC-1507	2. Government Accession No.	3. MDOT Project Manager Steve Kahl	
4. Title and Subtitle Evaluation of Prefabricated Composite Steel Box Girder Systems for Rapid Bridge Construction		5. Report Date February 12, 2008	
7. Author(s) Rigoberto Burgueño, Ph.D. and Benjamin S. Pavlich		6. Performing Organization Code	
9. Performing Organization Name and Address Michigan State University Department of Civil and Environmental Engineering 3546 Engineering Building East Lansing, MI 48824-1226		8. Performing Org Report No. CEE-RR – 2008/01	
12. Sponsoring Agency Name and Address Michigan Department of Transportation Construction and Technology Division P.O. Box 30049 Lansing, MI 48909		10. Work Unit No. (TRAIS)	
		11. Contract Number: 2002-0532	
		11(a). Authorization Number: 12	
15. Supplementary Notes		13. Type of Report & Period Covered 01-01-06 to 04-30-07	
		14. Sponsoring Agency Code	
16. Abstract <p>Prefabrication is a popular practice that has gained widespread use in the bridge engineering community. Often certain components of a bridge are prefabricated and then assembled at the job site. However, this report focuses on the possibility of prefabricating a box girder/slab unit and shipping the entire assembly to a job site, where only placement and transverse post-tensioning would be required to complete the construction. This could drastically reduce construction time, eliminating the need for lengthy and costly road closures.</p> <p>The objective of the project was to evaluate through numerical simulations the feasibility of creating an entirely prefabricated composite box girder bridge system and employing such a system for highway bridges. This included evaluating the global response of the system, local response of the composite girder/deck units and joints, and the vibration characteristics of the resulting bridge systems. The main issue to be resolved was the method for longitudinally joining the girder/deck units such that continuity between them can be maintained.</p> <p>The system was evaluated with a hierarchical suite of finite element analyses. Each analysis was specially designed to focus on one of the designated areas of study. The most complex models focused the behavior of transversely post-tensioned joints, capturing the contact interaction between individual girder/slab units. To ensure accuracy, the analytical models were checked against theoretical predictions and experimental data available outside the project.</p> <p>Results from the simulation studies of this work indicated that the prefabricated steel/concrete composite girder/deck units are a safe and viable system for short-span highway bridges. A parametric study found acceptable geometries for a range of spans and girder spacing. While the main concern with the system was maintaining continuity between the prefabricated units. 3D FE models indicated that this was indeed possible to achieve while remaining within the AASHTO limits for transverse post-tensioning. This was evidenced by a minimal deviation between the stress and deflection profiles of prefabricated bridges and corresponding models with a continuous slab. A minimum joint opening criterion equal to the crack control limits in reinforced concrete elements was adopted. It was shown that acceptable joint closure could be maintained below the AASHTO post-tensioning limits. Vibration characteristics were also evaluated and found to consistent with the performance of a continuous system.</p>			
17. Key Words Steel, Box Beams; Prefabricated Bridges; Rapid Construction; Analysis; Deck Joints; Transverse Post-Tensioning		18. Distribution Statement No restrictions. This document is available to the public through the Michigan Department of Transportation.	
19. Security Classification (report) Unclassified	20. Security Classification (Page) Unclassified	21. No of Pages 150	22. Price

Report No. CEE-RR – 2008/01

# **EVALUATION OF PREFABRICATED COMPOSITE STEEL BOX GIRDER SYSTEMS FOR RAPID BRIDGE CONSTRUCTION**

by

**Rigoberto Burgueño, Ph.D.**

*Associate Professor of Structural Engineering*

**Benjamin S. Pavlich**

*Graduate Research Assistant*

Technical Report to Michigan DOT under Contract No. 2002-0532 – Authorization 12  
MSU APP 90038

Department of Civil and Environmental Engineering  
Michigan State University  
East Lansing, MI 48824-1226

February 2008

## **DISCLAIMER**

The opinions, findings, conclusions and recommendations presented in this report are those of the authors alone and do not necessarily represent the views and opinions of Michigan State University or the Michigan Department of Transportation.

## ABSTRACT

Prefabrication is a popular practice that has gained widespread use in the bridge engineering community. Often certain components of a bridge are prefabricated and then assembled at the job site. However, this report focuses on the possibility of prefabricating a box girder/slab unit and shipping the entire assembly to a job site, where only placement and transverse post-tensioning would be required to complete the construction. This could drastically reduce construction time, eliminating the need for lengthy and costly road closures.

The objective of the project was to evaluate through numerical simulations the feasibility of creating an entirely prefabricated composite box girder bridge system and employing such a system for highway bridges. This included evaluating the global response of the system, local response of the composite girder/deck units and joints, and the vibration characteristics of the resulting bridge systems. The main issue to be resolved was the method for longitudinally joining the girder/deck units such that continuity between them can be maintained.

The system was evaluated with a hierarchical suite of finite element analyses. Each analysis was specially designed to focus on one of the designated areas of study. The most complex models focused the behavior of transversely post-tensioned joints, capturing the contact interaction between individual girder/slab units. To ensure accuracy, the analytical models were checked against theoretical predictions and experimental data available outside the project.

Results from the simulation studies of this work indicated that the prefabricated steel/concrete composite girder/deck units are a safe and viable system for short-span highway bridges. A parametric study found acceptable geometries for a range of spans and girder spacing. While the main concern with the system was maintaining continuity between the prefabricated units, 3D FE models indicated that this was indeed possible to achieve while remaining within the AASHTO limits for transverse post-tensioning. This was evidenced by a minimal deviation between the stress and deflection profiles of prefabricated bridges and corresponding models with a continuous slab. A minimum joint opening criterion equal to the crack control limits in reinforced concrete elements was adopted. It was shown that acceptable joint closure could be maintained below the AASHTO post-tensioning limits. Vibration characteristics were also evaluated and found to be consistent with the performance of a continuous system.

## **ACKNOWLEDGEMENTS**

The research described in this report was carried out under funding from the Michigan Department of Transportation, Contract 2002-0532 – Authorization 12, MSU APP 90038, with Mr. Steve Kahl as the project manager. The financial support of MDOT and the coordination of Mr. Kahl throughout the execution of the experimental program are gratefully acknowledged. Mr. Roger Till (MDOT) provided many helpful suggestions on the direction of the present study and his help is thankfully recognized. Finally, Mr. Guy Nelson (Nelson Engineering Services) provided invaluable knowledge and support to this research, which stemmed from his insightful bridge concept, supporting the analytical effort reported in this report with much needed information on the real construction and performance of prefabricated steel-box girder bridges.

# TABLE OF CONTENTS

<b>DISCLAIMER</b> .....	<b>i</b>
<b>ABSTRACT</b> .....	<b>ii</b>
<b>ACKNOWLEDGEMENTS</b> .....	<b>iii</b>
<b>TABLE OF CONTENTS</b> .....	<b>iv</b>
<b>LIST OF FIGURES</b> .....	<b>vii</b>
<b>LIST OF TABLES</b> .....	<b>xii</b>
<b>1. INTRODUCTION</b> .....	<b>1</b>
1.1 Summary.....	1
1.2 Research Objectives.....	2
1.3 Scope and Organization .....	3
<b>2. LITERATURE REVIEW</b> .....	<b>4</b>
2.1 General.....	4
2.2 Prefabricated Superstructure Systems.....	4
2.3. Prefabricated Steel Box Composite Superstructure Systems.....	6
2.3.1 Pressed-Formed Steel Box Girder Bridge System – West Virginia University .....	6
2.3.2 Composite Girders with Cold Formed Steel U Section – Tokai University, Japan.....	9
2.3.3 Texas Prefabricated Steel Tub-Girder System – University of Texas, Austin .....	10
2.3.4 Inverted Steel Box Bridge System – University of Nebraska, Lincoln .....	13
2.3.5 Con-Struct Bridge System – Nelson Engineering Services.....	14
2.3.6 Shallow U-shape Cold-bent Girders for Prefabricated Bridge Superstructure Units ..	16
2.4. Deck Systems.....	17
2.5. Longitudinal Girder-Deck Shear Connections.....	17
2.6. Transverse Deck Joints .....	18
2.7 Longitudinal Deck Connections .....	19
<b>3. DESIGN AND ANALYSIS CONSIDERATIONS</b> .....	<b>22</b>
3.1 General.....	22
3.2 Materials .....	22
3.3 Loading.....	22

3.4 Design Limit States.....	23
3.5 AASHTO Simplified Analysis and Design Methods .....	24
3.6 Refined Analysis Methods.....	29
3.7 Precast Decks .....	29
3.8 Parametric and Optimization Analyses.....	31
3.8.1 Optimization Problem.....	31
3.8.2 Problem Formulation .....	32
3.8.3 Implementation .....	35
3.8.4 Results.....	35
3.8.5 Discussion.....	36
<b>4. CONCEPT EVALUATION.....</b>	<b>37</b>
4.1 Flexural Performance of Con-Struct Bridge System .....	37
4.2 Concept Evaluation and Selection .....	42
<b>5. ANALYTICAL EVALUATION.....</b>	<b>47</b>
5.1 General.....	47
5.2. Stress Analysis of Bridge Components and System.....	47
5.2.1 Model Bridge Geometry .....	48
5.2.2 Model Bridge Loading.....	49
5.2.3 Grillage Model.....	50
5.2.4 Three-Dimensional Finite Element Model .....	56
5.2.5 Comparison of Models.....	56
5.2.6 Verification of Models Using Experimental Data .....	59
5.3 Global Parametric Analysis .....	65
5.3.1 Creation of 3D FE Models.....	67
5.3.2 Selection of Model Geometries .....	68
5.3.3 System Response .....	71
5.3.4 Discussion of Results.....	79
<b>5.4 Stress Analysis and Characterization of Connection Details.....</b>	<b>81</b>
5.4.1 General.....	81
5.4.2 Approach.....	81
5.4.3 Contact Interaction Modeling .....	82

5.4.4 Evaluation of Contact Interaction Modeling.....	85
5.4.5 Model Characterization.....	93
5.4.6 System Response .....	95
<b>5.5 Vibration Characteristics</b> .....	<b>110</b>
5.6 Dynamic Load Amplification Issues .....	115
<b>6. CONCLUSIONS AND RECOMMENDATIONS</b> .....	<b>117</b>
6.1 Observations .....	117
6.2 Recommendations for Design.....	118
6.3 Recommendations for Future Work.....	120
<b>REFERENCES</b> .....	<b>122</b>
Appendix I. Comparison of Analysis Tools .....	125
Appendix II. Bridge Case 1: FE Models Responses.....	126
Appendix III. Bridge Case 2: FE Models Responses .....	128
Appendix IV. Bridge Case 3: FE Models Responses .....	130
Appendix V. Bridge Case 4: FE Models Responses.....	132
Appendix VI. Bridge Case 5: FE Models Responses .....	134
Appendix VII. Bridge Case 6: FE Models Responses.....	136
Appendix VIII. Bridge Case 7: FE Models Responses.....	138
Appendix IX. Bridge Case 8: FE Models Responses .....	140
Appendix X. Bridge Case 9: FE Models Responses.....	143
Appendix XI. Bridge Case 10: FE Models Responses .....	145
Appendix XII. Bridge Case 11: FE Models Responses.....	147
Appendix XIII. Bridge Case 12: FE Models Responses.....	149

## LIST OF FIGURES

Figure 1. Composite Steel Box Girder Concept .....	1
Figure 2. Schematic of Prefabricated Steel Composite Superstructure with I-Girders .....	6
Figure 3. Press-Formed Composite Box Girder from Gangarao and Taly [16] .....	7
Figure 4. Shear Key Details for Pressed-Formed Steel Box Girders [Taly, 1979].....	8
Figure 5. Connection and Stiffener Details at Abutment Support (Taly, 1979).....	9
Figure 6. Dual U-shape Steel Girders with Composite RC Deck (Nakamura, 2002) .....	9
Figure 7. Texas DOT Steel Tub-Girder Section [Freeby, 2005] .....	11
Figure 8. Typical Bridge Cross-Section using Texas’ DOT Steel Tub-Girders [Freeby, 2005] ..	11
Figure 9. Transverse Deck Connection Detail for Steel Tub-Girder (Freeby, 2005) .....	12
Figure 10. Preliminary Concept for Composite Steel Box Girder [Nelson, 2004].....	14
Figure 11. Pedestrian Bridge over Tyler Creek (MI) with Cons-Struct System (Nelson, 2006)..	15
Figure 12. Deck Connection Detail using Reinforcement in Precast Pockets (Badie, 1999).....	20
Figure 13. Deck Connection Detail using Confined Reinforcement in Full-Depth Key (Badie, 1999) .....	21
Figure 14. Deck Connection Detail using Welded Steel Plate (Badie, 1999) .....	21
Figure 15. Design Truck Schematic.....	23
Figure 16. Bridge Geometry Used in AASHTO Analysis.....	24
Figure 17. Variables for AASHTO Nominal Plastic Moment of Composite Girders (AASHTO, 1998) .....	26
Figure 18. Composite Steel Box Girder Cross-Sectional Geometry .....	32
Figure 19. Bridge System Profile under Beam-Line Analysis Assumption .....	32
Figure 20. Typical Cross-Section of Con-Struct Test Units.....	37
Figure 21. Geometry of Shoreline Steel Lightweight Sheeting [5] .....	38
Figure 22. Test Unit with Cast-in-Place Concrete Deck.....	38
Figure 23. Test Unit with Precast Concrete Deck System.....	39
Figure 24. General Test Setup Views – C.I.P. Test Unit.....	40
Figure 25. Moment vs. Curvature Response of C.I.P. Test Unit at Mid-Span .....	41
Figure 26. Bridge being modeled for analysis approach comparison.....	48
Figure 27. Dimensions of model girder/slab unit .....	49

Figure 28. Schematic of grillage element cross-sections and grillage model.....	50
Figure 29. Nomenclature of box sides .....	51
Figure 30. Chart for distortion deflection parameter $w$ for simply supported beams and box without cross-bracing or diaphragms (Hambly, 1991) .....	52
Figure 31. Section A geometry and associated grillage properties.....	53
Figure 32. Section B and C geometry and associated grillage properties .....	53
Figure 33. Section D geometry and associated grillage properties.....	54
Figure 34. Application of wheel loads to grillage model.....	55
Figure 35. Completed grillage model and system transverse moment response .....	55
Figure 36. Girder modification in 3-D FEA model .....	56
Figure 37. Completed 3-D FEA model and von Mises stress contours.....	57
Figure 38. Location of forces chosen for comparison .....	57
Figure 39. Comparison of analysis tools on full scale bridge model (lane load only) .....	58
Figure 40. Comparison of analysis tools (full AASHTO loading) .....	59
Figure 41. Finite Element Model of Con-Struct System in Flexure. Contours Represent Vertical Displacement, in Inches.....	60
Figure 42. Con-Struct Test Unit Girder Cross Section.....	61
Figure 43. Experimental Test Setup.....	61
Figure 44. Load Displacement Response.....	62
Figure 45. Assembled 3D Model .....	64
Figure 46. Load Displacement Results .....	65
Figure 47. Response measures of interest in parametric studies .....	66
Figure 48. Typical Bridge Model Using Shell Elements.....	68
Figure 49. Typical Deformed Shape and Moment Distribution. Contours Represent Longitudinal Moment in kip-in/in. ....	72
Figure 50. Typical Deformed Shape and Moment Distribution. Contours Represent Transverse Moment in kip-in/in. ....	72
Figure 51. Typical Location of Paths. Contours Represent Transverse Moment in.....	73
Figure 52. 50' Span: Transverse Moment v. Transverse Distance Comparison .....	74
Figure 53. 50' Span: Transverse Moment v. Longitudinal Distance Comparison.....	75
Figure 54. 50' Span: Longitudinal Moment v. Longitudinal Distance Comparison.....	75

Figure 55. 75' Span: Transverse Moment v. Transverse Distance Comparison .....	76
Figure 56. 75' Span: Transverse Moment v. Longitudinal Distance Comparison .....	76
Figure 57. 75' Span: Longitudinal Moment v. Longitudinal Distance Comparison.....	77
Figure 58. 100' Span: Transverse Moment v. Transverse Distance Comparison With and Without Diaphragms.....	77
Figure 59. 100' Span: Transverse Moment v. Longitudinal Distance Comparison With and Without Diaphragms.....	78
Figure 60. 100' Span: Longitudinal Moment v. Longitudinal Distance Comparison With and Without Diaphragms.....	78
Figure 61. “Hard “ Contact Pressure-Overclosure Relation in ABAQUS (Simulia 2007) .....	83
Figure 62. Slip Regions for the Basic Coulomb Friction Model (Simulia 2007) .....	84
Figure 63. Schematic of Cube Contact Model with Pressure Normal to the Contact Plane.....	85
Figure 64. Cube model showing separation of nodes .....	86
Figure 65. Schematic of Cube Contact Model with Pressure Normal to the Contact Plane and Vertical Pressure .....	86
Figure 66. Bottom view of top-loaded model showing separation of nodes under load .....	86
Figure 67. Schematic of Updated Model with More Accurate Geometry.....	87
Figure 68. Updated Model with More Accurate Geometry.....	87
Figure 69. (a) Top view of deformed shape of model in Figure 68 and (b) Bottom view of model in Figure 68 showing node separation .....	88
Figure 70. Schematic of Rectangular Beam Used for Quantitative Evaluation .....	89
Figure 71. Model of rectangular beam.....	89
Figure 72. Deformed shape of rectangular beam model showing no opening at midspan (contours represent longitudinal stresses in ksi).....	89
Figure 73. Stress profile in rectangular beam model.....	90
Figure 74. Schematic of Male-to-Female Joint Model .....	91
Figure 75. ABAQUS Model with Male-to-Female Joint.....	91
Figure 76. FE Model of Male-to-Female Joint (Longitudinal Stress Contours in ksi).....	91
Figure 77. Comparison of longitudinal stress in FE model .....	92
Figure 78. Comparison of longitudinal stresses in models with and without joint.....	92
Figure 79. FE Model of Shear Key Joint Opening Under Loading.....	94

Figure 80. FE Model of Bridge Model 9. Contours Represent Longitudinal Stress in ksi.....	94
Figure 81. Parameters Studied in Models with Joints.....	96
Figure 82. FE Model with Solid Deck Elements and Joints Representing Model # 1 .....	97
Figure 83. Deformed Shape of Model in Figure 82. Contours Represent Vertical Displacement in Inches.....	97
Figure 84. Longitudinal Stress Variation by Girder (50-ft Model, Service Loading).....	98
Figure 85. Longitudinal Stress Variation by Girder (50-ft Model, Strength Loading).....	98
Figure 86. Transverse Profile of Vertical Displacement at Midspan Under Varying Post- tensioning Levels (50-ft Model, Service Loading).....	100
Figure 87. Transverse Profile of Vertical Displacement at Midspan Under Varying Post- tensioning Levels (50-ft Model, Strength Loading) .....	100
Figure 88. Joint 3 Opening Along Span (50-ft Model, Service Loading) .....	101
Figure 89. Joint 3 Opening Along Span (50-ft Model, Strength Loading).....	101
Figure 90. Joint 4 Opening Along Span (50-ft Model, Service Loading) .....	102
Figure 91. Joint 4 Opening Along Span (50-ft Model, Strength Loading).....	102
Figure 92. FE Model with Solid Deck Elements and Joints Representing Model # 9 .....	103
Figure 93. Deformed Shape of Model in Figure 92. Contours Represent Vertical Displacement in Inches.....	103
Figure 94. Longitudinal Stress Variation by Girder (100-ft Model, Service Loading).....	105
Figure 95. Longitudinal Stress Variation by Girder (100-ft Model, Strength Loading).....	105
Figure 96. Transverse Profile of Vertical Displacement at Midspan Under Varying Post- tensioning Levels (100-ft Model, Service Loading).....	106
Figure 97. Transverse Profile of Vertical Displacement at Midspan Under Varying Post- tensioning Levels (100-ft Model, Strength Loading) .....	106
Figure 98. Joint 2 Opening Along Span (100-ft Model, Service Loading) .....	107
Figure 99. Joint 2 Opening Along Span (100-ft Model, Strength Loading).....	108
Figure 100. Joint 3 Opening Along Span (100-ft Model, Service Loading) .....	108
Figure 101. Joint 3 Opening Along Span (100-ft Model, Strength Loading).....	109
Figure 102. Joint 4 Opening Along Span (100-ft Model, Service Loading) .....	109
Figure 103. Joint 4 Opening Along Span (100-ft Model, Strength Loading).....	110
Figure 104. Bending Mode Shape 1, 50' Bridge Model.....	111

Figure 105. Bending Mode Shape 2, 50' Bridge Model.....	111
Figure 106. Bending Mode Shape 3, 50' Bridge Model.....	112
Figure 107. Bending Mode 2 Cross-Section.....	112
Figure 108. Bending Mode 3 Cross-Section.....	113
Figure 109. Bending Mode Shape 1, 100' Model.....	114
Figure 110. Bending Mode Shape 2, 100' Model.....	114
Figure 111. Bending Mode Shape 3, 100' Model.....	115
Figure 112. Dynamic Load Allowance according to OHBDC (CAN/CSA-S6, 1988) .....	116

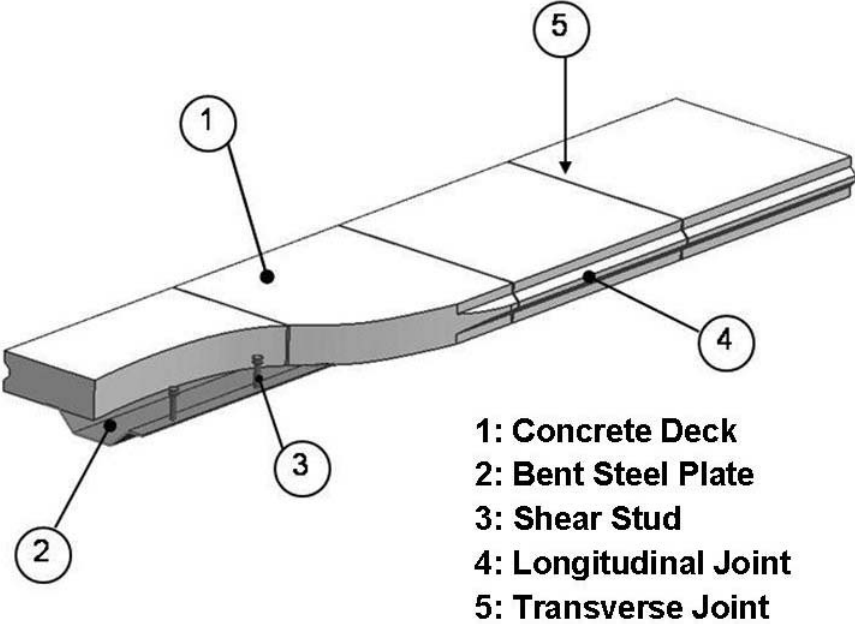
## LIST OF TABLES

Table 1. Material Properties.....	22
Table 2. Loading and Moment Demands for Beam Analysis.....	24
Table 3. Loading and Shear Demands for Beam Analysis .....	25
Table 4. Sample Results from Cross-Section Optimization Analyses.....	36
Table 5. Design Parameter Selection Criteria and Importance Factor.....	45
Table 6. Scoring and Ranking of Design Options .....	46
Table 7. Summary of limit states considered to evaluate bridge models.....	49
Table 8. Summary of grillage member properties .....	54
Table 9. Elements Used in Con-Struct 3D FE Model.....	63
Table 10. Material Properties used in 3D FE model.....	63
Table 11. Case Matrix for Global Parametric Analyses .....	66
Table 12. Element Data for Parametric Models with Shell Deck Elements.....	68
Table 13. Original Geometries Used for Models in Parametric Study.....	69
Table 14. Results of ABAQUS Analysis on Original Geometries .....	69
Table 15. Modified Geometries to Meet AASHTO Specifications.....	70
Table 16. Results of ABAQUS Analysis on Original Geometries .....	70
Table 17. Summary of Maximum Forces in Bridge Models .....	79
Table 18. Case Matrix of Post-Tensioning Levels and Loading Conditions.....	95
Table 19. Element Data for Full Models with Solid Deck Elements.....	95
Table 20. Fundamental Frequencies of the First Three Bending Mode Shapes, 50' Bridge Model .....	111
Table 21. Fundamental Frequencies of the First Three Bending Mode Shapes, 100' Bridge Model .....	113

# 1. INTRODUCTION

## 1.1 Summary

In order to offer faster and, in some cases, less expensive bridge construction, precast superstructures have recently become a topic of much interest to federal and state highway agencies (FHWA, 2004; Shahawy, 2003). Almost any component of a bridge can be precast, including girders, abutments, and decks (FHWA, 2004; Shahawy, 2003). The focus of this research is that of completely prefabricated composite steel box girder sections for rapid construction. While the exact geometry is to be developed with the work from this research project, the basic concept being investigated is presented in Figure 1 below and it clearly follows from the system that originated the Michigan Department of Transportation’s (MDOT) interest, shown in Figure 1.



**Figure 1. Composite Steel Box Girder Concept**

As shown in Figure 1, the prefabricated steel box superstructure system consists of a cast in place or precast deck connected to a press-formed or cold-bent steel plate by means of shear studs. These sections could then be place side by side and connected transversely, utilizing a shear keys or other similar mechanism. While the behavior, design, and analysis of composite

steel box girders is well established, several outstanding issues are unresolved for implementation of prefabricated concepts. The information needed in order to make the proposed prefabricated system viable is:

- What, if any systems are already in place
- Design of shear connections
- Design of longitudinal deck connection
- Design and analysis modeling techniques

These topics and their applicability to a prefabricated composite steel box girder system constituted the focus of the work performed in this project.

While the system that originally initiated MDOT's interest in this topic utilized a cold bent plate, the evaluation presented in this report is not limited to this concept. The size of the steel tub girder used in the longer span (100 foot) bridges, which were part of this study, would require the bending of rather thick and large plates. The feasibility of this process was not evaluated. The authors are not familiar with the current capabilities in the state of Michigan, or at a national level, on the cold bending of steel plates. Thus, the tub girders for longer spans may require welded plates. Although this would introduce additional cost into the system, it will not affect performance, and will not be discussed further.

## **1.2 Research Objectives**

The overall goal of the project was to gain a working knowledge of the bridge system at hand. This was considered to have been achieved when the following objectives had been met:

- Determine global system response of prefabricated composite steel box girder systems due to loads
- Determine localized behavior of joints
- Determine the effect of reduced post-tensioning on both global behavior and joint behavior
- Present design recommendations

The first three objectives were met by developing a hierarchical suite of finite element analyses that could address different aspects of the bridge behavior. While some models were conducive to global analysis, others were more suited for detailed joint analysis. Others yet had

reduced complexity that led to smaller run times, making them more adept to parametric studies. These finite element models were meticulously checked against theoretical and experimental results in order to ensure accuracy.

The final objective was accomplished by analyzing the data compiled throughout the first three objectives. These results allowed the research team to make recommendations for employing prefabricated composite steel box girder systems.

### **1.3 Scope and Organization**

The first step toward completing the project was to compile and study existing literature on related topics. This literature review can be found in Chapter 2 of this report. Although many similar systems were found, i.e., the use of cold-bent U-shape steel girders for prefabricated superstructure units, the studies were conceptual, experimental, or simply subjective. Thus, there has been no detailed study on the performance of this system under varying design parameters on the influence that post-tensioned longitudinal joints may have on their behavior and design. Therefore, the authors believe that this is the first study major study for this particular system. The design and analysis considerations for the project are listed in Chapter 3. These including loading conditions and limit states, analysis methods, and some preliminary optimization work.

Once the literature review was performed, the research team pared down the possible variations of the system to be studied by making use of a rating system which accounted for factors such as: cost efficiency, constructability, fatigue performance/durability, and ease of replacement/removal. The highest ranking designs were then chosen for analysis. This can be found in Chapter 4.

Chapter 4 also highlights information gathered from a separate project which involved experimental testing of a prefabricated steel box girder system. This experimental evaluation adds credibility to the analytical evaluations performed for this project.

The majority of the technical work done on this project can be found in Chapter 5. This section details the selection of analysis tools, parametric studies, and detailed studies of joints and connections. The information found here can be used to aid in the design of prefabricated composite box girder systems. Lastly, design recommendations are presented in Chapter 6.

## **2. LITERATURE REVIEW**

### **2.1 General**

A literature and survey review of current prefabricated complete superstructure systems have been conducted to identify prefabricated solutions similar to the system being studied or that address some of the issues noted in Section 1. The review considered available information at the conceptual, research, or implementation stage. As a reference, a brief account of concrete solutions is discussed and then more emphasis is placed on steel composite solutions. In the discussion of connection elements, the girder material type is not relevant and thus they are discussed as stand alone details.

### **2.2 Prefabricated Superstructure Systems**

As previously mentioned, national and state highway agencies have a high interest in using complete prefabricated bridge systems (AASHTO, 2002; FHWA, 2004; Shahawy, 2003, SDR, 2005). Technology progress is such that almost all the different elements composing a bridge system have been implemented into prefabricated solutions. Thus, superstructure elements are no different.

The most common type of prefabricated superstructure elements are clearly the girders, which could be considered prefabricated in either steel or prestressed concrete solutions in either I or box shapes. These prefabricated beams are usually made composite with a cast-in-place concrete deck. Thus, complete superstructure solutions are typically referred to as those that use prefabricated elements that *integrally* feature *both* the girder and the deck system. Under this definition, un-topped adjacent prestressed box girders could be considered a complete prefabricated system; and clearly so would be precast/prestressed concrete segmental bridges (typically cellular box girders). Both adjacent prestressed box girders and segmental cellular box girders are commonly and successfully used.

Prestressed double-tee beams have also been used as complete prefabricated superstructure solutions in several states (e.g., Colorado, New Mexico, and Wyoming) (Shahawy, 2003). Continuity between adjacent double-tee units is achieved by transverse post-tensioning. While this solution is aimed at highway bridges it has been mostly used for rural and secondary roads.

Complete superstructure deck systems have also been proposed, usually called full-depth prefabricated decks. Systems with and without the requirement of a cast-in-place topping have been developed (FHWA, 2004). Prefabricated prestressed and post-tensioned full-depth deck panels have also been used for complete superstructure replacement in Europe (Shahay, 2003).

A more recent concept is to use of precast/prestressed girder elements with full or partial deck flanges for a prefabricated superstructure element. A complete superstructure would then be assembled by a cast-in-place deck topping or connection of the prefabricated girder/deck elements through transverse connection of the deck flanges (Badie, 1999; FHWA, 2004; Freeby, 2005). These systems have been developed using I-or bulb-tee girders (FHWA, 2004), standard and modified closed box girders (Badie, 1999; Freeby, 2005), and U- or tub-shaped girders with deck flange overhangs (Badie, 1999; Freeby, 2005).

Prefabricated steel superstructure systems are less common but several have also been developed. Complete superstructure elements have been created by the pre-assembly of I girders with a composite concrete deck with partial overhangs as shown in Figure 2. If needed, the superstructure unit is prefabricated with transverse diaphragms. A superstructure of this type was used for the James River bridge replacement project in Richmond Virginia (FHWA, 2004; Ralls, 2003). The contractor used prefabricated steel I-girder/deck units for most of the 101 bridge spans. The girder-deck units were pre-constructed in a casting yard near the site. The old bridge was removed over night. Abutments were prepared for placement of the new bridge and the composite units were then set in place. The slab joints were sealed and the slab was post-tensioned transversely. For this project, the Virginia DOT did not consider any bids over 220 days. The winning bid was for 179 days and the contractor finished the job in 140 days. For each day under 179 the contractor received \$30,000 bonus, and was to be charged the same amount for each day over schedule.

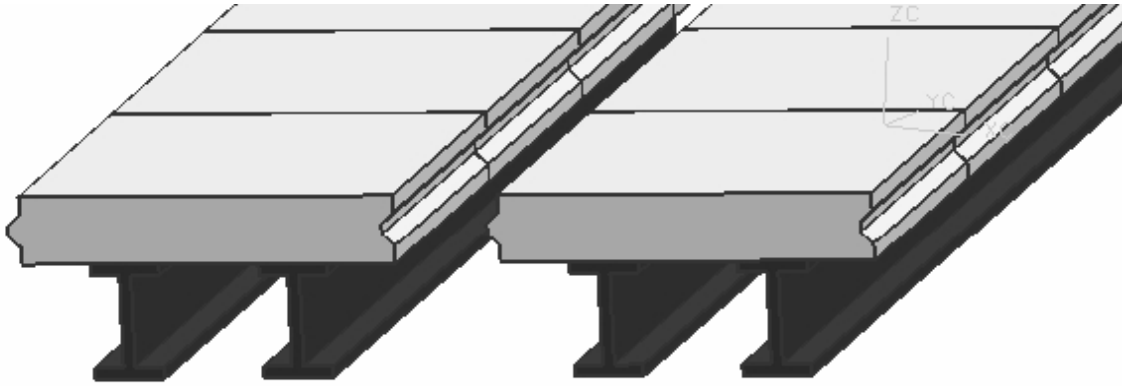


**Figure 2. Schematic of Prefabricated Steel Composite Superstructure with I-Girders**

### **2.3. Prefabricated Steel Box Composite Superstructure Systems**

Much to the surprise of the research team, a literature review on prefabricated steel box composite bridge superstructure elements showed that such a concept has been proposed several times during the past 35 years. The concept, as discussed in Section 1, consists on using a tub-shaped steel section as the girder element connected compositely to a concrete deck. The steel tub section and the composite deck thus define a box section. The prefabricated steel composite box girders are then to be used as complete superstructure units when placed side by side to make up the require bridge width.

#### **2.3.1 Pressed-Formed Steel Box Girder Bridge System – West Virginia University**

In the literature review thus far, the first finding of a prefabricated steel composite box girder system was the conceptual designs of Gangarao and Taly (Taly, 1979). Back in the early 1970s Gangarao and Taly developed and studied several modular bridge systems aimed at short and medium spans. Concepts for prefabricated press-formed steel box girder bridge superstructure elements were developed and found economical and suitable for span ranges of 40 to 100 ft under HS20-44 loading. The proposed system consists of a trapezoidal trough section which is press-formed from a 3/8-in. thick A36 steel plate, see Figure 3. The deck consists of 5-in. thick precast prestressed concrete panels. The concrete deck is to be precast with the stud-plate embedded in it and then the entire deck assembly is shop-welded to the steel through-section. The precast concrete planks are nominally prestressed to minimize shrinkage cracks.

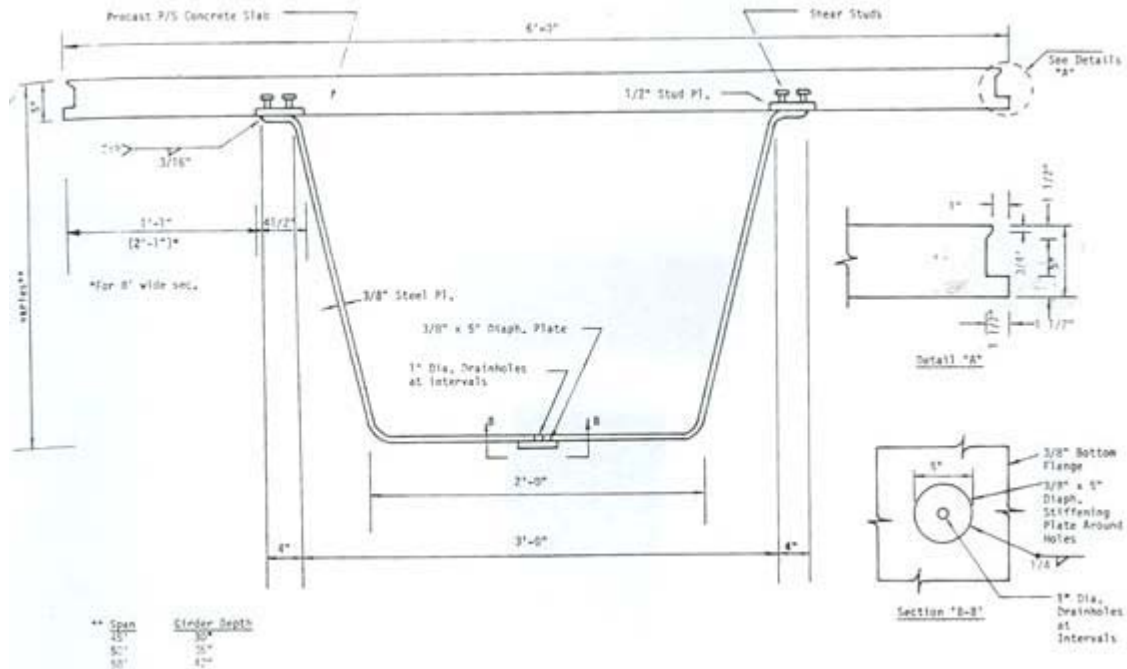


**Figure 3. Press-Formed Composite Box Girder from Gangarao and Taly [16]**

The composite solution was an alternate to an all-steel designed proposed by the same authors (Taly, 1979). The webs and the bottom flange are not stiffened internally or externally. Different girder sections were suggested for different span lengths. They envisioned the girders to be produced in two top-flange widths, 6 ft and 8 ft, each having three variations in depth: 2.5 ft, 3.0 ft, and 3.5 ft. Their studies showed that a suitable combination of these sections results in various deck width designs at 2 ft intervals for spans up to 65 ft.

Lateral load distribution between the adjacent girder units is achieved through shear keys with weld-ties at the junction of the two adjacent beam deck flanges as shown in Figure 4. The ends of the girders are closed by a 3/8-in. thick plate diaphragm welded all around the flanges and webs of the girders. Bearing stiffeners were provided at the beam ends. Drainage holes were proposed in the bottom flange (see Figure 5) to drain out moisture from the closed steel box section.

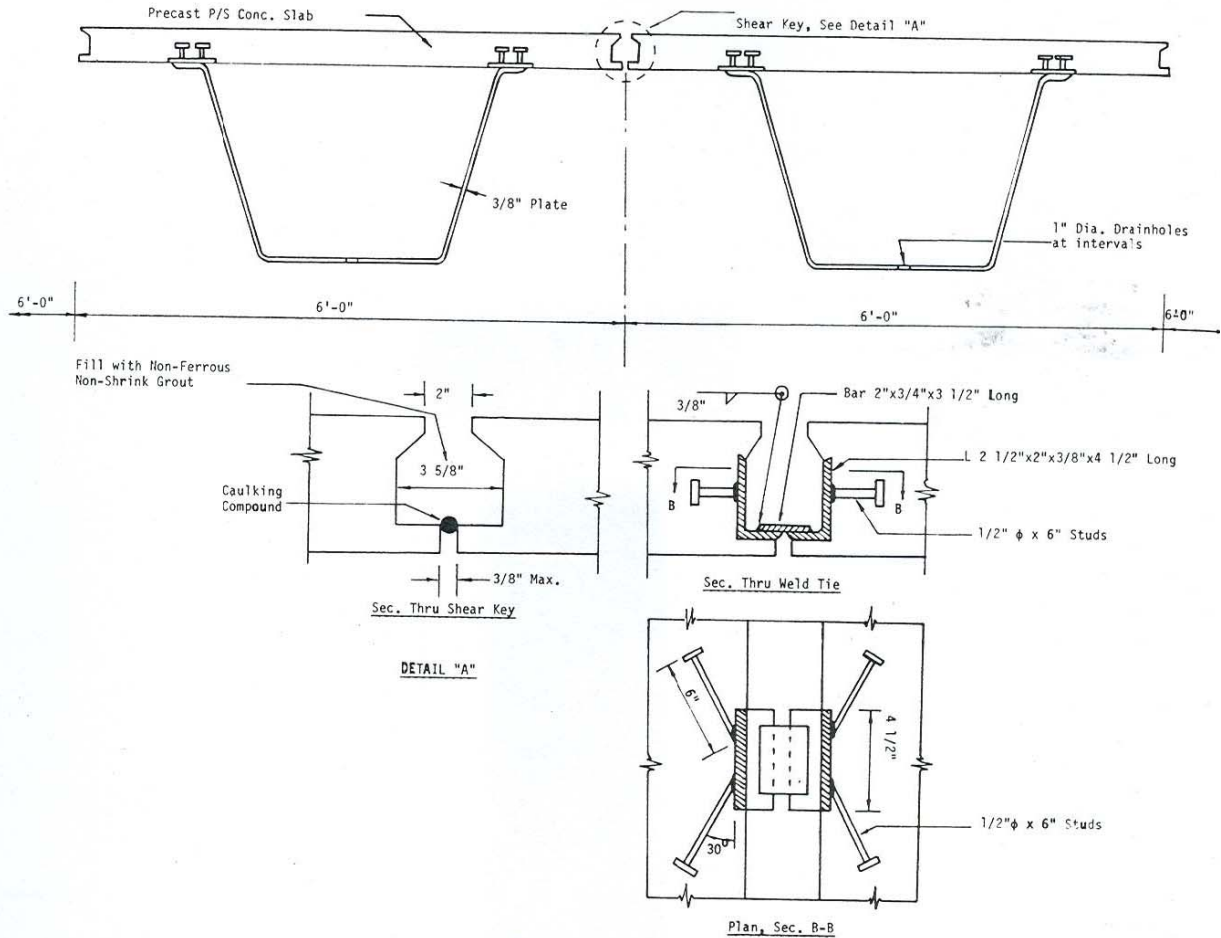


**Figure 4. Shear Key Details for Pressed-Formed Steel Box Girders [Taly, 1979]**

Since the American Association of Highway Transportation Officials (AASHTO) specifications did not provide any criteria for design with press-formed steel members, the proposed girder was checked according to the 1977 American Iron and Steel Institute specifications. Regarding the maintenance and durability of the system, the proponents note that investigations on several steel bridges with hollow members that had been in service for over 60 years had shown no signs of moisture or corrosion on the inside surfaces. Accordingly, they did not suggest corrosion-protective treatment for the interior of the proposed girders. For the exterior, they recommend painting the steel surface to protect it from corrosion, unless weathering steel, such as Corten or Mayari-R, is used for fabrication.

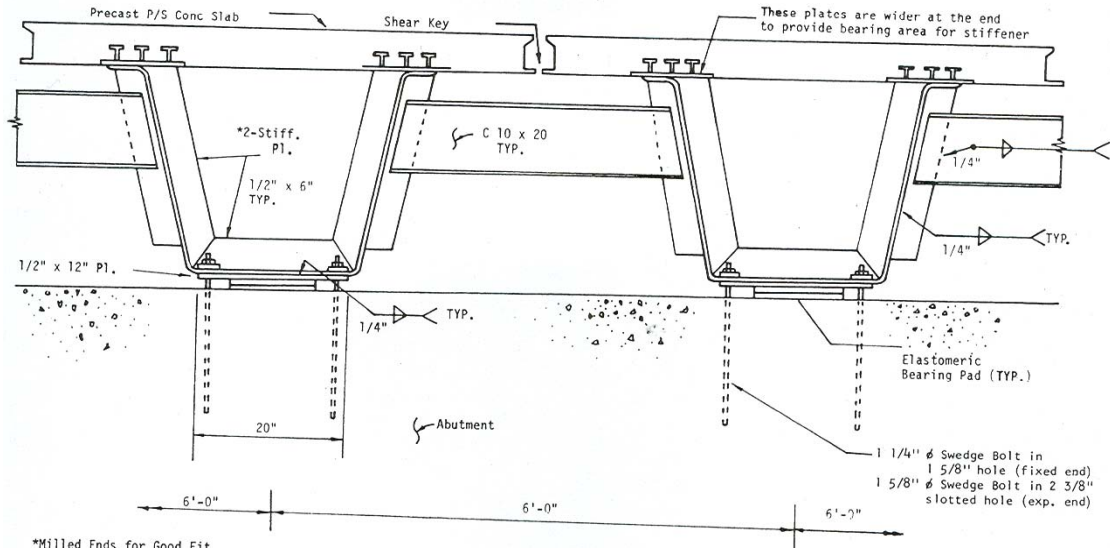


**Figure 5. Connection and Stiffener Details at Abutment Support (Taly, 1979)**

### 2.3.2 Composite Girders with Cold Formed Steel U Section – Tokai University, Japan

A similar concept to the pressed-formed girder system presented in Section 2.3.1 was later proposed by researchers from Tokai University in Japan (Nakamura, 2002). The system consisted prefabricated superstructure units of two U-shape steel girders composite with a reinforced concrete deck. The U-shape steel girders are cold formed from one sheet of steel with minimal welding of shear studs and intermediate diaphragms between the girders. Steel bulkheads welded inside the U-shape girder create regions to be filled with concrete at support locations.

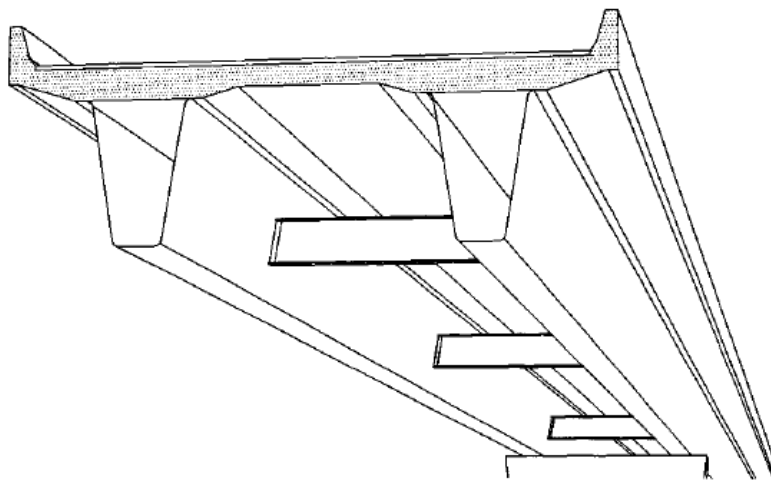


**Figure 6. Dual U-shape Steel Girders with Composite RC Deck (Nakamura, 2002)**

Flexure tests were conducted on three girder models in simply spans of 12.5 ft and loaded at the center by two loads 20 in. apart. The three girders tested were a girder in positive bending representing mid-span segments, a girder model in negative bending, representing segments over intermediate supports, and an alternative structure with a steel plate instead of concrete deck and tested in the inverted (negative bending) position. The models were approximately 40% scale and had a U-girder depth of 17.7 in., a wall thickness of 0.24 in., and the concrete deck was 4 in. thick and 26 in. wide. The experiments showed the composite girders to have sufficient bending strength and stiffness capacities and the researchers concluded that the system was practical and feasible.

### **2.3.3 Texas Prefabricated Steel Tub-Girder System – University of Texas, Austin**

A more recent effort to develop steel box girder systems for modular prefabricated bridge superstructures is the effort done at the University of Texas, Austin for the Texas Department of Transportation (Freeby, 2005). The effort was propelled by the pressure on the Texas DOT to upgrade and expand its on- and off-system roadways and, in particular, the need for the rapid construction of the nearly 150 bridges that cross I-35 in central Texas. Construction of these structures was scheduled to begin in spring 2005.

From the effort noted above, two new prefabricated bridge superstructure systems were developed: a steel tub-girder and a prestressed concrete pre-topped U-beam (Freeby, 2005). Both systems were developed for maximum span lengths of 115 ft and total superstructure depth of 38 in. Only the steel solution is discussed here.

The steel tub-girder system uses a conventional pre-fabricated trapezoidal steel girder topped with a cast-in-place concrete slab before transportation to the bridge site. To achieve a shallow superstructure depth, the beams are shored during placement of the concrete deck to make them composite for all loads. After slab placement, the beam is hauled to the bridge site and erected on the piers/abutments. A cast-in-place closure pour joints the deck girder sections after they are in place. Figure 6 shows a girder section for a 115 ft span. The steel tub-girder has a 29.5-in. deep steel section with an 8.5-in. slab for a total section depth of 38 in. The design used ASTM A709 Grade 50W steel. A typical transverse cross-section of a bridge is shown in Figure 7.

As shown in Figure 8, the steel tub is formed of welded steel plates, as opposed to the bent steel plate proposed in this project. This gives the advantage of variable widths for the webs and flanges, but comes at the expense of requiring costly welds. However, it should be noted that the Texas DOT opted for welded steel plates in order to avoid introducing new technology, not on the basis of performance (Freeby, 2006).

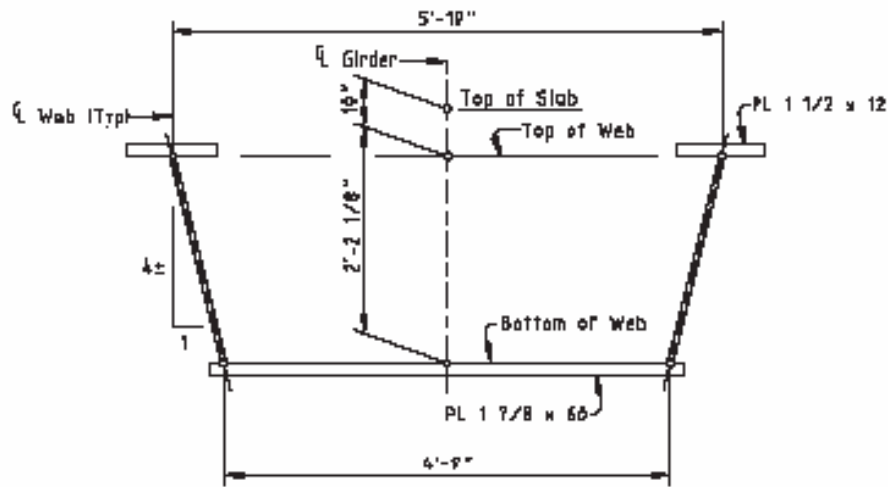


Figure 7. Texas DOT Steel Tub-Girder Section [Freeby, 2005]

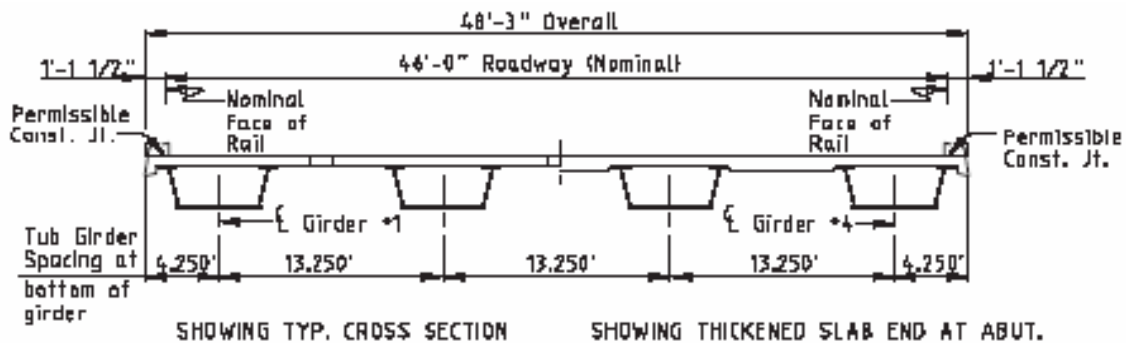
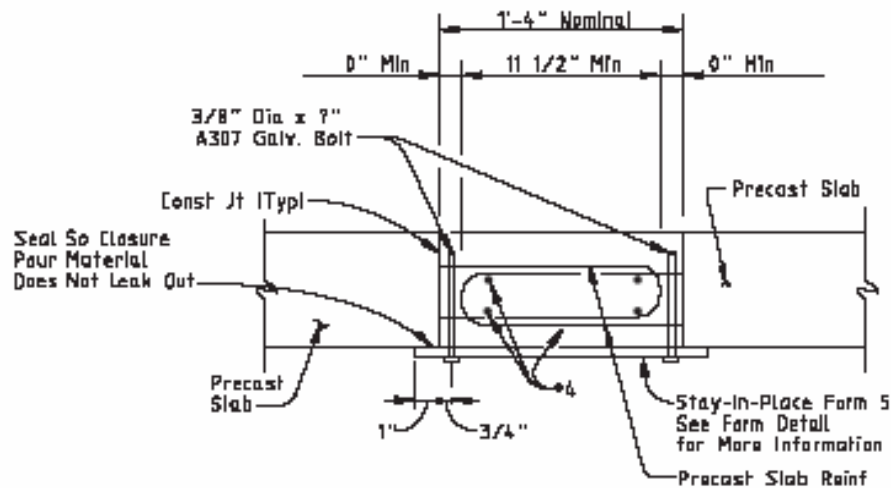


Figure 8. Typical Bridge Cross-Section using Texas' DOT Steel Tub-Girders [Freeby, 2005]

The girder design was developed using the AASHTO LRFD Bridge Design Specifications with HL93 loading (AASHTO, 1998). The design of the girder element was controlled by the Texas DOT imposed live load deflection limit of  $L/800$  and not by allowable strength

requirements. Due to the unusually shallow section, the girder was proportioned so that the deck would not crush before the steel tub reached yield.

The transverse deck connections for the prefabricated systems are reported to be undergoing testing at the University of Texas, Austin (Freeby, 2005). The concept for the joint detail for the steel tub-girder superstructure is shown in FIG. Preliminary research results reported in reference (Freeby, 2005) note that the closure joint behaves as designed and develops the predicted moment and shear capacities with failure due to yielding of the reinforcement exhibiting ductile behavior. While durability of the joints is a general issue, Texas DOT is not concerned with corrosion due to their weather but plan to monitor the structures closely.



**Figure 9. Transverse Deck Connection Detail for Steel Tub-Girder (Freeby, 2005)**

Weathering steel was specified for durable performance without maintenance costs. Drip tabs and other details were provided to reduce the potential for substructure staining from the weathering steel. A flexible lifting scheme was incorporated in the design to give the contractors more options on the lifting and placement of the prefabricated units.

The two competing prefabricated bridge designs were released for letting in August 2004 and the winning bid was of the pretopped prestressed U-beam design. It is felt that the recent rise in steel prices prevented the steel tub-girder design from being competitive. It should also be noted that the steel tub-girder is composed of welded plates, which add a considerable amount of labor.

The Texas DOT anticipates that both of the developed prefabricated bridge superstructures will be used over the next 10 years for the rapid construction of the I-35 corridor in central Texas.

#### **2.3.4 Inverted Steel Box Bridge System – University of Nebraska, Lincoln**

A new steel configuration for prefabricated steel-concrete composite superstructure bridge elements is currently being developed and studied at the University of Nebraska (UN), Lincoln under a contract from the Nebraska Department of Roads (TRB-RIP, 2006). The concept consists on the use of an inverted steel tub/box girder connected compositely with a concrete deck. The rationale for inverting the steel tub-girder section follows from the case that small box sections are not a good configuration since they do not permit maintenance workers inside the box for inspection. Thus, inverting the steel box eliminates this problem.

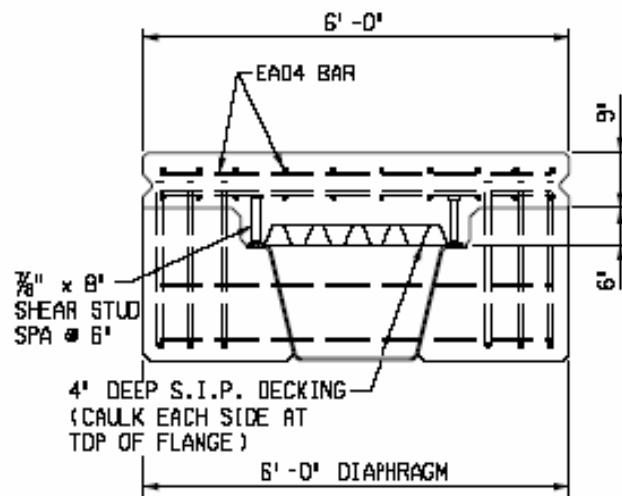
The inverted steel box girder features are:

- A girder consisting of an inverted steel box section. The web and top flange are of the same thickness and the bottom flanges are welded to the end of the web.
- The inverted box girder could be shop-welded or made by bending a flat plate into a U shape.
- Knee braces extending from the bottom flange ends can allow longer deck overhangs, if needed, and can provide horizontal restraint to the bottom flanges since they will have the tendency to “kick-out” (in plan) under flexural demands.
- Initial horizontal curvature (in plan) to the flanges could reduce the tendency of the bottom from “kicking-out” under flexural demands. This approach can also be used to generate an initial compressive force in the bottom flanges to counteract dead load stresses and increase the live load capacity of the girder.
- The wide top flange of the inverted box provides a convenient platform for construction workers but it may need to be stiffened.

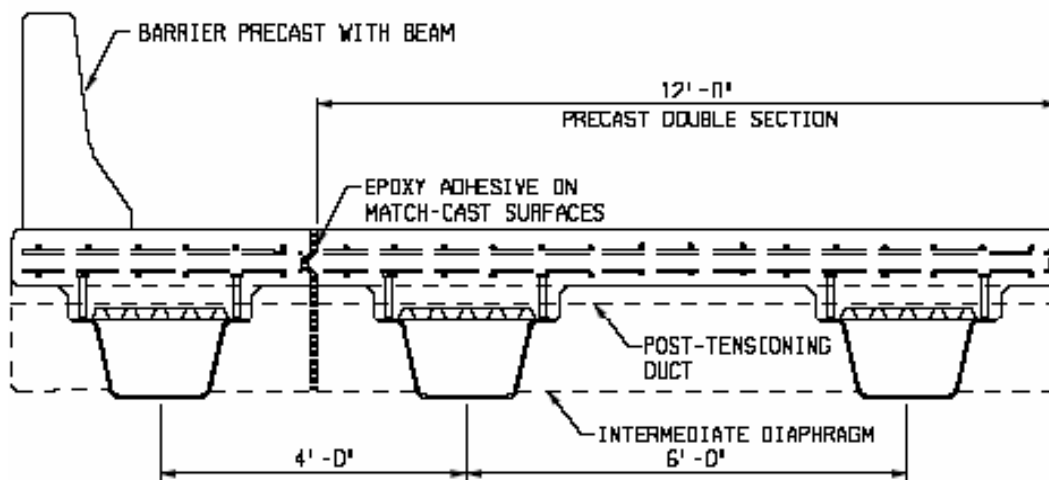
The mentioned research project is to investigate the system and develop design provisions. The project initiated in July 2000 and the end date was July 2004. The authors were unsuccessful in obtaining more information from the UN researchers on this project.

### 2.3.5 Con-Struct Bridge System – Nelson Engineering Services

Nelson Engineering Services (NES) has developed an innovative concept for a prefabricated composite steel box girder system with an integral road deck for shallow prefabricated bridge superstructures (AASHTO, 1998). The “Con-Struct” concept is that of a *shallow* girder element consisting of a cold-formed bent steel plate in the shape of a “bath-tub” connected compositely to a reinforced concrete deck (Figure 9a). The composite box shape is braced for placement by the prefabricrated deck, which eliminates the need for cross-frames. Prefabricated girder units can be placed side by side and post-tensioned transversely at the deck level or at intermediate concrete diaphragms to build up the desired superstructure width (Figure 9b).



a) Beam-Cross Section at Intermediate Diaphragm



b) Partial Deck Cross-Section

Figure 10. Preliminary Concept for Composite Steel Box Girder [Nelson, 2004]

Unique to the Con-Struct system from Nelson Engineering is their concept to prestress the steel plate to increase the composite girder capacity for live loads. This is achieved by propping the steel tub section at mid-span and stabilizing it, but not supporting it from its ends. A cast-in-place deck is then poured and a Styrofoam block or metal decking is used to form the deck on top of the tub-girder void. The self weight of the deck introduces negative bending on the steel plate when propped on its center. This negative moment introduces an initial compressive state in the bottom of the tub-girder soffit. Once cured, the concrete slab and the steel girder act compositely and the compressive stress in the steel tub is “locked-in.” This stress can be further controlled by using tensioning devices at the end of the steel tub-girder. The concept is to use the initial pre-compressive stress to provide camber to the section and to counteract dead load stresses. This also increases the service live load capacity of the section.

The Con-Struct system is built using galvanized steel for durability measures. To the knowledge of the research team, Nelson Engineering has not yet developed or validated transverse deck connection details to connect multiple girder sections for wider bridge solutions. The system, however, has been effectively used in several private pedestrian bridges in Michigan. A picture of a 40 ft long pedestrian bridge built using the Con-Struct system is shown in Figure 10.



**Figure 11. Pedestrian Bridge over Tyler Creek (MI) with Cons-Struct System (Nelson, 2006)**

### **2.3.6 Shallow U-shape Cold-bent Girders for Prefabricated Bridge Superstructure Units**

A recent report of a FHWA-sponsored research on prefabricated steel bridges provided a preliminary, yet subjective review of the Con-Struct system. With minimal justification, the authors concluded that the Con-Struct system did not meet AASHTO requirements for highway bridges. The criticism was that there AASHTO did not address the use of cold-bent steel shapes. The authors, however, did note that the AISC Manual of Steel Construction does address cold-bending with limitations that bend lines longer than 36 inches may require large radii to avoid fatigue problems. In addition, the authors cite little benefits of using a box girder since they are usually needed when requiring torsional stiffness; and that otherwise they tend to be more expensive. Finally, they site that the biggest drawback is maintenance and inspection since the shallow depth of the U-shape girder would make it very difficult for access by maintenance crews.

While the concerns leading to critique cited above are reasonable, the overall conclusion that that the shallow prefabricated superstructure systems using cold bent plates do not meet AASHTO requirements for highway bridge systems s seems overarching. Concerns related to fatigue of the cold bent plates can be addressed by increasing the radii of the bent, which can be easily provided given the outer sloping geometry of the tub girder webs. In addition, there are published studies with information on the fatigue behavior of cold bent members that can assist this design issue (Hassan et al.. 1998). Regarding capacity, the flexural performance of shallow prefabricated systems such as the Con-Struct system has been shown via experiments to be adequate and to satisfy with AASHTO criteria (Burgueño and Pavlich, 2006). The inefficiency of the box sections for straight bridges is true but its impact in cost does not seem to be consistent with the noted critique. Implementations of the Con-Struct system thus far have indicated that the system is cost competitive with conventional solutions as well as other prefabricated systems (Nelson, 2006). Finally, the issue of inspection is one that can certainly be circumvented via the provision of access holes at the girder ends for the use of robotic inspection systems. Furthermore, the difficulty in inspecting shallow U-shape steel bridges is no different than the inability to inspect prestressed concrete box girders, whose void is actually inaccessible with a foam block that could trap moisture and lead to corrosion of the steel reinforcement. Thus, inspection of the system alone should not be seen as a deterrent for consideration of the system under study.

Thus, there are certainly certain issues that can initially raise the attention of bridge engineers on the suitability of prefabricated bridge systems using shallow U-shape cold bent steel girders. However, as noted above, most of the concerns can be logically addressed. The systems thus seem worthy of investigation.

## **2.4. Deck Systems**

In designing a composite bridge girder system, even if it is a prefabricated one, a decision must be made between decks cast-in-place, decks made of precast elements with cast-in-place overlays, decks made of precast elements with wet joints, and totally precast decks.

Decks cast in place have strong advantages. They are simple to erect and easy to connect. However, these deck systems may suffer high tensile strains produced by shrinkage, which are restrained by the steel beam. Slabs made from precast elements also have advantages: low cost, fast construction, and high product quality. Connection of a precast deck to a steel girder is achieved by distributing the connection in groups that are anchored in pockets left in the precast deck and which, after placement, are filled with no-shrink grout. Problems with this solution may include connector density, corrosion between the girder and the deck, and shrinkage of the concrete in the pockets. The best solution is to prefabricate the deck and to prestress it longitudinally before connecting it to the steel girder (Virlogeux, 1999). The only concern would be creep in the concrete, which could be reduced through prefabrication. Thus, the slab could be made of precast elements made continuous through longitudinal joints before prestressing the deck; leaving the connection to the steel girder last.

## **2.5. Longitudinal Girder-Deck Shear Connections**

Shear connections in composite beams are obviously essential. The nature of composite action induces large shear forces at the interface between the steel and concrete. Traditionally, these shear forces have are carried by means of a shear stud welded to the steel, which is then embedded into the concrete deck. When a cast-in-place deck is used, embedding of the shear studs is simple. Shear studs are shop-welded and the deck is poured around them. However, if the deck is prefabricated, pockets are left in the precast slabs that correspond to the location of the shear studs on the steel. These pockets are then filled with a non-shrink grout, which hardens

to achieve the composite action. The design of the shear studs, as well as the properties of the grout used, can have large effects on the response of the entire section.

Considerable information exists both in code guidelines and research findings to guide the design of girder-deck shear connections. This research will study further the guidelines in the AASHTO LRFD specifications as the main source. Considerable information was also found from activities in Korea on the development of composite box girder sections with precast decks (Chang, 2001). This findings and general guidelines on steel and concrete composite construction (Ohelers, 1995) will continue to be studied.

## **2.6. Transverse Deck Joints**

Also of consideration are the longitudinal connections between prefabricated deck segments. Transverse deck joints will be less critical for the concept under investigation here since the sections are to be used as simple spans. Therefore, negative moments, and the associated tensile stresses will not occur at the transverse joints. Despite this, transverse deck connections between prefabricated panels should not be ignored as they are responsible for transferring the longitudinal shear in the deck element. An inadequate longitudinal shear deck connection can lead to slip between adjacent precast panels and limit the flexural and shear capacity of the overall component and system.

Typically, the joints connecting prefabricated panels are made by means of *shear keys* of two basic types: female-to-female or tongue-and-groove type joints. After installation, the joints are filled with high-strength non-shrink grout or with an epoxy mortar. Longitudinal post-tensioning is sometimes necessary to provide sufficient compression to keep the joints from opening.

Use of precast concrete panels for full depth decks has been in use since the 1970s (Taly, 1979) and new efforts closely related to steel box construction have been recently published (Chang, 2001). Thus, extensive literature exists on the topic (Issa, 1995). Thus, this research only considered a handful of relevant sources on this detail.

## 2.7 Longitudinal Deck Connections

The capacity of a deck system to distribute loads transversely between girders defines the load distribution characteristics of the bridge system. Thus, the ability to connect the prefabricated sections transversely, at the deck flanges, will be of great importance for the system under consideration. The longitudinal deck connections for prefabricated decks seems to be designed on a project specific basis for connecting prefabricated double tees (Shahawy, 2003) as well as the prefabricated steel box tub-girder concepts presented in Section 2.3.1 and Section 2.3.2. An overview of the concepts identified thus far follows.

In general, to maintain continuity between adjacent prefabricated deck elements (or the flanges of prefabricated girder/deck elements), the flange edges, or sides, are shaped to create a continuous shear key that can be filled with a non-shrink grout or epoxy mortar. Different types of longitudinal deck connections are feasible:

1. Grouted female-to-female shear keys. In this connection detail shear is transferred by friction and by the creation of an internal diagonal compression strut inside the shear key cavity.
2. Grouted tongue-and-groove shear keys. In this connection detail shear is transferred largely by friction and by the diagonal compression transferring load between the grove part of the key onto the tongue part in the other component.,
3. Reinforced (confined or unconfined) shear keys blocks. This connection requires the provision of long pockets inside the prefabricated deck system. The pockets are asymmetrical such that the reinforcement is placed first on one side and then slid across the joint once the adjacent member is in place, see Figure 11.
4. Reinforced (confined or unconfined) female-to-female shear keys. In this connection, a full depth shear key is reinforced with splicing bars extending from the adjacent panels. The reinforcement could be a simple splice or confined as shown in Figure 12.
5. Post-tensioned grouted female-to-female shear keys. This connection concept is as described in (1) above with additional post-tensioning forces to avoid cracking or opening of the joint and increase its shear capacity.

6. Post-tensioned grouted tongue-and-groove shear keys. This connection concept is as described in (2) above with additional post-tensioning forces to avoid cracking or opening of the joint and increase its shear capacity.
7. Welded plate grouted shear key blocks. In this concept, a steel plate or reinforcement bar is embedded at the end of the flange and fabricated with the precast deck. A plate is then welded in the field to provide a shear connection. The block-out cavity is then grouted. This connection detail is shown in Figure 13. This concept was utilized for the connection design of Gangarao & Taly's pressed-formed steel box girder bridge system, see Figure 4.
8. Reinforced grouted moment key blocks. A full-depth block-out is reinforced with hair-pin reinforcement protruding from both sides of the prefabricated deck component and crossing in the region of the connection block. The region is grouted and the joint becomes a moment resisting connection. This concept was proposed for the Texas DOT steel tub-girder concept, see Figure 8.
9. Post-tensioned grouted female-to-female moment keys. This connection concept is an extension of that in (5) with the difference that the tendon would be placed such as to give the section moment capacity. Passive compression reinforcement would probably be necessary to control cracking induced from the post-tensioning.
10. Post-tensioned grouted tongue-and-groove moment keys. This connection concept is the same as that in (9) but applied to a tongue-and-groove geometry.

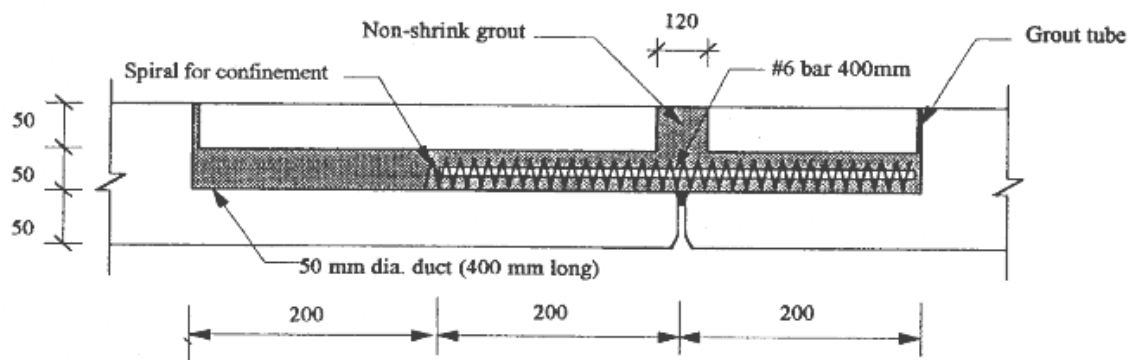


**Figure 12. Deck Connection Detail using Reinforcement in Precast Pockets (Badie, 1999)**

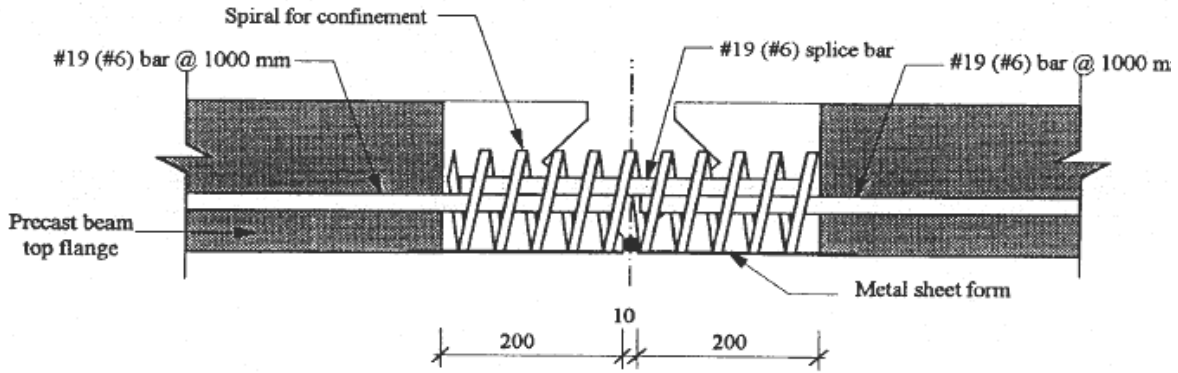


**Figure 13. Deck Connection Detail using Confined Reinforcement in Full-Depth Key (Badie, 1999)**

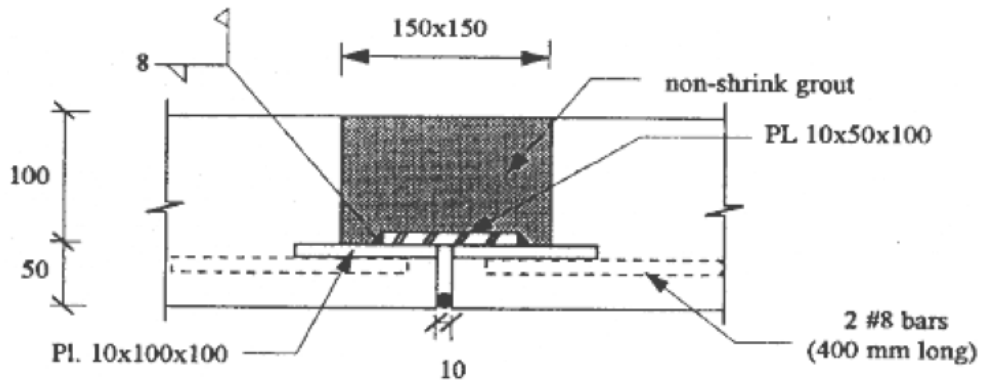


**Figure 14. Deck Connection Detail using Welded Steel Plate (Badie, 1999)**

The advantages and disadvantages of all of the above listed connections was considered with respect to cost, structural performance, constructability, design ease, etc., in order to identify approximately three options for further study under this project.

### 3. DESIGN AND ANALYSIS CONSIDERATIONS

#### 3.1 General

This Chapter provides the details of the standardized parameters for all of the analyses used in this project. In general, the project followed the design and analysis guidelines in the AASHTO LRFD Bridge Design Specifications (AASHTO, 1998). Deviations from these specifications are noted in the respective sections. In addition to general analysis and design specifications, this section also presents the implementation of these guidelines in a design optimization process aimed at providing a parametric evaluation.

#### 3.2 Materials

The material properties for the design and analysis tasks in this study are listed in Table 1. While the construction of the steel/concrete composite prefabricated bridges require diverse materials, only a few parameters of these are needed for the preliminary design tasks and for the service-load numerical modeling. Further, some specific details are not required such as the type of post-tensioning strands for the transverse connection of the units since only the pressure by them is considered in the analysis and is consistent with code recommendations.

**Table 1. Material Properties**

<b>Material</b>	<b>Properties</b>		
Concrete	$f'_c = 4,000$ psi	$E_c = 3,605$ ksi	$\gamma = 8.68 \times 10^{-5}$ kips/in <sup>3</sup>
Structural Steel	$F_y = 50,000$ psi	$E_s = 29,000$ ksi	$\gamma = 2.83 \times 10^{-4}$ kips/in <sup>3</sup>

#### 3.3 Loading

Loading for this study followed the AASHTO LRFD Bridge Design Specifications (AASHTO, 1998). Only the considerations applying to dead load (DC), live load (LL), and impact factor (IM) were considered. Dead loads consisted of the self weight of the superstructure and the road barriers. The material densities listed in Table 1 were used to make the load estimates.

Live loading consisted of the vehicular truck loading only. The AASHTO HL-93 design truck was used for all analyses. The loading consists of a lane load of 0.064 kips/ft<sup>2</sup> and an HS20-44 design truck (see Figure 15) along the 10 ft wide design lane. The MDOT Bridge Design Specifications require the use of a heavier design truck (HS-25) that is 25% heavier than the HS-20. The reason to use the HS-20 truck was to be consistent with the AASHTO loading criteria in order to check the specifications for the transverse post-tensioning of deck joints. Assessment of the impact of HS25 on the response of the studied systems indicated that the HS25 would increase moments by 10-12% and increase deflections by approximately 18%.

The systems considered in this study were simple spans. Thus, the axle configuration shown in Figure 15 was used for all analyses. The truck direction was changed on the bridge when considering multiple traffic lanes. For the 3D models, the truck axle loads were applied to an area patch 20 inches wide and 10 inches long. An impact factor on the truck axle loads was considered as specified in the AASHTO design specifications.

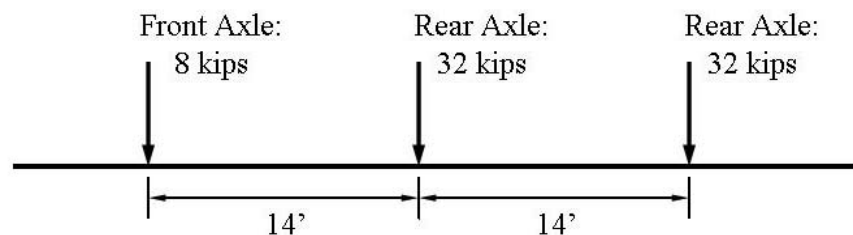


**Figure 15. Design Truck Schematic**

### 3.4 Design Limit States

The design limit states considered for the design and analysis of the prefabricated steel/concrete bridge structures were: Strength I (to assess strength under basic load combination to represent normal operating conditions of a bridge), Service II (to control yielding of steel structures under vehicular loading) and the optional Deflection Control (under live load only) limit state (AASHTO, 1998). The load combinations used for these limit states were:

- Strength I:  $1.25D + 1.75(L \times IM)$
- Service II:  $1.0D + 1.30(L \times IM)$
- Deflection Control:  $1.0(L \times IM)$

where  $D$  = dead load,  $L$  = vehicular live load, and  $IM$  = impact factor = 1.33.

### 3.5 AASHTO Simplified Analysis and Design Methods

Although the prefabricated systems being studied here are not directly addressed by the AASHTO code, the specifications for composite steel box girders are considered applicable to the type of structure under study and are thus followed.

To demonstrate the AASHTO method, a sample bridge was analyzed. The bridge is assumed to be a 50-ft simple span composed of five girder/deck prefabricated units as shown in Figure 16. The loads and corresponding bending moment and shear demands are listed in Table 2 and Table 3, respectively.

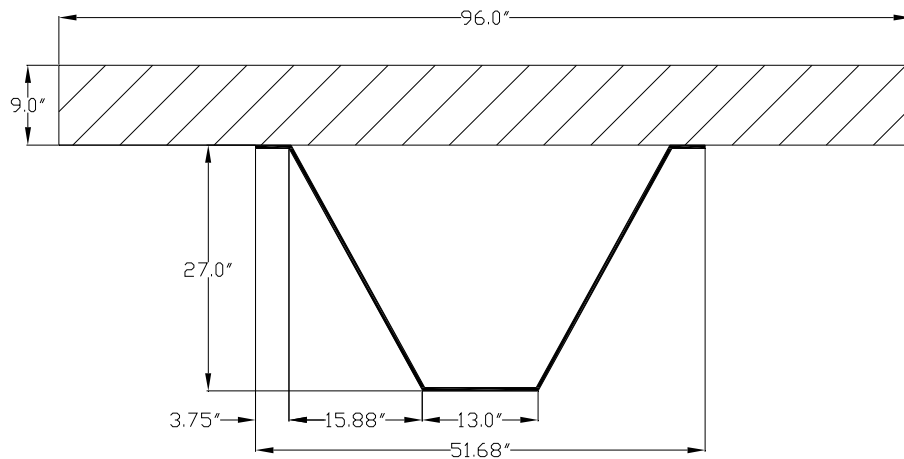


**Figure 16. Bridge Geometry Used in AASHTO Analysis**

**Table 2. Loading and Moment Demands for Beam Analysis**

AASHTO Load	Component	Magnitude	Moment at Midspan (kip*ft)
DC	Concrete Self-Weight	0.90 kip/ft	281.3
	Steel Self-Weight	0.156 kip/ft	23.3
	Barrier	0.18 kip/ft	55.1
	Total:		359.7
LL	Vehicular Lane Load	0.64 kip/ft	200
	Design Truck (Axle 1)	8 kip	34
	Design Truck (Axle 2)	32 kip	360
	Design Truck (Axle 3)	32 kip	216
	Total:		810
IM	All Cases Other Than Fatigue: 1.33		

**Table 3. Loading and Shear Demands for Beam Analysis**

AASHTO Load	Component	Magnitude	Shear @ 1 (kips)	Shear @ 2 (kips)
DC	Concrete Self-Weight	0.90 kip/ft	22.5	22.5
	Steel Self-Weight	0.156 kip/ft	3.9	3.9
	Barrier	0.18 kip/ft	4.5	4.5
	Total:		30.9	30.9
LL	Vehicular Lane Load	0.64 kip/ft	16	16
	Design Truck (Axle 1)	8 kip	6.6	1.4
	Design Truck (Axle 2)	32 kip	17.6	14.4
	Design Truck (Axle 3)	32 kip	8.6	23.4
	Total:		48.8	55.2
IM	All Cases Other Than Fatigue: 1.33			

Distribution of moment and shear demands on the individual girder units was estimated with the AASHTO load-distribution factors. The distribution factor for a box section with a steel girder is given by (AASHTO, 1998):

$$DF = 0.05 + \left( 0.85 \frac{N_L}{N_B} \right) + \frac{0.425}{N_L} \quad (3-1)$$

For the bridge under consideration, Equation (3-1) becomes:

$$DF = 0.05 + \left( 0.85 \cdot \frac{2}{5} \right) + \frac{0.425}{2} = 0.6 \quad (3-2)$$

The maximum bending moment ( $M_u$ ) under the Strength-I load case is determined with Equations (3-3).

$$[(DC)(1.25) + (VLL)(1.25) + (DT)(IM)(1.75)] \times DF \quad (3-3a)$$

$$[(359.6)(1.25) + (200)(1.25) + (610)(1.33)(1.75)] \times 0.6 = 1337 \text{ kip} \cdot \text{ft} \quad (3-3b)$$

Design follows from satisfying

$$M_u = \phi_f M_n \quad (3-4)$$

where  $M_u$  is the moment demand,  $M_n$  is the flexural capacity and the strength reduction factor  $\phi_f$  is given to be 1.0 in AASHTO Article 6.5.4.2.

To determine the section capacity, the AASHTO bridge design specifications outline a simplified approach for obtaining the nominal plastic moment of composite sections in its Appendix 6-A (AASHTO, 1998).

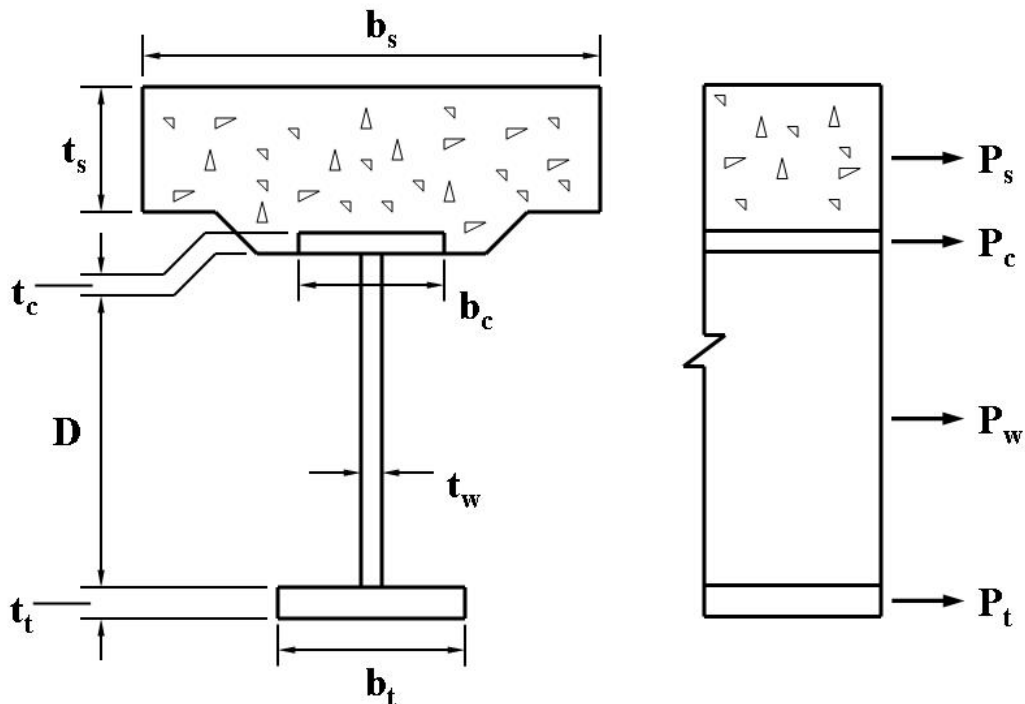


**Figure 17. Variables for AASHTO Nominal Plastic Moment of Composite Girders (AASHTO, 1998)**

Inspection of force equilibrium for the bridge model units showed that in all cases the section neutral axis was located in the slab above the level of the bottom deck reinforcement. This situation is defined as Case III, IV, or V in Appendix 6-A of the AASHTO Specifications (all three cases are identical when no deck reinforcement is present). For such cases, with reference to Figure 17, section force equilibrium, the plastic neutral axis depth, and the section plastic moment is given, respectively by:

$$P_t + P_w + P_c + P_{rb} = \left( \frac{c_{rb}}{t_s} \right) P_s + P_{rt} \quad (3-5)$$

$$\bar{y} = t_s \left[ \frac{P_{rb} + P_c + P_w + P_t - P_{rt}}{P_s} \right] \quad (3-6)$$

$$M_p = \left( \frac{-\bar{y}^2 P_s}{2t_s} \right) + [P_{rt}d_{rt} + P_{rb}d_{rb} + P_c d_c + P_w d_w + P_t d_t]. \quad (3-7)$$

For the test units under consideration, the force components at the deck reinforcement can be neglected and thus  $P_{rb}$  and  $P_{rt}$  are set equal to zero. Considering a deck concrete compressive strength of 3.6 ksi, solution of the above equations yields a plastic neutral axis depth ( $\bar{y}$ ) of 3.66 inches and a nominal plastic capacity ( $M_p$ ) of 1987 kip-ft. Since the deck is nine inches deep, the plastic neutral axis is in the deck.

AASHTO Article 6.10.4.1.2-1 (AASHTO, 1998) states that the section is compact if

$$\frac{2D_{cp}}{t_w} \leq 3.76 \sqrt{\frac{E}{F_y}} \quad (3-8)$$

Since the plastic neutral axis is in the deck, the depth of web in compression at the plastic moment is zero. Hence, the left side of the inequality in Equation (3-8) is also zero, and the section is compact. For compact sections, the AASHTO specifications direct the user to Article 6.10.4.2.2. Here, a variable  $D'$  is defined as

$$D' = \beta \frac{d + t_s + t_h}{7.5} \quad (3-9a)$$

$$D' = 0.9 \frac{27 + 9 + 0}{7.5} = 4.32 \quad (3-9b)$$

where  $\beta$  is given as 0.9 for  $F_y = 36$  ksi,  $d$  is the depth of the steel,  $t_h$  is the haunch thickness, and  $t_s$  is the slab thickness. For the section in Figure 16  $D'$  is 4.32 inches. Since  $D'$  is less than the plastic neutral axis depth then  $M_n = M_p = 1969$  kip-ft (found with Equation (3-7) above) and  $M_u \leq M_r$  making the section adequate in flexure.

The loading values used for the shear calculations are showed in Table 3. As Table 3 shows, the highest shear value occurs at Support 2. The maximum shear demand ( $V_u$ ) under the Strength-I limit state is determined as shown in Equation (3-10):

$$[(DC)(1.25) + (VLL)(1.25) + (DT)(IM)(1.75)] \times DF \quad (3-10a)$$

$$[(30.9)(1.25) + (16)(1.25) + (39.2)(1.33)(1.75)] \times 0.6 = 94.7 \text{ kips} \quad (3-10b)$$

Equation (3-10b) gives the  $V_u$ , which is described in AASHTO Section 6.10.9.1 as shear in the web at the section under consideration due to factored loads [ref#]. Now the shear resistance of the section must be found.

The maximum shear resistance,  $V_n$ , of the section is given by (AASHTO, 1998):

$$V_r = \phi_v V_n \quad (3-11)$$

where  $\phi_v$  is given in AASHTO Article 6.5.4.2 as 1.0, and  $V_n$  is found using Equation (3-12) below:

$$V_n = \frac{4.55 t_w^3 E}{D} \quad (3-12a)$$

$$V_n = \frac{4.55(0.375)^3(29,000)}{27} = 258 \text{ kips} \quad (3-12b)$$

where  $t_w$  is the thickness of the web, and  $D$  is the depth of the steel girder. With a maximum shear demand ( $V_u$ ) of 94.7 kips, the section is adequate in shear.

### **3.6 Refined Analysis Methods**

There are many other methods to analyze a bridge structure with improved refinement. In this project, two other methods will be employed. The first is the grillage method. A grillage model is a means of representing a structure with a series of line type elements that have been giving properties appropriate for representing the stiffness, torsion and unit weight properties of the structure being modeled. Grillage models reduce the number of required elements and degrees of freedom, thereby reducing the number equations that need to be solved to evaluate system response. Grillage models can be two- or three-dimensional, although only two-dimensional models were used in this project.

The second analysis method that was used is the finite element (FE) method. The finite element method is an approximate method of structural analysis that breaks the structure into discrete pieces, or elements, connected by means of nodes. The nodes are enforced to satisfy compatibility requirements and the way in which they interact with nodes of other elements or boundary conditions is determined by the force-deformation properties of the elements. This method is very powerful, and it can be used to analyze very complex structures to a high degree of accuracy. Care must be taken, however, to ensure the method is used correctly. In this project, three-dimensional FE models were created and analyzed with linear elements.

### **3.7 Precast Decks**

The AASHTO Bridge Design (AASHTO, 1998) specifications provide some general guidelines for the design of precast decks. They are defined as precast concrete units placed adjacent to each other in the longitudinal direction and then transversely joined together to form a deck system. The minimum thickness of the deck is to be 5.5 in and reinforcement needs to be provided by analysis and for the control of transverse cracking.

Precast longitudinal components are to be connected transversely by shear keys not less than 7 inches in depth. The specifications note that for purposes of analysis shear transfer joints should be modeled as hinges. The purpose of this study was to investigate the performance of moment (or shear-flexure) transfer joints, thus shear joints were not further considered in the design or analysis tasks.

Shear-flexure transfer joints require that the precast longitudinal components be jointed together by transverse posttensioning, closure joints, a structural overlay or a combination of these. An overview of these different options with schematics to some of them was presented in Section 2.7. With regards to modeling, the specifications note that decks connected by these joints should be modeled as continuous plates. This approach was followed in the parametric studies presented in Section 5.3 using 3D finite element models.

For posttensioned deck joints, the specifications indicate that uniform transverse posttensioning should be uniformly distributed in the longitudinal direction. The compressed depth of the joint should not be less than 7 inches. And the minimum amount of prestressing is specified as 0.25 ksi after all losses. It should be noted that this is a high level of prestressing force. If 0.5-in. strand were to be used on a 9 in. deep deck, this level of prestressing would amount to a longitudinal distribution of approximately 1 strand every 12 inches. The possibility of relaxing this criterion was part of the detailed stress analyses presented in Sections 5.4.

In order to evaluate the possibility of relaxing the required level of transverse posttensioning on the longitudinal precast joints from a prescriptive criterion to a performance-based criterion requires establishing such a performance level. No previously defined performance criterion for precast posttensioned joints was found from the literature or the AASHTO Bridge Design Specifications. It is clear that the performance of the shear-flexure transfer joint must satisfy the bending and shear demands from the service and strength limit states. However, these levels may be resisted by the posttensioned joint with different levels of joint opening on the tension side of the joint and compressive stresses on top of the joint. Compressive stress levels are thought to be already addressed by the design of the deck system as a continuous plate. However, adopting an allowed level of joint opening is more difficult. For this purpose, the criterion postulated in the AASHTO specifications for the control of cracking in reinforced concrete decks was used as the basis for joint opening acceptability.

The AASHTO specifications note that cracking in reinforced concrete members should be controlled with reinforcement and that crack width should be kept to certain limits to improve durability. This acceptability threshold is discussed in the commentary to Article 5.7.3.4. The crack is noted to be based on a crack width of 0.017 in. and directly modified by an exposure factor  $\gamma_e$ . This exposure factor is unity for a Class 1 exposure condition, that is, when cracks can

be tolerated due to reduced concerns of appearance and/or corrosion, and it is given as 0.75 for Class 2 exposure conditions, corresponding to segmental concrete box girders for any loads prior to full concrete strength and when there is increased concern for appearance and/or corrosion. The limit of crack width is thus given by:

$$w_c = 0.017\gamma_e = 0.017 \times 0.75 = 0.0128 \text{ in.} \quad (3-13)$$

where  $w_c$  is the maximum width of a crack. Therefore, the acceptability threshold for this project was set at 0.0128 inches.

This threshold has been included in the plots of the joint opening of the models in Section 5.4.4. However, it should be kept in mind that this is simply a comparison that the research team found to give a reasonable benchmark, not an actual requirement by any code or governing body. It should be further noted that the AASHTO specifications note that the individual Authority with jurisdiction may specify a different (more stringent) exposure factor  $\gamma_e$ . This indicates the subjectivity in establishing this performance level.

### **3.8 Parametric and Optimization Analyses**

To create a starting point for bridge geometries to be studied in this project, a simple optimization program was created using Microsoft Excel. The program incorporated the AASHTO criteria detailed in Section 3.5. This section describes the way the spreadsheet optimization program was created and the obtained results.

#### **3.8.1 Optimization Problem**

“Level-1” optimization analyses have been formulated and conducted at the section level in order to identify possible improvements to the basic design concept of a composite steel box girder component and also to conduct parametric studies. The optimization analysis was conducted using the nonlinear quadratic solver of Microsoft Excel. The section being investigated is shown in Figure 22, and a view of the system, using a beam-line analysis assumption, is shown in Figure 23. The problem at hand is to find the best combination of dimensions for the girder represented in these figures such that cost is minimized.

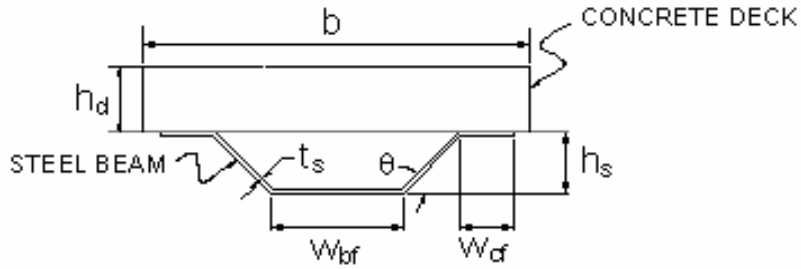


**Figure 18. Composite Steel Box Girder Cross-Sectional Geometry**

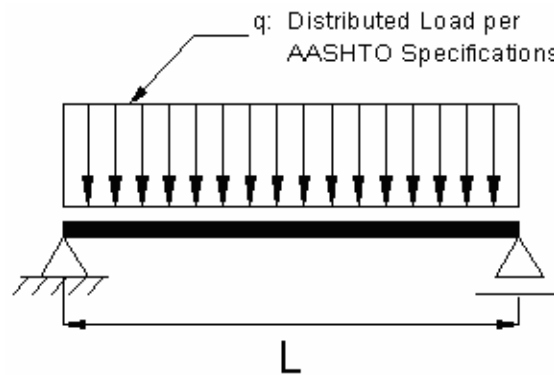


**Figure 19. Bridge System Profile under Beam-Line Analysis Assumption**

### 3.8.2 Problem Formulation

Optimization algorithms are numerical methods that allow selection of structural or material parameters for maximum efficiency through an objective function that measures the “goodness” or “efficiency” of a structural design. The objective function is defined by design variables, which are parameters that change during the design process. Design variables can be continuous or discrete depending on whether they can take values from a continuum or are limited to a set of discrete values. The optimization process is then to improve the goodness of the design by automatic changes in the design variables. Optimization processes are generally performed with some limits that constrain the choice of a design. Such limits are called constraints and usually include performance criteria. Optimization algorithms are thus a general and versatile technique for optimal structural design.

An optimization problem is typically defined in standard mathematical terms as:

Objective: Minimize  $f(\mathbf{x})$

Subject to:  $g_i(\mathbf{x}) \leq 0 \quad i = 1 \text{ to } m$

$h_j(\mathbf{x}) = 0 \quad j = 1 \text{ to } p$

$\mathbf{X}^L \leq \mathbf{x} \leq \mathbf{X}^U$

where  $\mathbf{x}$  is the design variables vector,  $\mathbf{X}^L$  and  $\mathbf{X}^U$ , are the lower and upper bound vectors of the design variables,  $f(\mathbf{x})$  is the objective function, and  $g_i(\mathbf{x})$  and  $h_j(\mathbf{x})$  are the equality and inequality constraints, respectively.

As far as the component geometry being sought, the design variables are obviously chosen as the dimensions of the different components that govern the cross section of the girder component. The selection of the objective function depends on the application. For example, the objective for current problem could be to maximize stiffness, maximize strength or minimize cost. Finally, the constraints are used to implement design limits such as maximum stresses and displacements for the achievement of an optimum objective.

### **1) Objective Function**

The basis for determining the optimal section was that the section is the least expensive. Consequently, the objective function was to minimize the cross-sectional area of the steel tub-girder. The area of steel used in this optimization was not the area per girder, but rather the area of all the girders required to form a three lane bridge (the bridge width can easily be modified, as noted in subsequent sections). In this way, the individual section is not being optimized, but instead the bridge as a whole is being considered.

### **2) Independent Variables**

The independent variables are the variables that are changed by the solver in order to reach the optimal result. The current bridge optimization problem used six independent variables to optimize the section. These variables and their corresponding labels in Figure 18 were:

- Deck Width,  $b$
- Steel Plate Thickness,  $t_s$

- Compression Flange Width,  $w_{cf}$
- Tension Flange Width,  $w_{bf}$
- Web Angle of Inclination,  $\theta$
- Steel Section Depth,  $h_s$

### **3) Parameters**

Parameters constitute those values in the design that do not change during the optimization process. The parameters included in the current analyses and their values were:

- Deck Height,  $h_d = 9$  in.
- Concrete Compressive Strength,  $f'_c = 6$  ksi
- Concrete Modulus of Elasticity,  $E_c = 4,415$  ksi
- Steel Yield Strength,  $f_y = 36$  ksi
- Steel Modulus of Elasticity,  $E_s = 29,000$  ksi

### **4) Constraints**

When changing the independent variables, limits must be set in order to ensure the optimal solution is a feasible design. The constraints to the independent variable were as shown below:

- $48 \text{ in.} \leq b \leq 96 \text{ in.}$
- $0.179 \text{ in.} \leq t_s \leq 0.375 \text{ in.}$  (7 ga. – 3/8" plate)
- $4 \text{ in.} \leq w_{cf} \leq 6 \text{ in.}$
- $10 \text{ in.} \leq w_{bf} \leq 24 \text{ in.}$
- $60^\circ \leq q \leq 76^\circ$
- $12 \text{ in.} \leq h_s \leq 54 \text{ in.}$

Other constraints related to design values were also incorporated, namely:

- Moment Capacity > Nominal Moment
- Steel Section Width < Slab Width
- Enforce Compactness (AASHTO Eq. 6.10.4.1.2-1)

### 3.8.3 Implementation

The final step in the optimization is to create a set of dependent variables that will change based on the changes made to the independent variables. The dependent variables and the calculations used to obtain them are given below.

As presented in Section 3.5, the nominal moment was calculated per the AASHTO LRFD Bridge Design Specifications (AASHTO, 1998). The moment demand per bridge girder component was based on Service II limit state requirements. The loads considered in the analysis were dead load, vehicular live load, and a dynamic load allowance. Distribution factors were calculated based on the AASHTO-LRFD recommendations.

Lastly, the desired span,  $L$ , and number of lanes,  $N_L$ , was specified. These were constant for a single run of the optimizer, but are user defined in order to find optimal sections for varying bridge lengths and widths.

### 3.8.4 Results

Because of the high number of variables, there are many local minima in the problem space and the gradient-based search algorithm in Excel easily gets “stuck” in local minima. Therefore, the solution found is highly dependent on the starting values of the independent variables. A table of results returned by the optimizer with the reduced number of variables is shown in Table 4. As mentioned above, Excel has trouble with finding local minima. Therefore, in order to achieve a solution, some of the values were given a specific starting point in order to arrive at a solution.

**Table 4. Sample Results from Cross-Section Optimization Analyses**

Parameter	Symbol	Units	Span			
			40'	50'	60'	70'
Deck width (Spacing)	$b$	in	96.00	96.00	96.00	96.00
Plate thickness	$t_s$	in	0.234	0.268	0.289	0.309
Compression Flange Width	$w_{cf}$	in	4	4	4	4
Bottom Flange Width	$w_{bf}$	in	10.0	12.0	13.4	14.7
Angle (web-to-horizontal)	$\gamma$	deg	76	76	76	76
Steel Depth	$h_s$	in	19.8	27.4	31.6	35.6
<b>Total Steel Area:</b>	<b><math>A_s</math></b>	<b>in<sup>2</sup></b>	<b>68.8</b>	<b>102.5</b>	<b>125.1</b>	<b>148.2</b>
Parameter	Symbol	Units	Span			
			80'	90'	100'	
Deck width (Spacing)	$b$	in	96	96	96	
Plate thickness	$t_s$	in	0.327	0.344	0.361	
Compression Flange Width	$w_{cf}$	in	4	4	4	
Bottom Flange Width	$w_{bf}$	in	15.9	17.1	18.5	
Angle (web-to-horizontal)	$\gamma$	deg	76	76	76	
Steel Depth	$h_s$	in	39.3	42.8	46.1	
<b>Total Steel Area:</b>	<b><math>A_s</math></b>	<b>in<sup>2</sup></b>	<b>171.8</b>	<b>195.4</b>	<b>219.4</b>	

### 3.4.5 Discussion

The following trends were observed in the data:

- The optimization algorithm seems to always choose the largest available deck width.
- Steeper web angles improve the optimal moment capacity.
- The section geometry generally causes the plastic neutral axis to be located in the slab, eliminating compression forces in the steel.
- Acceptable geometries were found for spans ranging between 40'-100', but spans greater than 100' have not been investigated.
- Spans ranging from 20' to 50' had identical results, implying that the lower bounds on some of the independent variables may have been set too high.

It should also be noted that steel is not available in arbitrary thicknesses or widths. Thus, the results found here would have to be increased to the next available standard size, which could impact the cost of the system. As increasing the steel thickness always results in an increase in moment capacity, the section will not become inadequate when the steel thickness is increased.

## 4. CONCEPT EVALUATION

### 4.1 Flexural Performance of Con-Struct Bridge System

Due to MSU's involvement with this MDOT project, the PI was approached by Nelson Engineering Services to evaluate the flexural capacity of two scale units of their Con-Struct system, which is the concept that motivated the present investigation. This testing project, while separate from the MDOT research has given the team an excellent opportunity to evaluate the prefabricated steel box systems under consideration. With the permission of Nelson Engineering Services (hereafter referred to as NES), an overview of the testing conducted and the evaluation of the results and concept follow.

Two three-point bending tests were conducted on small-scale prototypes of the Con-Struct bridge girder system with cast-in-place and precast decks. The test units were designed by NES and also built under their direction. The test beams were small-scale replicas of the full-scale sections of the Con-Struct system used by NES in field applications. A typical cross section of the low-profile steel-concrete composite box girder section is shown in Figure 14. The steel plate used for the test unit was a lightweight 7-gage steel sheeting unit with geometry as shown in Figure 15 [5]. The test units were manufactured so that they had an effective span of 12 ft with the beam ends encased on a concrete block for support purposes. The overall geometry of the cast-in-place and precast deck test units are shown in the in Figure 16 and Figure 17, respectively. These drawings and the specifications outlined in them were provided by NES for manufacturing purposes.

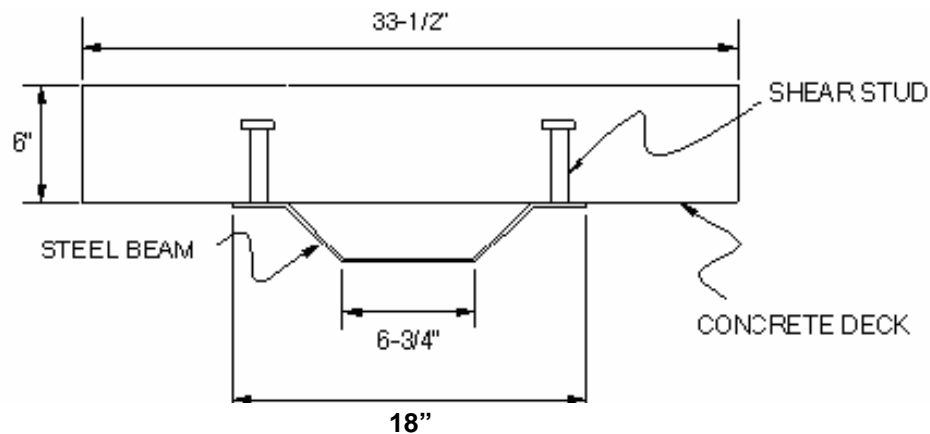
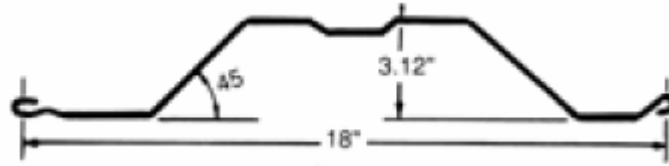
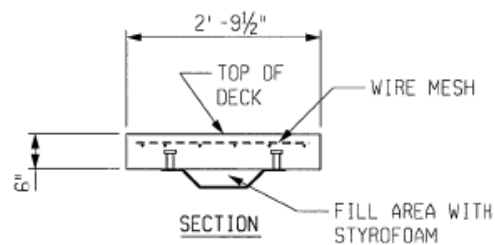
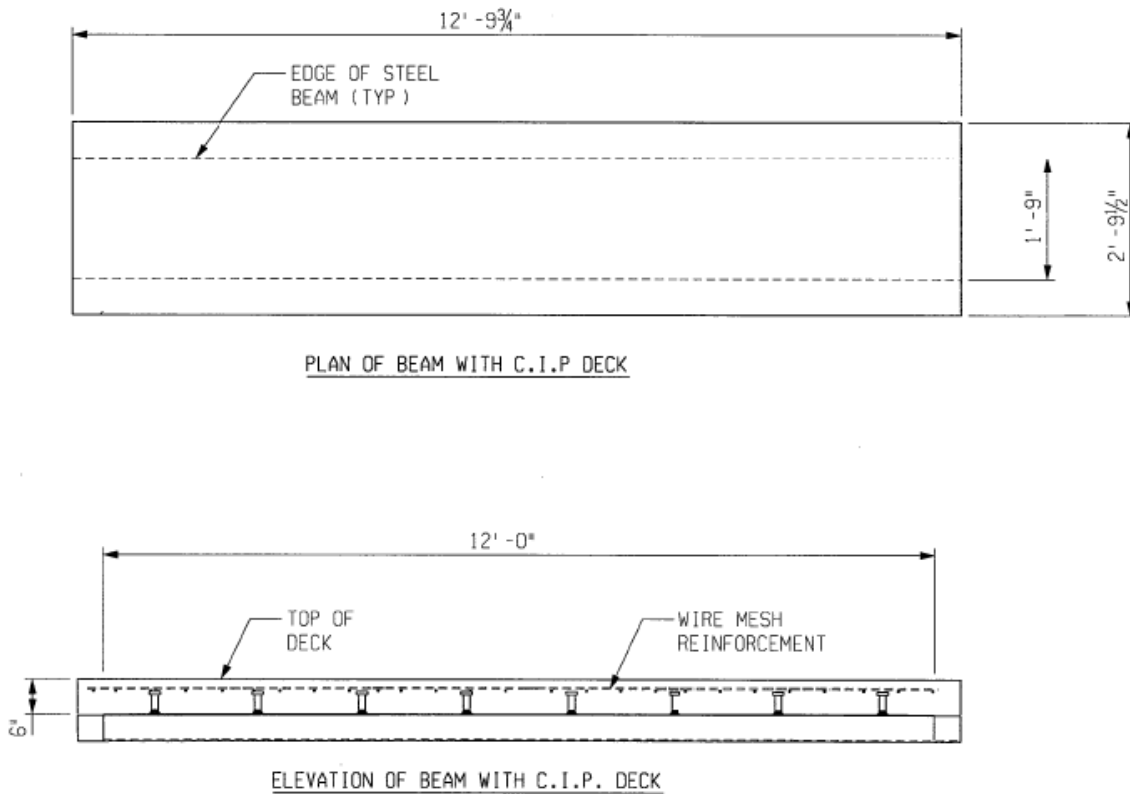


Figure 20. Typical Cross-Section of Con-Struct Test Units



**Figure 21. Geometry of Shoreline Steel Lightweight Sheeting [5]**



**Figure 22. Test Unit with Cast-in-Place Concrete Deck**

The flexural behavior of the Con-Struct beams was assessed through three-point bending tests. The beams were simply supported on end-blocks so that the effective span was 12 feet. Laminated elastomeric pads were used between the test unit and support blocks. Overall views of the test setup are shown in Figure 18.

The flexural tests showed that the overall behavior of the low profile composite box girder system is reliable and that it can effectively exceed the nominal flexural capacity determined according to current AASHTO specifications (see Figure 19). Overall, the performance of both the cast-in-place and precast composite girders was essentially equal. In both cases, their ultimate capacity was limited by detailing of the deck system to effectively carry the longitudinal shear demands.

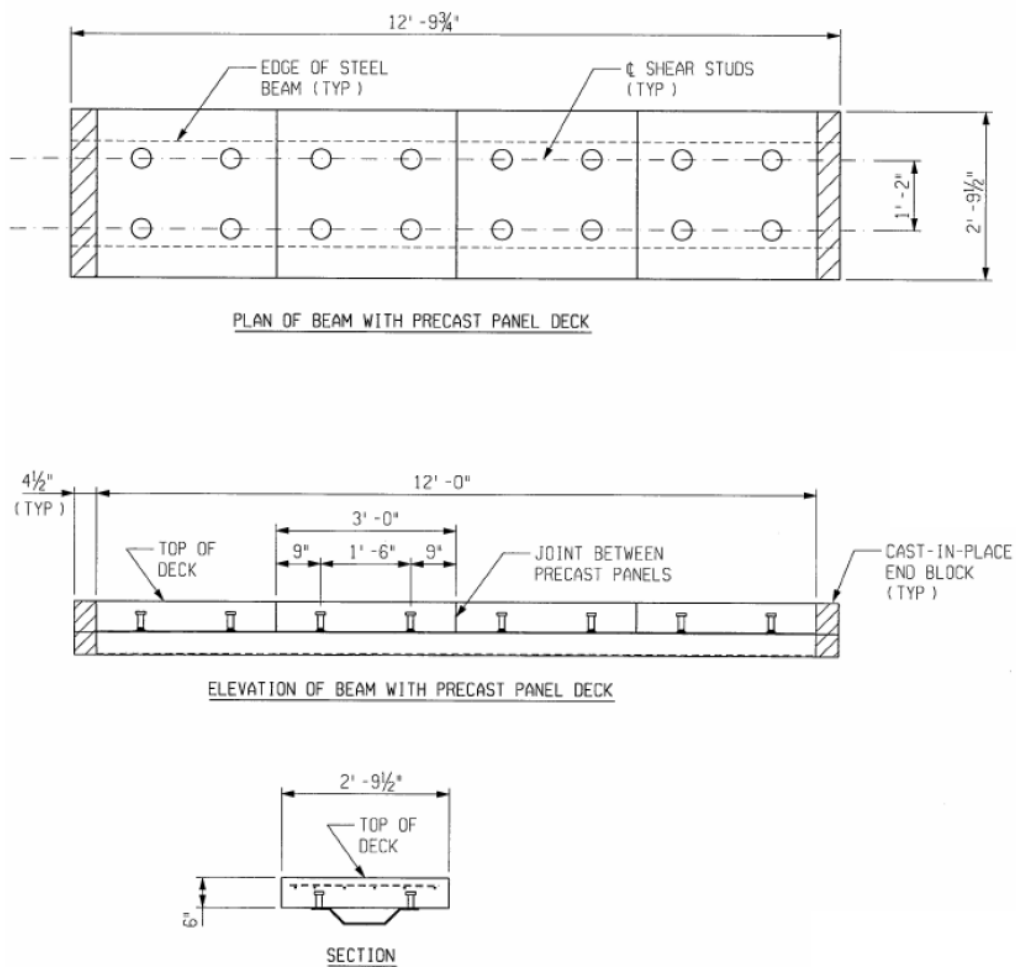


**Figure 23. Test Unit with Precast Concrete Deck System**



a) Overview



b) Underside View

**Figure 24. General Test Setup Views – C.I.P. Test Unit**

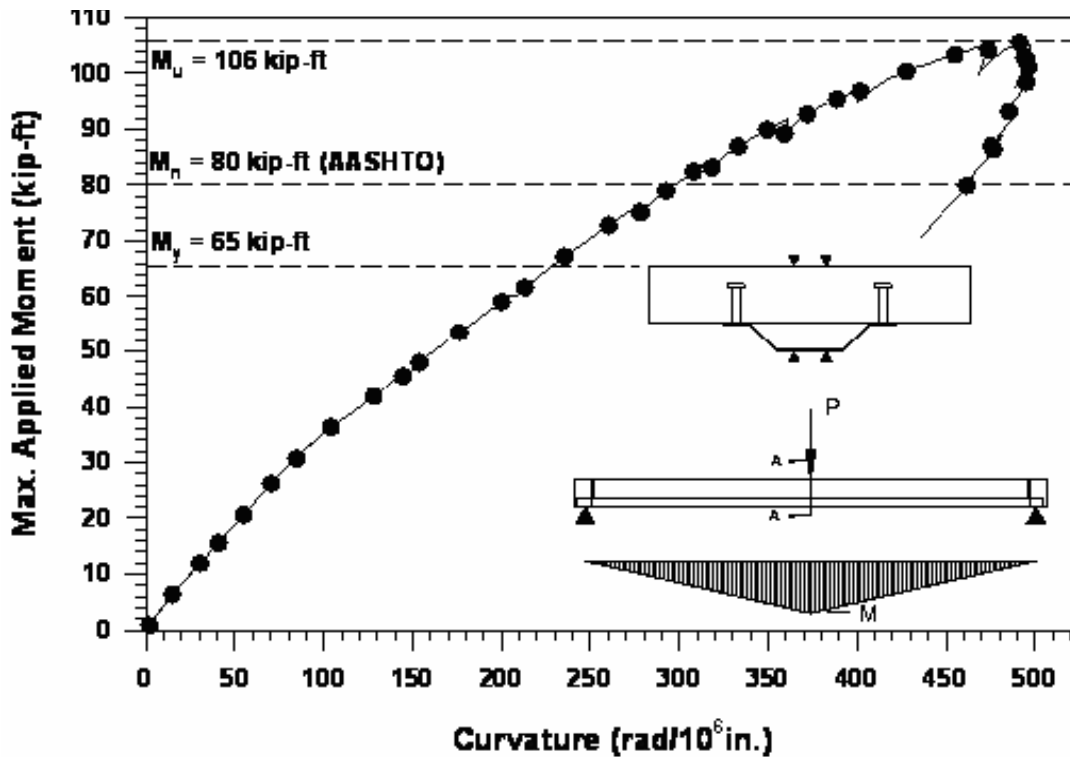


Figure 25. Moment vs. Curvature Response of C.I.P. Test Unit at Mid-Span

For the cast-in-place unit the force transfer at the shear connectors introduced longitudinal shear demands in the concrete deck that exceeded the shear strength of the concrete element. In the case of the precast unit, the lack of longitudinal shear keys to transfer shear forces across the joints of the precast panels composite the deck led to the deterioration of the beam load carrying mechanism. In both cases, the failure modes are clearly undesired, but they are not believed to compromise the overall efficiency of the concept as these problems can be easily addressed. Improved performance of the cast-in-place deck can be achieved by better assessment of the forces imposed by the shear connectors and by providing appropriate deck reinforcement to arrest the development of longitudinal shear cracks. Improvements in the precast system can be easily achieved by providing well detailed longitudinal shear keys to the precast panels. Integration of both of these detailing aspects will without a doubt improve the performance of the Con-Struct system at ultimate conditions. Clearly, this also applies to the generic prefabricated steel box girder systems being investigated under this MDOT research project.

In addition to the use of a shallow cold-bent steel profile for the composite beam, the Con-Struct concept introduces prestressing to the steel beam during construction by pre-cambering it. This is done to increase the yield moment capacity and offset dead load deformations. The efficiency gained from prestressing the steel plate during the construction operation is a unique feature of the Con-Struct system and one that should be considered for the general goals of the MDOT research project. It should be recognized, however, that the prestressing effect is really beneficial only up to the onset of yield in the critical section response for the system. Thus, benefits are to be gained while satisfying serviceability stress limits. However, gains in ultimate strength are minor since at full plastification of the steel section ultimate section capacity is more heavily controlled by the effective lever arm between tensile and compression forces and the location of the plastic neutral axis. In addition, consideration should be given to the “longevity” of the prestressing benefits since creep effects in the concrete slab and stress relaxation of the prestressed steel plate will most likely reduce the initial stress conditions.

The experimental study also permitted evaluating the applicability of code guidelines to assess the capacity of composite sections and that the shallow composite girder system can be well predicted by conventional theory of steel-concrete composite structures.

#### **4.2 Concept Evaluation and Selection**

Based on the literature review collected from Task 1, this task has as a goal to preliminarily evaluate prefabricated steel box composite systems to explore their advantages, disadvantages, possible improvements, and the development of new similar concepts. While the systems, components, and connection details identified thus far have been informally evaluated, a complete compilation of the aforementioned evaluation is in progress and will be presented in the next progress report.

Another goal of this task was to perform a preliminary study that would permit identifying three to five concepts with high potential that would become the focus of this research project. All concepts are to be evaluated under a common set of structural, construction, and durability requirements; and a ranking method would be used to assess their potential.

As discussed in the introduction section, final recommendations to the system under investigation will be the outcome of the research project. Thus, no specific designs are available at this stage. However, the general concept and its components have been clearly identified in Section 1 (Introduction) and are repeated in Figure 20 above.

With reference to Figure 20 and based on what has been learned thus far from the literature review presented in Chapter 2, a list of design alternatives based on permutations of different features can be generated. The variable parameters will be the type of steel plate, the type of concrete deck, and the type of transverse deck joint. The different options for each of these variables are listed next.

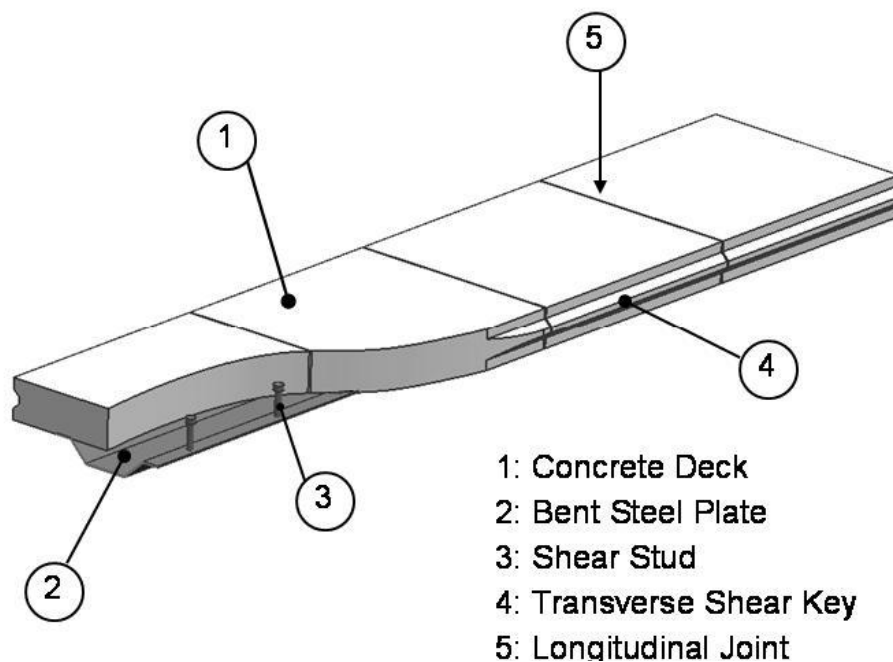


**Figure 20. Composite steel box girder concept**

**A) Steel Plate.** From the literature review, the research team believes that the inverted steel box solution will not be as effective as its developers envision. Thus, only the use of a “right-side-up” steel box will be considered. Four types of steel tub-plates will be considered based on their method of construction and implementation:

- 1) Pressed-formed or cold-bent – unstressed
- 2) Shop-welded – unstressed
- 3) Pressed-formed or cold-bent – prestressed
- 4) Shop-welded – prestressed

**B) Concrete Deck.** The literature review has shown advantages and disadvantages for different types of concrete decks and different solutions have been adopted for the prefabricated steel box systems proposed thus far. Thus, the following *prefabricated* deck options, based on their construction method, will be considered as options:

- 1) Cast-in-place at shop/yard
- 2) Modular Precast made continuous with passive wet longitudinal joints at shop/yard
- 3) Modular Precast made continuous with passive wet longitudinal joints at shop/yard and prestressed at shop/yard before making composite with steel girder.
- 4) Hybrid – precast stay-in-place form with exposed reinforcement for a cast-in-place topping and closure pour at job site.

**C) Transverse Deck Connection.** As shown by the literature review, this detail is the one that presents the most options. Based on the design alternatives presented in Section 2, the following are considered viable options for the system under consideration (see Section 2.6):

- 1) Grouted female-to-female shear keys
- 2) Grouted tongue-and-groove shear keys
- 3) Reinforced (confined or unconfined) shear keys blocks
- 4) Reinforced (confined or unconfined) female-to-female shear keys
- 5) Post-tensioned grouted female-to-female shear keys
- 6) Post-tensioned grouted tongue-and-groove shear keys
- 7) Welded plate grouted shear key blocks
- 8) Reinforced grouted moment key blocks
- 9) Post-tensioned grouted female-to-female moment keys
- 10) Post-tensioned grouted tongue-and-groove moment keys

In order to evaluate the potential design concepts that could develop from the permutation of the different design options, a common set of performance criteria was preliminarily used. The criteria is aimed at *qualitatively* ranking the *perceived* by the research team on the performance of the *individual* design options listed above, i.e., steel plate, deck, and transverse deck connections. In addition, each of the criteria was assigned a weighting factor of “importance” on a scale of 1 to 3 with 1 being low, 2 being medium and 3 being high. The criteria and their weight factors are given in Table 5.

Each of the design options was given a score for each of the criteria on a scale of 1 to 5, where 1 represented the lowest mark and 5 the highest. The tabulated results for each of the system components are presented in Table 6. The last column in this table shows the total “score” of the bridge component upon factoring the score in each category by the importance factors in Table 5. The highest scores for each of the design components are shown in bold font. It should be noted that the researchers are aware that the criteria and the associated importance factors are based on best judgment and thus the ultimate choice will be dictated by the DOT such that it best fits its current practice.

**Table 5. Design Parameter Selection Criteria and Importance Factor**

<b>Criteria ID</b>	<b>Description</b>	<b>Importance Factor</b>
<b>A</b>	Cost efficiency	3
<b>B</b>	Structural efficiency	2
<b>C</b>	Design versatility	1
<b>D</b>	Design/analysis ease	1
<b>E</b>	Construction ease	3
<b>F</b>	Fatigue performance	3
<b>G</b>	Durability & corrosion resistance	3
<b>H</b>	Replacement/removal ease	2

\* Importance Factor: 1 = Low; 2 = Medium; 3 = High

**Table 6. Scoring and Ranking of Design Options**

Design Option		Criteria*						Score	
<b>Plate</b>									
	<b>A</b>	<b>B</b>	<b>C</b>	<b>D</b>	<b>E</b>	<b>F</b>	<b>G</b>	<b>H</b>	
1	5	3	2	5	5	5			58
2	3	4	4	4	2	2			37
3	5	3.5	2.5	5	4.5	5			<b>58</b>
4	3	4.5	4.5	4	2	2			<b>38.5</b>
<b>Deck</b>									
	<b>A</b>	<b>B</b>	<b>C</b>	<b>D</b>	<b>E</b>	<b>F</b>	<b>G</b>	<b>H</b>	
1	5	4	4	5	4		3	3	<b>59</b>
2	4	4	3	4	5		3.5	3	<b>58.5</b>
3	3	5	4	3	4		4	2	54
4	3	4	3	2	3		3	3	46
<b>Deck Connection</b>									
	<b>A</b>	<b>B</b>	<b>C</b>	<b>D</b>	<b>E</b>	<b>F</b>	<b>G</b>	<b>H</b>	
1	5	2	2	5	5	5	5	5	<b>81</b>
2	5	2	2	5	4.5	5	5	5	79.5
3	4	3	3	4	4	4	3	4	66
4	4	3	3	4	4	4	3	4	<b>66</b>
5	3	4	4	3	3	5	4	3	<b>66</b>
6	3	4	4	3	2.5	5	4	3	64.5
7	3.5	3	3.5	3	4	2	3	4	58
8	3	3	3.5	4	4.5	4	3	4	<b>65</b>
9	2.5	4.5	4.5	2	3	5	4	3	65
10	2.5	4.5	4.5	2	2.5	5	4	3	63.5

\* Evaluation: 1 = Low to 5 = High

## 5. ANALYTICAL EVALUATION

### 5.1 General

The objective of the analytical evaluation is to develop a suite of hierarchical finite element models to investigate issues related to structural performance, with particular attention to connection detailing and design. The different levels of model refinement will support each other to investigate system performance. The conducted analyses were:

**A) Stress Analysis of Bridge Component and System.** 3D finite element analyses of component and system to evaluate detailed performance of the prefabricate element.

**B) Global Parametric Analysis.** 3D finite element analyses of bridge systems to perform system parametric studies.

**C) Stress Analysis and Characterization of Connection Details.** 3D finite element analyses of connection details.

### 5.2. Stress Analysis of Bridge Components and System

The original goal of the research was to use 3D skeletal-type (frame element) models to perform system parametric studies to evaluate the need for any intermediate diaphragms and the load transfer demand and performance of deck connections. The use of full 3D finite element models was not considered appropriate for the parametric studies due to their computational expense and effort to develop. Thus, grillage models were initially selected for these studies. Despite this, the research team chose to create both models and evaluate their performance to decide which method to use. This section presents the development of both model types and a comparison of their performance.

For an initial check of compatibility between the grillage and 3-D FE models, simple plate models were created and moment responses were compared. To begin this comparison, two sets of models were created. One set of models were square plates, while the other set modeled rectangular plates with sides in a 2:1 ratio. Two loading conditions were considered. The first was a distributed load over the entire plate, while the second was a point load at the center of the plate. The bending moment distribution of each model was then compared in three different

ways: at mid-span under both distributed and concentrated loads, and its transverse distribution under the concentrated load. The results of this comparison indicated a sufficient agreement between the two methods to move to a more sophisticated comparison. A graphical representation of the results can be seen in Appendix II. It should be noted that the loads and dimensions were arbitrarily and that the results were normalized for clearer presentation. After this simple verification, the two modeling approaches were then applied to actual bridge models under consideration and compared.

### **5.2.1 Model Bridge Geometry**

The bridge chosen to model was a two-lane bridge with a 50-foot span. It consisted of five girder/deck units, as shown in Figure 26. The geometry of the girder/deck units was developed by making use of the Excel optimization spreadsheet detailed in Section 3.4. However, the purpose of this exercise was not to find an optimum design, but rather to compare the two analysis models (i.e., grillage vs. 3D FE). The geometry of the girder/deck units used in the comparison is shown in Figure 27.

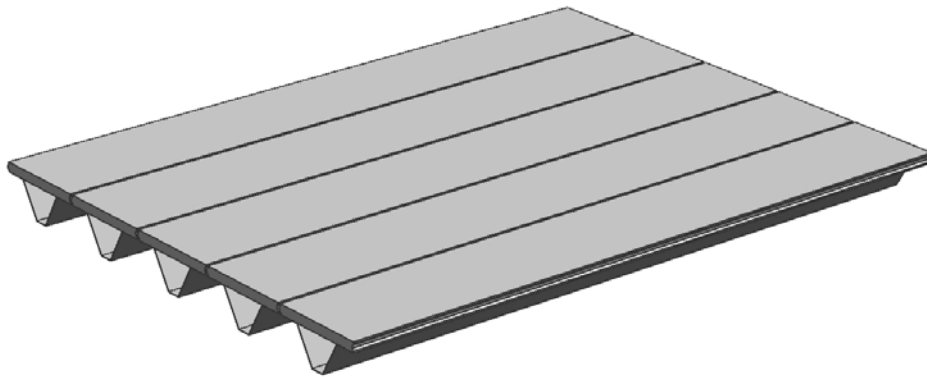


**Figure 26. Bridge being modeled for analysis approach comparison**

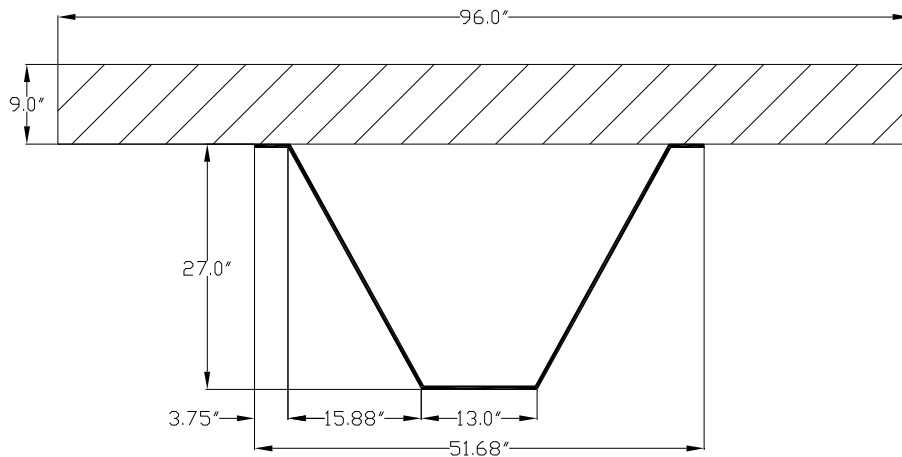


**Figure 27. Dimensions of model girder/slab unit**

### 5.2.2 Model Bridge Loading

Loading for the bridge models was according to the AASHTO LRFD Bridge Design Specifications [AASHTO, 1998]. Dead load and vehicular live load were considered. Dead load consisted of self-weight and barrier weight. The cross section of the barrier was that of a New Jersey Concrete Barrier as specified by the Federal Highway Administration (FHWA) [FHWA, 2006]. The vehicular live load consisted of the design lane load and the design truck load with an axle spacing of 14-ft. Three different AASHTO limit states were evaluated, namely, live-load deflection, Service-II, and Strength-I. A summary of the limit states and associated loads and load factors is given in Table 7.

**Table 7. Summary of limit states considered to evaluate bridge models**

Load Case	Loads and Load Factors			
	Dead Load	Load Factor	Live Load	Load Factor
Strength-I	No	n/a	Yes	1.00
Service-II	Yes	1.00	Yes	1.30
Deflection	Yes	1.25	Yes	1.75

### 5.2.3 Grillage Model

A grillage model is a means of representing a structure with a series of beam elements that have been given properties appropriate for representing the stiffness, torsion and unit weight properties of the structure being modeled. Grillage models reduce the number of required elements and degrees of freedom, thereby reducing the number equations that need to be solved to evaluate system response. Grillage models can be 2D or 3D. For this project, a two-dimensional grillage model was created and analyzed, as detailed in this section.

#### 5.2.3.1 Derivation of Grillage Member Properties

The grillage model followed the recommendations presented in Hambly (1991) and Barker and Puckett (1997). To capture the behavior of the bridge, several sections were chosen for grillage members to represent the bridge as shown in Figure 28.

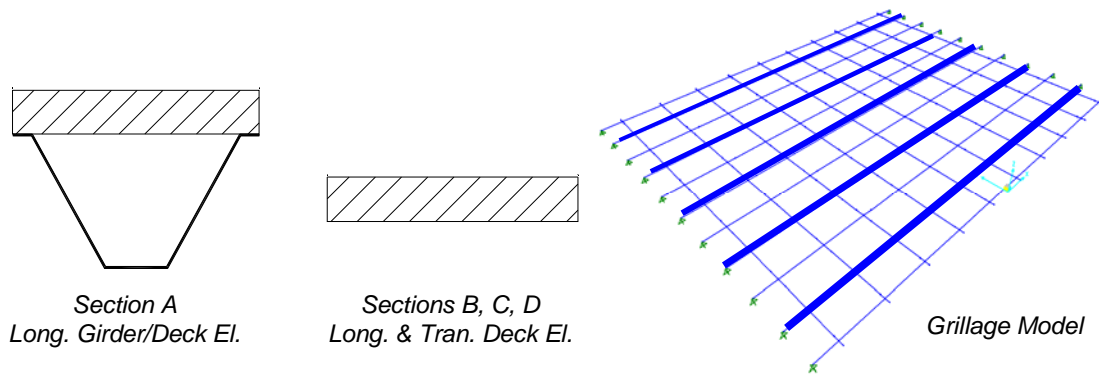


**Figure 28. Schematic of grillage element cross-sections and grillage model**

The longitudinal section representing the girder/deck units (see Figure 28) was termed section A. The section moment of inertia,  $I$ , was calculated for a section transformed to steel properties. The torsion constant,  $J$ , was also calculated for a transformed section, but instead of changing the width, the height was modified. Then, the torsion constant for a thin walled hollow section was determined with equation (5-1) (Hambly, 1991):

$$J_t = \frac{4A^2}{\oint \frac{ds}{t}} \quad (5-1)$$

where  $A$  is the area enclosed by the center line of the walls,  $ds$  is the length of each individual wall and  $t$  is the wall thickness. This value is known as the pure torsion constant, or  $J$ . However, due to local deformations of the open box section, the pure torsion constant is not valid. Thus, an equivalent torsion constant that accounts for distortion,  $J_d$ , must also be found (Hambly, 1991). The process to obtain  $J_d$  follows.

The flexural rigidity of the individual sides of the box (see Figure 29) is obtained by applying equation (5-2) (Hambly, 1991):

$$D_a = \frac{E_a t_a^3}{12(1-\nu_a^2)} \quad (5-2)$$

where  $D$  is the flexural rigidity,  $E_a$  is the elastic modulus,  $t_a$  is the wall thickness and  $\nu_a$  is Poisson's ratio; and the subscript  $a$  refers to side  $a$  (see Figure 29).

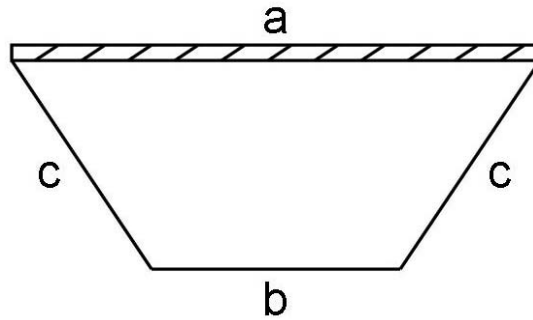


**Figure 29. Nomenclature of box sides**

After calculating the flexural rigidity of each side with equation (5-2) above, the out-of-plane shear in the bottom flange per unit torsional load,  $v$ , is given by equation (5-3) [Hambly, 1991]

$$v = \frac{\frac{1}{D_c}[(2a+b)abc] + \frac{1}{D_a}[ba^3]}{(a+b) \left[ \frac{a^3}{D_a} + \frac{2c}{D_c}(a^2+ab+b^2) + \frac{b^3}{D_b} \right]} \quad (5-3)$$

where  $D_a$ ,  $D_b$  and  $D_c$  and  $a$ ,  $b$  and  $c$  are the flexural rigidities and the lengths of the walls in Figure 29, respectively.

Once  $v$  is calculated, the vertical deflection of one web per unit torsional load,  $\delta_1$ , is given by equation (5-4) below

$$\delta_1 = \frac{ab}{24(a+b)} \left\{ \frac{c}{D_c} \left[ \frac{2ab}{a+b} - v(2a+b) \right] + \frac{a^2}{D_a} \left[ \frac{b}{a+b} - v \right] \right\}. \quad (5-4)$$

Next, a parameter,  $\beta$ , used in the analysis of beams-on-elastic-foundations (BEF), the theory from which the previous equations were derived, is calculated as shown in equation (5-5) [Hambly, 1991]

$$\beta = \left\{ \frac{1}{EI_c \delta_1} \right\}^{0.25} \quad (5-5)$$

where  $I_c$  is the moment of inertia of the box girder cross-section.

Next a dimensionless distortion-induced deflection term,  $w$ , is obtained from a chart presented in Hambly (1991) and reproduced in Figure 30. For this example  $w$  was found to be equal to 1.0.

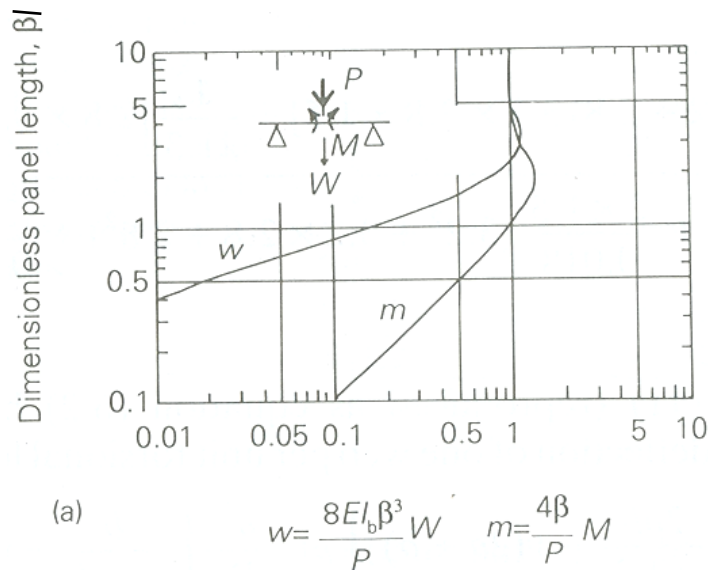


**Figure 30. Chart for distortion deflection parameter  $w$  for simply supported beams and box without cross-bracing or diaphragms (Hambly, 1991)**

The final formula to find  $J_d$  is given in Equation (5-6) below:

$$J_d = \frac{a^2 I_c (\beta l)^3}{l^2 1.6w} \quad (5-6)$$

The values of  $J_t$  and  $J_d$  are then combined to give the value of  $J$  used for the grillage member,  $J_{dt}$ , as shown in equation (5-7) [Hambly, 1991]. For further information and references on this method, the reader is referred Chapter 6.5 of Hambly (1991):

$$\frac{1}{J_{dt}} = \frac{1}{J_d} + \frac{1}{J_t} \quad (5-7)$$

The final properties of the longitudinal girder/deck members are shown in Figure 31.

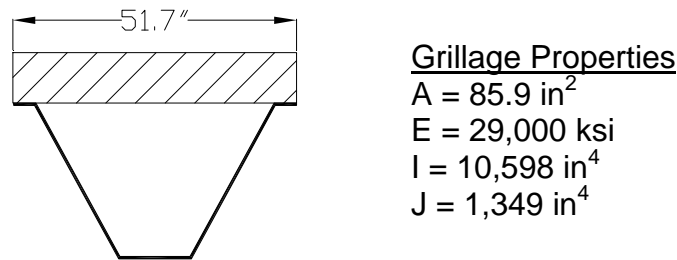


**Figure 31. Section A geometry and associated grillage properties**

Longitudinal deck elements of different widths were also included in the model to improve its accuracy. Sections B and C and their properties are given in Figure 32. The moment of inertia for these elements was found with equation (5-8) [Barker, 1997]

$$I = \frac{bh^3}{12} \quad (5-8)$$

The torsional constant was taken as twice the moment of inertia [Barker, 1997], or

$$J = \frac{bh^3}{6} \quad (5-9)$$

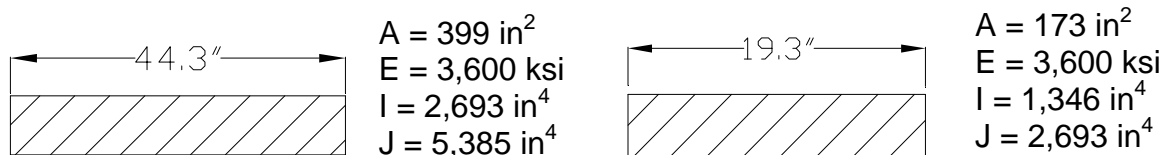


**Figure 32. Section B and C geometry and associated grillage properties**

Transverse grillage members pm;u represented the concrete deck. All transverse elements had the same cross section, which was labeled section D. Their properties were found in the same manner as for sections B and C, resulting in the values shown in Figure 33. Because the weight of the concrete deck was already included in the weight of the longitudinal members, the transverse deck elements were not assigned any self-weight. A summary of the properties for the grillage members is given in Table 8.

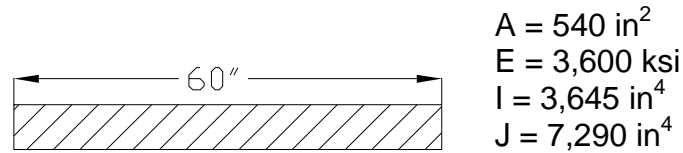


**Figure 33. Section D geometry and associated grillage properties**

**Table 8. Summary of grillage member properties**

Section Name	Description	Area (in <sup>2</sup> )	Elastic Modulus (ksi)	Moment of Inertia (in <sup>4</sup> )	Torsion Constant (in <sup>4</sup> )
A	Long. Box Section	85.9	29,000	10,598	1,349
B	Long. Deck Section	399	3,600	2,693	5,385
C	Long. Deck Edge Section	173	3,600	1,346	2,693
D	Transverse Deck Section	540	3,600	3,645	7,290

### 5.2.3.2 Application of Loads

Vehicular lane load was applied by defining a tributary area for each longitudinal member and applying a distributed load of appropriate magnitude along the length of the member. Applying the concentrated truck loads required determining equivalent loads and moments to be applied to the existing members due to the tire locations not corresponding with the location of the grillage members. This was accomplished by creating a separate model of two beams intersecting at the location of the tire load and fixed at their ends, which coincided with points on the grillage model mesh. The truck load was then applied at the intersection of the beams and the reaction forces (fixed- end forces) at the endpoints were obtained. These forces were then applied at their corresponding location on the actual model. This approach is schematically

shown in Figure 34. The grillage model was created and computed with the general finite element program SAP2000 (CSI, 2000). A figure of the completed grillage model, as well as its transverse moment response under the described loading, is shown in Figure 35. A discussion of the results and their comparison with those from a finite element continuum model is provided in Section 5.1.5.

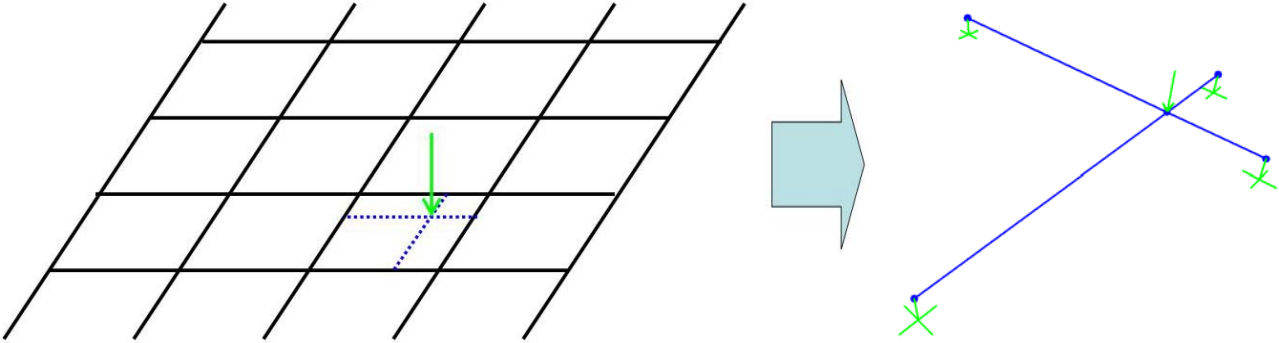


**Figure 34. Application of wheel loads to grillage model**

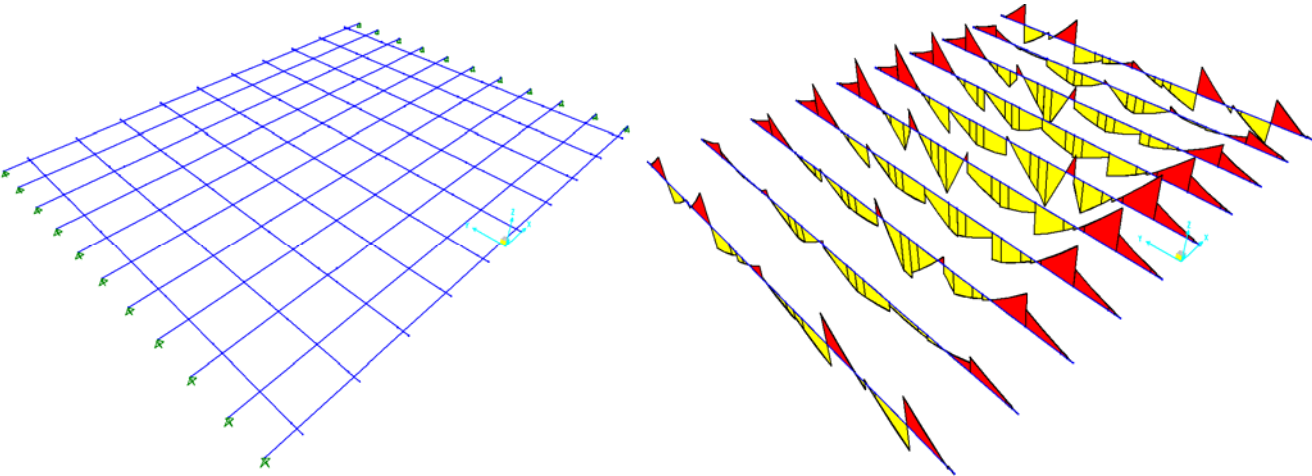


**Figure 35. Completed grillage model and system transverse moment response**

### 5.2.4 Three-Dimensional Finite Element Model

The 3-D finite element model was created completely (both deck and girder) of 4-noded shell elements (S4R, [Simulia, 2007]) – both deck and girder. This was done by positioning the deck elements at the neutral axis of the actual deck. The model geometry of the typical girder/deck unit is shown in Figure 36.

In these models the deck is modeled as one continuous slab. This assumes full moment transfer at the joints, which may not be representative of actual behavior, depending on the type of joints that are used. However, because the same is true of the grillage model, this was not a problem for comparing the two modeling approaches. Yet, it is recognized that future models will need to address this issue (See Section 5.3). Also, the model assumes full shear interaction, meaning there is no relative slip between the deck and the girders. The completed 3-D FEA model and von Mises stress contours on the underside of the bridge can be seen in Figure 37.

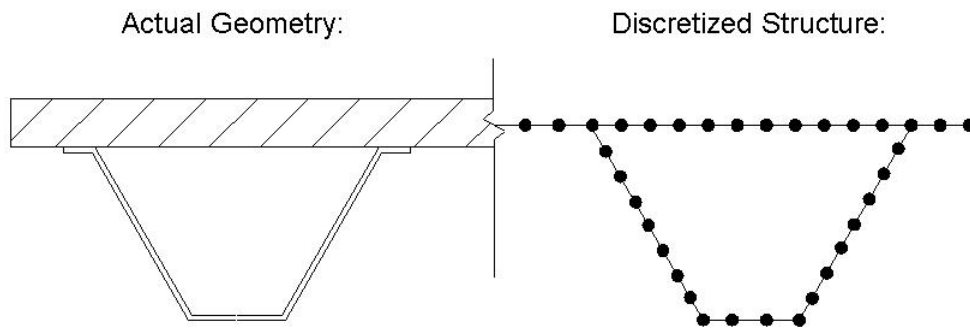


**Figure 36. Girder modification in 3-D FEA model**

### 5.2.5 Comparison of Models

The grillage and continuum models were first compared with only the design lane load applied. The response quantities chosen for comparison were the transverse moment forces along a line coincident with what would potentially be a longitudinal joint between girder units, as shown in Figure 38. The transverse moment demand for both strength and service conditions along line A-A (see Figure 38) is shown in Figure 39. It can be seen that the finite element response is smoother than the grillage output, which is to be expected due to the finer resolution of the nodes in comparison with grillage intersections. Nonetheless, both models are considered

to compare favorably. All other joint lines were also checked, and the result comparison was similar.

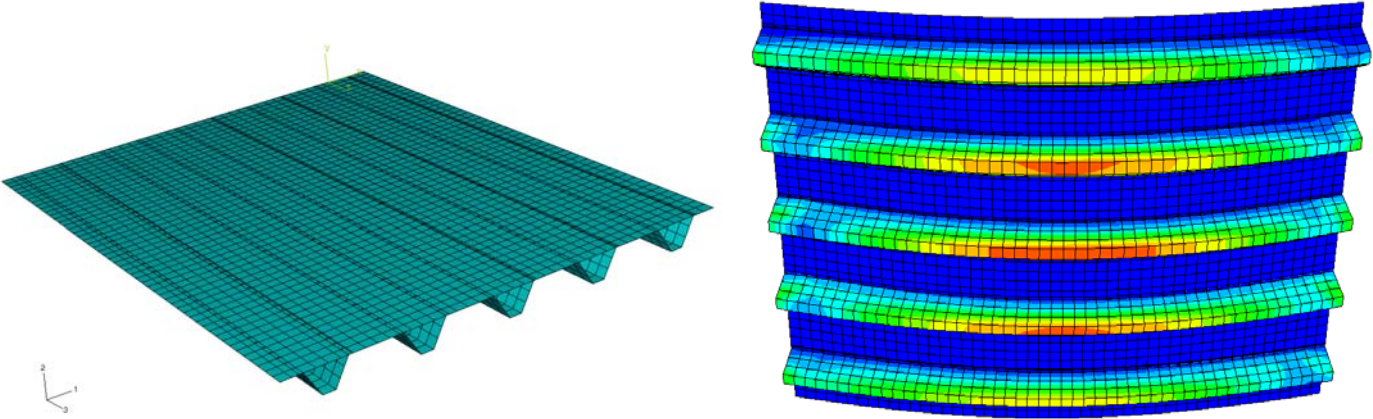


**Figure 37. Completed 3-D FEA model and von Mises stress contours**

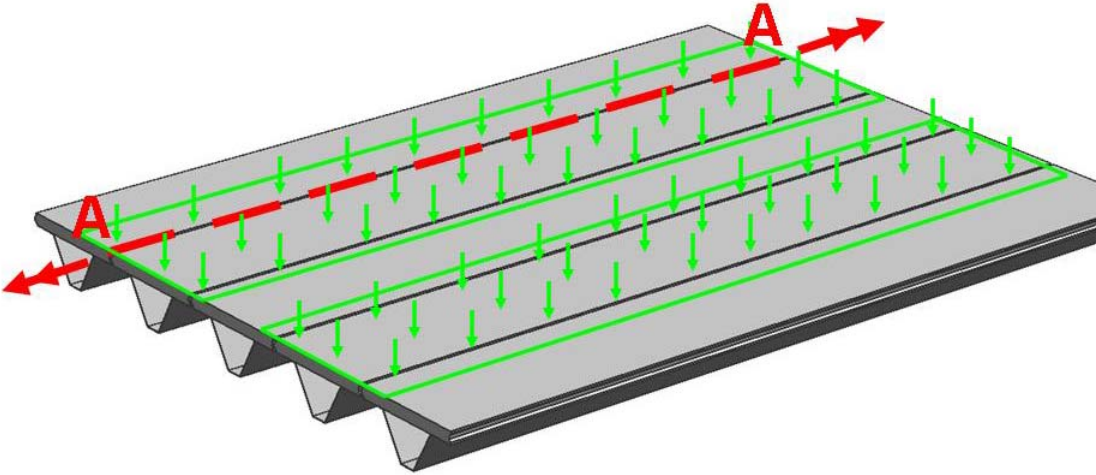


**Figure 38. Location of forces chosen for comparison**

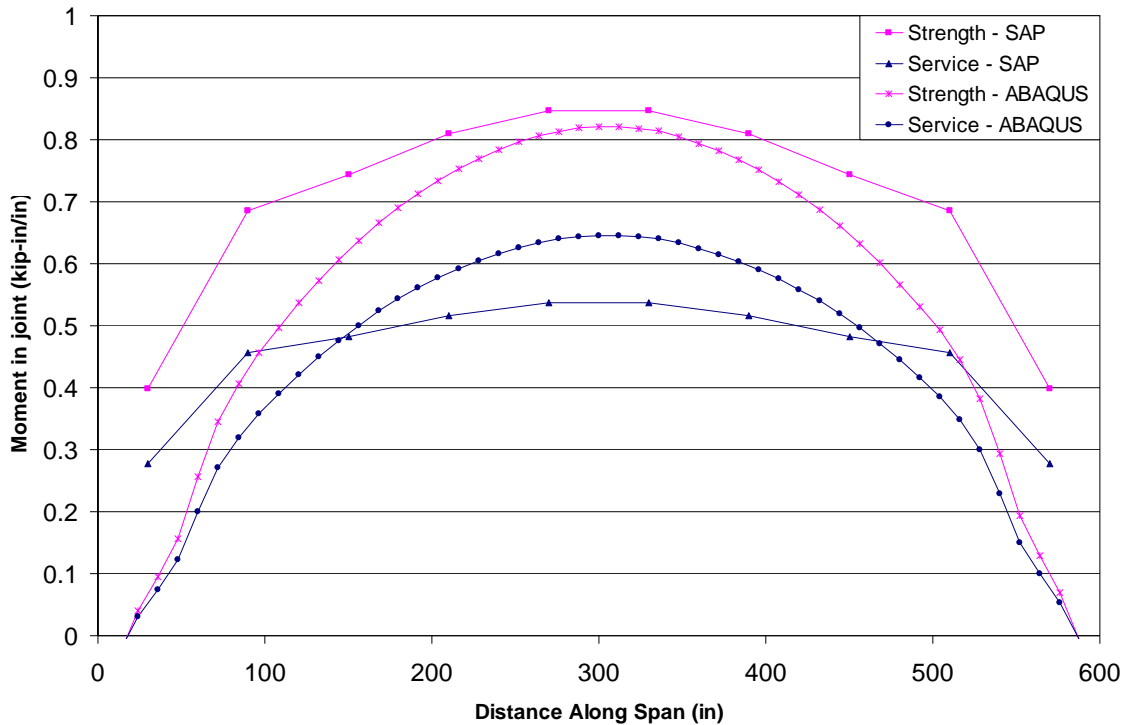


**Figure 39. Comparison of analysis tools on full scale bridge model (lane load only)**

After the initial verification had been established, both models were updated to incorporate the AASHTO design truck loading. The transverse moment distribution along joint line A-A (see Figure 38) for the full live loading from both models is shown in Figure 40. These results are again in close agreement, with the finite element model showing a greater resolution. Upon evaluating these results, the research team determined that both the grillage model and the 3-D FEA model gave coinciding results, and that either could provide accurate representation of the forces in the joints, as well as in the bridge system as a whole. It follows that either model could be used for parametric studies of the system. While the original research plan was to use the grillage model for parametric studies due to its low computational demand, running the 3-D FEA model only took 1-2 minutes longer than running the grillage model. Yet, as noted in the comparison of results, the FEA model provides better resolution. Additionally, the FEA models were easier to create due to the use of the program's (Simulia, 2007) graphical user interface. For these reasons, the research team decided to supersede the grillage model and use 3-D

continuum FEA models with shell elements not only for the detailed analyses, but for parametric studies as well.

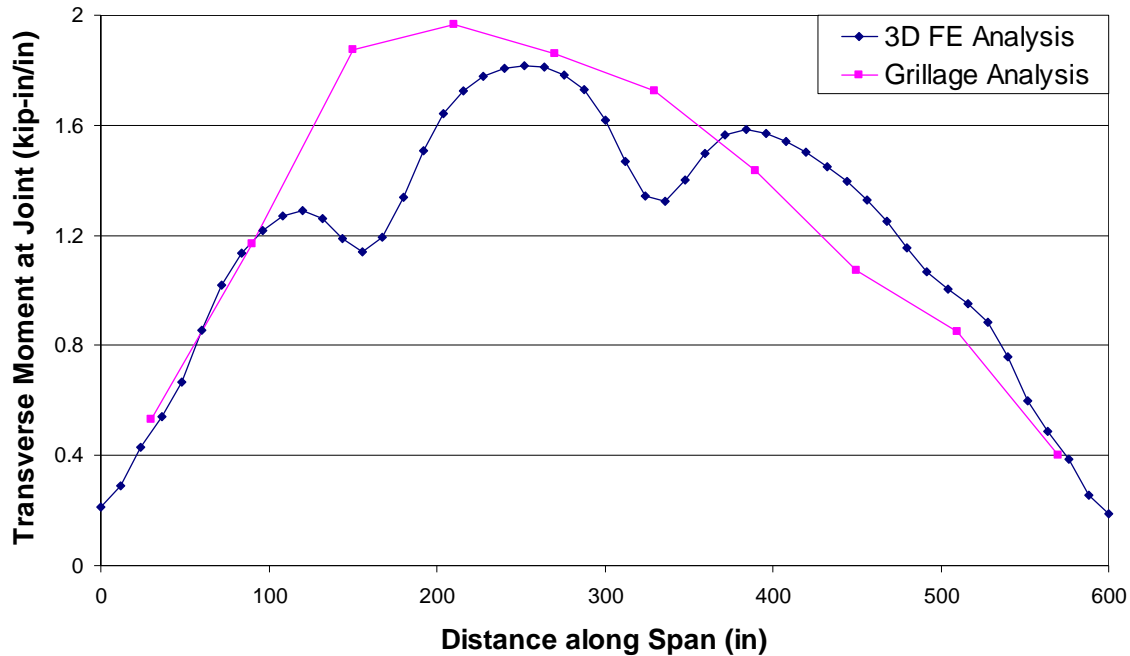


**Figure 40. Comparison of analysis tools (full AASHTO loading)**

### 5.2.6 Verification of Models Using Experimental Data

As detailed in Section 3.1, previous research performed by members of the research team provided experimental data that directly correlated to the system being studied (Burgueño and Pavlich, 2006). Hence, this data could be used to verify that the models of the box-girder system are producing results that match what happens in experimental situations.

General information on the Con-Struct test units and the conducted experiments was given in Section 3.1 and complete information can be found in Reference (Burgueño and Pavlich, 2006). A general view of stress contours on the developed 3D finite element model is shown in Figure 41. The model was created using the general purpose finite element program ABAQUS (Simulia, 2007). The steel tub-girder was modeled with four-node shell elements (S4R). The deck was also modeled with these elements, corresponding with the models to be used in the parametric study of Section 5.2. These elements incorporated reduced integration and hourglass deformation control. Longitudinal shear interaction between the deck and the steel girder has

been modeled as rigid, i.e., full shear interaction. This assumption is considered adequate to assess service performance of composite steel box bridge systems. Nonetheless, since failure in the tested Con-Struct beam units was controlled by the shear interaction, incorporation of partial shear interaction between the surfaces of the concrete deck and the top steel flanges through ABAQUS’s contact and surface interaction modeling options might be considered for future modeling efforts. As this type of failure was not directly applicable to the system being studied, it was ignored in this project.

It should be noted that the modeling efforts reported here were an attempt to gain confidence in our ability to accurately model the behavior of the bridge components by developing a good modeling strategy and validating the modeling assumptions against experimental data.

In the aforementioned project, a prototype of the ‘Con-Struct System,’ which was the concept that motivated the present study, was tested at MSU’s Civil Infrastructure Laboratory. The cross-section dimensions of the Con-Struct test girder are shown in Figure 42. The concrete deck was 33.5 inches wide and 6 inches deep. The bent steel plate has a thickness of 0.179 inches. The plate had compression flanges that were 2.5 inches wide and a tension flange that was 6.75 inches wide. The depth of the bent steel plate was 2.75 inches.

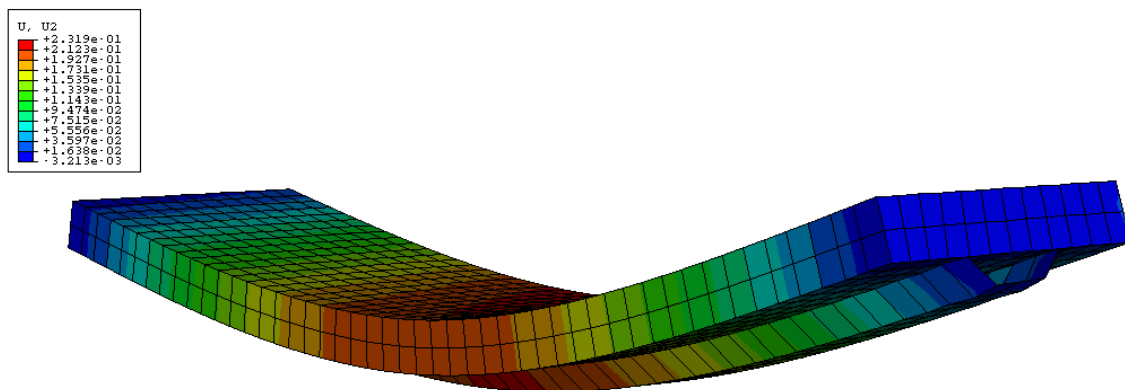


**Figure 41. Finite Element Model of Con-Struct System in Flexure. Contours Represent Vertical Displacement, in Inches.**

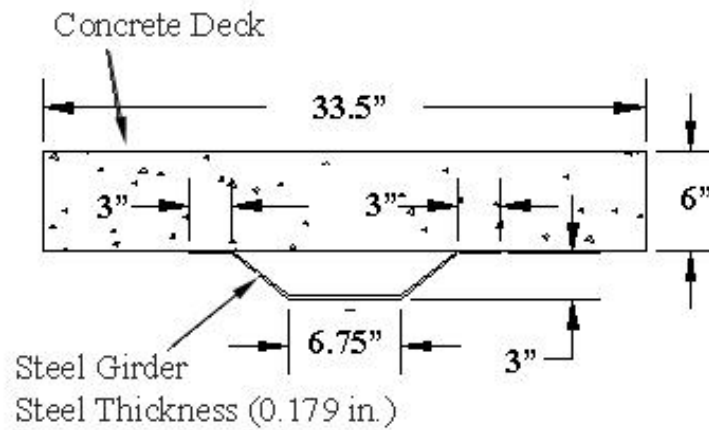


**Figure 42. Con-Struct Test Unit Girder Cross Section**

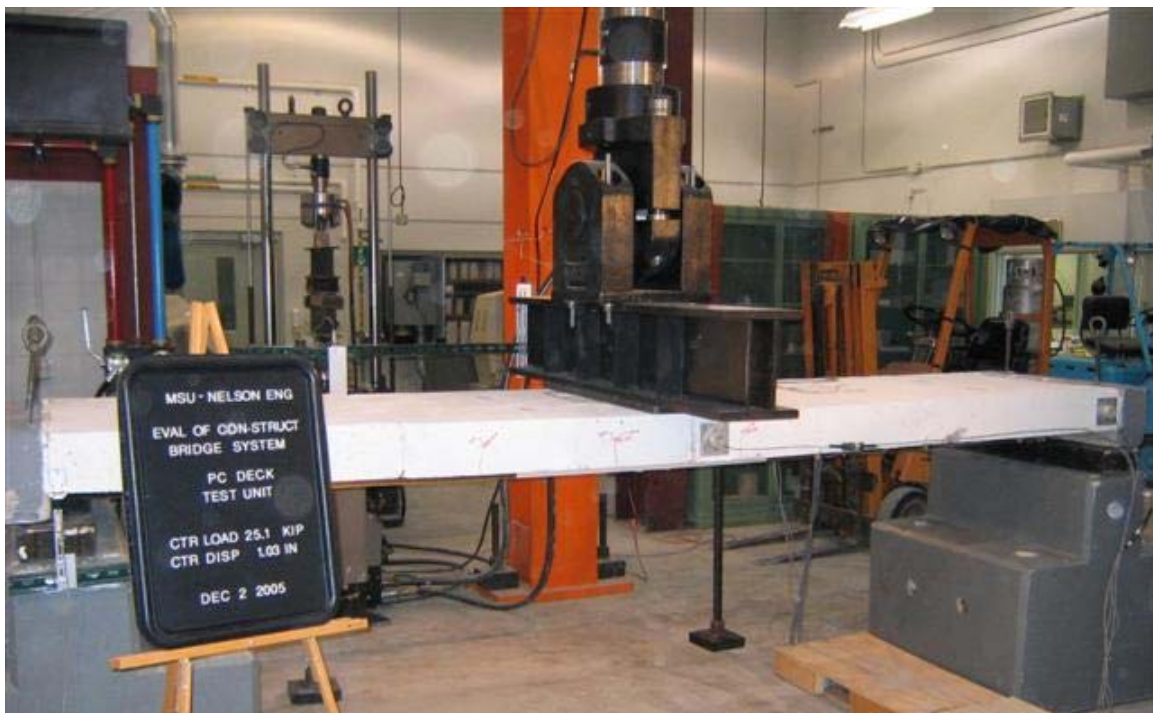


**Figure 43. Experimental Test Setup**

The test setup for the experimental testing program is shown in Figure 43. The test was a simple three point bending test on a girder with a length of 12 ft. Continuous displacement and applied load measurements were recorded during the test. The displacements were measured at

the girder mid-span by linear potentiometers. The applied load was measured with a load cell in the actuator.

The load displacement response from the girder with a cast-in-place deck is shown in Figure 44. From the graph it can be seen that the maximum applied load achieved during the test was approximately 35 kips. The maximum displacement of the 12 ft girder was approximately 2 inches. The response can be separated into two portions, an assumed linear portion, and a non-linear portion. The linear of the portion is assumed as it is not perfectly linear. This assumed linear portion of the response is from a load of 0 kips up to a load of 12.5 kips. The 12.5 kip point was chosen as the end of the linear portion because after this point the slope of the load displacement response in each of the successive load increments has a different, smaller slope. Between loads of 0 and 12.5 kips the slope remains approximately constant. It is this pseudo-linear portion of the response that was to be modeled using a full 3D finite element model.

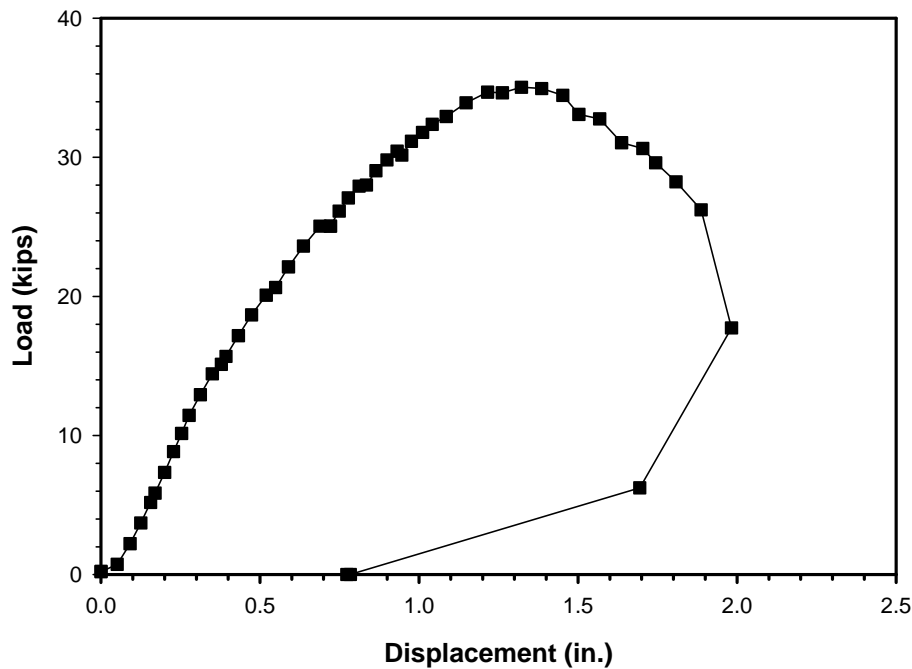


**Figure 44. Load Displacement Response**

The 3D FE model of the Con-Struct system was generated by creating two parts: one representing the deck, and one representing the steel girder. The steel tub girder was modeled with shell elements while the deck was modeled with solid elements. Details are given in Table 9. The dimensions of the modeled girder matched exactly with the dimensions of the actual girder (see Figure 42). The modulus of elasticity used for the concrete was 4576 ksi, which was the value obtained from material tests in the experimental evaluation project. Material properties for concrete and steel are given in

Table 10. The 3D model also utilized a no-slip constraint at the concrete-steel interface. The 3D model can be seen in Figure 45.

**Table 9. Elements Used in Con-Struct 3D FE Model**

<b>Part</b>	<b>Material</b>	<b>Shell Thickness (in)</b>	<b>Element Type</b>	<b>Hourglass Control</b>	<b>Reduced Integration</b>	<b>Element Size (in)</b>
Deck	Concrete	n/a	C3D8R	Active	Active	4.5
Tub	Steel	0.375	S4R	Active	Active	6

**Table 10. Material Properties used in 3D FE model**

<b>Material</b>	<b>Elastic Modulus (ksi)</b>	<b>Poisson's Ratio</b>	<b>Unit Weight (kips/in<sup>3</sup>)</b>
Concrete	4576	0.2	8.68 E-5
Steel	29000	0.3	2.83 E-4

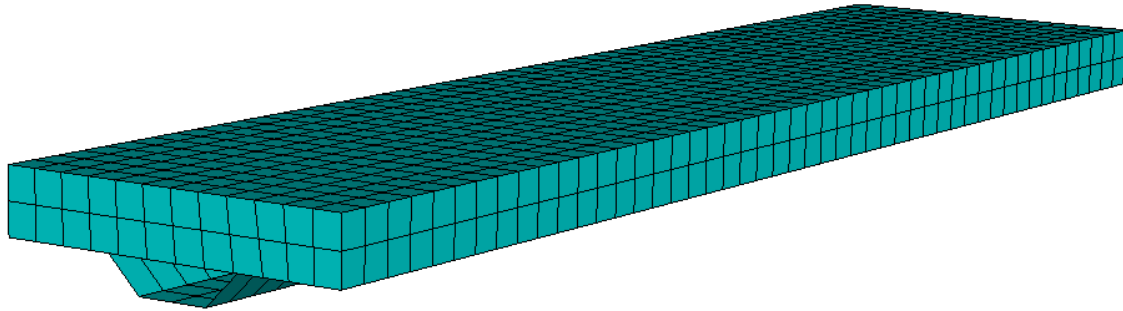


**Figure 45. Assembled 3D Model**

Comparative results of the experimental and analytical load displacement response are shown in Figure 46. This plot shows the assumed linear range of the experimental data only, to appropriately compare with eh linear elastic FE model. The experimental data has been shifted to correct for nonlinearities at the beginning of the loading due to the compressing of the elastomeric pads at the beam end supports. The shift was calibrated so that the two sets of data would be at the same value of displacement when the load was one kip. From the figure it is possible to see that the results from the FE model were stiffer than the experiment. The maximum displacement value of the FE model was 0.216 inches, while the experimental model had a maximum displacement of 0.256 inches. This difference can be attributed in part to the flexibility of the end supports (elastomeric pads) and slip at the girder/deck interface. Additionally, it is well known that the finite element models typically give results that are stiffer than reality.

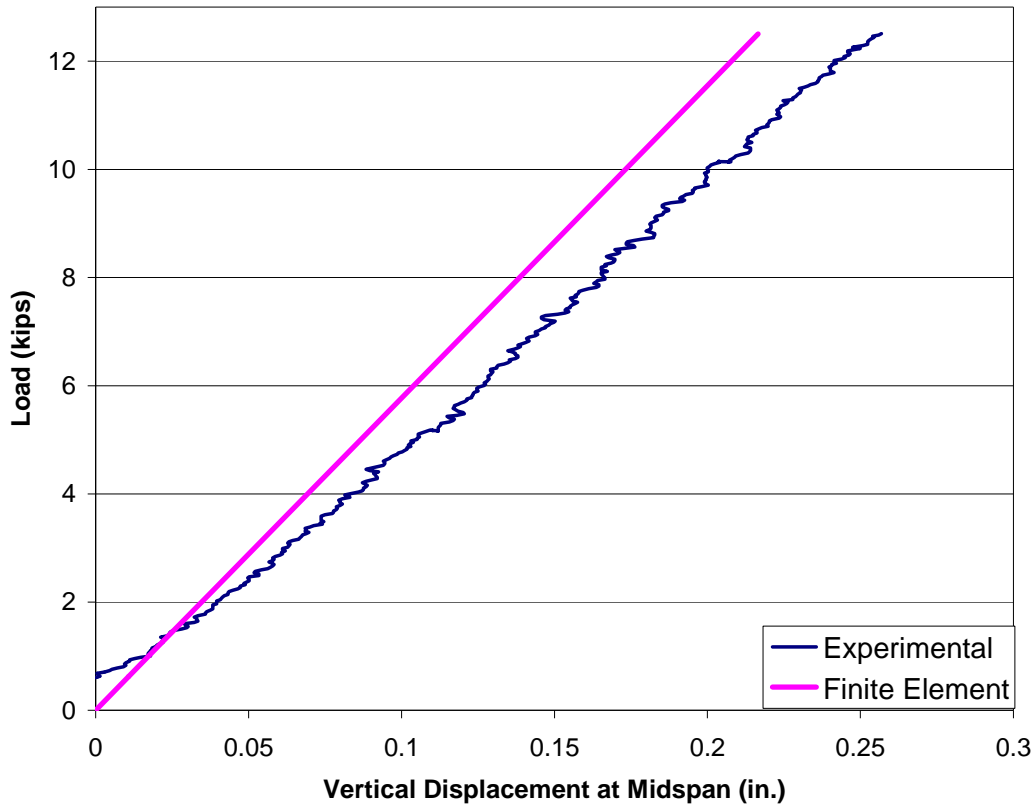


**Figure 46. Load Displacement Results**

### 5.3 Global Parametric Analysis

To evaluate the behavior of feasible bridge systems built with the prefabricated girder/deck units under consideration, a parametric study was performed. In the study, the parameters under evaluation were: (1) span length, (2) girder spacing, and (3) existence/location of intermediate diaphragms. The proposed case matrix for the parametric studies is given in Table 11. The bridge models were assumed to carry two design lanes of traffic, with one design truck in each (see Section 3.3). The limit states and material properties are given in Sections 3.4 and 3.2, respectively.

The parametric study was performed in order to investigate three separate responses: (1) transverse load distribution, (2) transverse moment demands along longitudinal joints, and (3) longitudinal moment demands along longitudinal joints. The response measures of interest are schematically shown in Figure 47.

**Table 11. Case Matrix for Global Parametric Analyses**

Case #	Span Length (ft)	Girder Spacing (ft)	Diaphragm
1	50	4	None
2	50	6	None
3	50	8	None
4	75	6	None
5	75	6	½ pt
6	75	8	½ pt
7	100	6	None
8	100	6	1/3 pts
9	100	8	None
10	100	8	1/3 pts
11	100	10	None
12	100	10	¼, ½ pts

A parameter of interest not included in the above cases is that of the type of longitudinal joint used in a given bridge. While joint types will certainly influence system behavior, they are not included in the parametric studies because modeling of their behavior is difficult and computationally expensive. Thus, the research team proposes to study the effect of joint type and behavior through a reduced set of selective case studies (see Section 5.3). The parametric studies will then focus on overall behavior assuming that full moment continuity has been achieved through the longitudinal joint.

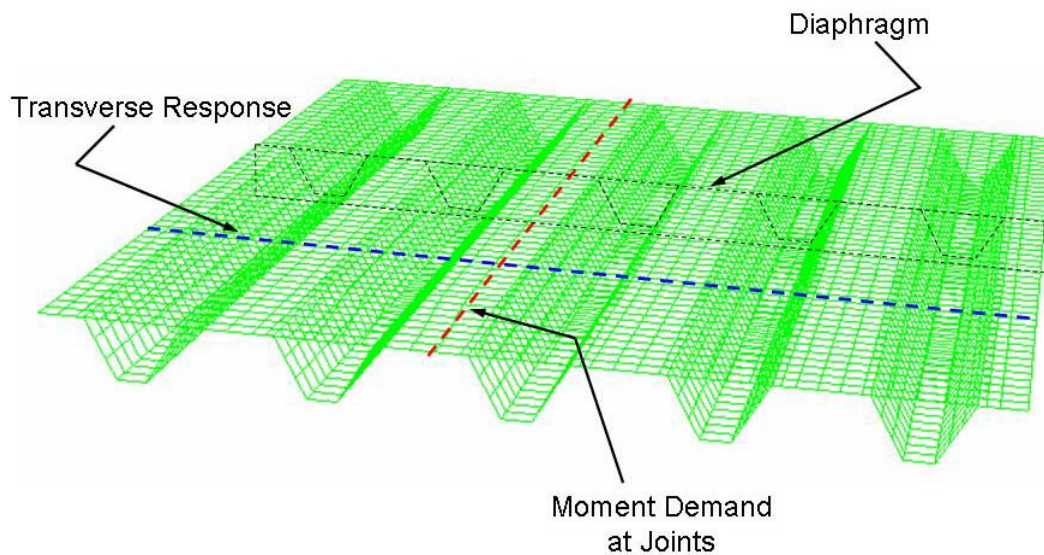


**Figure 47. Response measures of interest in parametric studies**

### 5.3.1 Creation of 3D FE Models

To improve computational efficiency, the models generated in the matrix shown in Table 11 were created using shell elements. More specifically, the ABAQUS (Simulia, 2007) element S4R was used. This is defined by ABAQUS as “a 4-node doubly curved thin or thick shell, [with] reduced integration, hourglass control, [and] finite membrane strains”. In addition, the deck was considered to be one continuous slab. This assumption can be considered valid if it can be shown that the longitudinal joints can be held closed under service loads by a reasonable amount of prestressing. This check is performed in Section 5.3. A sample bridge model can be seen in Figure 48.

As seen in Figure 48, the bridge models have end-blocks, and some models (see Table 11), such as the model in the figure, have diaphragms. The end-blocks were modeled with shell elements, and were assigned a thickness of 24 inches. The material used was concrete. The diaphragms were also modeled using shell elements. They were made of steel, and assigned a thickness of 0.5 inches. Steel diaphragms were chosen for the simulation studies due to their lower weight. However, concrete diaphragms could also be used for this bridge system. The end-blocks were then simply supported, creating the boundary conditions for the bridge. The sizes of the different elements vary. The original element size was 6 inches for deck and girder elements. End-block and diaphragm responses were not being studied, and consequently they were composed of a coarser 12 inch mesh. However, after running some analyses the research team found that the deck and end-block meshes needed to be finer than the girder mesh to prevent the girders from passing through the deck and end-blocks. Therefore, the mesh size of the deck and end-block elements was reduced to 4 inches. The final selection of elements is detailed in Table 12.

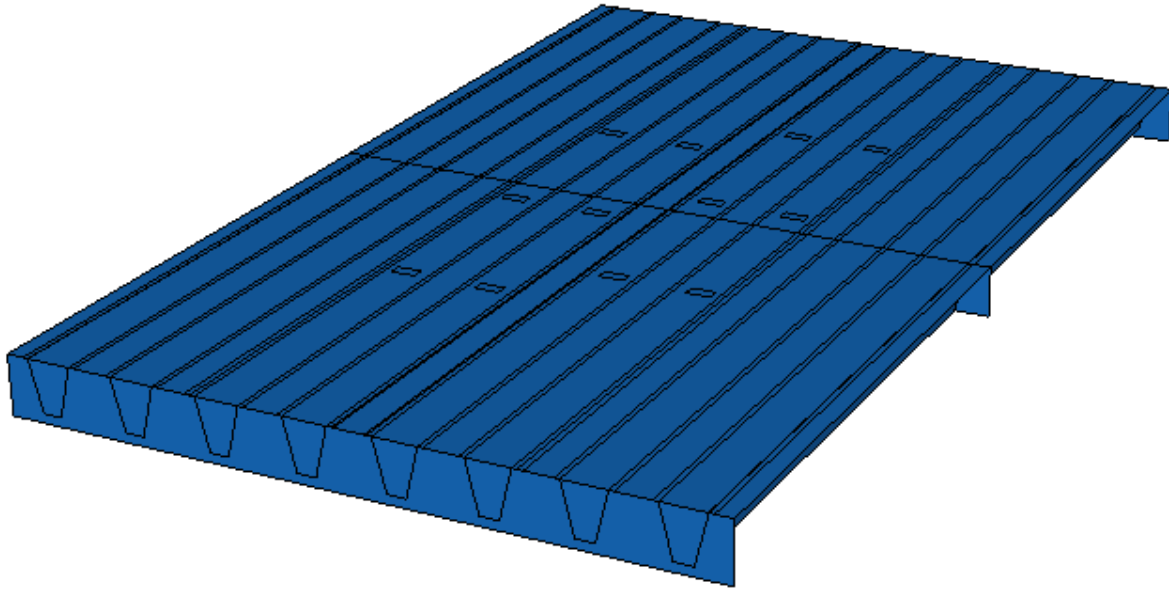


**Figure 48. Typical Bridge Model Using Shell Elements**

**Table 12. Element Data for Parametric Models with Shell Deck Elements**

<b>Part</b>	<b>Material</b>	<b>Shell Thickness (in)</b>	<b>Element Type</b>	<b>Hourglass Control</b>	<b>Reduced Integration</b>	<b>Element Size (in)</b>
Deck	Concrete	9	S4R	Active	Active	4
Tub	Steel	0.375	S4R	Active	Active	12
Diaphragm	Steel	0.5	S4R	Active	Active	4
End Block	Concrete	24	S4R	Active	Active	4

### 5.3.2 Selection of Model Geometries

In order to obtain realistic and usable geometries for the sample bridges used in the parametric study, the initial dimensions were selected by making use of the Excel spreadsheet developed for preliminary system analysis (see Section 3.4). The combinations of span and spacing defined in Table 11 were entered into said spreadsheet, and the preliminary dimensions that were obtained have been listed in Table 13. These models were then created and analyzed using ABAQUS. The results of these analyses were then compared against AASHTO

specifications for midspan deflection and maximum tub stress to check their feasibility. This comparison can be found in Table 14.

**Table 13. Original Geometries Used for Models in Parametric Study**

Model No.	Span/Spacing	Diaphragm	Section Depth (in)	Equivalent Depth (in)	Tension Flange (in)	Compression Flange (in)	Number of Girders	Spacing (in)	
1	50'	4'	19.5	24	10	4	12	47	
2		6'	20.5	25	10	4	8	70.5	
3		8'	21.5	26	10	4	6	94	
4	75'	6'	31.5	36	13	4	8	70.5	
5		6'	31.5	36	13	4	8	70.5	
6		8'	1/2 pt.	33	37.5	13.5	4	6	94
7	100'	6'	41.5	46	16.5	4	8	70.5	
8		6'	1/3 pt.	41.5	46	16.5	4	8	70.5
9		8'	none	43.5	48	17.5	4	6	94
10		8'	1/3 pt.	43.5	48	17.5	4	6	94
11		10'	none	45.5	50	20	4	5	112.8
12		10'	1/4, 1/2 pt.	45.5	50	20	4	5	112.8

**Table 14. Results of ABAQUS Analysis on Original Geometries**

Model No.	Span/Spacing	Results (ABAQUS)		Predicted (Excel)		AASHTO Limits		
		Max. Tub Stress (ksi)	Midspan Deflection (in)	Max. Tub Stress (ksi)	Midspan Deflection (in)	Max. Tub Stress (ksi)	Midspan Deflection (in)	
1	50'	4'	23.5	0.695	19.7	0.728	50	0.750
2		6'	31.1	0.861	25	0.718	50	0.750
3		8'	35.2	1.95	30	0.722	50	0.750
4	75'	6'	33.8	1.44	27.7	1.11	50	1.125
5		6'	32.3	1.22	27.7	1.11	50	1.125
6		8'	38.1	1.34	32.8	1.10	50	1.125
7	100'	6'	32.1	1.66	29.4	1.48	50	1.500
8		6'	29.3	1.56	29.4	1.48	50	1.500
9		8'	34.8	1.84	34.3	1.46	50	1.500
10		8'	32.2	1.73	34.3	1.46	50	1.500
11		10'	42.6	1.84	35.8	1.36	50	1.500
12		10'	39.2	1.69	35.8	1.36	50	1.500

As Table 14 indicates, many of the geometries obtained by using the spreadsheet optimization were inadequate, despite incorporation of the AASHTO criteria into the spreadsheet. This could be due to several things, but the most likely cause, as determined by the research team, is an inability of the AASHTO distribution factors to accurately model the true load distribution. The reason for skepticism toward these distribution factors is their inherent vagueness- the same equation is used for both shear and bending for interior and exterior beams. In addition, the only factors considered are number of lanes and number of beams. These

observations seem to indicate that minimal time has been spent developing distribution factors for the system being studied, and this is reflected in their inaccuracies, as observed in this study.

To make the parametric study more practical, the bridges were redesigned so that they would meet the AASHTO criteria for stress and for deflection. In addition, for the 75-foot span and the 100-foot span models, a “standard geometry” was chosen to be used for several different bridge models. This was done in order to show that a single girder geometry could have the versatility to be used for a variety of situations. The updated geometries are shown in Table 15, and the corresponding system responses are shown in Table 16.

**Table 15. Modified Geometries to Meet AASHTO Specifications**

Model No.	Span/Spacing	Diaphragm	Section Depth (in)	Equivalent Depth (in)	Tension Flange (in)	Compression Flange (in)	Number of Girders	Spacing (in)
1	50'	4'	19.5	24	10	4	12	47
2		6'	23	27.5	10	4	8	70.5
3		8'	26	30.5	12	4	6	94
4	75'	6'	36	40.5	13	4	8	70.5
5		6'	36	40.5	13	4	8	70.5
6		8'	36	40.5	13.5	4	6	94
7	100'	6'	44	48.5	16.5	4	8	70.5
8		6'	44	48.5	16.5	4	8	70.5
9		8'	50	54.5	17.5	4	6	94
10		8'	50	54.5	17.5	4	6	94
11		10'	50	54.5	18.5	4	5	112.8
12	10'	1/4,1/2 pt.	50	54.5	18.5	4	5	112.8

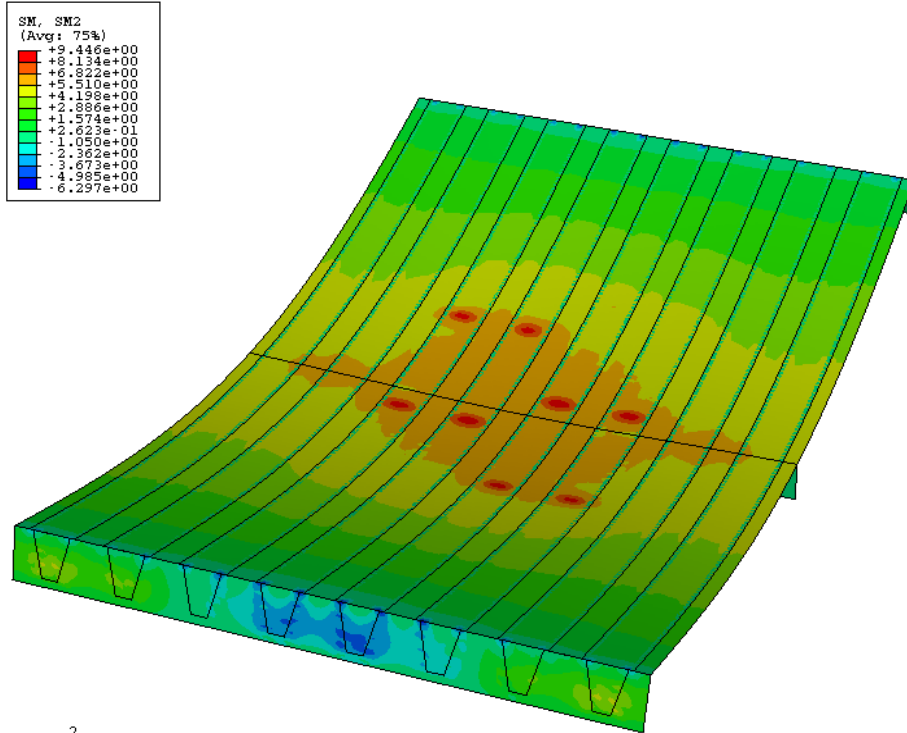
**Table 16. Results of ABAQUS Analysis on Original Geometries**

Model No.	Span/Spacing	Results (ABAQUS)		AASHTO Limits		
		Max. Tub Stress (ksi)	Midspan Deflection (in)	Max. Tub Stress (ksi)	Midspan Deflection (in)	
1	50'	4'	23.2	0.667	50	0.750
2		6'	26.9	0.670	50	0.750
3		8'	26.9	0.635	50	0.750
4	75'	6'	27.5	0.951	50	1.125
5		6'	30.2	0.857	50	1.125
6		8'	34.8	1.07	50	1.125
7	100'	6'	29.5	1.45	50	1.500
8		6'	26.8	1.38	50	1.500
9		8'	28.5	1.28	50	1.500
10	100'	8'	28.8	1.12	50	1.500
11		10'	36.3	1.48	50	1.500
12		10'	34.8	1.32	50	1.500

### 5.3.3 System Response

Once it had been verified that the models for the study fit within AASHTO parameters for stress and deflection, the response at the joints was analyzed. Specifically, the three responses investigated were: transverse moment response along a transverse path across the bridge, transverse moment response along a theoretical longitudinal joint, and longitudinal moment response along a theoretical longitudinal joint (see Figure 47). A graphical representation of these responses for individual bridges, as well as a schematic of measurement locations, can be found in Appendices II-XIII. The vertical lines in these plots represent the location of the tires from the design truck(s). The paths were chosen by selecting a line passing through the areas of the deck with the highest magnitude of the moment under consideration (located under the design truck tires). For a visual representation of the system response, see Figure 49 and Figure 50.

To display the response graphically, a number of plots were generated which show system response over a specified path. These paths were chosen to show the most extreme forces that would be experienced by the bridge. The location of the paths varied slightly from model to model, and thus all paths are shown in the Appendices. In addition, Figure 51 shows where these paths were typically found. Contours were shown in black and white to make the paths easier to see in black-and-white printed versions of this document.



2

**Figure 49. Typical Deformed Shape and Moment Distribution. Contours Represent Longitudinal Moment in kip-in/in.**

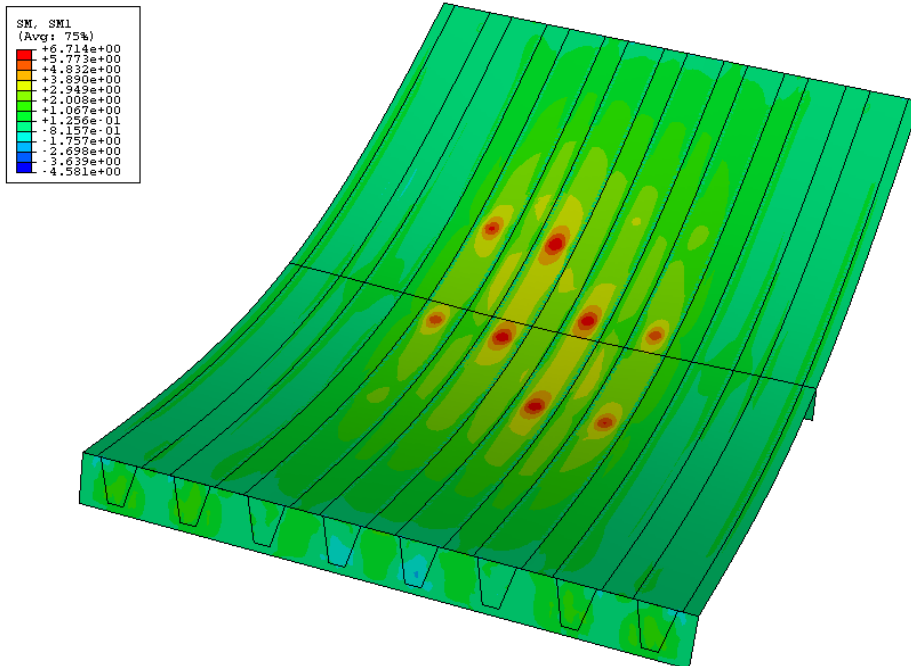


**Figure 50. Typical Deformed Shape and Moment Distribution. Contours Represent Transverse Moment in kip-in/in.**

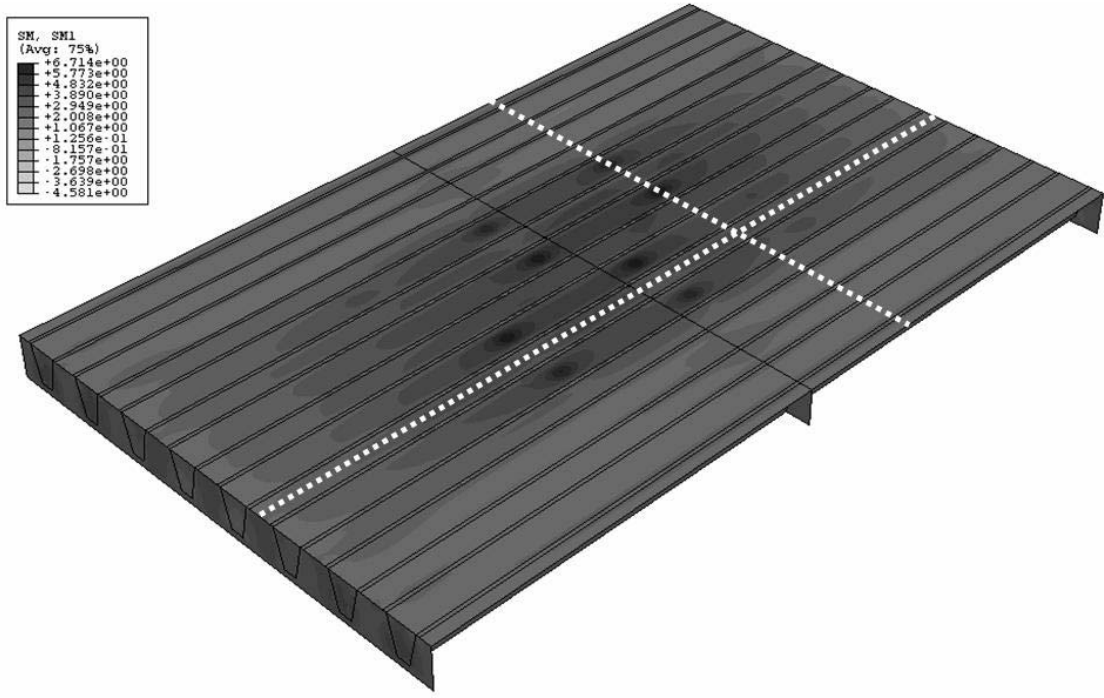
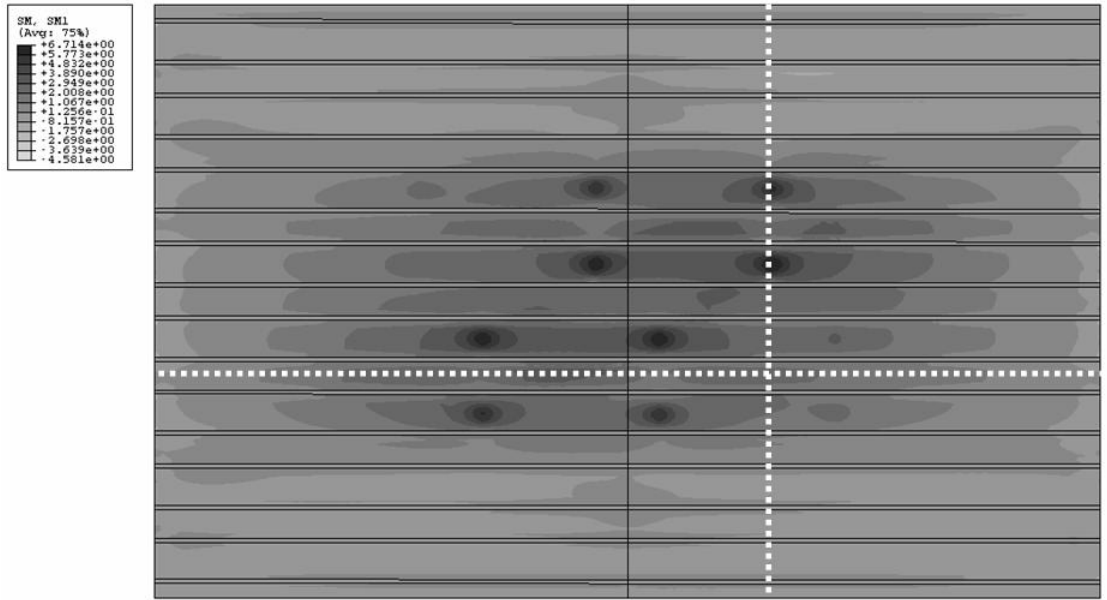


**Figure 51. Typical Location of Paths. Contours Represent Transverse Moment in kip-in/in.**

While the individual plots have been relegated to the Appendices, several comparisons between models will be provided here. First the data for the 50' span bridge models are shown in Figure 52, Figure 53, and Figure 54. The data for the 75' span bridge models are shown in Figure 55, Figure 56, and Figure 57. Finally, the data for the 100' span bridge models are shown in Figure 58, Figure 59, and Figure 60.

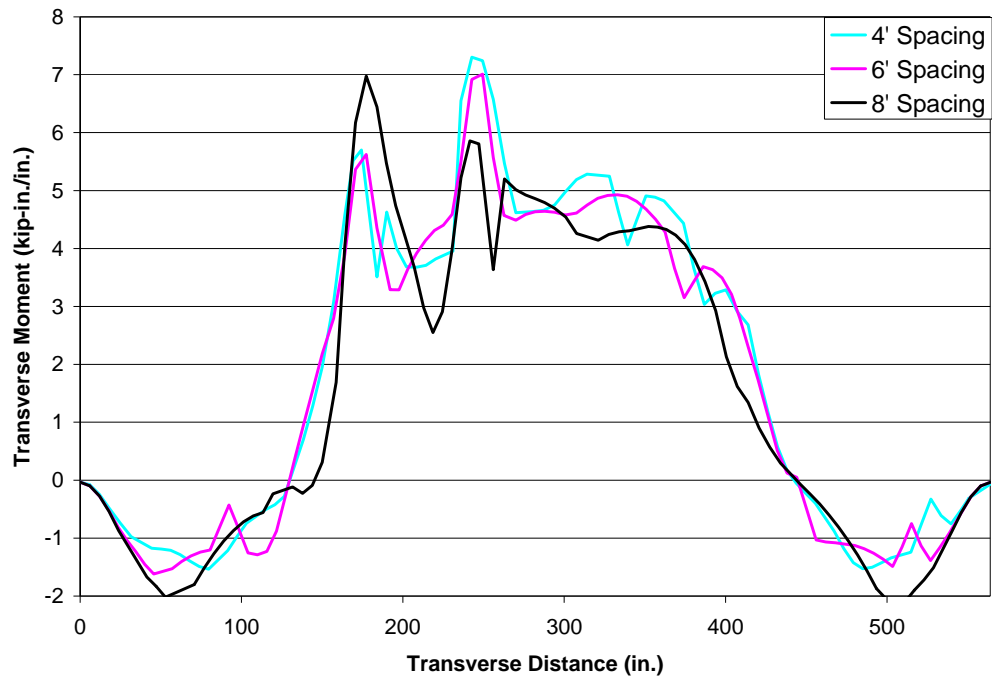


**Figure 52. 50' Span: Transverse Moment v. Transverse Distance Comparison**

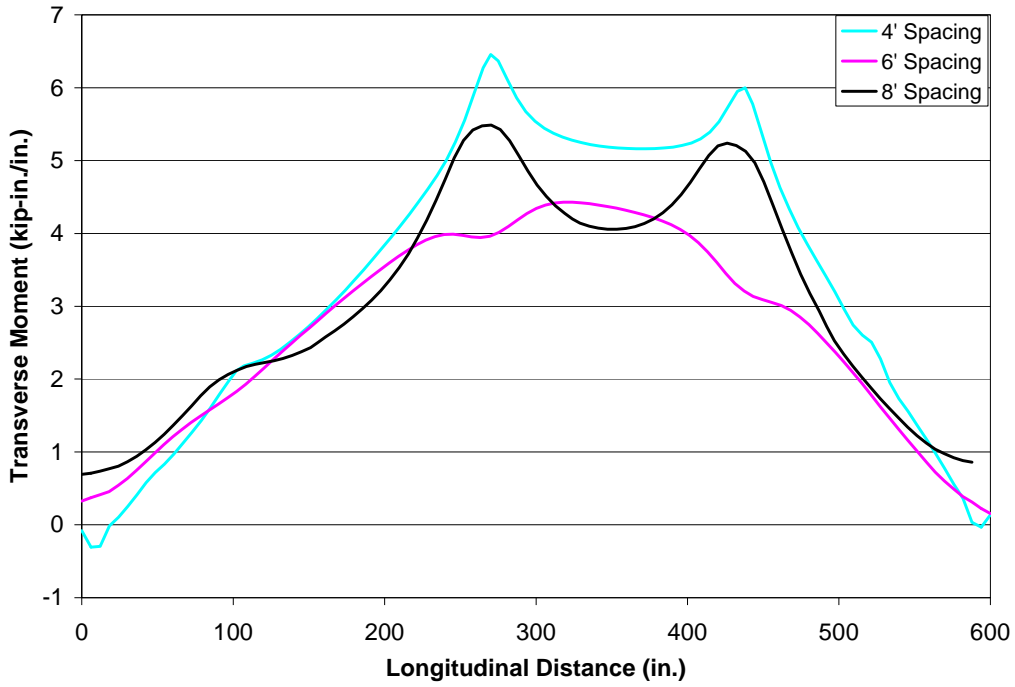


**Figure 53. 50' Span: Transverse Moment v. Longitudinal Distance Comparison**

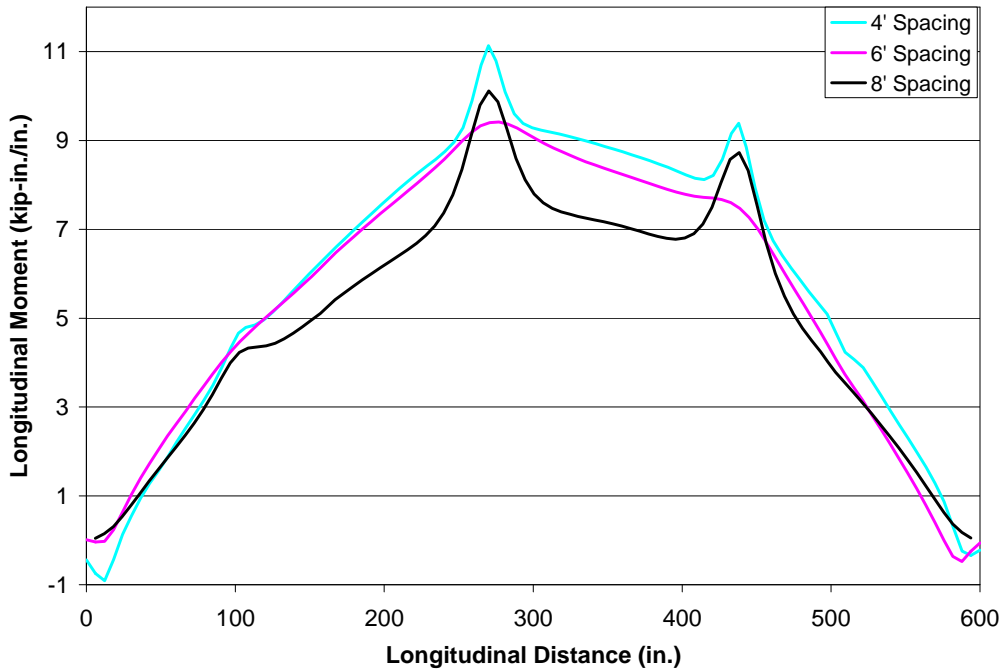


**Figure 54. 50' Span: Longitudinal Moment v. Longitudinal Distance Comparison**

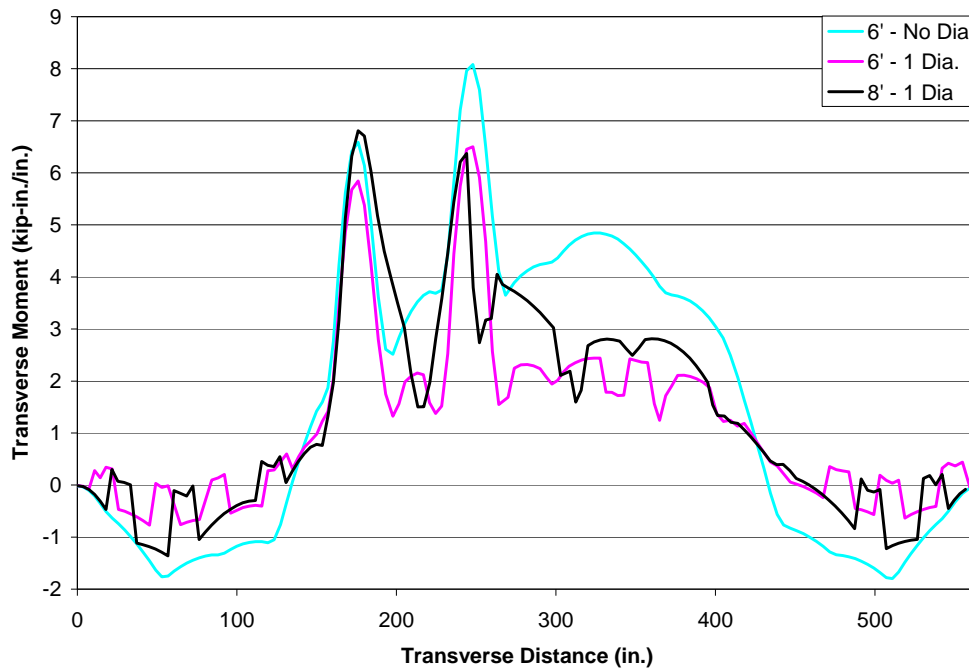


**Figure 55. 75' Span: Transverse Moment v. Transverse Distance Comparison**

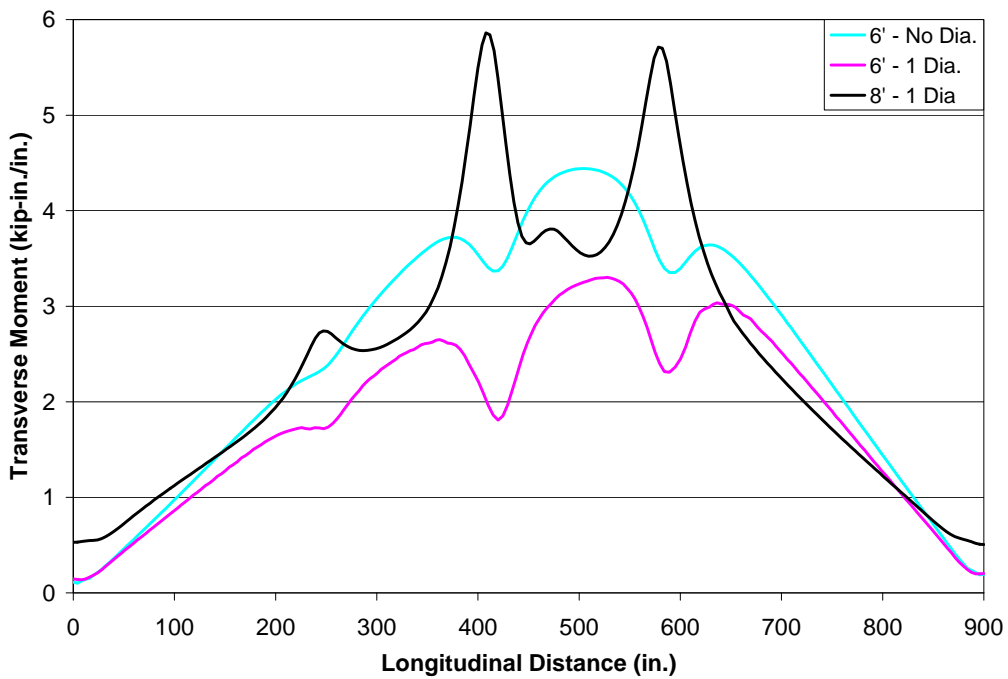


**Figure 56. 75' Span: Transverse Moment v. Longitudinal Distance Comparison**

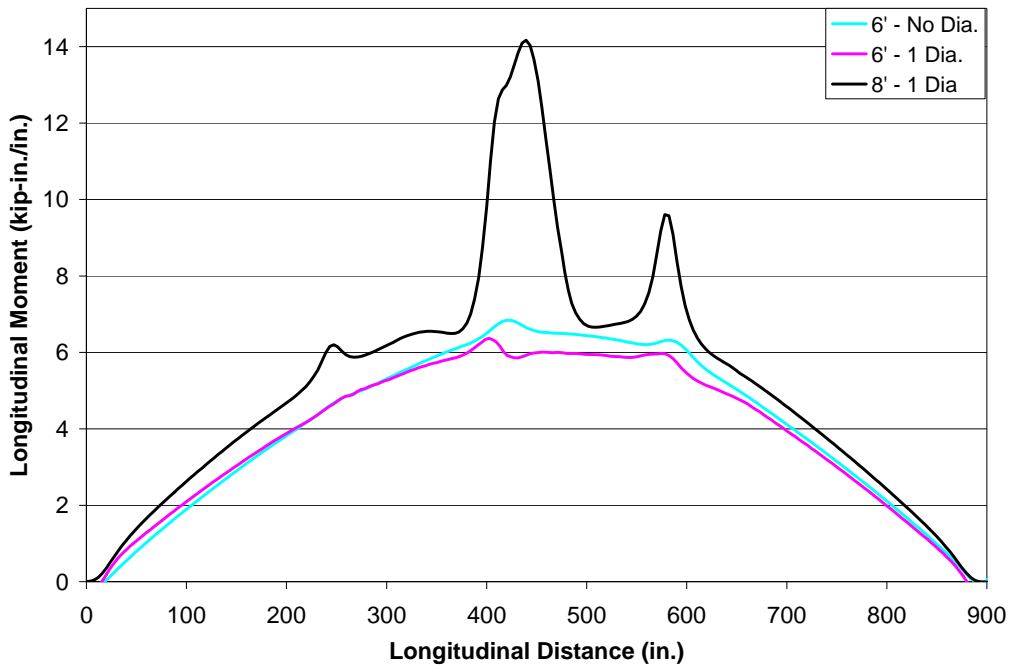


**Figure 57. 75' Span: Longitudinal Moment v. Longitudinal Distance Comparison**

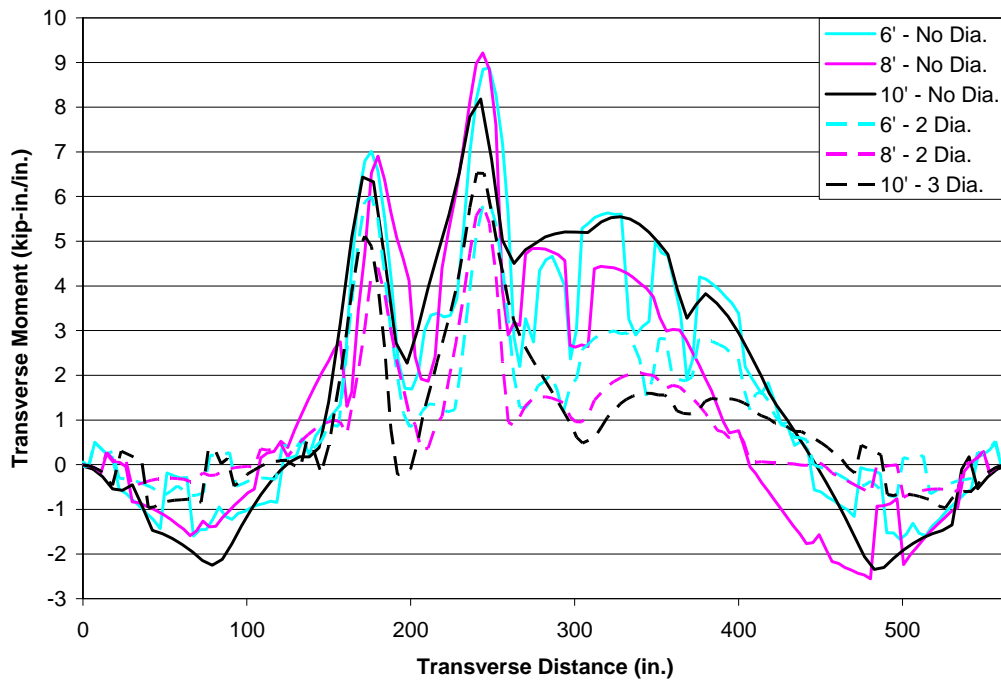


**Figure 58. 100' Span: Transverse Moment v. Transverse Distance Comparison With and Without Diaphragms**

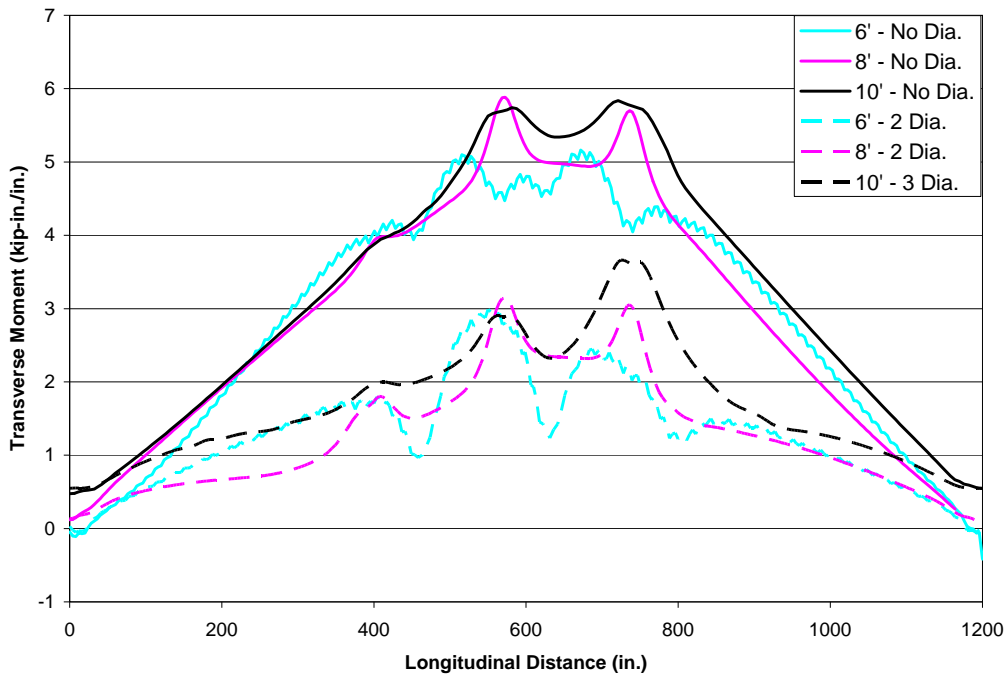


**Figure 59. 100' Span: Transverse Moment v. Longitudinal Distance Comparison With and Without Diaphragms**

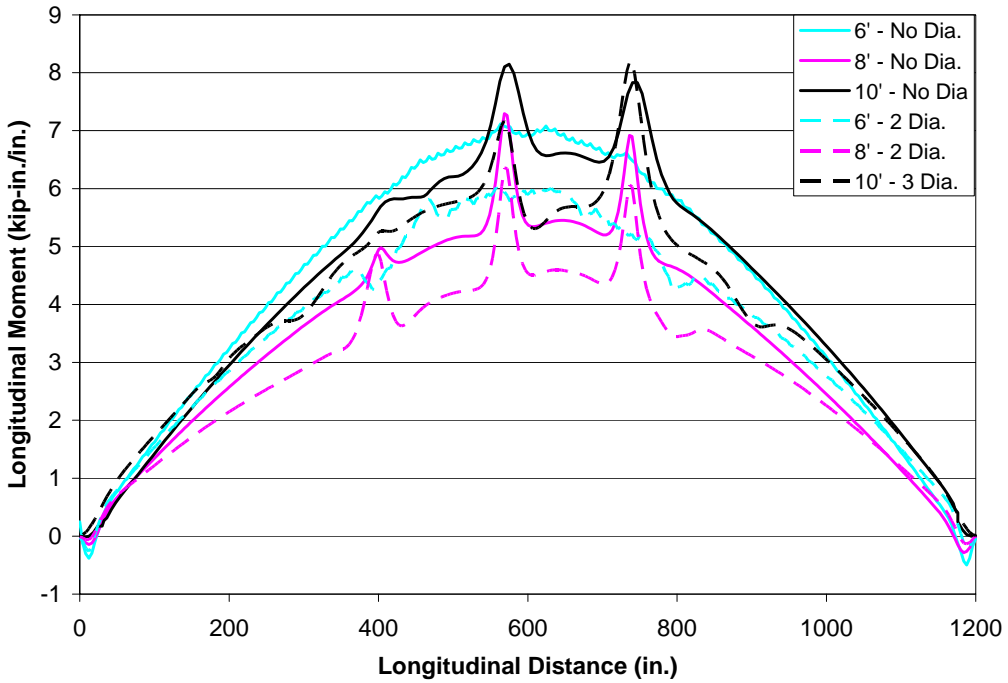


**Figure 60. 100' Span: Longitudinal Moment v. Longitudinal Distance Comparison With and Without Diaphragms**

A summary of the forces represented in Figure 52 to Figure 60 are shown below in Table 17.

**Table 17. Summary of Maximum Forces in Bridge Models**

Bridge No.	Max. Tran. Moment (kip-in/in)	Max. Tran. Moment at Joint (kip-in/in)	Max. Long. Moment at Joint (kip-in/in)
1	7.30	6.46	11.13
2	7.01	4.43	9.42
3	6.98	5.49	10.11
4	8.08	4.44	6.84
5	6.50	3.30	6.37
6	6.81	5.86	14.17
7	8.88	5.16	7.12
8	6.00	2.99	6.02
9	9.21	5.88	7.30
10	5.81	3.15	6.36
11	8.18	5.84	8.15
12	6.52	3.66	8.19
Avg.	7.27	4.72	8.43
Max.	9.21	6.46	14.17

### 5.3.4 Discussion of Results

The results presented in Section 5.2.3 show some interesting trends. These trends and possible explanations will be offered here. First, the transverse moment response along the transverse paths will be discussed. These graphs show a trend to spike at positions where design tire loads are applied. The magnitude of the moment that is developed increases slightly on average as the span increases, but the increase is small. As shown in Table 17, the maximum transverse moment force that was developed in any of the models was 9.21 kip-in/in.

The transverse moment response along a longitudinal path (meant to represent the location of a joint) provided the most intriguing results. As seen in Figure 53, Figure 56, and Figure 59, certain models showed a *decrease* in the magnitude of the transverse moment directly beneath the wheel load. This is at odds with conventional logic. Careful inspection of the schematics showing where the forces were extracted (Appendix II - Appendix XIII) reveal that in the models showing the decrease in magnitude, the wheel load falls between two girders. However, when the wheel load falls in a location above a girder, the predicted increase in transverse moment occurs. The research team believes this phenomenon is caused by the girders absorbing much of the force due to their increased rigidity in comparison with the deck. The maximum transverse

moment developed was 6.46 kip-in/in. This is lower than the maximum found along the transverse path, indicating that in these simulations the maximum transverse moment does not occur at a joint. However, the maximum transverse moment along the transverse path (9.21 kip-in/in) should be kept in mind for design purposes, as the wheel loads' locations will vary during live traffic.

The longitudinal moment along the longitudinal path shows a typical moment diagram for a distributed load with spiked increases under the wheel loads. The longitudinal moment does not appear to be affected by the placement of the wheel loads over the girders. One notable anomaly in the data can be seen in Figure 57. Here the increase in moment under the wheel load is extremely pronounced. Once again, this can be explained by looking at the schematic of the bridge in Appendix VII. The figure clearly shows the longitudinal path crossing very near to the wheel loads. This close proximity to the wheels creates a more distinct increase. This fact should again be carefully considered by a designer. Trucks could certainly drift in their lane, or change lanes and in doing so drive over a joint. Therefore, the maximum longitudinal moment developed (14.17 kip-in/in) should be used for design.

Another trend in the data that is decisively shown in Figure 58, Figure 59, and Figure 60 is the effect of diaphragms on design forces. In every case the moment magnitudes are reduced by the presence of diaphragms. However, the reductions are most notable when considering transverse moment. Although there are also decreases in longitudinal moment, they are not as prominent. Correspondingly, if moment values are of concern to the designer, the addition of diaphragms may be a viable way to reduce forces.

## **5.4 Stress Analysis and Characterization of Connection Details**

### **5.4.1 General**

The final step in the hierarchical suite of analyses outlined at the beginning of this chapter was to evaluate the performance of longitudinal joints between the prefabricated girder/deck units through detailed 3D stress analyses. This step involved the largest and most complex FE models as it required three-dimensional simulation of the connection detail and the forces being transferred. This section describes the modeling procedure, validation, and the results that are relevant to this project.

### **5.4.2 Approach**

This subtask deals with evaluating the performance of connection details for the prefabricated steel/concrete superstructure units. The research team conceptualized different options to realize the longitudinal joints of the concrete deck flanges. While specific design options were outlined they fall within the following categories:

- 1) Cast-in-place reinforced concrete joints.
- 2) Shear keys (keyed, grouted or reinforced with steel dowels)
- 3) Post-tensioned shear keys/joints

From the three main joint categories, cast-in-place reinforced concrete joints (type 1) are designed as a full moment connection joint and thus expected to behave accordingly. Thus, no special analytical evaluation is considered to be required for this connection type. In addition, system performance with this type of connection detail will be covered through the parametric studies (see Section 5.3).

Shear keys (type 2) that are not designed to transfer moments are not permitted according to the AASHTO LRFD specifications. Rather, a minimum post-tensioning force is specified. Thus, characterization of connection type 3, of the list above, is considered to be of most relevance to this project. Therefore, the effort will be in studying the behavior of post-tensioned shear key joints to evaluate their load transfer efficiency and determining the required transverse post-tensioning level required for adequate performance. In addition, successful modeling of this connection type can allow for modeling of the shear key connection (type 2) as a special case

where the transverse post-tensioning level is not enough to provide significant moment transfer across the joint.

Finite element simulation of post-tensioned shear key/joints requires modeling disconnected girder/deck units that are in contact only at the joints of the concrete deck. This is achieved in finite elements through contact and interaction modeling. Successful modeling of interaction problems is difficult. Thus, the next sections present a summary of the efforts taken to ensure that the contact and interaction modeling options to be used in the joints were applied properly.

### **5.4.3 Contact Interaction Modeling**

ABAQUS permits modeling of contact interactions using surfaces or contact elements. This research used the approach of surface-based contact interaction. Within this type of interaction, the type of problem that was simulated was one of contact between two deformable bodies. The sides of deck joint are in three-dimensional space and can undergo small or finite sliding. Definition of the mechanical contact simulation between bodies may include different parameters and definitions. The ones used for the current study were:

- A constitutive model for the contact pressure-overclosure relation that governs the motion of the surfaces.
- A friction model that defines the force resisting the relative tangential motion of the surfaces.

The behavior of the surface-to-surface interaction is achieved in ABAQUS by defining *contact pressure-overclosure relations*. For this research, the “hard” contact relation was used, which is the most common contact pressure-overclosure relation. This relation, as shown in FIG, consists on a zero-penetration condition of the two surfaces such that any contact pressure can be transmitted between them if they are in contact. Conversely, the surfaces would separate if the contact pressure reduces to zero. Separated surfaces come into contact when the clearance between them reduces to zero.

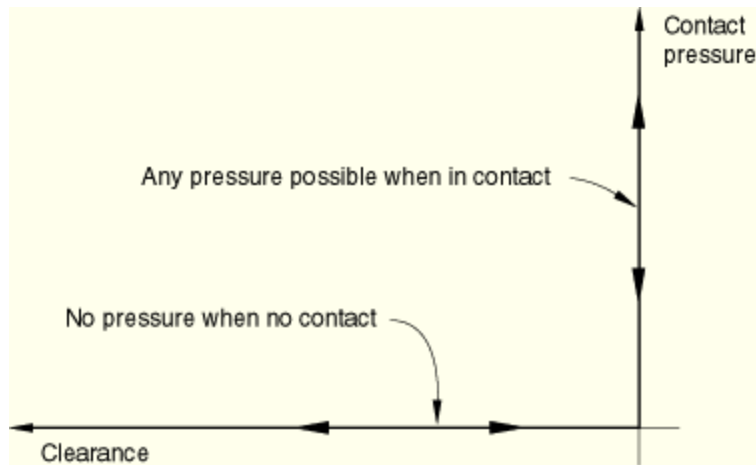


**Figure 61. “Hard “ Contact Pressure-Overclosure Relation in ABAQUS (Simulia 2007)**

By default, ABAQUS assumes that the contact between the surfaces is frictionless. A friction model can be added as part of a surface interaction definition. The friction relation between contacting bodies defines the relation between the shear and normal force components acting across the interface of surfaces that are in contact. ABAQUS has several friction models, including the classical isotropic Coulomb friction model, shear-stress limited and anisotropic Coulomb models, and “softened” interfaces for sticking friction.

The basic Coulomb friction model was used in this study. The model relates the maximum allowable frictional (shear) stress across an interface to the contact pressure between the contacting bodies. In its basic form, the model allows the two contacting surfaces to carry shear stresses up to a certain magnitude across their interface before they start sliding relative to one another (a state defined in ABAQUS as “sticking”). The Coulomb friction model defines this critical shear stress  $\tau_{crit}$  at which the sliding of the surfaces starts as a fraction of the contact pressure,  $p$ , between the surfaces ( $\tau_{crit} = \mu p$ ). The stick/slip calculations determine when a point transitions from sticking to slipping or from slipping to sticking. The fraction  $\mu$  is the friction coefficient.

The basic friction model assumes that  $\mu$  is the same in all directions (isotropic friction). For a three-dimensional simulation, the two orthogonal components of shear stress are averaged (square root of the sum of the squares) to an equivalent shear stress for the stick/slip calculations. In addition, ABAQUS determines and combines the orthogonal slip velocity components into an

equivalent slip rate. The stick/slip calculations thus define a surface in the pressure-shear stress space that defines when a point transitions from sticking to slipping. A two-dimensional representation of the Coulomb friction model is shown in Figure 62.

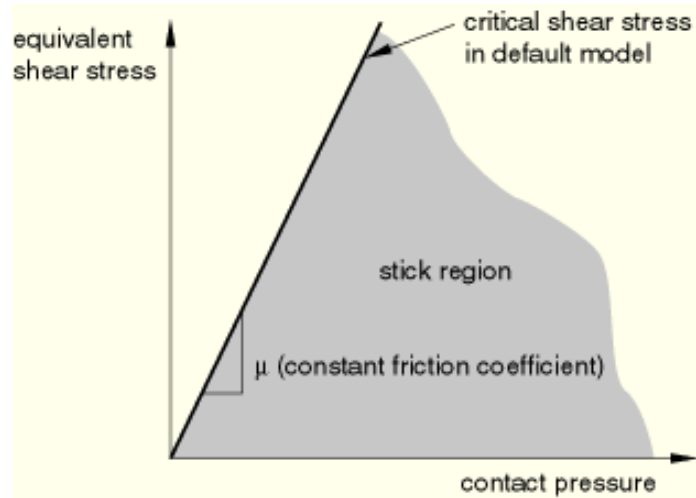


**Figure 62. Slip Regions for the Basic Coulomb Friction Model (Simulia 2007)**

There are two ways of defining the basic Coulomb friction model in ABAQUS: (1) the friction coefficient is defined as a function of the equivalent slip rate and contact pressure, or (2) the static and kinetic friction coefficients are defined. Option 1 was chosen in this study. The friction coefficient in this option depends on slip rate, contact pressure, temperature and field variables. For this study, the default option of a friction coefficient independent of temperature and field variables was used. Based on literature review of similar modeling efforts, a friction coefficient of 0.5 was conservatively chosen.

Although the robustness of the interaction models in ABAQUS are well documented, several checks were performed in order to verify that the interaction properties used in the model were behaving as desired. Details of the evaluation measures follow.

## 5.4.4 Evaluation of Contact Interaction Modeling

### 5.4.4.1 Qualitative Evaluation

To properly represent the behavior of the joint, the contact property needed two characteristics. First, when nodes come into contact, the interaction property needs to prevent them from passing through each other. Second, if the nodes lose the pressure pressing them together, the model needs to allow them to separate. Verifying that these two behaviors are occurring was the aim of this first evaluation.

The model created to perform this check consisted of two simply supported cubes with pressure applied inward on the outer face of each block, as shown in Figure 63. The motivation for choosing this setup was to create a situation where the blocks would come into contact, and then separate. This first objective was achieved, as shown in Figure 64. Loading was then applied to the top of the cubes in order to achieve a separation at the bottom of the interface, as an actual loaded joint would behave. This is shown in Figure 65. The separation was achieved, as shown in Figure 66.

As Figure 64 and Figure 66 show, these models exhibited major deformations at the element level in areas of high stress. This effect is partly due to graphical representation of the small displacements introduced in this model. This problem could have been remedied by increasing the number of elements or changing to a quadratic element. However, this evaluation was qualitative; thus it was instead decided to evaluate a model with a geometry closer to that of a bridge deck.

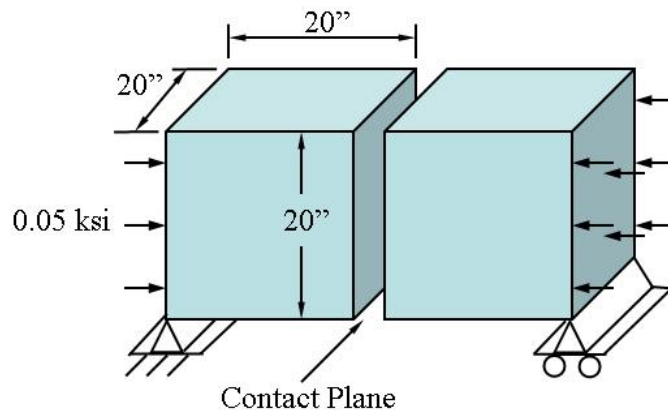


**Figure 63. Schematic of Cube Contact Model with Pressure Normal to the Contact Plane**

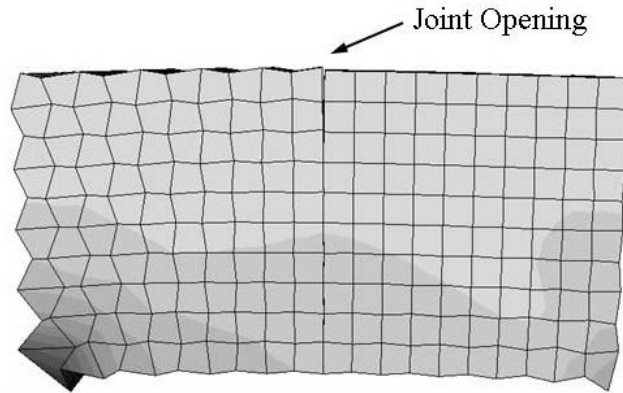


**Figure 64. Cube model showing separation of nodes**

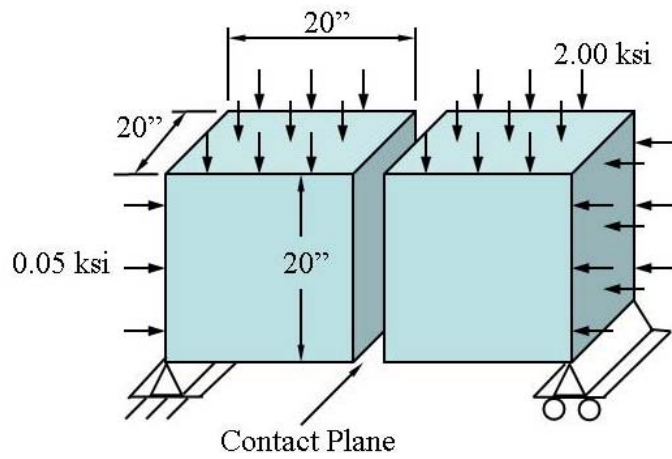


**Figure 65. Schematic of Cube Contact Model with Pressure Normal to the Contact Plane and Vertical Pressure**

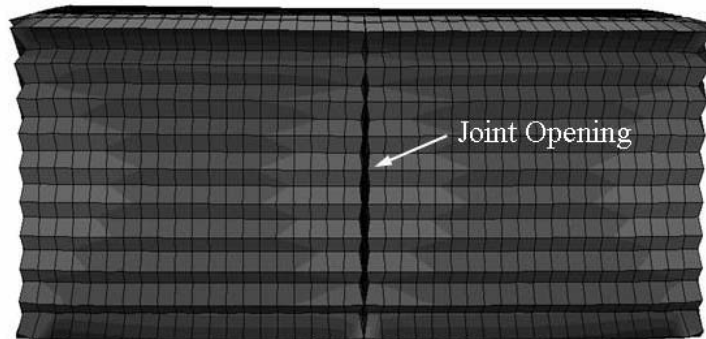


**Figure 66. Bottom view of top-loaded model showing separation of nodes under load**

As shown in Figure 67 and Figure 68, the model was modified to use shallower parts which more closely approximate deck slabs. The objective with this model was to learn more about creating an accurate way of modeling the connections to be used when analyzing a joint with no moment transfer, as well as to observe the qualitative behavior of a joint modeled with the contact interaction. The results of this analysis can be seen in Figure 69.

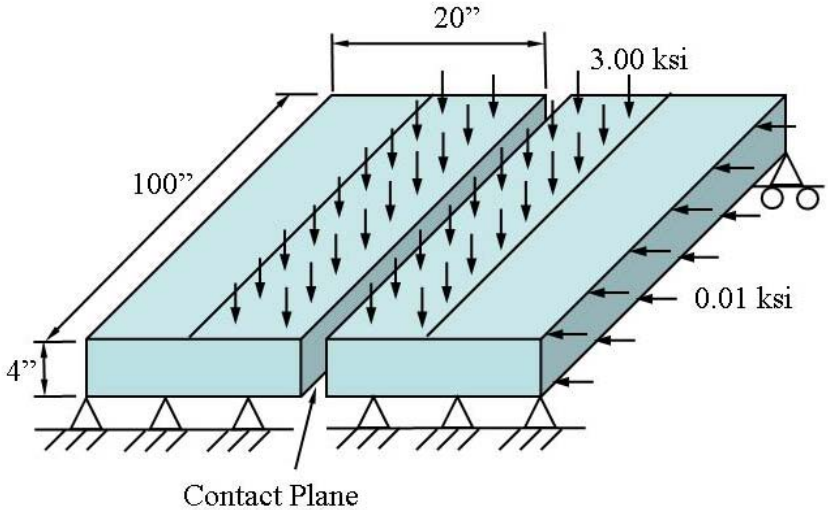


**Figure 67. Schematic of Updated Model with More Accurate Geometry**

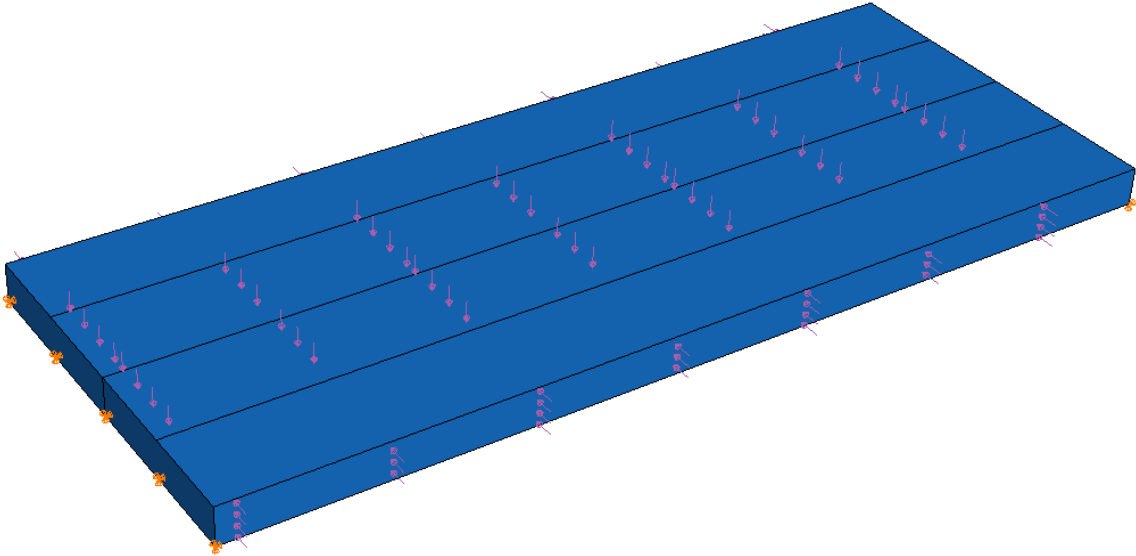


**Figure 68. Updated Model with More Accurate Geometry**

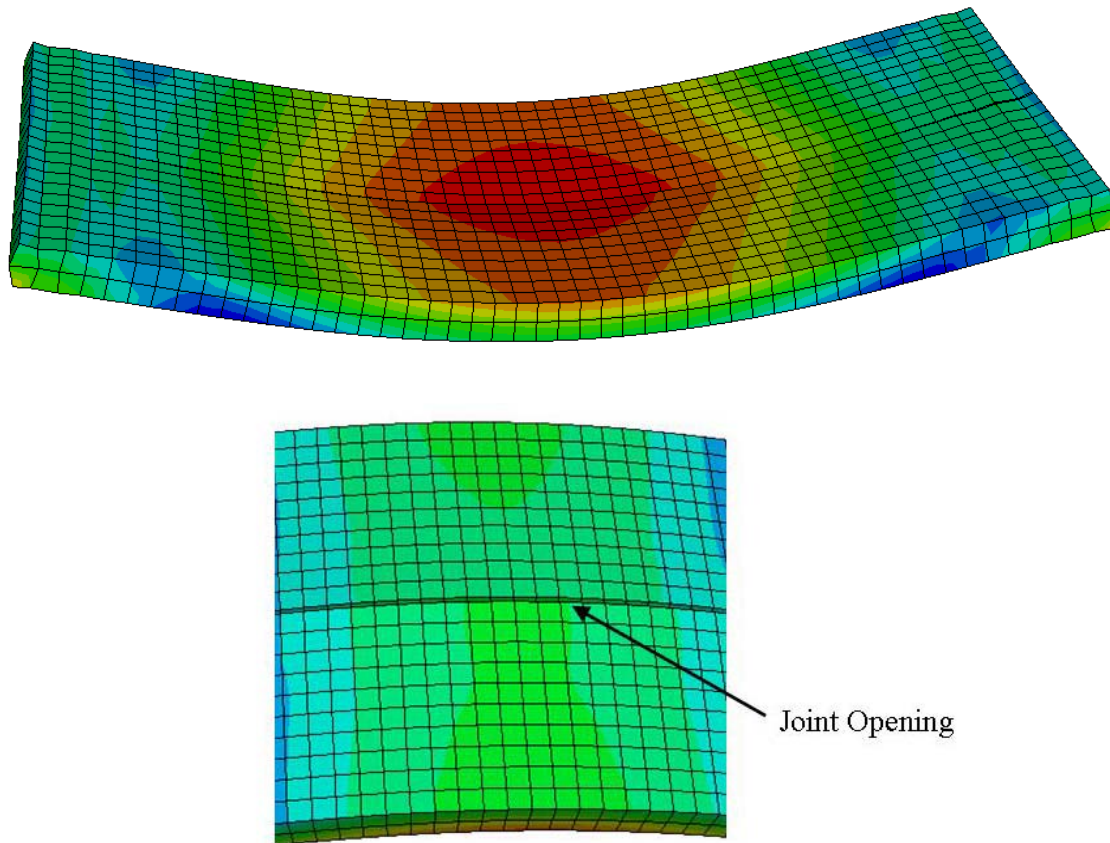


**Figure 69. (a) Top view of deformed shape of model in Figure 68 and (b) Bottom view of model in Figure 68 showing node separation**

#### **5.4.2.2 Quantitative Evaluation**

Once it was observed that the interaction property was behaving qualitatively correctly, a series of quantitative evaluations were performed in order to ensure that these observations were in fact correct, and not merely a misrepresentation in the post-processor. The first model used for this check consisted of a simply supported rectangular beam divided in two sections at mid-span loaded transversely and “held together” by a longitudinal post-tensioning force (see Figure 71).

To calibrate the model, hand calculations were performed to choose the magnitude of post-tensioning required for zero longitudinal stress at the bottom fiber of the beam at mid-span. This level of post-tensioning was chosen in order to check that the interface would remain closed as theoretically predicted. The FE simulation showed that the beam did remain closed under loading as shown in Figure 72. Figure 72 also shows that the stress is very close to zero at the bottom fiber (1.0037 ksi, compressive). This matches with the theoretical prediction.

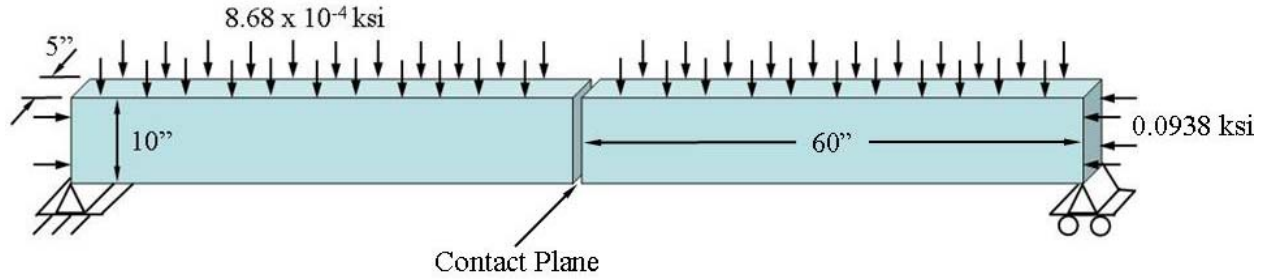


**Figure 70. Schematic of Rectangular Beam Used for Quantitative Evaluation**

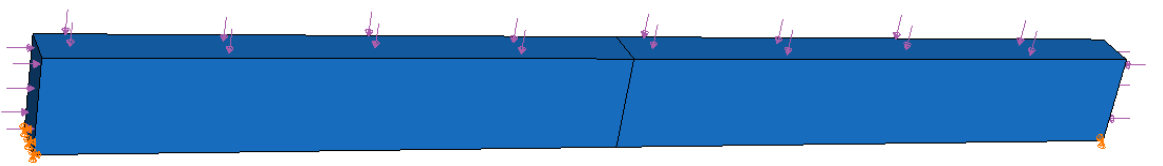


**Figure 71. Model of rectangular beam**

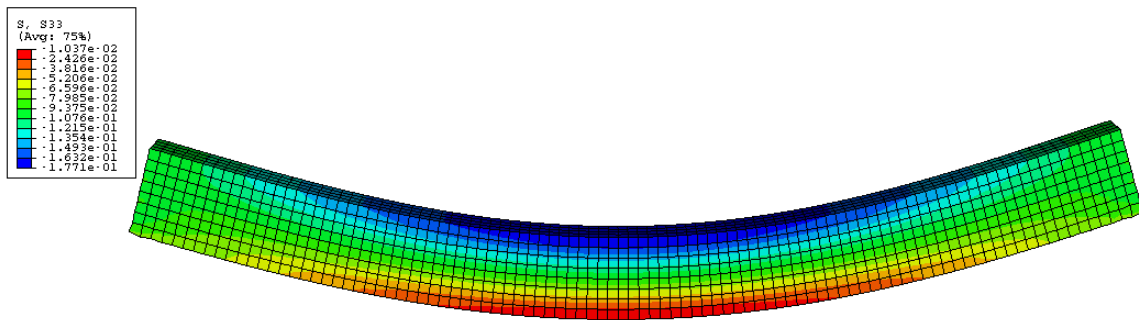


**Figure 72. Deformed shape of rectangular beam model showing no opening at midspan (contours represent longitudinal stresses in ksi)**

A stress profile was then determined from beam theory, and compared with the results of the ABAQUS model. This comparison is shown in Figure 73. The results showed close agreement (<5% error) with the theoretical calculations, except at the extreme fibers, where there was greater error. However, the research team believes that the FE model is actually correct, because beam theory assumes that plane sections remain plane, which does not hold true for a deep beam as the one modeled here. This assumption was investigated further with the next model.

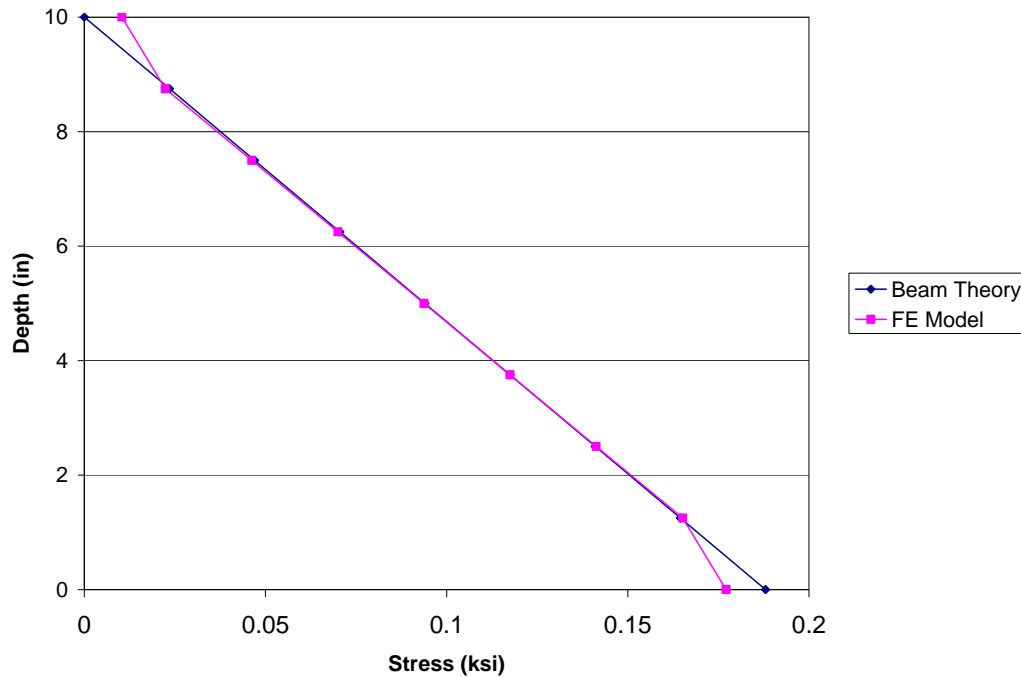


**Figure 73. Stress profile in rectangular beam model**

After verifying the accuracy of a model with a flat butt joint, a more complex male-to-female joint geometry that would more closely resemble the joint types 2 or 3 (see Section 5.3.1) in an actual bridge superstructure was investigated, as shown in Figure 74 and Figure 75. This model was subjected to a post-tensioning force and vertical loading similar to the rectangular beam with the flat butt joint. However, in this model the post-tensioning was proportioned so that the entire joint would remain in compression. This kept the joint closed, as shown in Figure 76. When this model was analyzed, it matched closely with predicted longitudinal stress values, again with the exception of the extreme fibers. These results are shown in Figure 77. As previously mentioned, this discrepancy was believed to be caused by shear deformations due to the relatively thick beams being modeled. To check that the departure from theoretical predictions at the extreme fibers were being caused by shear deformations and not a numerical problem caused by modeling the joint, a beam was modeled with the same dimensions as shown in Figure 74, but without a joint. These results, shown in Figure 78, also showed the nonlinear stress profile exhibited in Figure 73 and Figure 77. This indicates that this nonlinearity is due to shear deformations and is not related to a modeling issue.

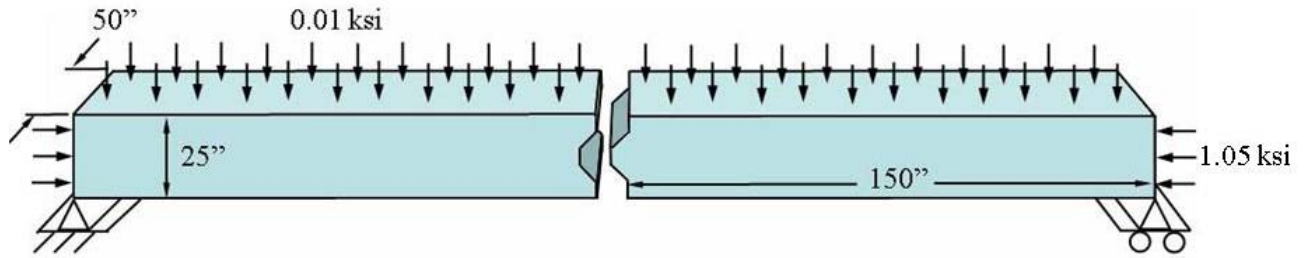


**Figure 74. Schematic of Male-to-Female Joint Model**

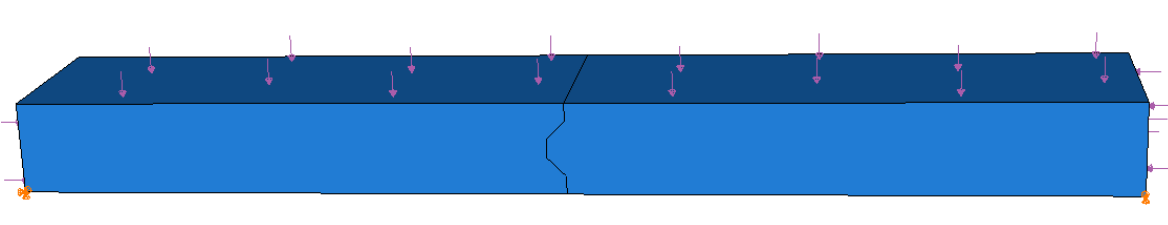


**Figure 75. ABAQUS Model with Male-to-Female Joint**

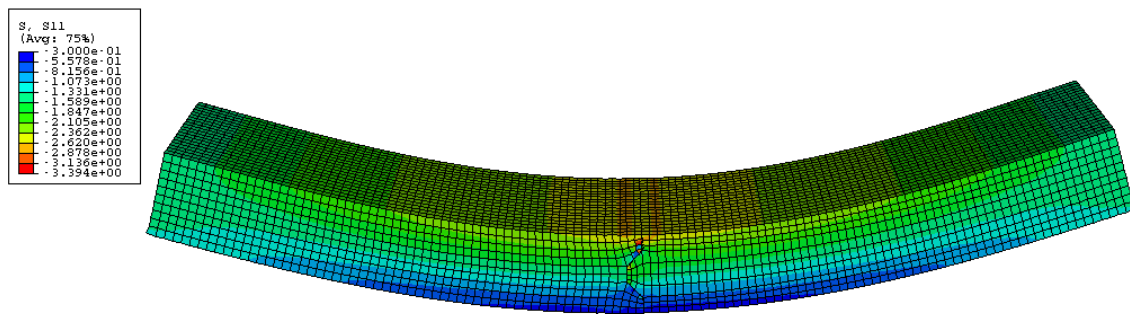


**Figure 76. FE Model of Male-to-Female Joint (Longitudinal Stress Contours in ksi)**

After completing these checks, the research team is satisfied that the method for modeling the interaction property is adequate. The results of these models agree with predicted results and the physical behavior coincides with what is expected. Therefore, a similar model can be used to assess the behavior of the longitudinal joints in the prefabricated composite steel box girder system and determine the level of post-tensioning required for proper system performance.

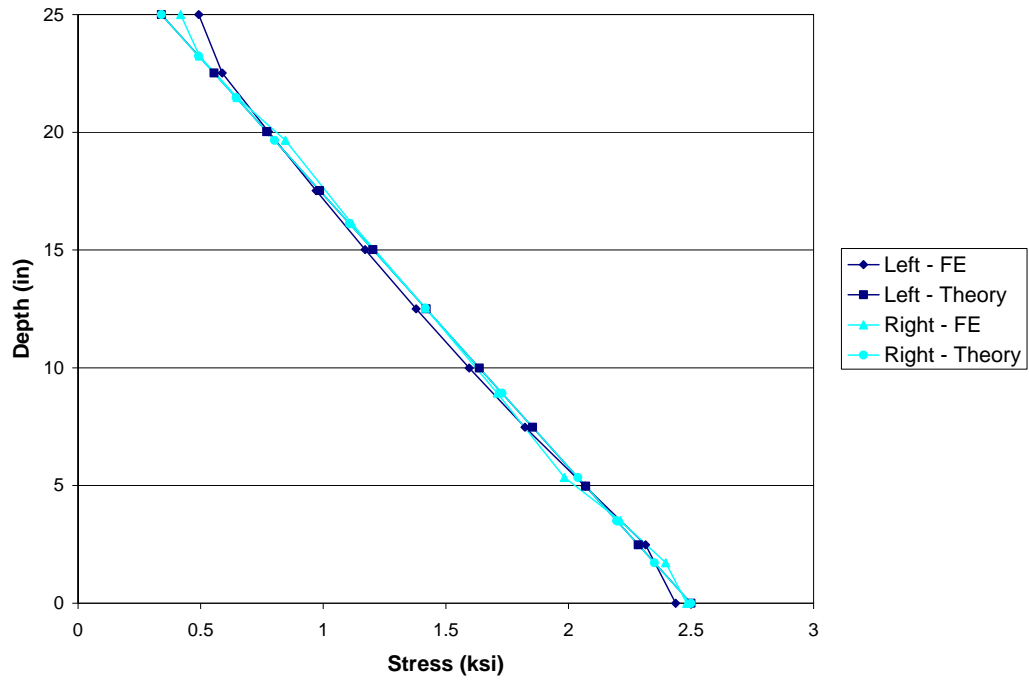


**Figure 77. Comparison of longitudinal stress in FE model**

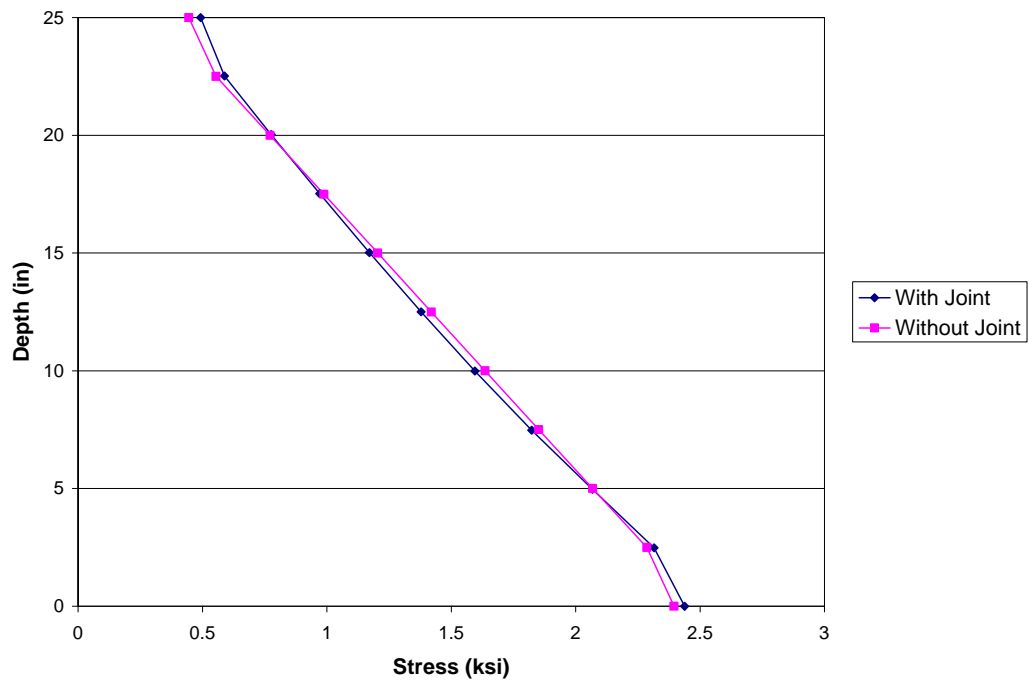


**Figure 78. Comparison of longitudinal stresses in models with and without joint**

#### 5.4.5 Model Characterization

Having established the functionality of the contact interaction when modeling joints, the research team began modeling a typical joint geometry that could be used in an actual bridge. The goal is to show that joints can be kept closed with a reasonable amount of post-tensioning. This will be done by performing a global analysis with detailed joint modeling in order to establish the post-tensioning force required to maintain closure of the joints under AASHTO service loading. If joint closure can be maintained, a full moment connection model can be assumed to carry out parametric studies.

To verify that the deck was acting as a continuous slab, and hence could be analyzed using a single shell-element deck two FE models were created with solid-element decks and shear-key type joints. Model 1 was a 50 ft bridge with double girder units, each individual girder spaced at 4 ft. Model 2 was a 100 ft bridge with single girder units and a girder spacing of 8 ft.

The joints were modeled to represent a typical shear key joint (type 2 or 3 from Section 5.3.1). The FE representation of such a joint can be seen in Figure 79. Although the FE model incorporates one male and one female side of the joint, in practice both flanges would likely be female, with a grouted “key” running through the void created by the two female flanges.

Globally, the models (particularly the 100-ft model) were very large and extremely cumbersome computationally. Therefore, it was advantageous to reduce the model using symmetry. With a symmetric geometry and an anti-symmetric loading, the model could be cut in half at mid-span, and given a shear-mechanism boundary condition. A completed model is shown in Figure 80.

By checking the system response under different levels of post-tensioning, the minimum amount of post-tensioning required can be determined. Therefore, multiple combinations of varying post-tensioning levels and loading conditions were prescribed. A matrix of these combinations is presented in Table 18. Finally, the element types and sizes can be found in Table 19.

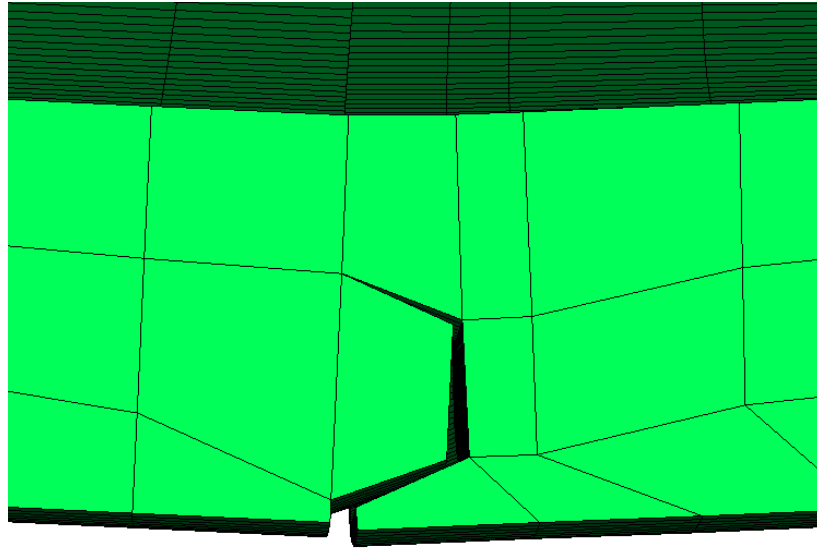


**Figure 79. FE Model of Shear Key Joint Opening Under Loading**

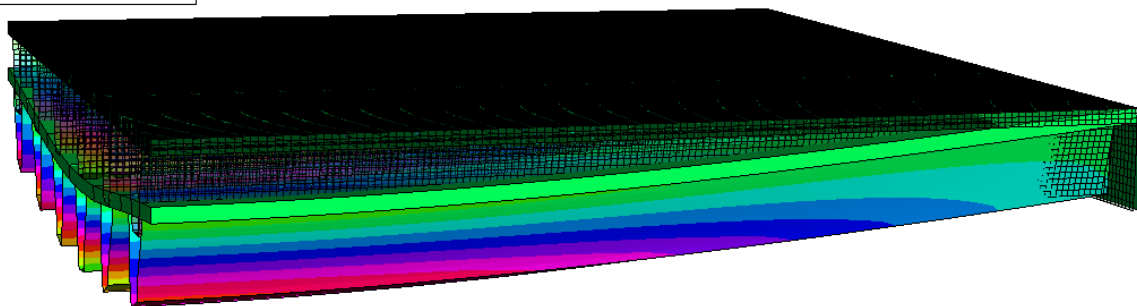
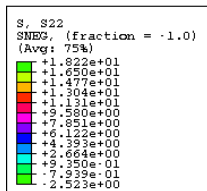


**Figure 80. FE Model of Bridge Model 9. Contours Represent Longitudinal Stress in ksi.**

**Table 18. Case Matrix of Post-Tensioning Levels and Loading Conditions**

Load Case	Post-Tensioning (ksi)	Loading Condition (AASHTO)
1	0.250	Service II
2	0.225	Strength I
3	0.200	Service II
4	0.175	Strength I
5	0.150	Service II
6	0.125	Strength I
7	0.250	Service II
8	0.225	Strength I
9	0.200	Service II
10	0.175	Strength I
11	0.150	Service II
12	0.125	Strength I

**Table 19. Element Data for Full Models with Solid Deck Elements**

Part	Material	Shell Thickness (in)	Element Type	Hourglass Control	Reduced Integration	Element Size (in)
Deck	Concrete	n/a	C3D8R	Active	Active	4.5
Tub	Steel	0.375	S4R	Active	Active	6
End Block	Concrete	24	S4R	Active	Active	4

## 5.4.6 System Response

### 5.4.6.1 General

The results of these analyses were favorable for this system. Three areas of interest were evaluated in order to determine the viability of the using shear-key joints in a prefabricated system such as the one being studied. They were:

Longitudinal Stress in Steel Tubs

Deflection Profile

Joint Opening

These parameters were derived for the two models with joints, and then compared to a model that was identical in geometry, except the jointed deck had been replaced with a deck slab which

was continuous over the width of the bridge. This approach aimed to show that a prefabricated system could function similarly to a superstructure with a traditional cast-in-place deck.

#### 5.4.6.2 Interpretation of Results

Figure 81 shows the location of the measurements taken to evaluate responses (1), (2), and (3). The first parameter studied was longitudinal stress in the steel tubs. The stress in each tub was extracted at mid-span, in the middle of the bottom (tension) flange. The second parameter studied was the vertical deflection of the bridge deck. The deflection at each node along the deck surface was extracted at mid-span. The third parameter studied was the joint opening along the span of the bridge. To obtain this data, the lateral coordinate of each node along either side of the joint was extracted, and the difference of the two was taken to be the joint opening. Hence, the value reported here represents the lateral distance between nodes, not the true distance between the two. Since there is minimal vertical differential between the nodes, this difference is negligible. To see the naming convention used to define each individual joint, see Figure 81. Also presented in the graphs of joint opening is an “acceptability threshold” as discussed in Section 3.7.

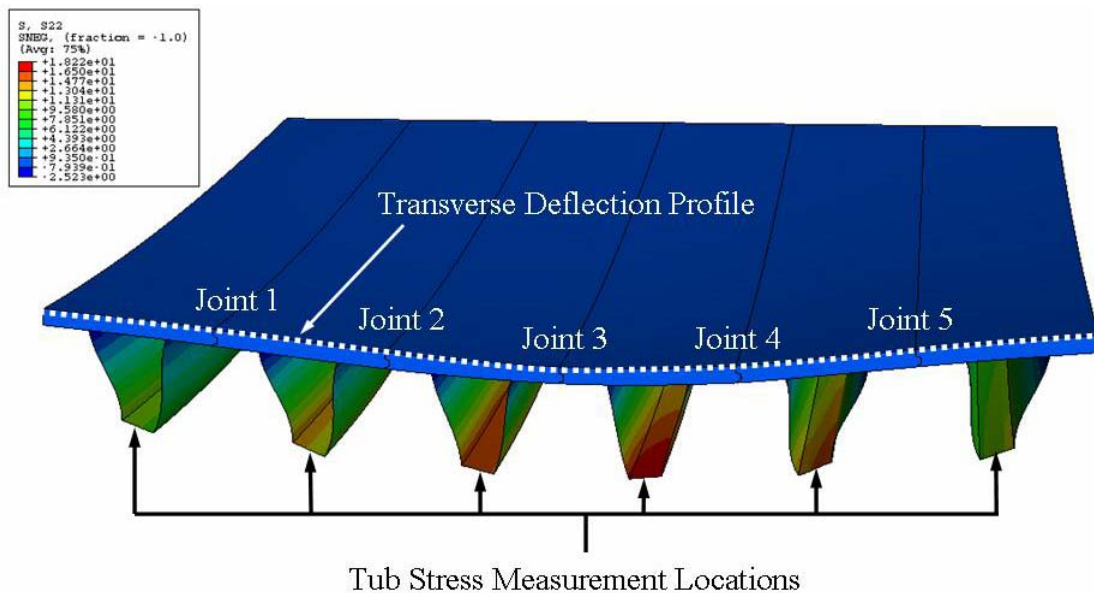


**Figure 81. Parameters Studied in Models with Joints**

### 5.4.6.3 50-ft Bridge Model

The results for the 50-ft bridge model are presented here. The FE model used to analyze this bridge is shown in Figure 82. The dimensions of the girders are those of bridge Model 1 of the parametric study. The model information can be found in Table 11. The deformed shape is also presented in Figure 83.

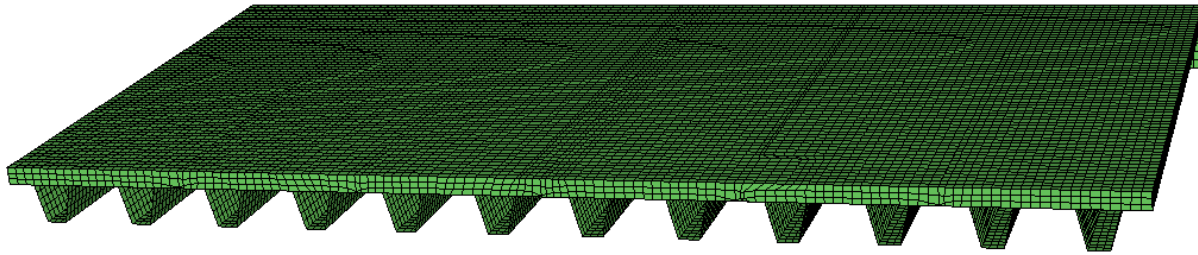


**Figure 82. FE Model with Solid Deck Elements and Joints Representing Model # 1**

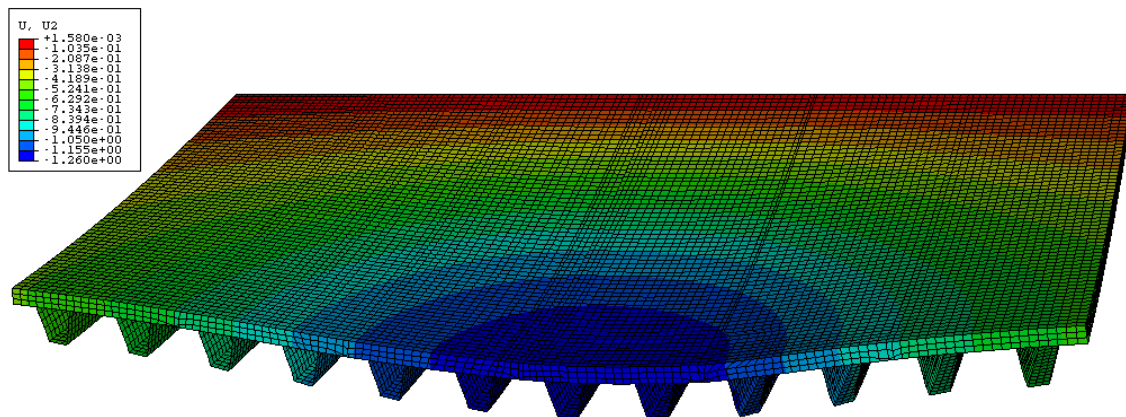


**Figure 83. Deformed Shape of Model in Figure 82. Contours Represent Vertical Displacement in Inches.**

As shown in Figure 84 and Figure 85, the stress in the tubs is largely unaffected by post-tensioning levels. The variation between the models with prefabricated decks is very small (less than 1 ksi). However, some of the tubs in the model with a continuous deck have stresses that differ greatly when compared with the corresponding tubs in the segmental models. The charts show a much more uniform distribution of stress across the width of the bridge when there is a continuous deck. However, the critical central tubs that experience the highest stress do not see a

significantly higher stress with the segmental deck. Therefore, using prefabricated girder units does not diminish performance when compared with a continuous-slab bridge of the same dimensions.

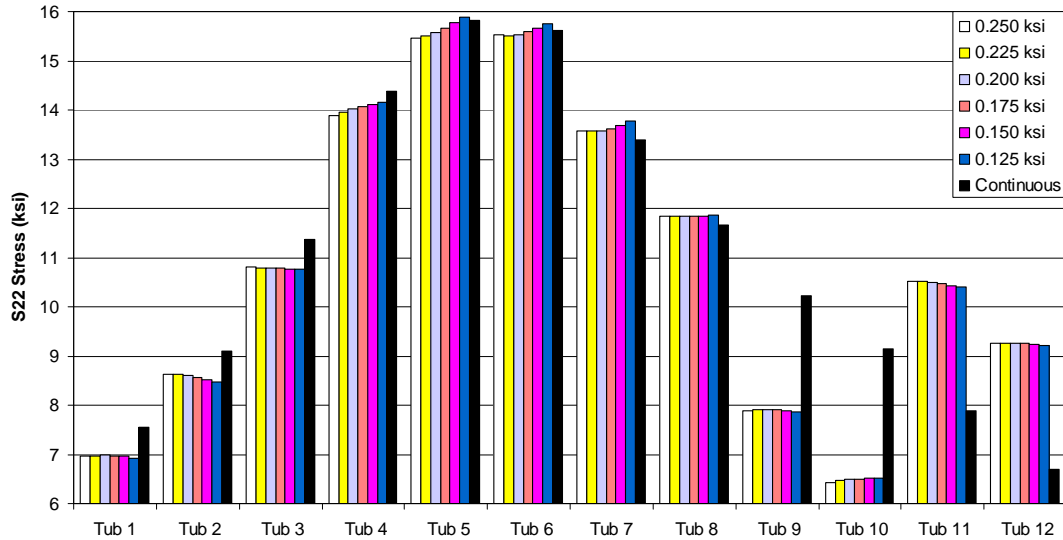


**Figure 84. Longitudinal Stress Variation by Girder (50-ft Model, Service Loading)**

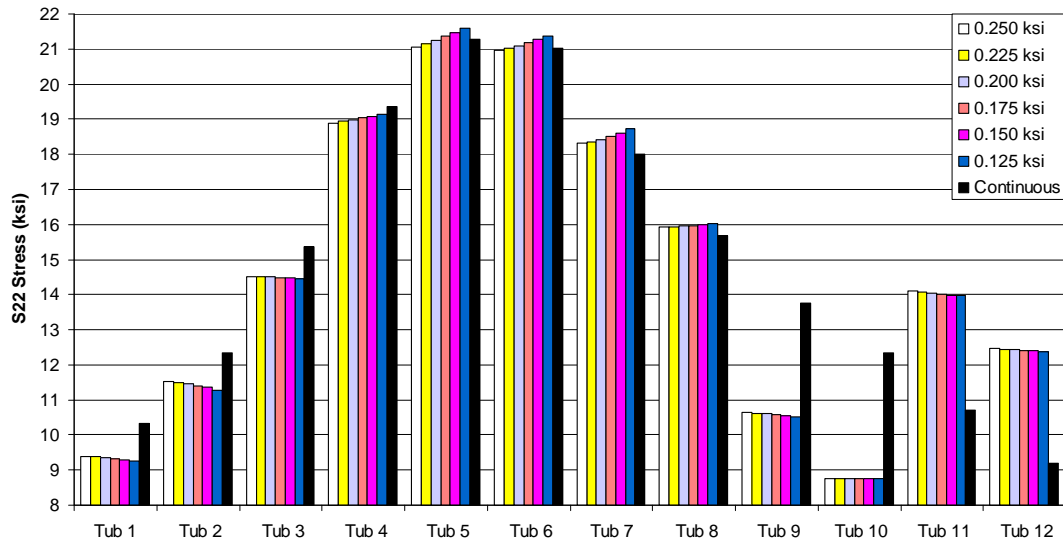


**Figure 85. Longitudinal Stress Variation by Girder (50-ft Model, Strength Loading)**

The deflection profile of the bridge deck is plotted in Figure 86 and Figure 87. As indicated by the graphs, it is again noticeable that the load is better distributed by the continuous slab deck. However, similarly to the longitudinal stresses, the maximum values of deflection do not differ significantly in the segmental model. The increase in maximum deflection for the model with 0.250 ksi of post-tensioning is about 0.025 inches over that of the model with a continuous slab. The increase in deflection of the model with the lowest post-tensioning, 0.125 ksi, is about 0.050 inches over that of the model with a continuous slab.

Another important trend in this data is the “kinking” of the deck profile at joint locations in the segmental models. This is most prominent in Figure 89 at 282 inches and 376 inches (the locations of Joint 3 and Joint 4). This kinking is undesirable, as it indicates the bridge superstructure is functioning as individual pieces and not one unified entity. This behavior occurs when the post-tensioning is 0.150 ksi or lower under service loading, and when the post-tensioning is 0.200 ksi or lower under strength conditions. Although this kinking may be tolerable under strength loading, it should be prevented under service conditions.

For the 50-ft span bridge, only Joint 3 and Joint 4 show significant opening, and the opening of those joints only have been presented. These plots of the joint opening along the span can be found in Figure 88 - Figure 91. As the plots show, the “acceptability threshold” developed by the research team was only exceeded under strength loading conditions at Joint 4. In this circumstance, models with a post-tensioning level of 0.200 ksi or lower do not meet the maximum opening criteria.

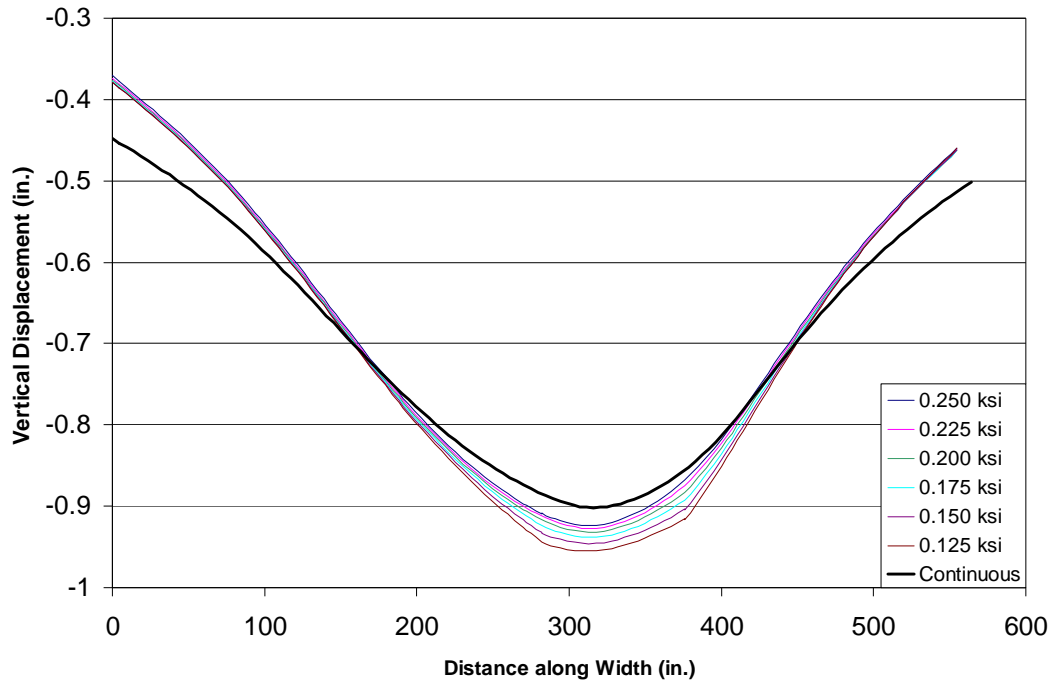


**Figure 86. Transverse Profile of Vertical Displacement at Midspan Under Varying Post-tensioning Levels (50-ft Model, Service Loading)**

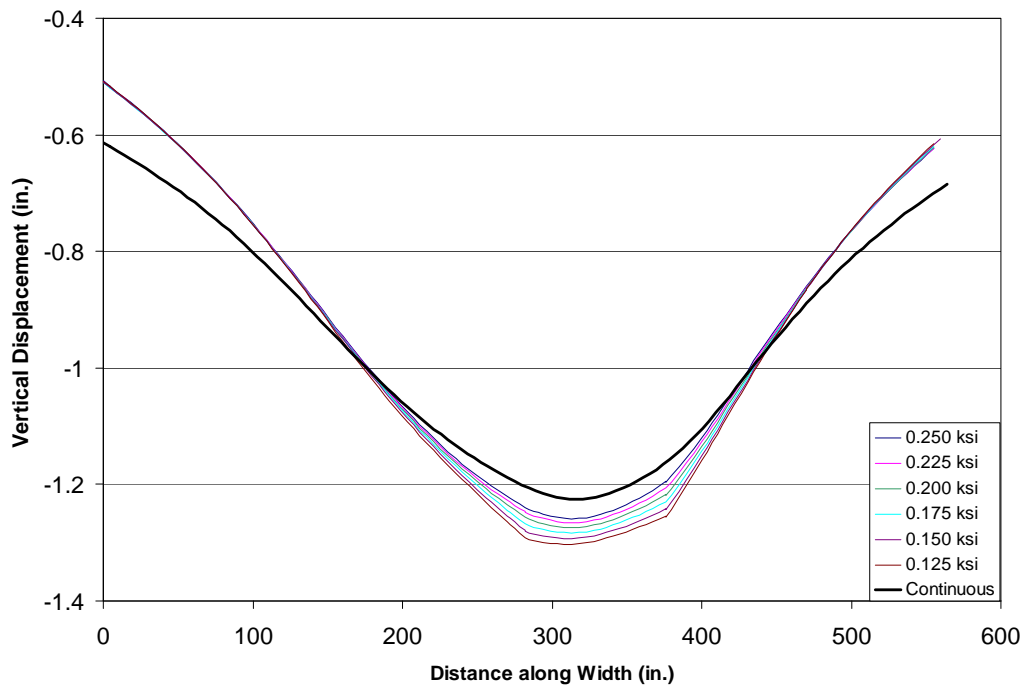


**Figure 87. Transverse Profile of Vertical Displacement at Midspan Under Varying Post-tensioning Levels (50-ft Model, Strength Loading)**

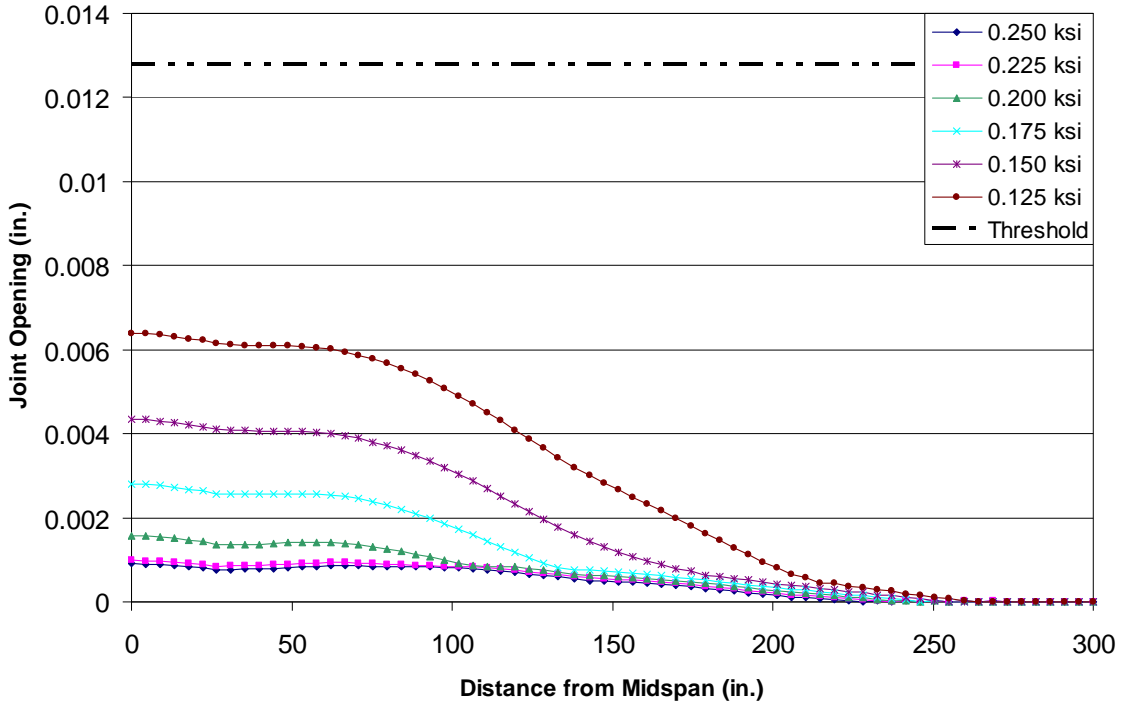


**Figure 88. Joint 3 Opening Along Span (50-ft Model, Service Loading)**

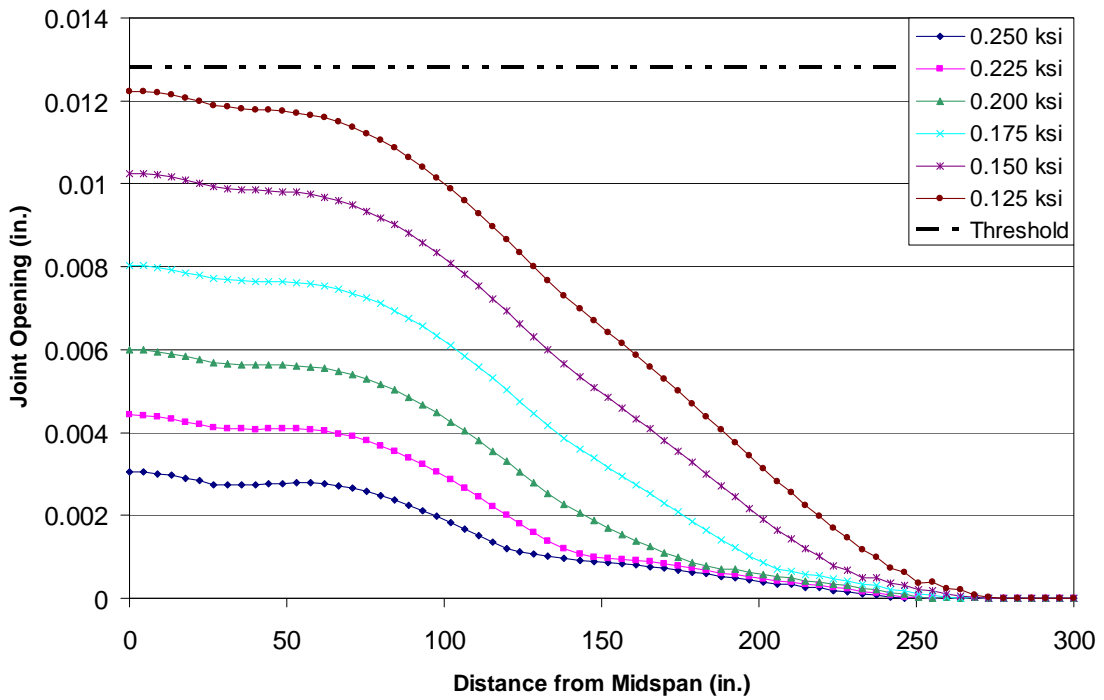


**Figure 89. Joint 3 Opening Along Span (50-ft Model, Strength Loading)**

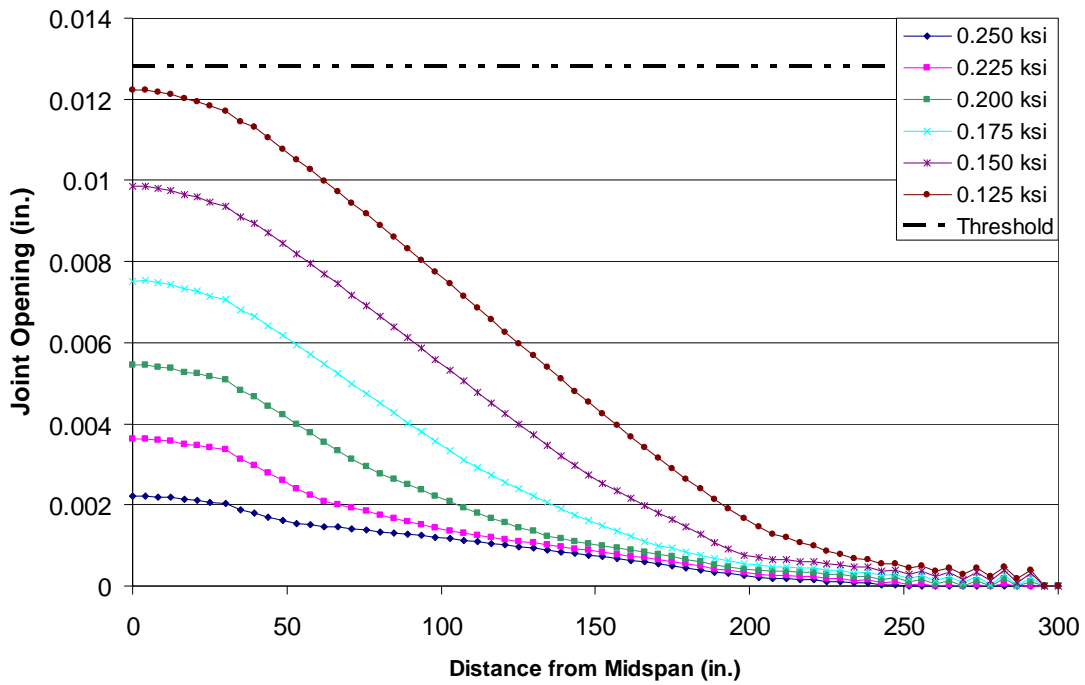


**Figure 90. Joint 4 Opening Along Span (50-ft Model, Service Loading)**

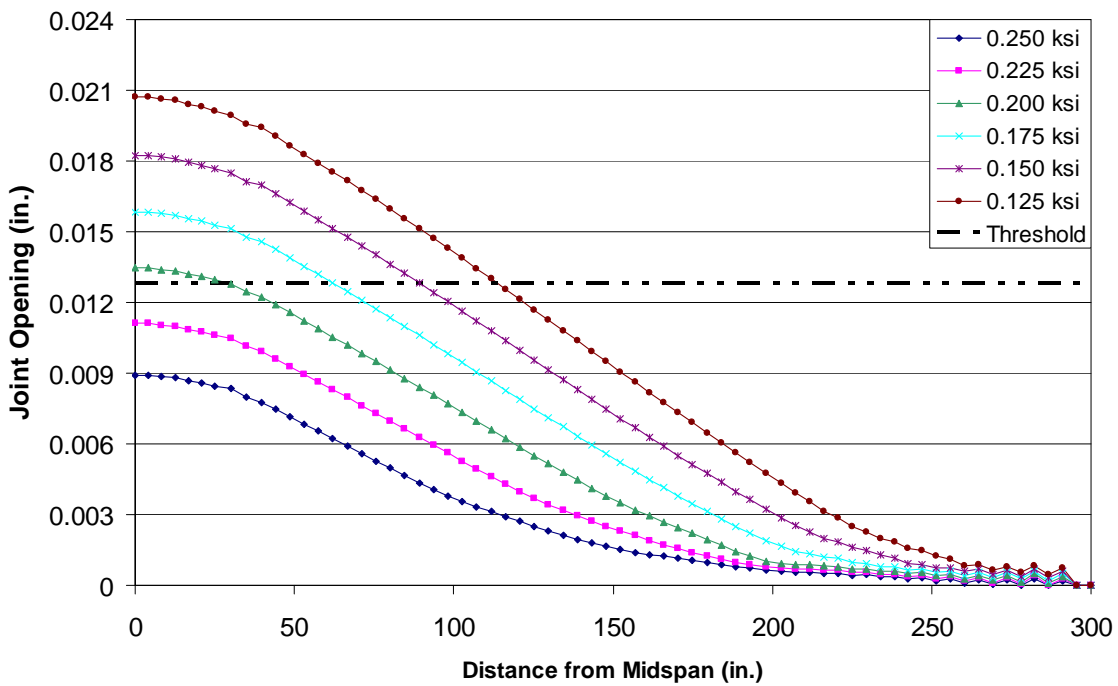


**Figure 91. Joint 4 Opening Along Span (50-ft Model, Strength Loading)**

#### 5.4.6.4 100-ft Bridge Model

The results for the 100-ft bridge model are presented here. The FE model used to analyze this bridge is shown in Figure 92. The dimensions of the girders are those of bridge Model 9 of the parametric study. These model information can be found in Table 11. The deformed shape is also presented in Figure 93.

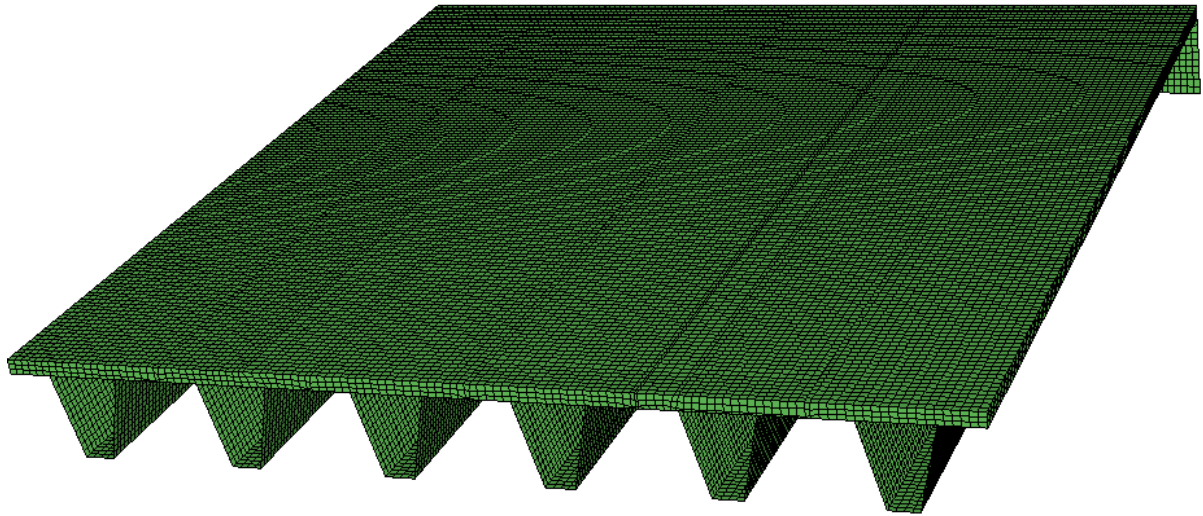


**Figure 92. FE Model with Solid Deck Elements and Joints Representing Model # 9**

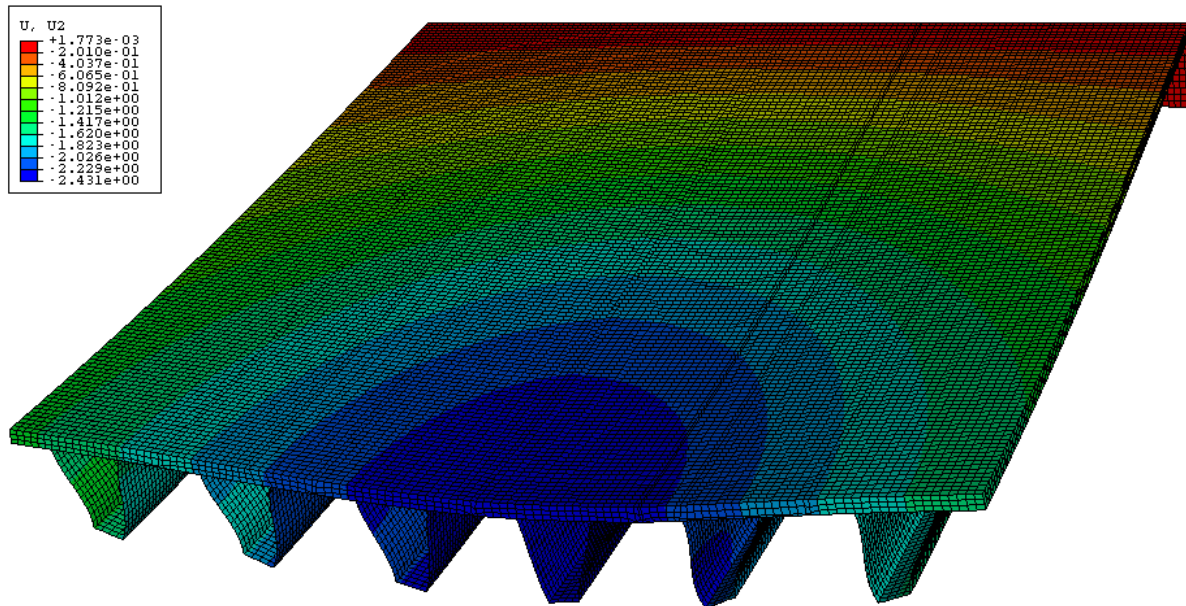


**Figure 93. Deformed Shape of Model in Figure 92. Contours Represent Vertical Displacement in Inches.**

The same parameters studied with 50-ft model were again evaluated for the 100-ft model. The first parameter studied was longitudinal stress in the steel tubs. As shown in Figure 94 and Figure 95, the stress in the tubs is largely unaffected by post-tensioning levels. As was the case in the 50-ft bridge, the variation between the models with prefabricated decks is very small (less than 1 ksi). Consequently, the same conclusions drawn in Section 5.3.4.1 can be drawn here: the segmental bridge does not distribute load as well, but the maximum stresses increase only slightly.

The second parameter studied was the vertical deflection of the bridge deck. The deflection at each node along the deck surface was extracted at mid-span and then plotted in Figure 96 and Figure 97. As indicated by the graphs, it is again noticeable that the load is better distributed by the continuous slab deck. However, similarly to the longitudinal stresses, the maximum values of deflection do not differ significantly in the segmental model. The increase in maximum deflection for the model with 0.250 ksi of post-tensioning is about 0.100 inches over that of the model with a continuous slab. The increase in deflection of the model with the lowest post-tensioning, 0.125 ksi, is about 0.125 inches over that of the model with a continuous slab.

Another important trend in this data is the “kinking” of the deck profile at joint locations in the segmental models. This is most prominent in Figure 97 at 282 inches and 376 inches (the locations of Joint 3 and Joint 4). This kinking is undesirable, as it indicates the bridge superstructure is functioning as individual pieces and not one unified entity. This behavior occurs when the post-tensioning is 0.175 ksi or lower under service loading, and when in all cases under strength conditions. Although this kinking may be tolerable under strength loading, it should be prevented under service conditions.

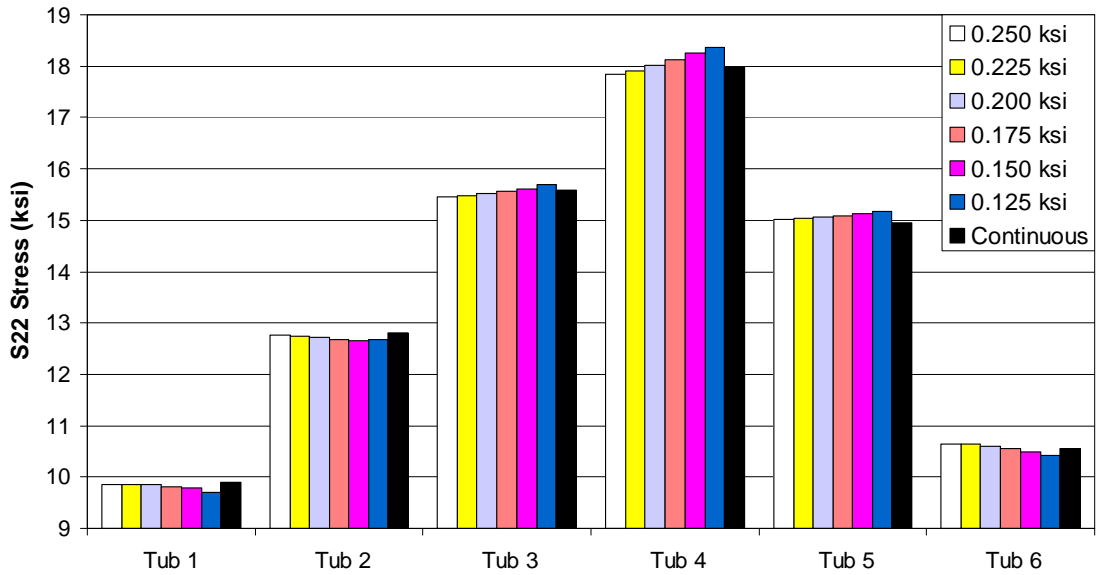


**Figure 94. Longitudinal Stress Variation by Girder (100-ft Model, Service Loading)**

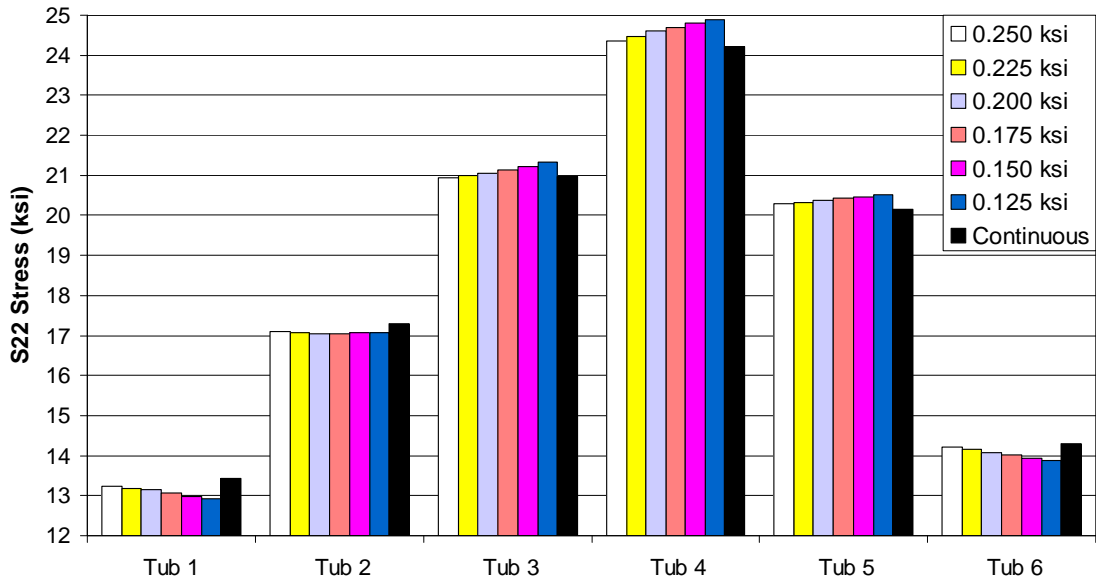


**Figure 95. Longitudinal Stress Variation by Girder (100-ft Model, Strength Loading)**

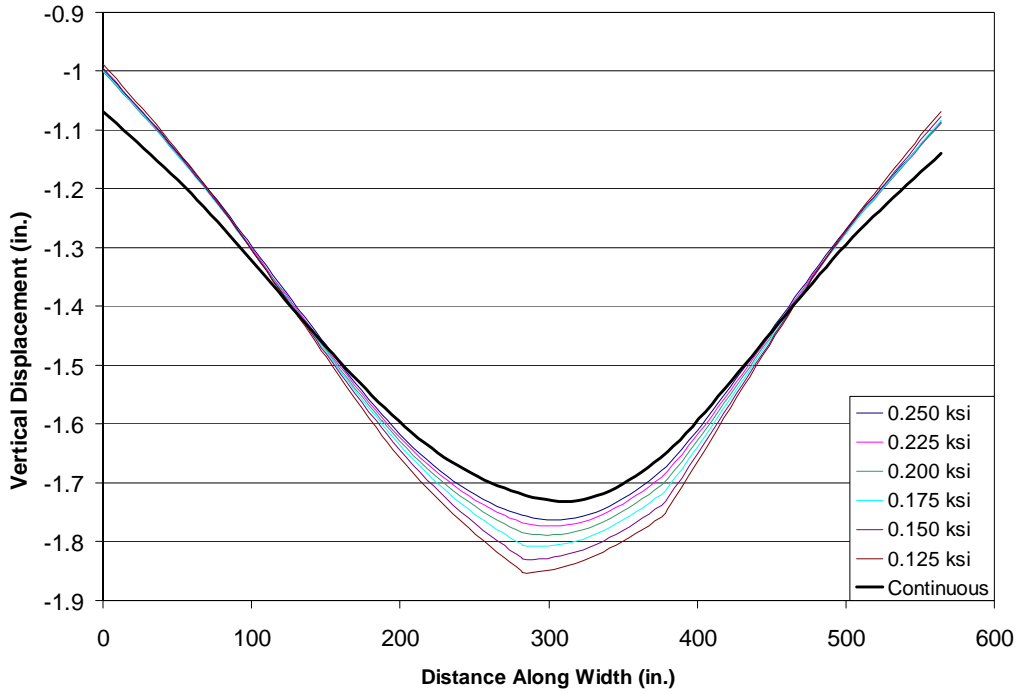


**Figure 96. Transverse Profile of Vertical Displacement at Midspan Under Varying Post-tensioning Levels (100-ft Model, Service Loading)**

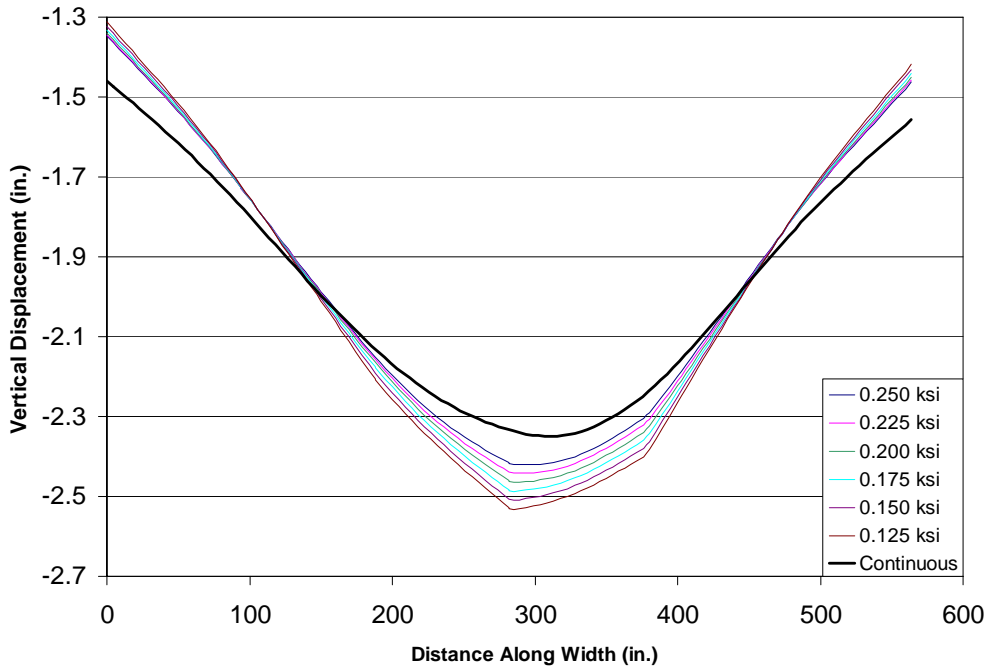


**Figure 97. Transverse Profile of Vertical Displacement at Midspan Under Varying Post-tensioning Levels (100-ft Model, Strength Loading)**

The third parameter studied was the joint opening along the span of the bridge. The joint naming scheme is shown in Figure 81. In this bridge, Joints 2, 3, and 4 showed significant opening. Plots of the joint opening along the span can be found in Figure 98 - Figure 103.

As the plots show, the threshold is exceeded under service loading conditions at Joint 3 and Joint 4. However, models with a post-tensioning level of 0.175 ksi or higher always meet the maximum opening criteria under service loading. In contrast, strength loading causes all models to exceed the criteria at Joint 4, and all but the 0.250 ksi post-tensioning fail at Joint 3. Again, this criteria applies more directly to service loading than to strength loading, so this analysis indicates that 0.175 ksi should be sufficient for post-tensioning a 100-ft span bridge such as the one model. Joint 2 never opens far enough to exceed the criteria. It should be recalled that this criterion is simply a guideline from the research team, not an official standard.

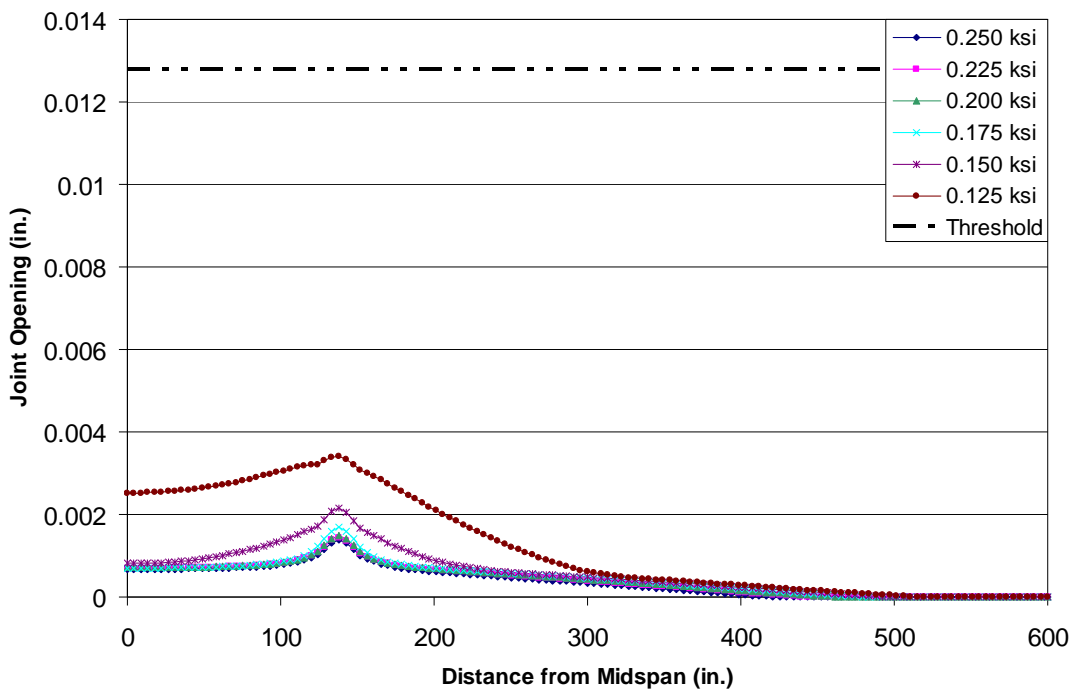


**Figure 98. Joint 2 Opening Along Span (100-ft Model, Service Loading)**

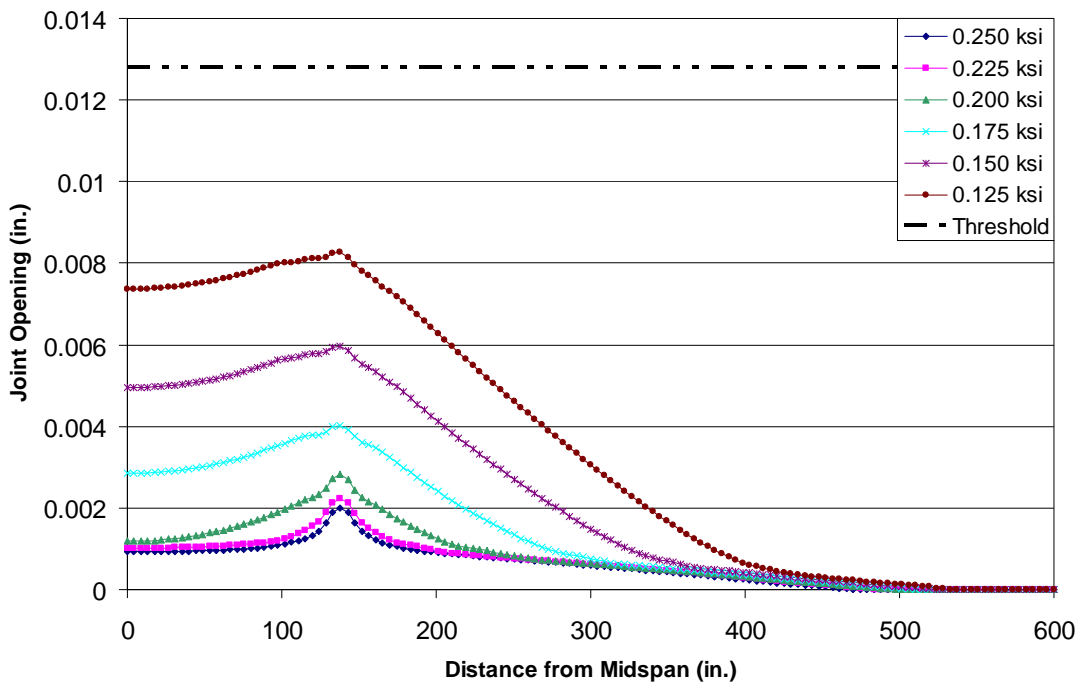


**Figure 99. Joint 2 Opening Along Span (100-ft Model, Strength Loading)**

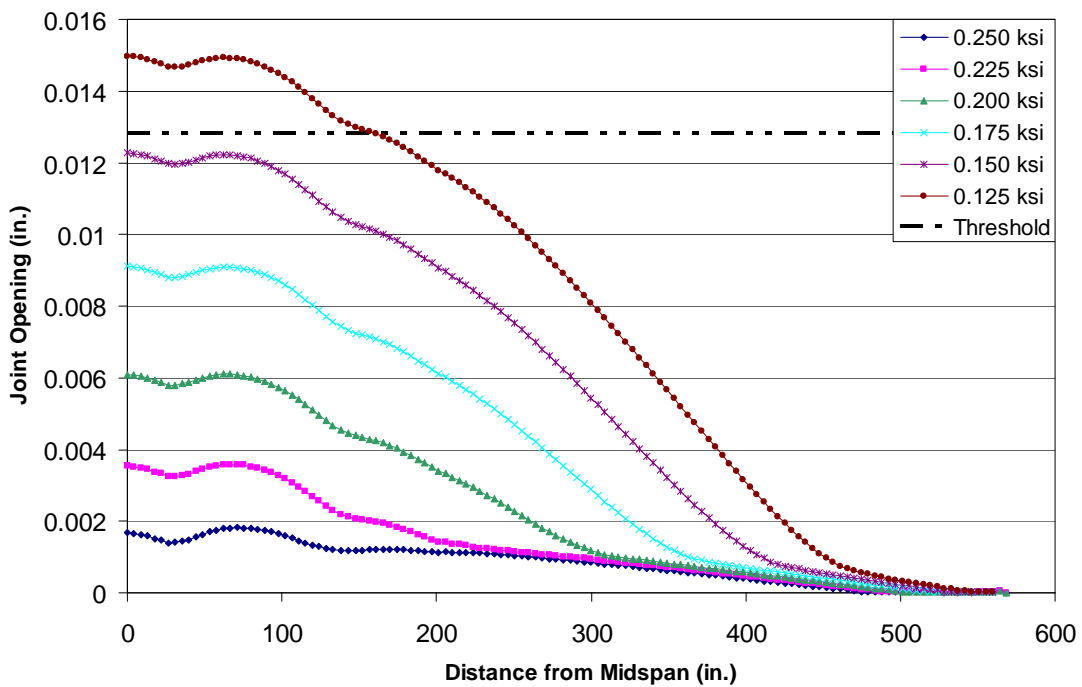


**Figure 100. Joint 3 Opening Along Span (100-ft Model, Service Loading)**

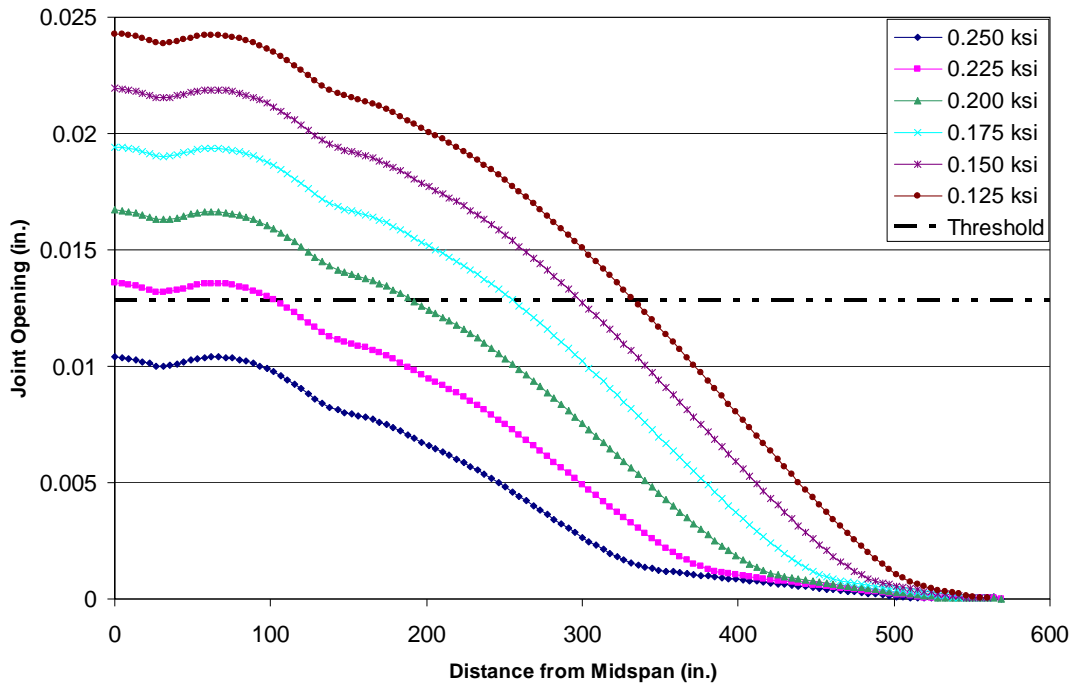


**Figure 101. Joint 3 Opening Along Span (100-ft Model, Strength Loading)**

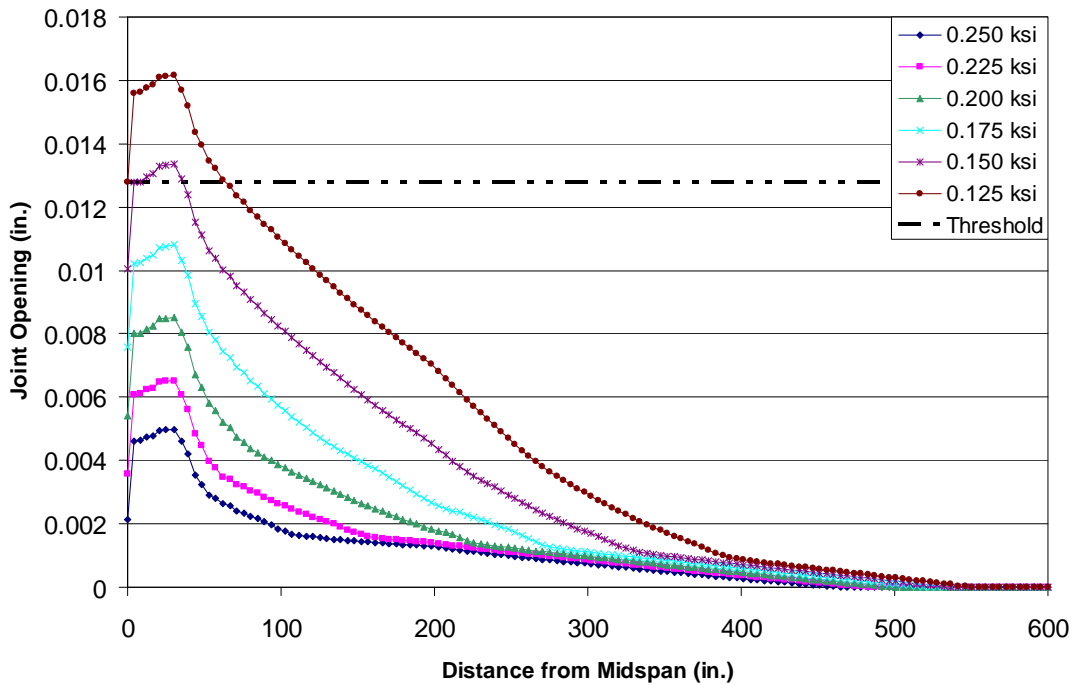


**Figure 102. Joint 4 Opening Along Span (100-ft Model, Service Loading)**

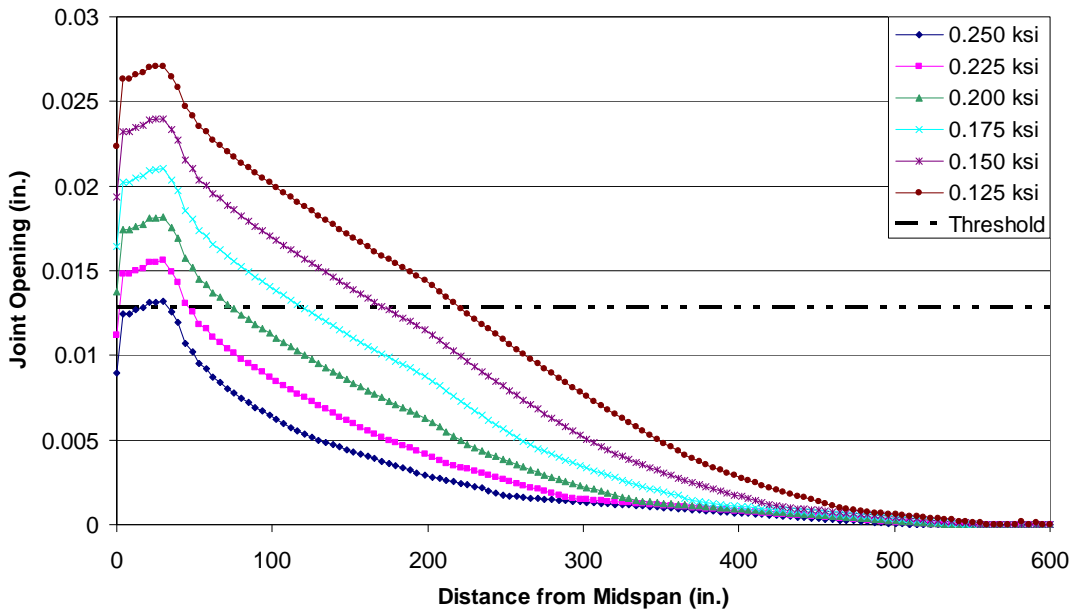


**Figure 103. Joint 4 Opening Along Span (100-ft Model, Strength Loading)**

### 5.5 Vibration Characteristics

The last task performed with the two FE models with solid decks (Section 5.3) was to determine the fundamental frequencies and mode shapes of these bridge systems. This was performed in ABAQUS using a linear perturbation step that was capable of running an eigenvalue analysis on the system mass matrix. Since Section 5.3.4 showed that continuity could be established with adequate post-tensioning, the dynamic analyses were performed on the models with continuous slabs. This avoided computational difficulties that arise out of modeling the base state of a segmental model.

The first three bending mode shapes were extracted, eliminating other mode shapes that were not of concern (i.e., transverse/longitudinal stretching). The first three mode shapes, and the corresponding fundamental frequencies for the 50-ft bridge model are presented in Figure 104-Figure 106 and Table 20, respectively.

**Table 20. Fundamental Frequencies of the First Three Bending Mode Shapes, 50' Bridge Model**

Bending Mode	Fundamental Frequency	
	rad/time	cycles/time
Mode 1:	28.450	4.5280
Mode 2:	48.714	7.7530
Mode 3:	68.467	10.897

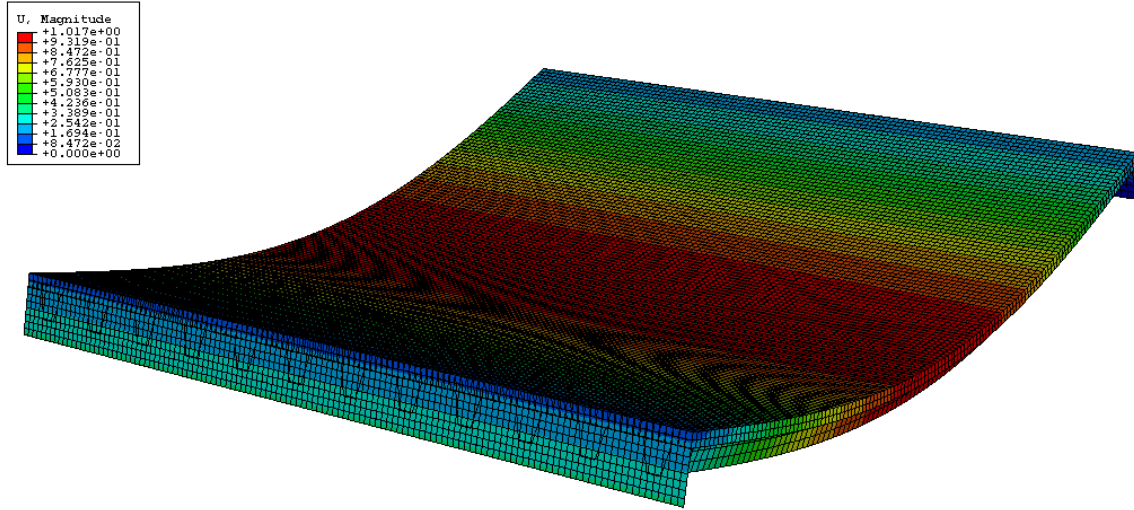


**Figure 104. Bending Mode Shape 1, 50' Bridge Model**

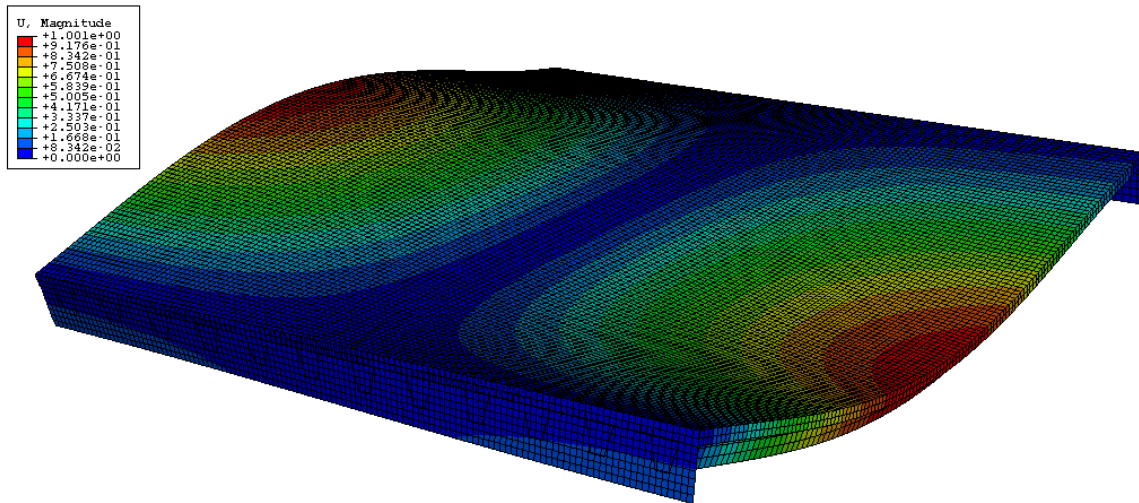


**Figure 105. Bending Mode Shape 2, 50' Bridge Model**

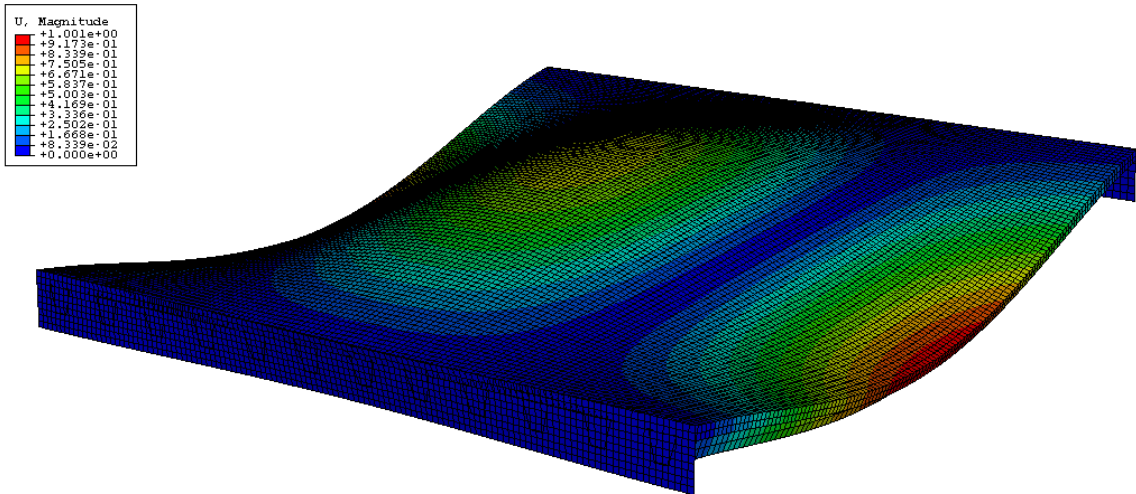


**Figure 106. Bending Mode Shape 3, 50' Bridge Model**

As the above figures show, the three bending mode shapes correspond to the first longitudinal bending mode, followed by the first two transverse bending modes. This is the qualitative expected result. To better visualize the bending behavior in Mode 2 and Mode 3, Figure 107 and Figure 108 are provided.

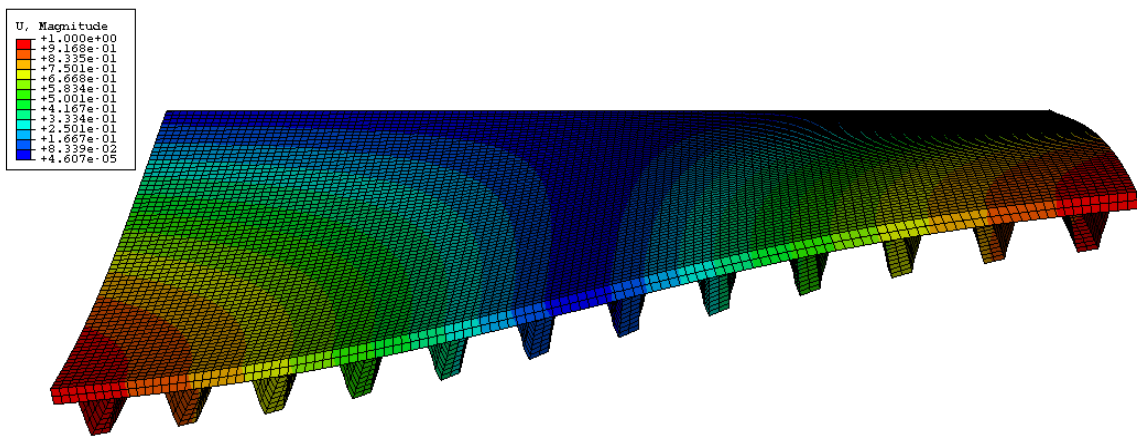


**Figure 107. Bending Mode 2 Cross-Section**

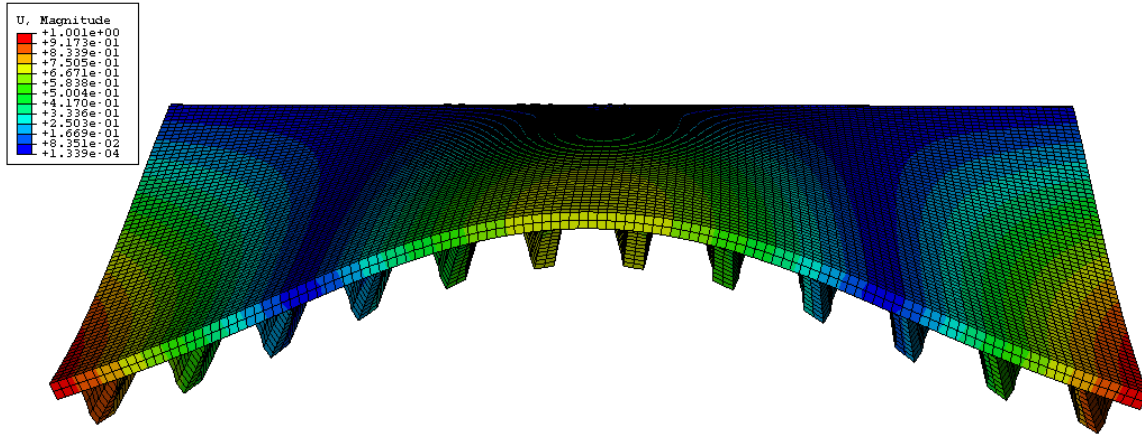


**Figure 108. Bending Mode 3 Cross-Section**

Qualitatively, the results of the dynamic analysis on the 100-ft model yielded the similar results. However, the value of the frequencies decreased significantly. The first three mode shapes, and the corresponding fundamental frequencies for the 100-ft bridge model are presented in Figure 109-Figure 111 and Table 21 , respectively.

**Table 21. Fundamental Frequencies of the First Three Bending Mode Shapes, 100' Bridge Model**

Bending Mode	Fundamental Frequency	
	rad/time	cycles/time
Mode 1:	16.312	2.5962
Mode 2:	28.679	4.5644
Mode 3:	45.434	7.2310

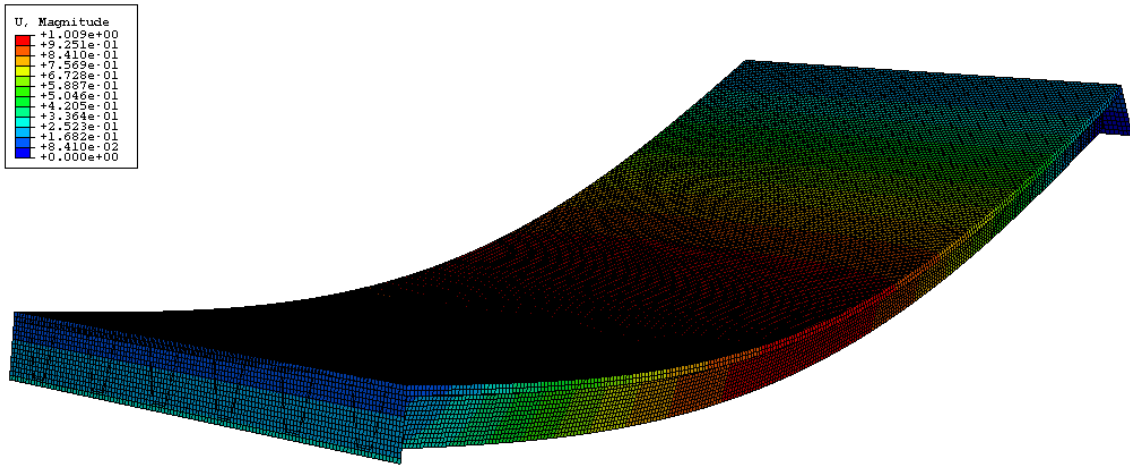


**Figure 109. Bending Mode Shape 1, 100' Model**

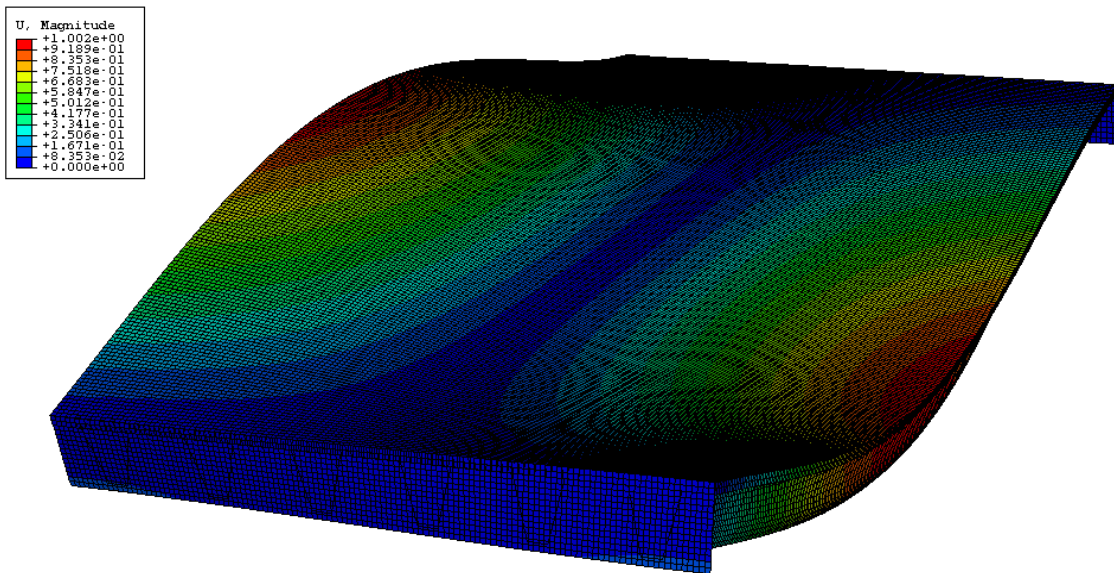


**Figure 110. Bending Mode Shape 2, 100' Model**

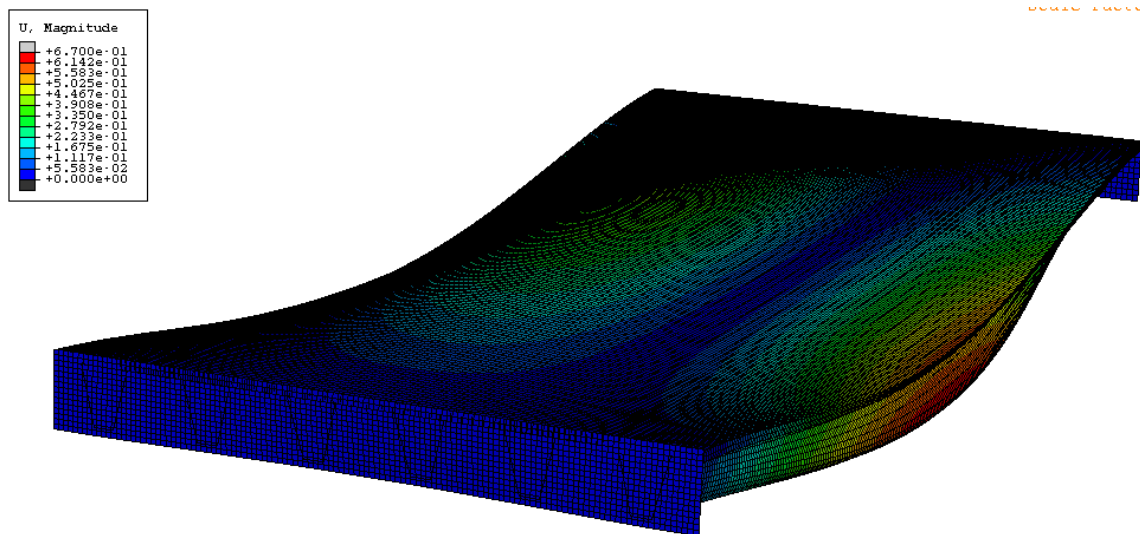


**Figure 111. Bending Mode Shape 3, 100' Model**

## 5.6 Dynamic Load Amplification Issues

The dynamic action of moving loads on bridges has long been recognized and the interaction of moving loads and the bridge superstructure results in dynamic amplification of the moving loads and thus increased stresses (AASHTO 1998, CAN/CSA-S6 1988, OHBDC 1983). The dynamic load allowance given in codes is generally a function of the span of the bridge or the natural frequency of the bridge dynamic interaction. Several methods have been developed to evaluate dynamic load amplification effects including vehicle and bridge. Some of these models are quite complex since they involve detailed modeling of the vehicles speed, mass, and suspension in addition to all other parameters governing the dynamic behavior of the bridge. Further, roadway roughness and pavement irregularities have a strong influence on the dynamic amplification effect.

In spite of the many parameters affecting the dynamic response of the bridge, the dynamic amplification effect has been most commonly related to the fundamental vibration frequency of the bridge. The Ontario Highway Bridge Design Code has recognized the significant influence of the natural frequency of the bridge superstructure on its dynamic response, and its 1983 edition specified values of impact factor based on the first flexural frequency of the bridge. This criterion is shown graphically in Figure 112. However, this provision has been changed and new

empirical values of the dynamic load allowance have been prescribed. It can be seen that the dynamic response of the systems evaluated in this study are approximately the same as the prescribed AASHTO amplification factor of 33%.

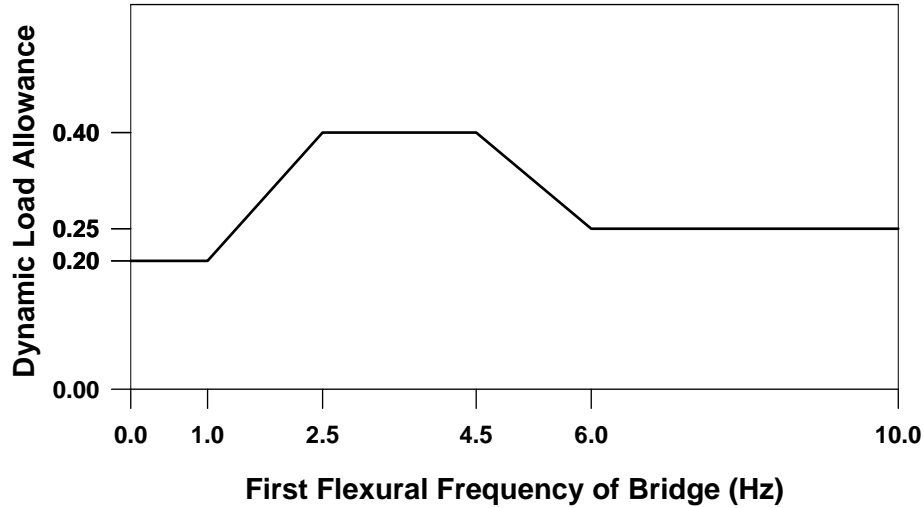


**Figure 112. Dynamic Load Allowance according to OHBDC (CAN/CSA-S6, 1988)**

Other studies have estimated the dynamic amplification factor by relating the maximum system deformation under dynamic loading to that under maximum static deformation. The dynamic load amplification can then be estimated based on the fundamental vibration characteristics of the bridge according to (Seible et al., 1990):

$$DMF = \frac{1}{1 - (V / 2Lf_b)} \quad (5-10)$$

where  $V$  is the moving load speed,  $L$  is the simply supported beam span and  $f_b$  is the bridge fundamental vibration frequency.

Using a speed of 90 mph the dynamic amplification factors for the 50 ft and 100 ft bridges considered in the dynamic characterization studies would yield dynamic magnification factors of 25 and 21 percent, respectively. Both of these are less than the prescribed AASHTO value. Thus, this preliminary analysis of the dynamic properties of the prefabricated system under study indicates that dynamic behavior and its effect on dynamic load amplification do not seem to be a concern.

## 6. CONCLUSIONS AND RECOMMENDATIONS

### 6.1 Observations

After performing the analyses detailed in Chapter 5, the following observations can be drawn after evaluating the obtained results:

The simplified analysis method presented in the AASHTO LRFD Design Specifications (AASHTO, 1998) were found to be generally applicable for analyzing the prefabricated composite steel box girder bridges studied in this work. However, this method seems to be lacking when it comes to distribution factors. Due to their geometry, box girders distribute load differently than traditional W-shape girders, or bulb-shape girders that are often used in highway bridges. Hence, their distribution factors require additional research. Nevertheless, it appears that minimal research has gone into the development of distribution for these bridges, as evidenced by the single “blanket” equation to describe the distribution of both moment and shear demands to interior and exterior girders alike. Therefore, it is recommended that a refined analysis is performed to accompany an AASHTO analysis of a composite box girder bridge system.

The grillage method is a well-established simplified method for analyzing bridge structures. By idealizing a structure into a set of beam elements, the number of degrees of freedom in a system can be greatly reduced. This subsequently reduces the number of equations that need to be solved in order to complete a system analysis, which in turn reduces computation time. However, with the increase in computing technology, running more refined three-dimensional finite element analyses with continuum-type elements does not significantly increase computation time. In addition, when compared with grillage models, an experienced user can create complex continuum-type finite element models with relative ease. Therefore, it is recommended that when performing analytical evaluations similar to the type performed in this project, the finite element method should be used in lieu of the grillage method.

## 6.2 Recommendations for Design

The results of the parametric analysis in Section 5.3 indicate that at the global level, the composite steel box girder system can easily be designed in a way that will allow it to perform within the AASHTO specifications for stress and deflection. As seen in the figures and tables of Section 5.3.3, adequate designs have been developed for a range of spans and girder spacing. In addition, several of the span/spacing combinations have been satisfied using the same girder, indicated that a single girder could be versatile enough to be manufactured in bulk and used in a variety of situations. The frequency analyses that were performed also returned acceptable results. Therefore, the design should be controlled by ensuring satisfactory behavior of the joints.

In Section 5.4, the joint behavior was investigated. First, the prefabricated bridges were compared with another bridge model which was identical, with the exception that the deck was replaced with a continuous slab. This was done to study the continuity that could be achieved with a transversely post-tensioned longitudinal joint as the connection element between the prefabricated girder/deck units. As noted in Section 5.4.4, the AASHTO LRFD Bridge Design Specifications require that this type of joints be provided with a minimum of 0.250 ksi pressure of transverse post-tensioning (after all losses). As seen in Section 5.4.4, the prefabricated bridges were able to achieve continuity close to that of the continuous slab bridge with stress values across the joints lower than the AASHTO specified level. Stress and deflection profiles remained largely unchanged between the segmental models and the continuous models. However, when the level of post-tensioning gets too low (below 0.150 ksi in the 50 foot model, below 0.175 ksi in the 100 foot model) a kinking behavior occurs at the joints, which is undesirable. Hence, a post-tensioning level which is greater than these values should be specified.

As described in Section 5.4.4.2, a benchmark limit to judge the adequacy of the joint closure was proposed by the research team. Based on the AASHTO LRFD Bridge Design Specifications for crack opening in a reinforced concrete structures, it was recommended that this limit should not be exceeded under service conditions at the longitudinal deck joints connecting the prefabricated girder/deck bride units. Using this guideline, the transverse post-tensioning level should not fall below 0.175 ksi for the 100 foot model. All post-tensioning levels studied passed this criterion for the 50 foot bridge.

Summarizing the analysis results, the 50 foot bridge is controlled by kinking behavior at the joints. This occurs at a post-tensioning level of 0.150 ksi, which is then considered the minimum design value for this span length. The 100 foot bridge model is controlled by both kinking behavior and joint opening. These both become unacceptable at post-tensioning levels of 0.175 ksi. This level should be the minimum design value for these bridges of this length. These results are logical in that the transverse post-tensioning stress level required to maintain an emulative reinforced concrete joint increases with span length.

In summary, this study has confirmed that prefabricated steel/concrete composite girder/deck units that are connected together with longitudinal deck joints are safe and viable option for rapid bridge construction. The parametric studies indicated that adequate performance can be obtained for short spans ranging from 50 to 100 ft. Transverse diaphragms can improve load distribution and thus lower the moment demands on individual girder/deck units. However, cost-benefit assessment of the added time to bridge construction related to the addition of the diaphragms compared to the improved efficiency gained needs to be evaluated. The vibration characteristics of the prefabricated systems indicated that the joints are fully active and thus the behavior of the system is no different than a fully continuous bridge. Thus, there are no concerns with added fatigue damage due to the prefabricated nature of these bridge systems. For the short spans for which the prefabricated steel/concrete composite sections are considered, transversely post-tensioning level required by the AASHTO code will provide full emulative behavior of the joint. While the results from this investigation indicate that lower post-tensioning stress levels may be adequate, it should be mentioned that the current study has not considered concrete volume effects on the post-tensioning force and its influence on joint behavior. These considerations should be done before a reduced post-tensioning level from that recommended by AASHTO can be fully justified.

While the concerns leading to critique cited above are reasonable, the overall conclusion that that the shallow prefabricated superstructure systems using cold bent plates do not meet AASHTO requirements for highway bridge systems seems overarching. Concerns related to fatigue of the cold bent plates can be addressed by increasing the radii of the bent, which can be easily provided given the outer sloping geometry of the tub girder webs. In addition, there are published studies with information on the fatigue behavior of cold bent members that can assist this design issue (Hassan et al.. 1998). Regarding capacity, the flexural performance of shallow

prefabricated systems such as the Con-Struct system has been shown via experiments to be adequate and to satisfy with AASHTO criteria (Burgueño and Pavlich, 2006). The inefficiency of the box sections for straight bridges is true but its impact in cost does not seem to be consistent with the noted critique. Implementations of the Con-Struct system thus far have indicated that the system is cost competitive with conventional solutions as well as other prefabricated systems (Nelson, 2006). Finally, the issue of inspection is one that can certainly be circumvented via the provision of access holes at the girder ends for the use of robotic inspection systems. Furthermore, the difficulty in inspecting shallow U-shape steel bridges is no different than the inability to inspect prestressed concrete box girders, whose void is actually inaccessible with a foam block that could trap moisture and lead to corrosion of the steel reinforcement. Thus, inspection of the system alone should not be seen as a deterrent for consideration of the system under study.

Thus, there are certainly certain issues that can initially raise the attention of bridge engineers on the suitability of prefabricated bridge systems using shallow U-shape cold bent steel girders. These include fatigue issues with the cold-bent plates, the efficiency of box sections, and the difficulty of internal inspection of the shallow depth box girders. However all of these concerns can be logically addressed as discussed in Section 2.3.6. These observations, together with the adequate performance observed through experiments and simulations support the feasibility of this type of system as a rapid-construction alternative to highway bridges.

### **6.3 Recommendations for Future Work**

To further the state-of-the-art in this field, several items for future work are possible: The work in this project has allowed evaluation of the prefabricated bridge concept only through numerical simulations. However; there are many aspects of the modeling and theory behind the simulation that need to be verified. For example, the analytical models used to assess the global behavior of the bridge system should be trusted to a high degree of accuracy. However, the detailed 3D stress models used to evaluate joint behavior should be confirmed experimentally. Although the contact interaction used in the finite element models of the joints should give accurate results, it is recommended that they are checked. Thus, experimental verification on the system and connection behavior that parallel the analytical evaluation conducted in this study is recommended.

It is proposed that any experiment used to verify the work done in this project be designed to address and confirm the following findings from the project:

1) Component Stiffness: The numerical models should closely match with experimental results. However, longitudinal shear slip, nonlinear deformations, and other factors could affect the system response.

2) Joint Behavior: The analytical models in the project showed that adequate joint closure could be achieved with the levels of post-tensioning that were specified. The actual joint openings should be checked experimentally. Further, the performance of these types of joints under fatigue loading and volume concrete changes should be experimentally assessed.

3) System Response: The analytical models indicated that a kinking occurs at low post-tensioning levels. The actual limits of needed post-tensioning for adequate behavior should be verified. Thus, system-level experiments that permits understanding joint behavior under realistic loading simulation and load distribution effects on multiple girders needs to be performed.

Finally, the Cons-Struct System by NES has gained interest from private parties and local governments, and a few prefabricated bridge systems with reinforced concrete joints (not transversely post-tensioned) have been built in heavy traffic locations. Thus, opportunities to gain further knowledge on this type of bridge system might be gained from field demonstration project(s) together with instrumentation monitoring of existing or new projects.

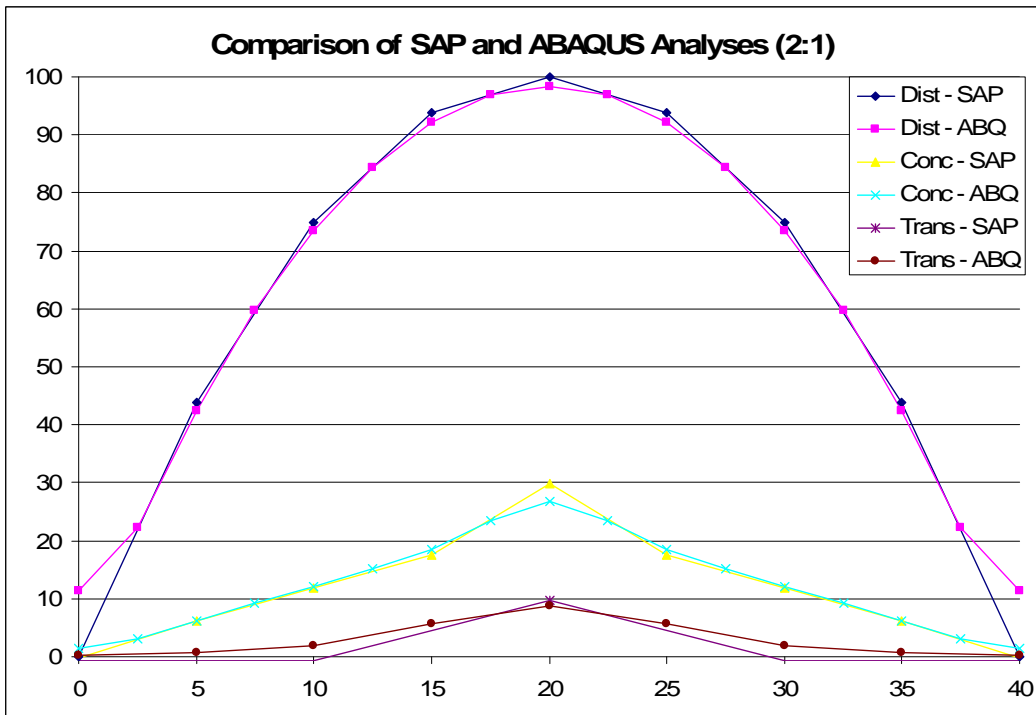
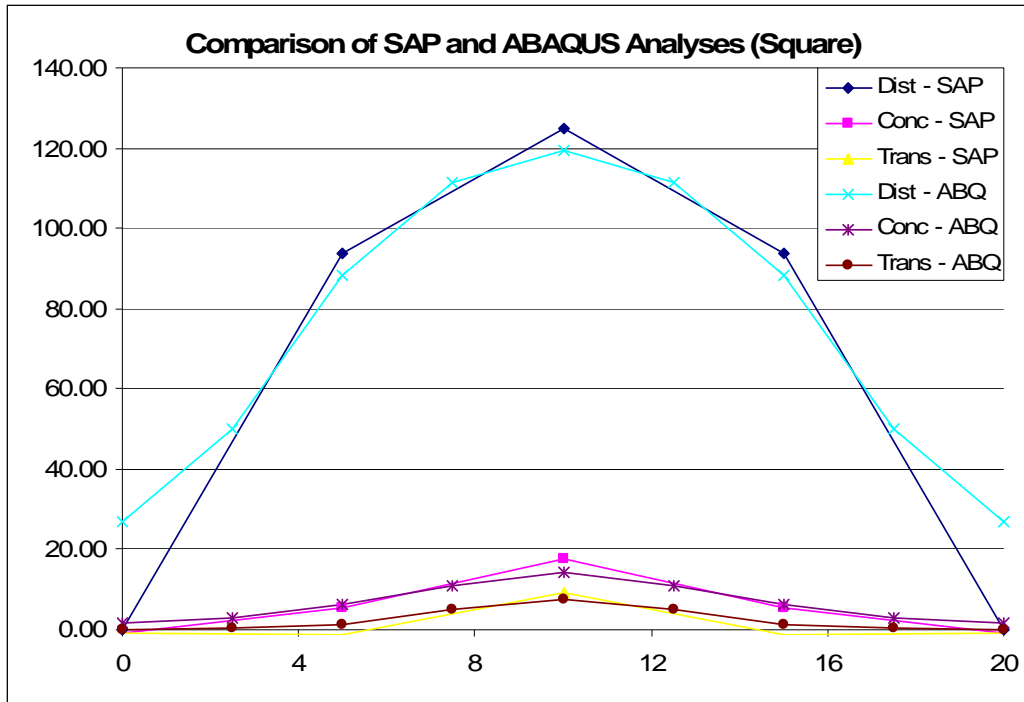
## REFERENCES

- AASHTO Technology Implementation Group (TIG), “Prefabricated Bridges – Get in, get out, stay out,” American Association of State Highway and Transportation Officials, Washington, DC, May 2002.
- American Association of Highway Transportation Officials (AASHTO), AASHTO-LRFD Bridge Design Specifications – 2nd Edition, Washington DC, 1998.
- Badie, S.S., Kamel, M.R., and Tadros, M.K. (1999). “Precast Pretensioned Trapezoidal Box Beam for Short Span Bridges”, *PCI Journal*, 44(1): 48-59.
- Barker, R.M. and Puckett, J.A. (1997) Design of Highway Bridges. John Wiley & Sons. New York, NY.
- Burgueño, R. and Pavlich, B.S. (2006). “Flexural Performance of Prefabricated Composite Bridge Girder Units,” Technical Report CEE-TR-2006-01, Department of Civil and Environmental Engineering, Michigan State University, East Lansing, Michigan.
- CAN/CSA-S6, (1988). Design of Highway Bridges, Canadian Standards Association, Rexdale, Ontario.
- Chang, S.-P. and Shim, C.-S. (2001). “Continuous Composite Bridges with Precast Decks,” *Steel Structures*, 1:123-132.
- Computers and Structures (CSI). (2000). SAP 2000 v.7.1 – Integrated Software for Structural Analysis & Design.
- Federal Highway Administration, (2004). “Prefabricated Bridge Elements and Systems in Japan and Europe,” Federal Highway Administration, International Technology Exchange Program.
- Federal Highway Administration. Bridge Rail Guide – New Jersey Barrier. <http://www.fhwa.dot.gov/BRIDGE/bridgerail/br054106.cfm>. Accessed 5/17/2006.
- Freeby, G.A. (2005). “Texas’s Totally Prefabricated Bridge Superstructures,” *Transportation Research Record: Journal of the Transportation Research Board*, CD 11-S, Transportation Board of the National Academies of Sciences, Washington, D.C., pp. 169-174.

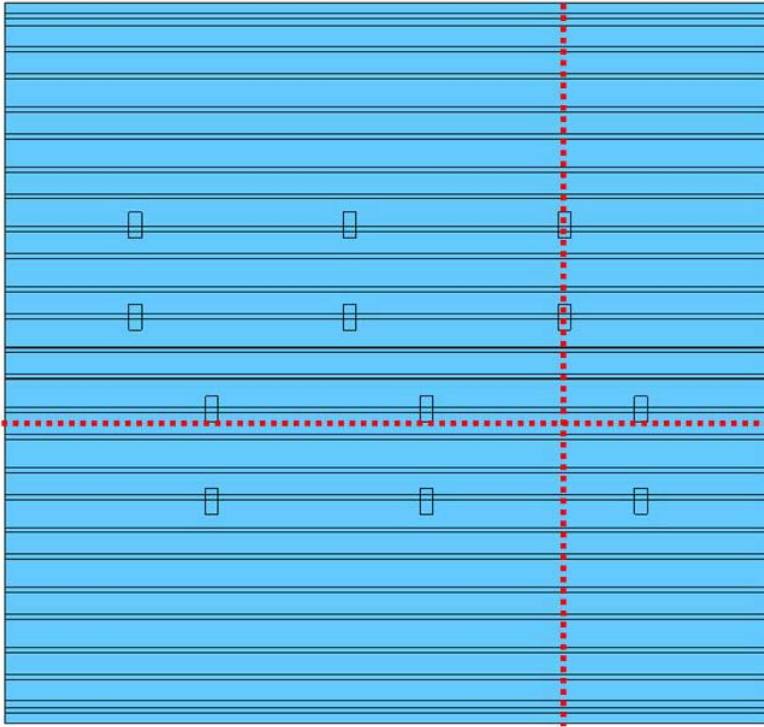
- Freeby, G.A., (2006). Personal Communication with B. Pavlich.
- Hambly, E.C. (1991) Bridge Deck Behaviour, 2<sup>nd</sup> Edition. E & FN Spon. London, UK.
- Hassan, S.K., Polyzois, D. and Morris, G. (1998). “Axial Fatigue Performance of Cold-Formed Steel Sections,” *Journal of Structural Engineering*, 124(2): 149-157.
- Issa, M.A., Idrs, A.-T., Kaspar, I.I., and Khayyyat, S.Y. (1995). “Full-Depth Precast and Precast Prestressed Concrete Bridge Deck Panels,” *PCI Journal*, 40(1): 59-80.
- Issa, M.A., et al. (1995) “Field Performance of Full Depth Precast Concrete Panels in Bridge Deck Reconstruction,” *PCI Journal*, 40(3): 82-108.
- Nakamura, S. (2002). “Bending Behavior of Composite Girders with Cold Formed Steel U Section,” *Journal of Structural Engineering*, 128(9): 1169-1176.
- Nelson, G.C., “Composite Cold-Formed Steel Plate Box Beam,” Communication to Michigan Department of Transportation, URS Corporation, Grand Rapids, MI, Spring 2004.
- Nelson, G.C. (2005). “Con-Struct Prefabricated Bridge System,” 2005 World Steel Bridge Symposium Presentation
- Nelson, G.C. (2005). Prefabricated, Prestressed Bridge System and Method of Making the Same Patent Application No. 11/337,206.
- Nelson, G.C., (2006). Personal Communications with R. Burgueño
- Ohelers, D.J., and Bradford, M.A. (1995). Composite Steel and Concrete Structural Members: Fundamental Behaviour, Elsevier Science, Tarrytown, NY.
- OHBDC, Ontario Highway Bridge Design Code, (1983). Highway Engineering Division, Ontario Ministry of Transportation and Communications, Downsview, Ontario.
- Ralls, M.L. and Tang, B.M. (2003). “Laying the Groundwork for Fast Bridge Construction,” *Public Roads*, 67(3).
- SDR Engineering Consultants Inc., “Prefabricated Steel Bridge Systems – FHWA Solicitation No. DTFH61-03-R-00113,” Final Report to the Federal Highway Administration, Structure Design and Rehabilitation (SDR), Inc., Tallahassee, FL, September 2005.

- Seible, F., Priestley, M.J.N., Krishnan, K., Nagy, G., and Sharabi, N., (1990). "Simulation of Rolling Loads on the Gepford Overhead Bridge Section," Structural Systems Research Project Report No. SSRP-90/05, Department of Applied Mechanics and Engineering Sciences, University of California, San Diego, La Jolla, CA.
- Shahawy, M.A. (2003). "Prefabricated Bridge Elements and Systems to Limit Traffic Disruption during Construction – A Synthesis of Highway Practice," NCHRP Synthesis 324, National Cooperative Highway Research Program, Transportation Research Board, Washington, D.C.
- Simulia. (2007). ABAQUS FEA v.6.7
- Taly, N. and Gangarao, H.V.S. (1979). "Prefabricated Press-Formed Steel T-Box Girder Bridge System," *Engineering Journal*, American Institute of Steel Construction, Third Quarter, pp. 75-83.
- TRB-RIP, (2006) "Short Span Steel Bridge: Inverted Steel Box," Transportation Research Board of the National Academies, Research in Progress, <http://rip.trb.org/browse/dproject.asp?n=5087>, accessed online 4/20/06.
- Turmo, J., Ramos, G., Aparicio, A.C. (2006) "Shear strength of dry joints of concrete panels with and without steel fibres. Application to precast segmental bridges," *Engineering Structures*, 28: 23-33.
- Virlogeux, M. (1999). New Trends in Prestressed Concrete Bridges," *Transportation Research Record* 1696, Paper No. 5B0135, pp. 238-248.

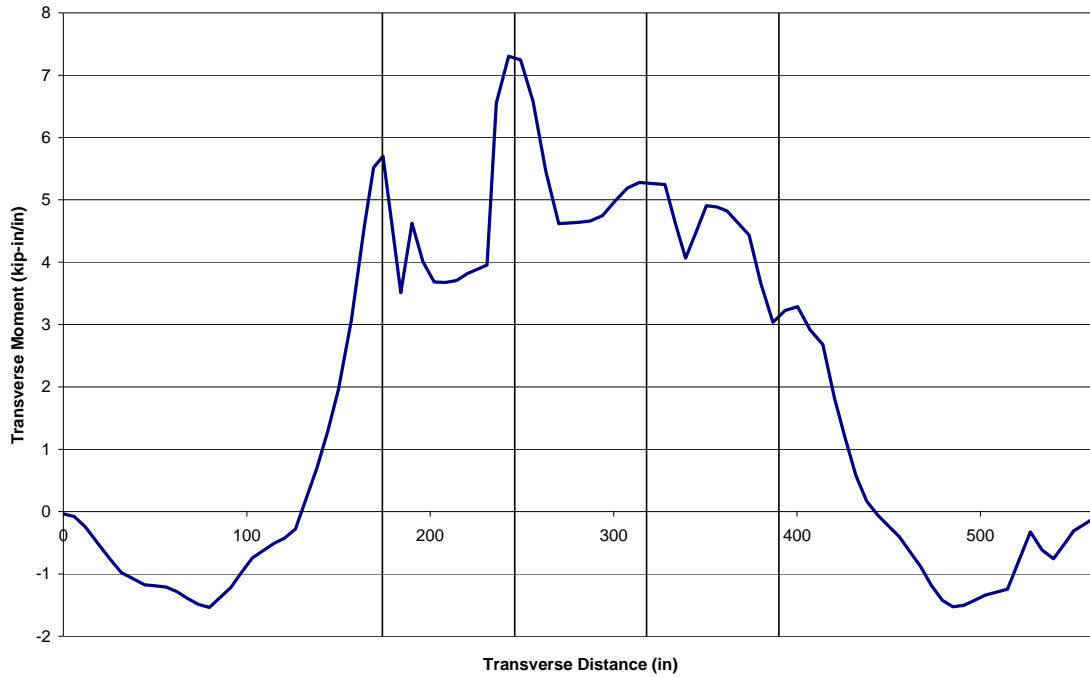
## Appendix I. Comparison of Analysis Tools



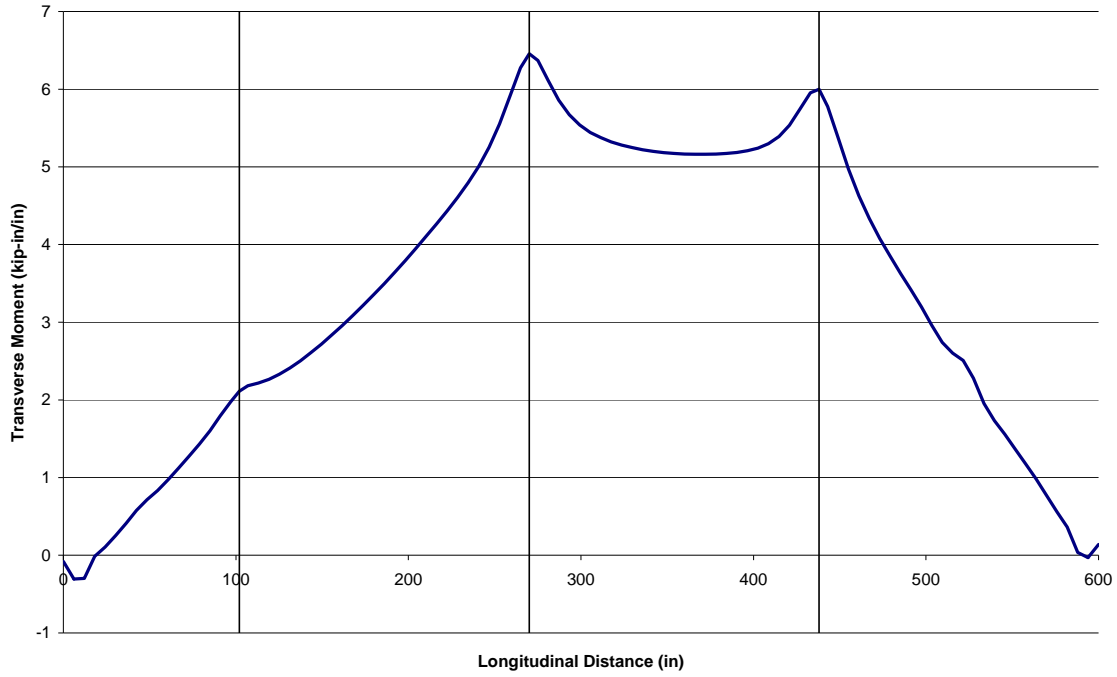
## Appendix II. Bridge Case 1: FE Models Responses



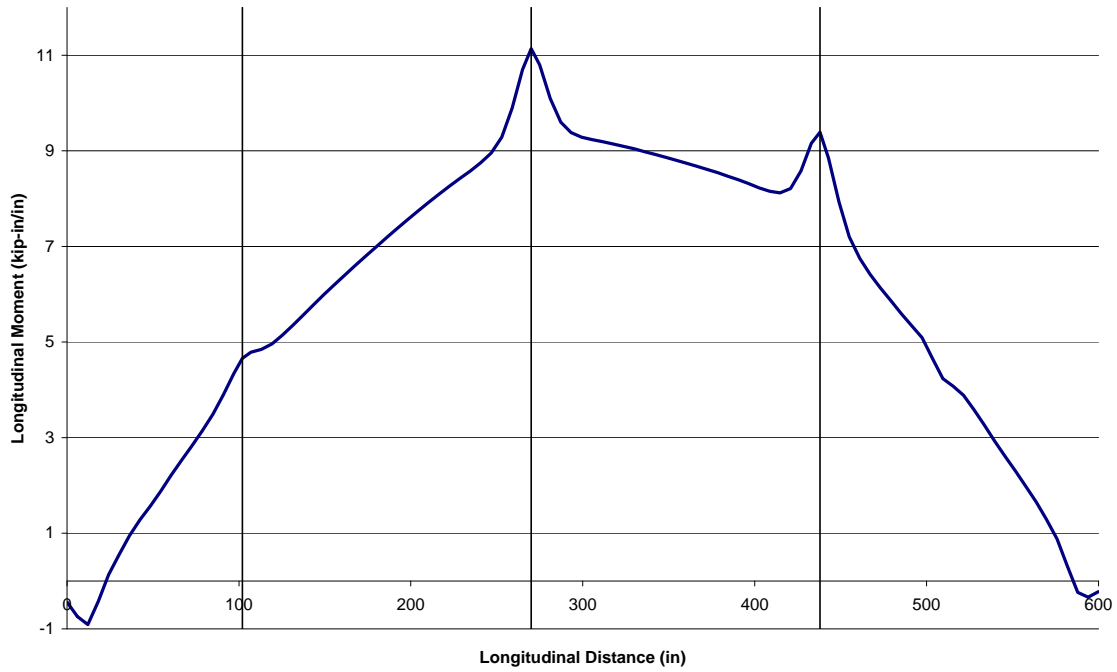
50' Span, 4' Girder Spacing: Transverse Moment v. Transverse Distance



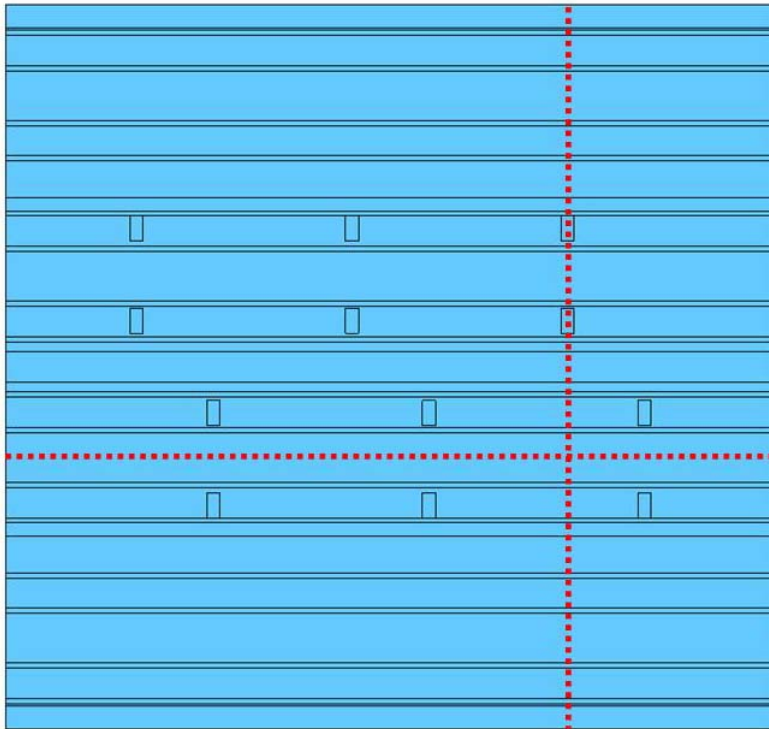
50' Span, 4' Girder Spacing: Transverse Moment v. Longitudinal Distance



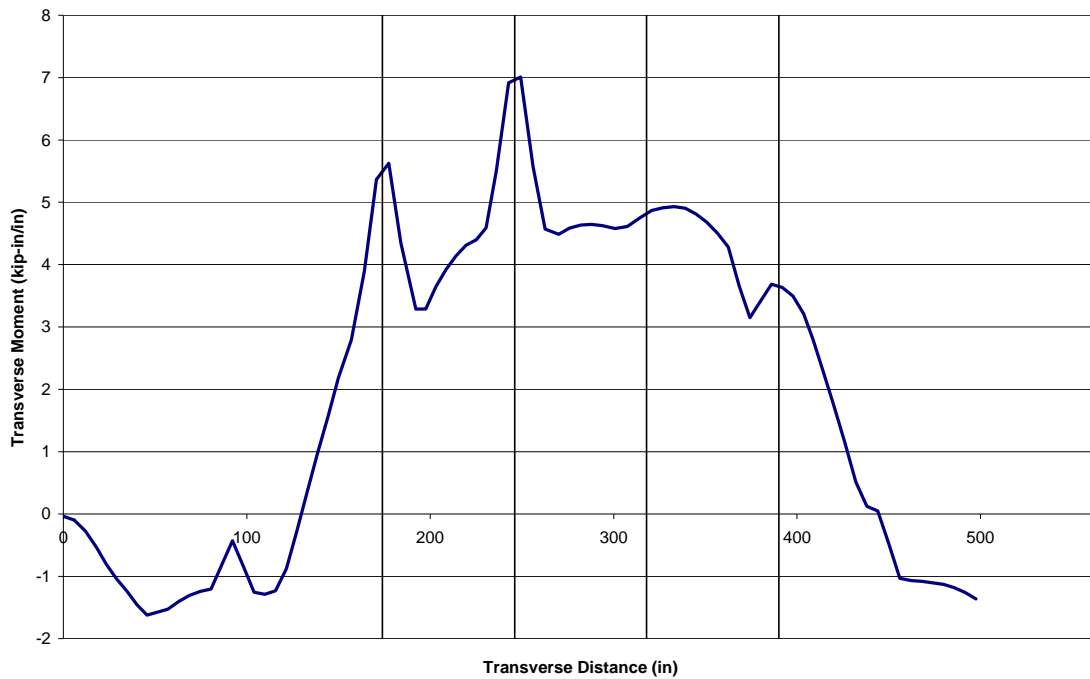
50' Span, 4' Girder Spacing: Longitudinal Moment v. Longitudinal Distance



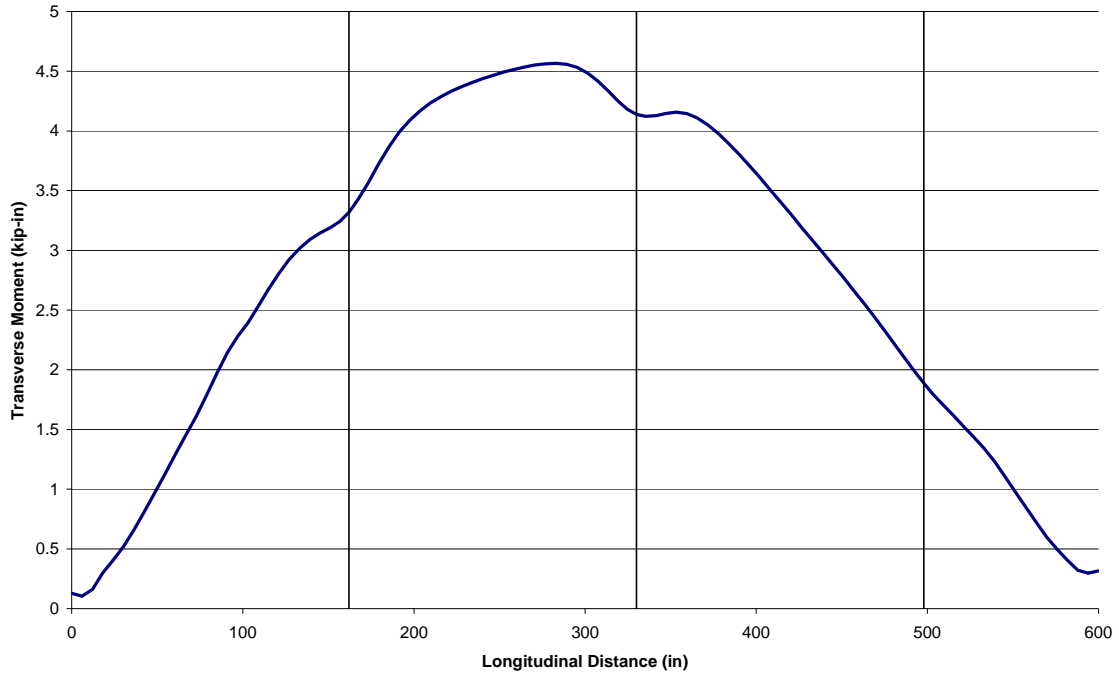
### Appendix III. Bridge Case 2: FE Models Responses



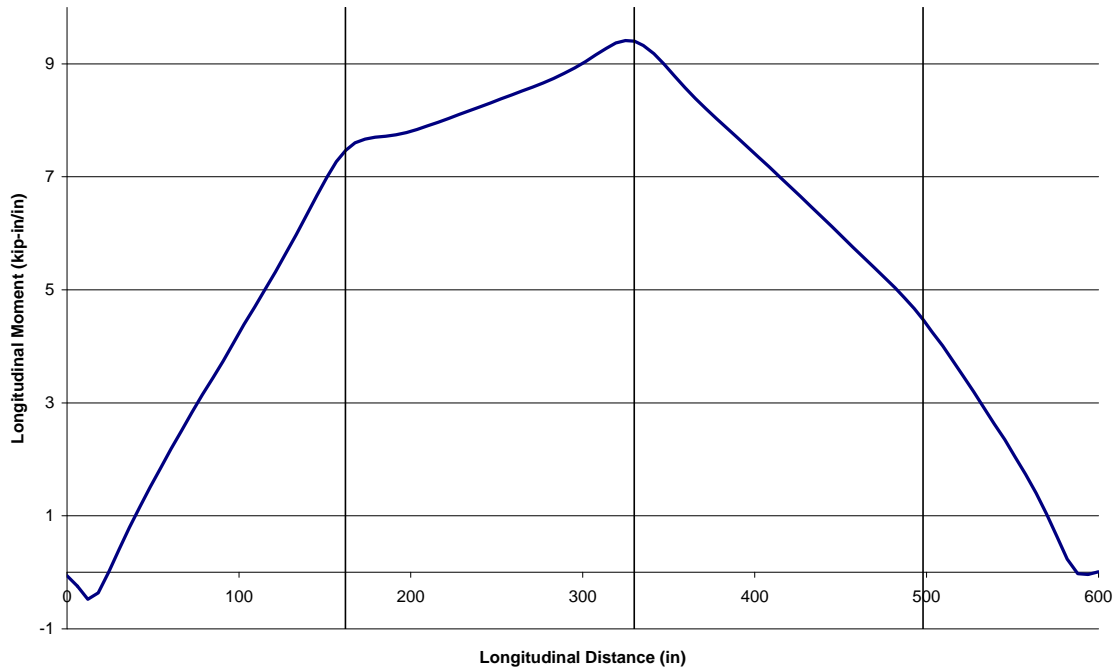
50' Span, 6' Girder Spacing: Transverse Moment v. Transverse Distance



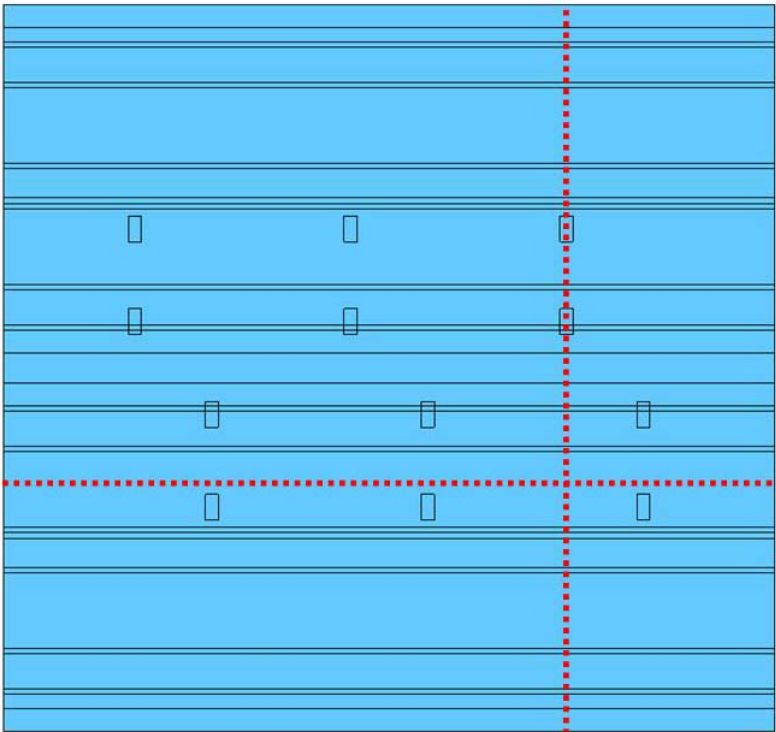
50' Span, 6' Girder Spacing: Transverse Moment v. Longitudinal Distance



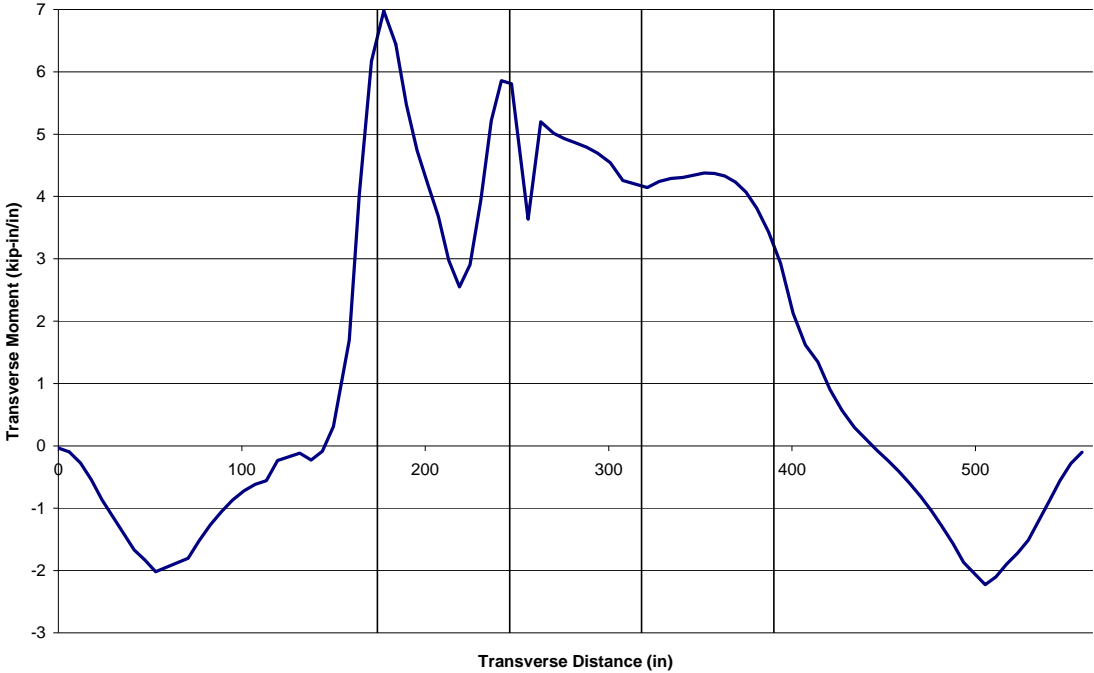
50' Span, 6' Girder Spacing: Longitudinal Moment v. Longitudinal Distance



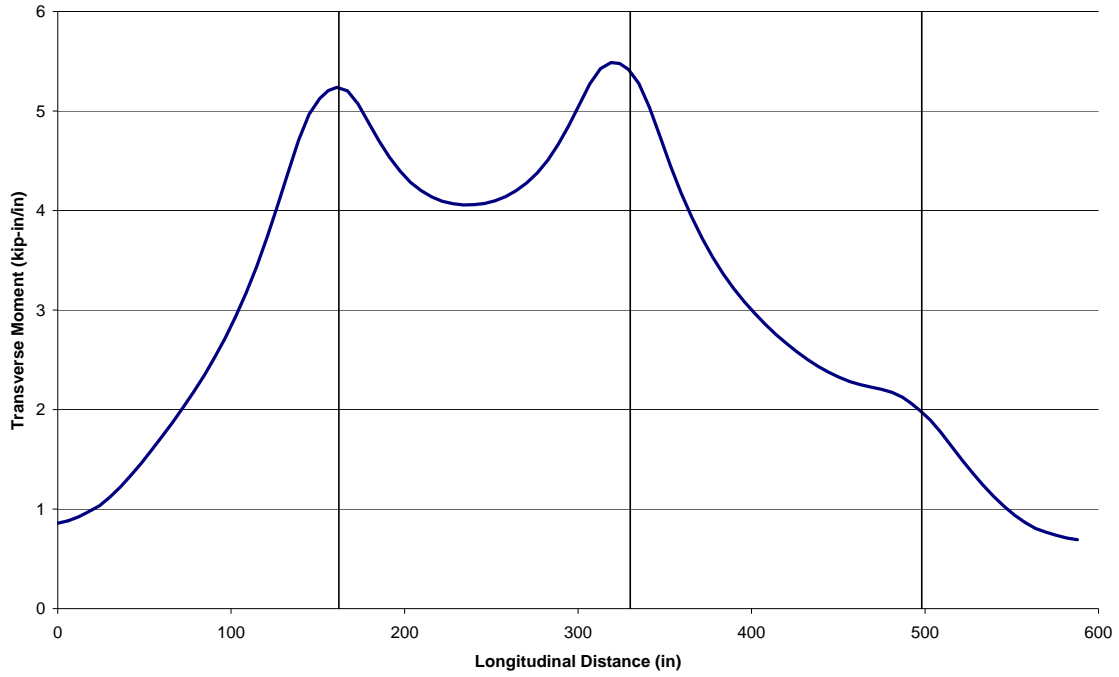
**Appendix IV. Bridge Case 3: FE Models Responses**



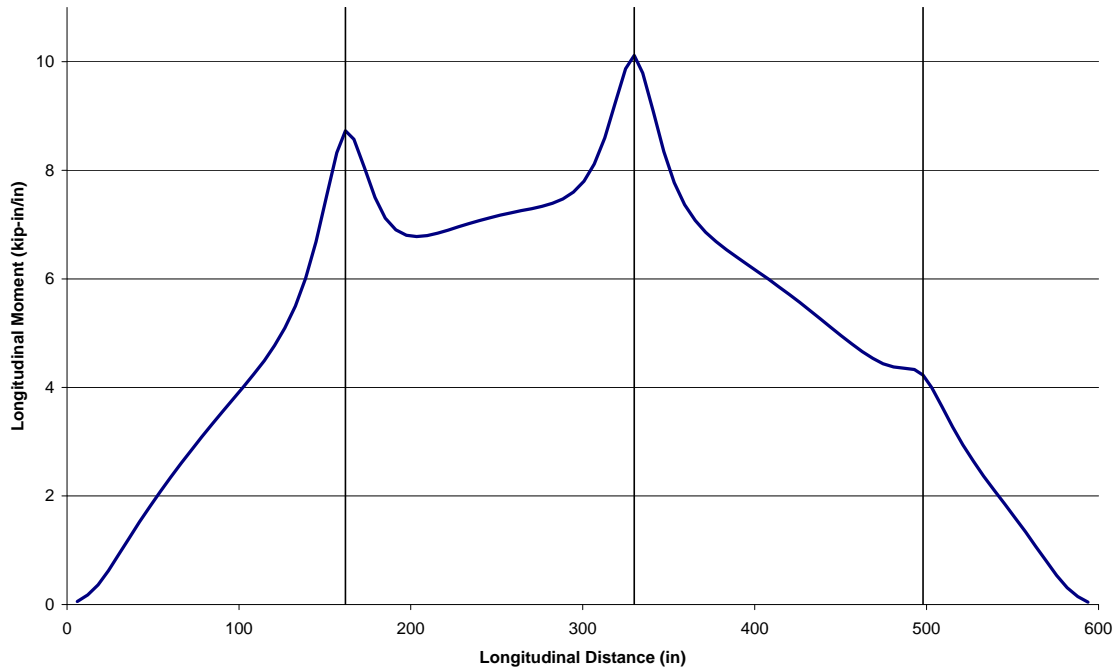
**50' Span, 8' Girder Spacing: Transverse Moment v. Transverse Distance**



50' Span, 8' Girder Spacing: Transverse Moment v. Longitudinal Distance



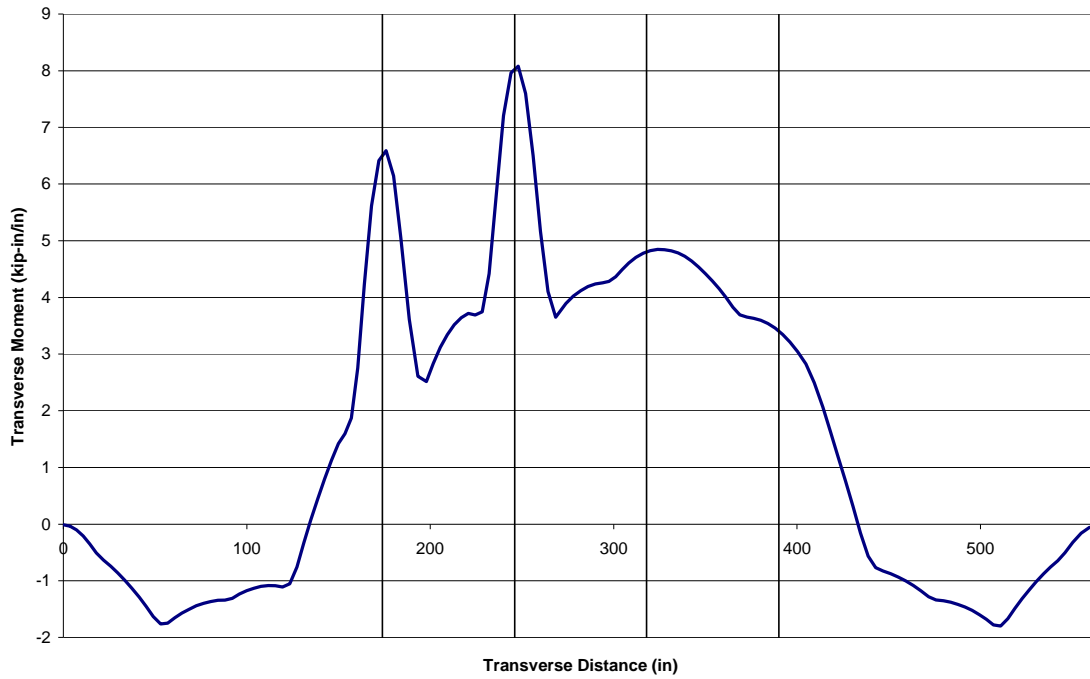
50' Span, 8' Girder Spacing: Longitudinal Moment v. Longitudinal Distance



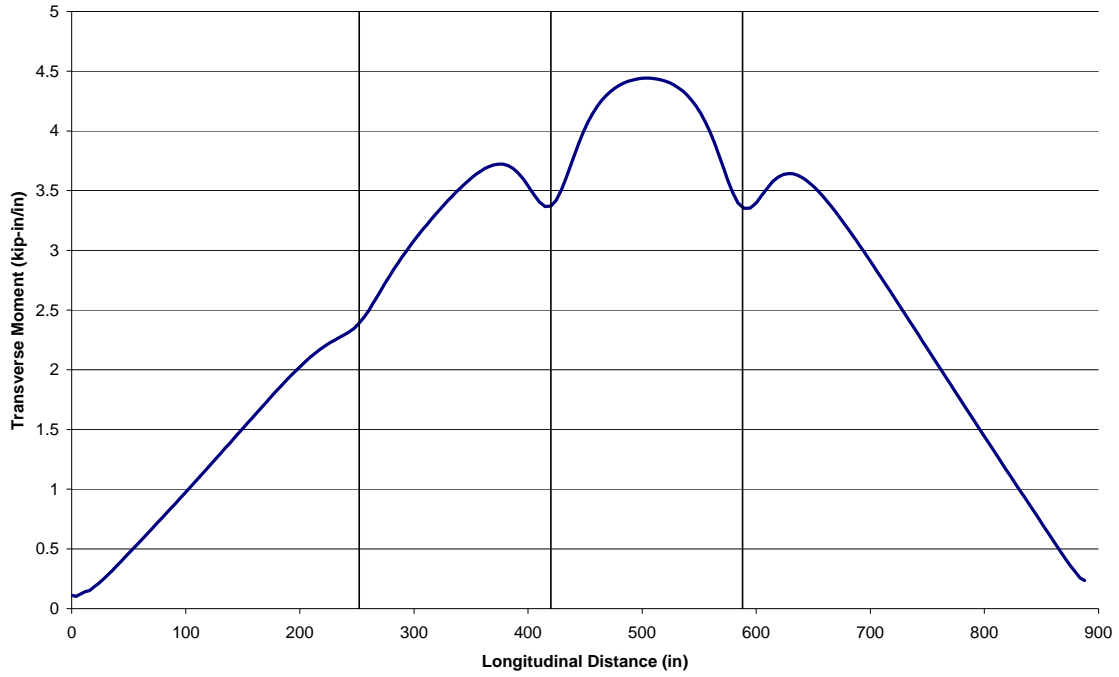
## Appendix V. Bridge Case 4: FE Models Responses



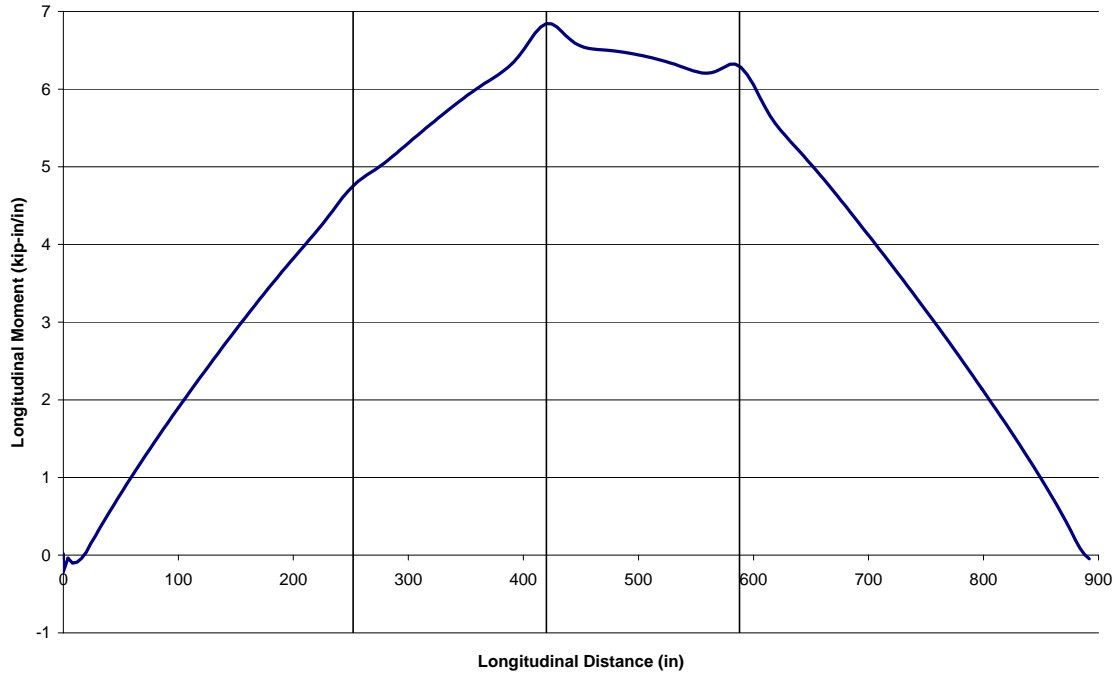
75' Span, 6' Girder Spacing: Transverse Moment v. Transverse Distance



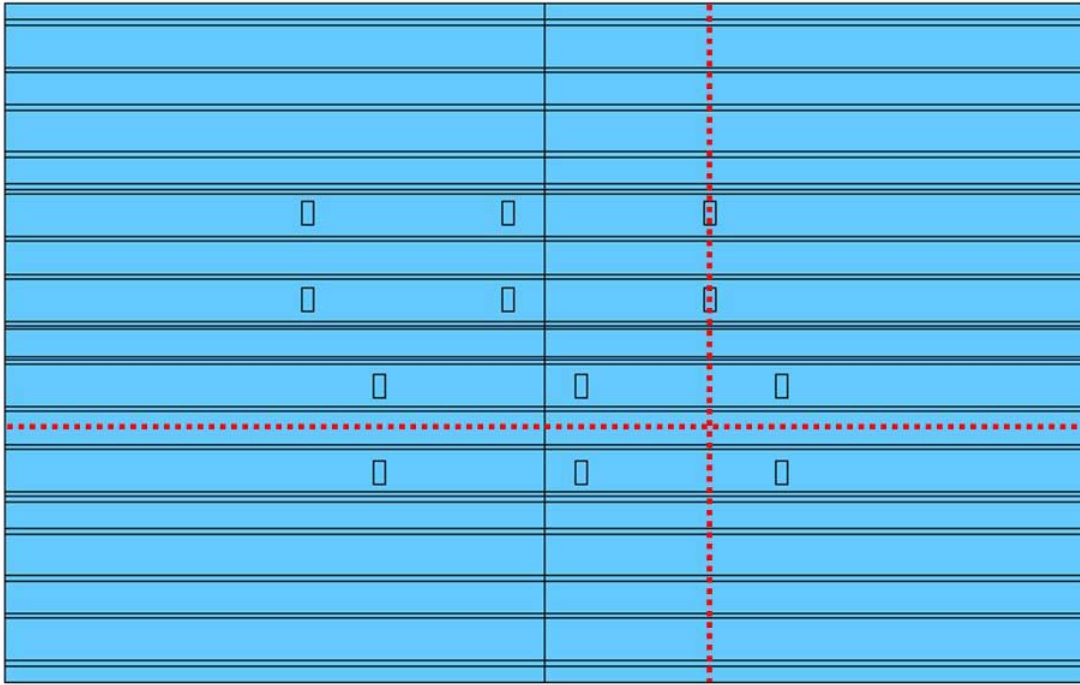
75' Span, 6' Girder Spacing: Transverse Moment v. Longitudinal Distance



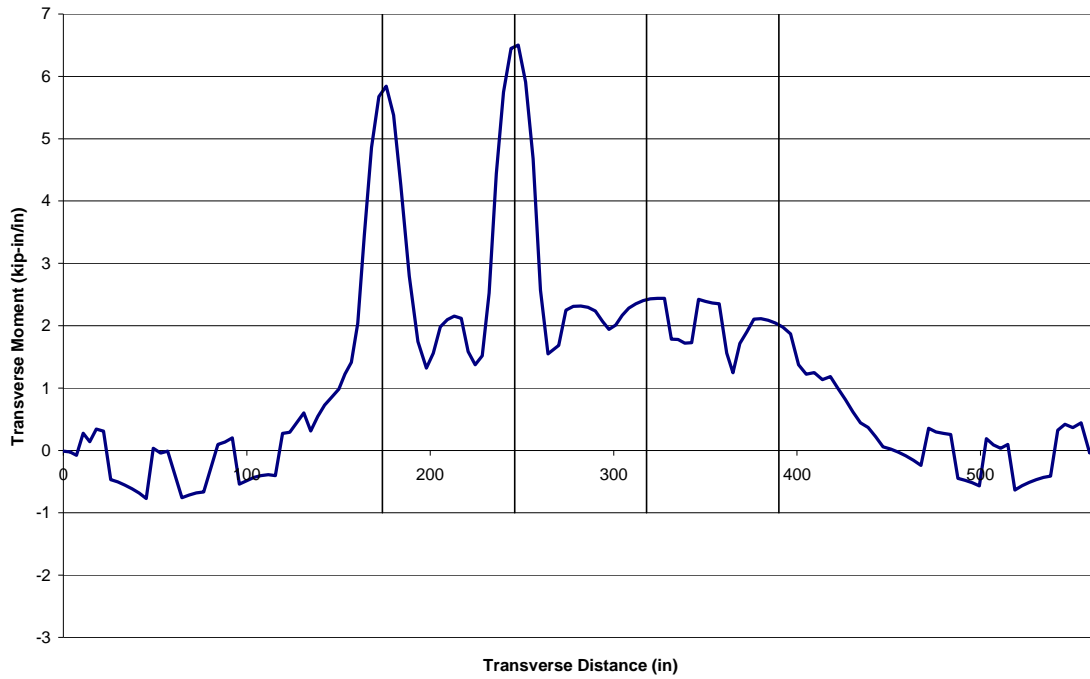
75' Span, 6' Girder Spacing: Longitudinal Moment v. Longitudinal Distance



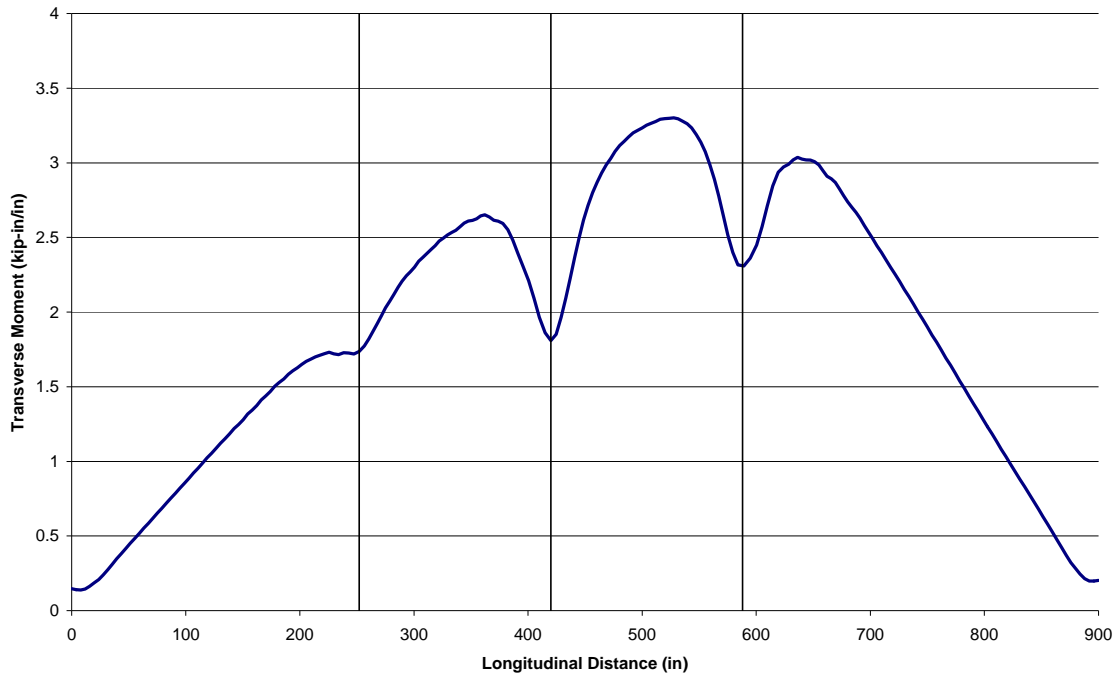
## Appendix VI. Bridge Case 5: FE Models Responses



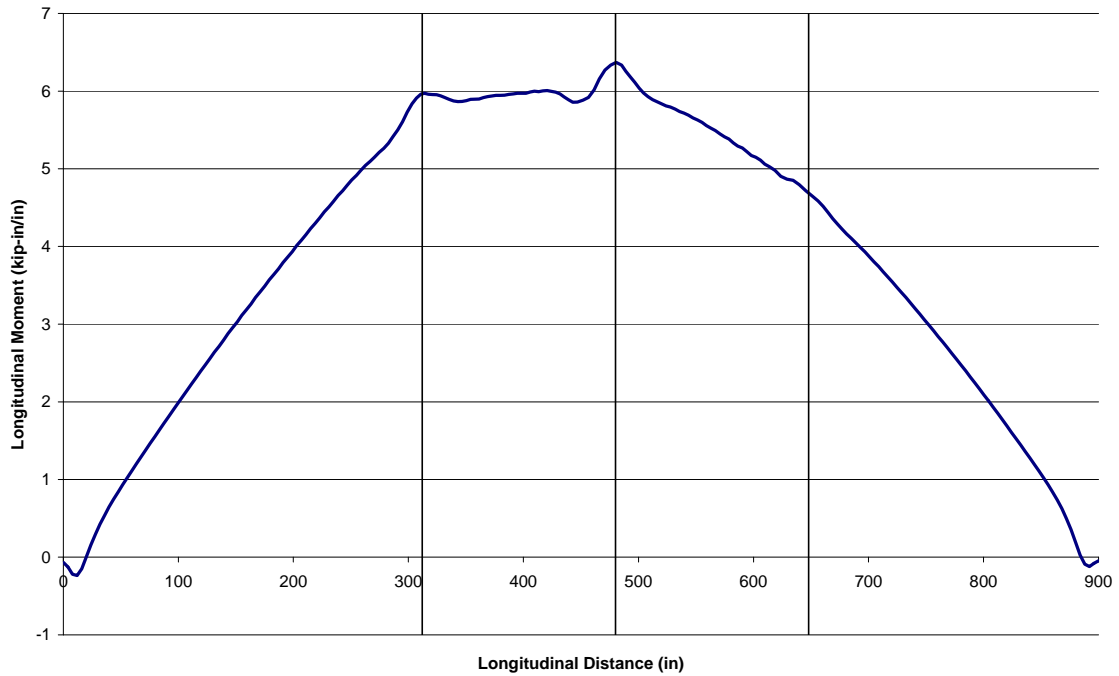
75' Span, 6' Girder Spacing, One Diaphragm: Transverse Moment v. Transverse Distance



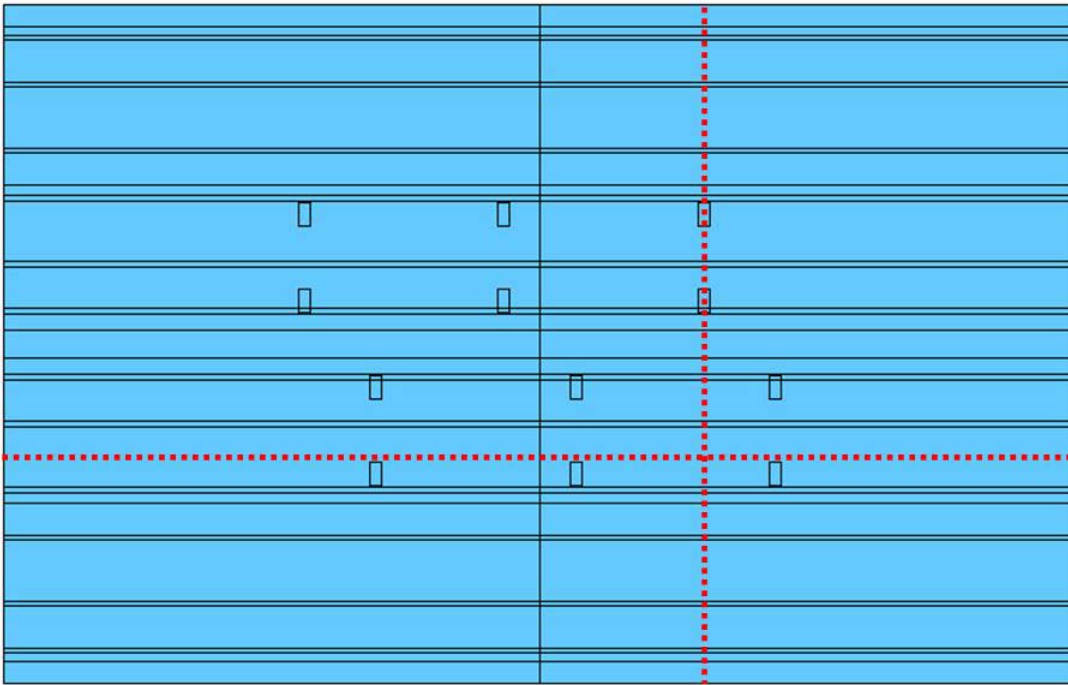
75' Span, 6' Girder Spacing, One Diaphragm: Transverse Moment v. Longitudinal Distance



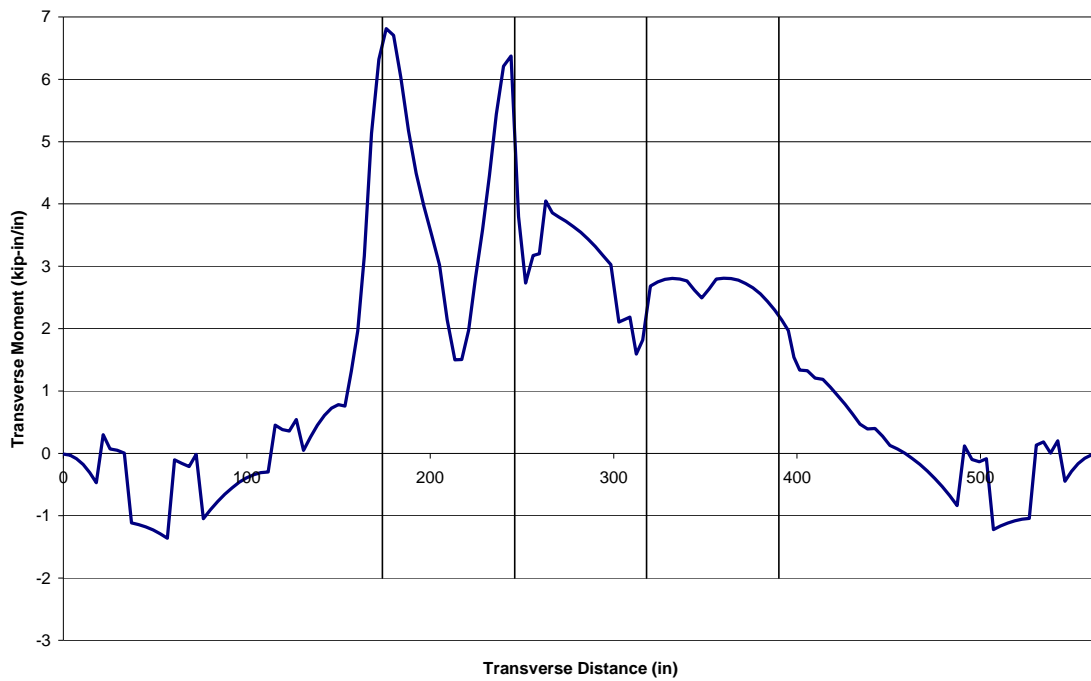
75' Span, 6' Girder Spacing, One Diaphragm: Longitudinal Moment v. Longitudinal Distance



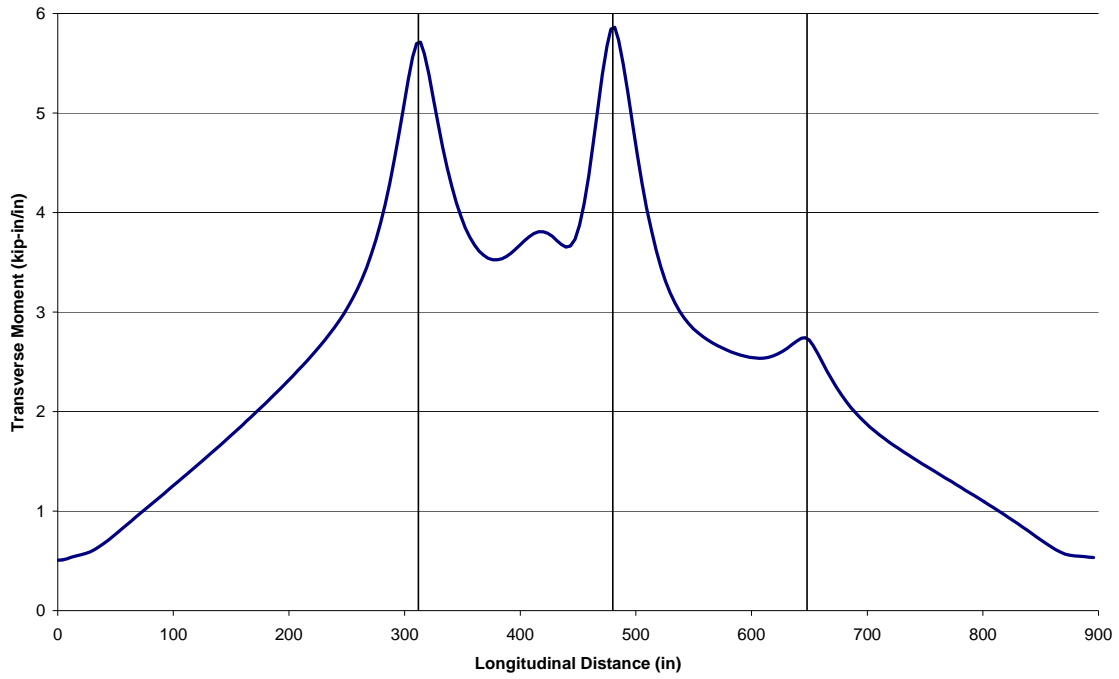
## Appendix VII. Bridge Case 6: FE Models Responses



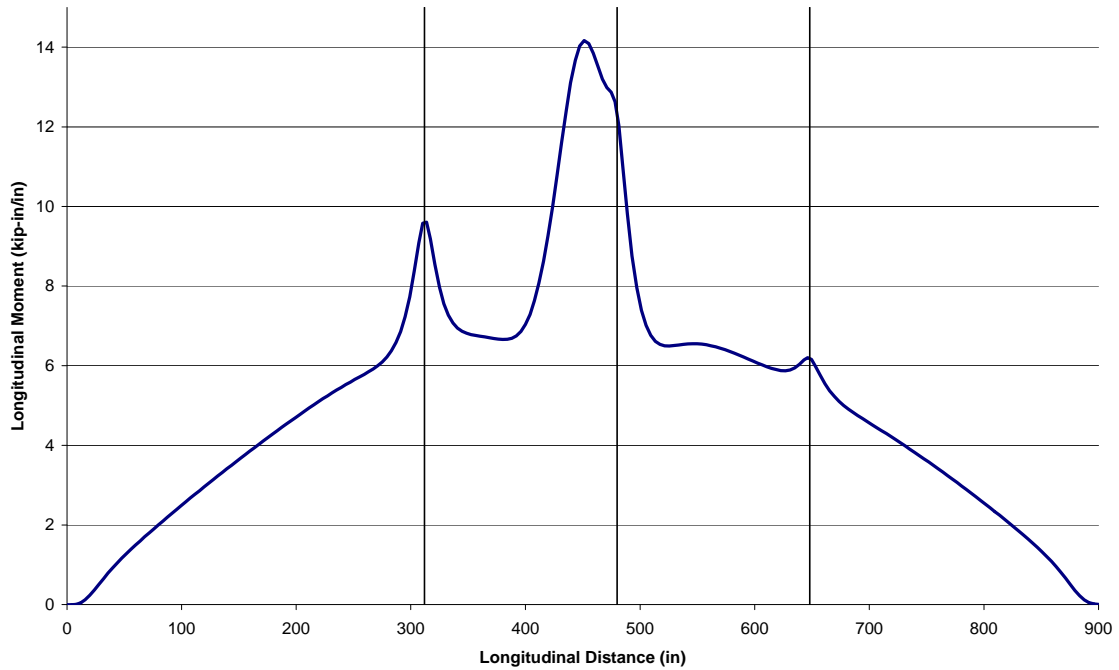
75' Span, 8' Girder Spacing, One Diaphragm: Transverse Moment v. Transverse Distance



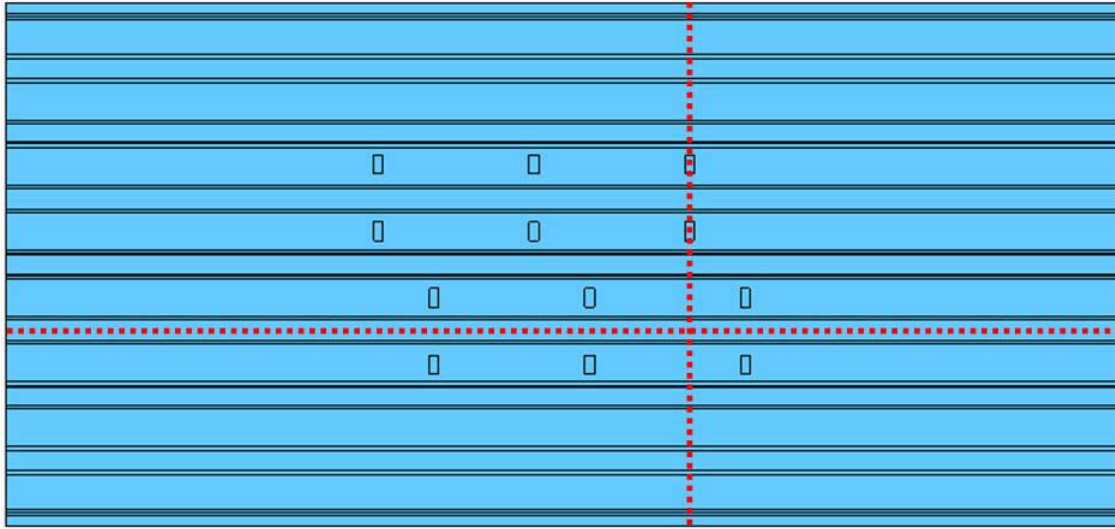
75' Span, 8' Girder Spacing, One Diaphragm: Transverse Moment v. Longitudinal Distance



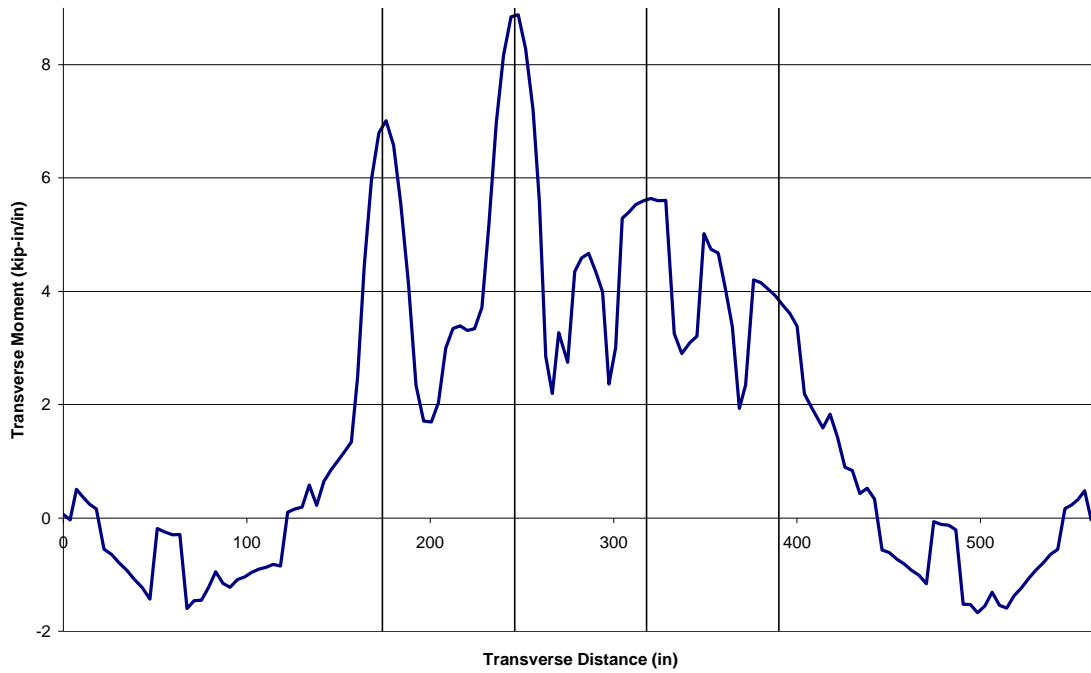
75' Span, 8' Girder Spacing, One Diaphragm: Longitudinal Moment v. Longitudinal Distance



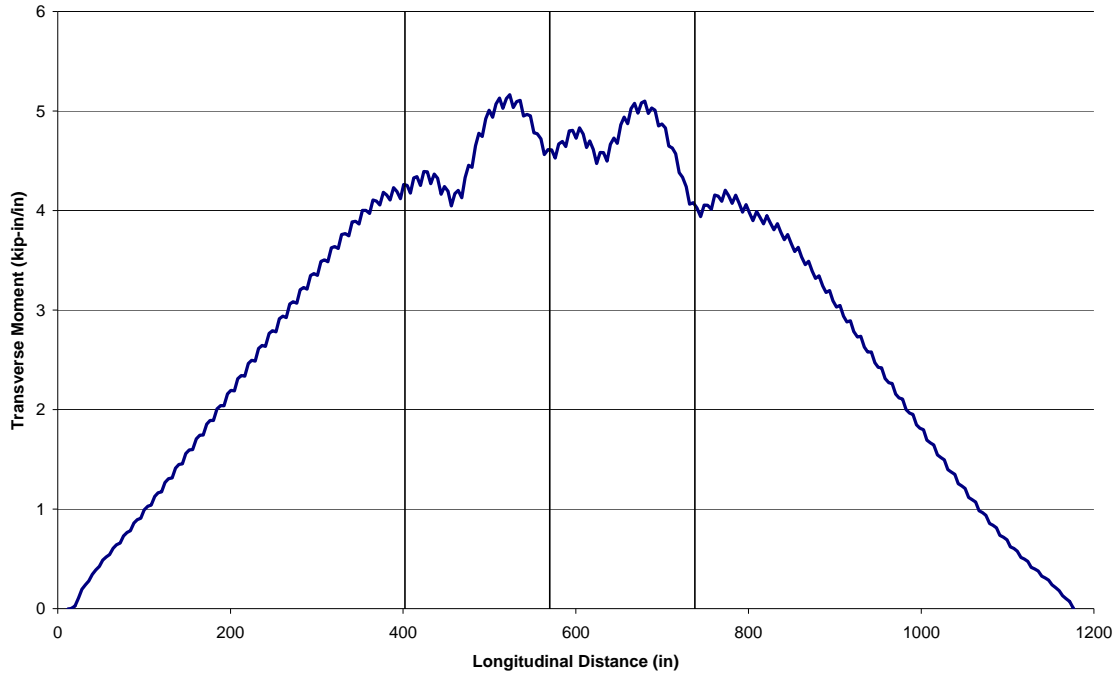
## Appendix VIII. Bridge Case 7: FE Models Responses



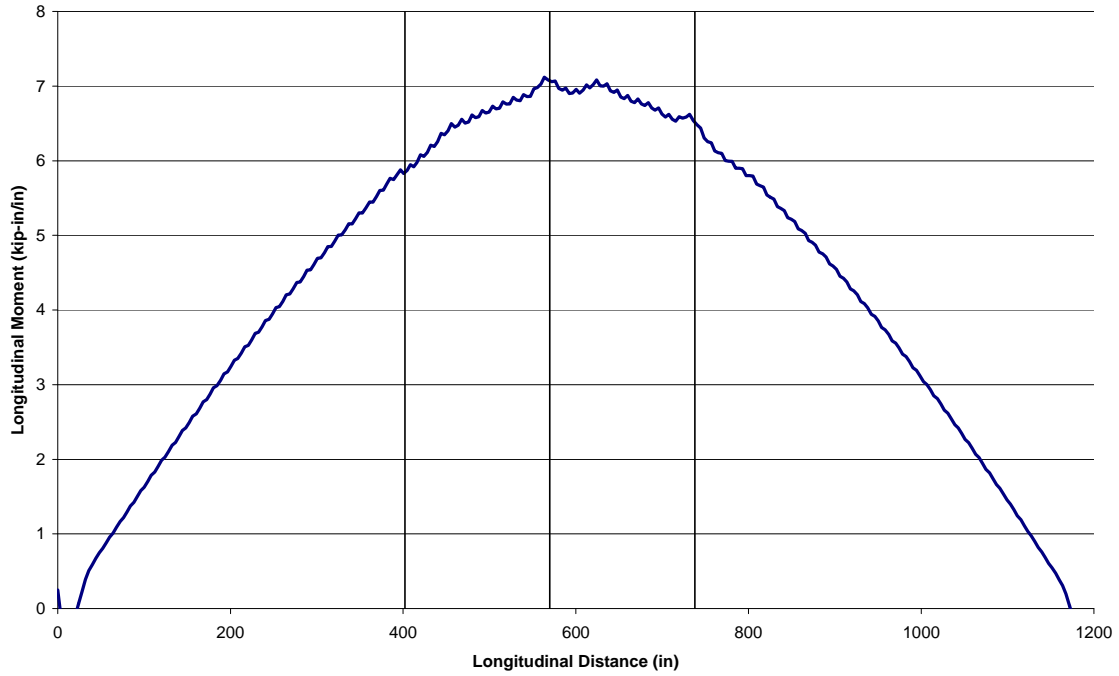
100' Span, 6' Girder Spacing: Transverse Moment v. Transverse Distance



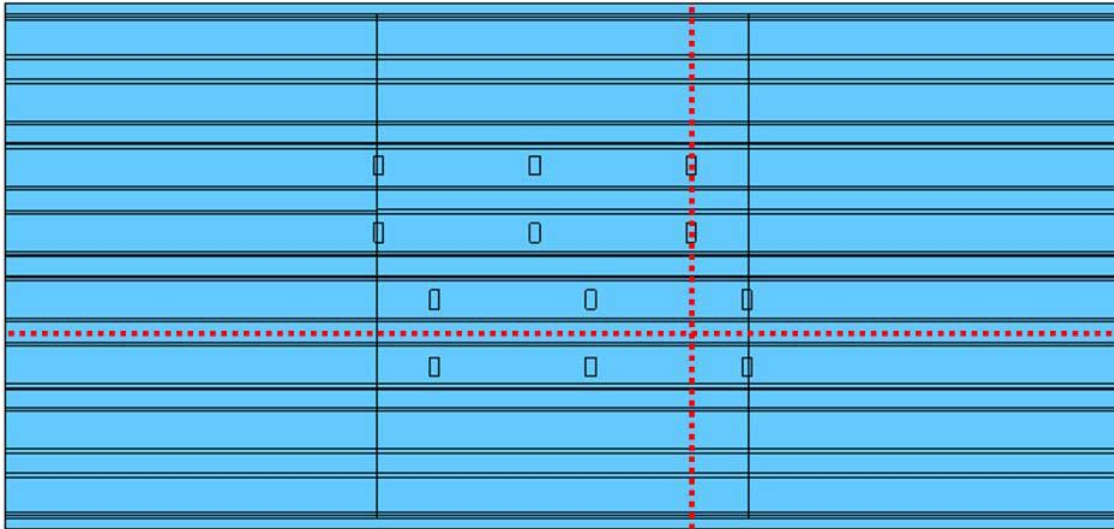
100' Span, 6' Girder Spacing: Transverse Moment v. Longitudinal Distance



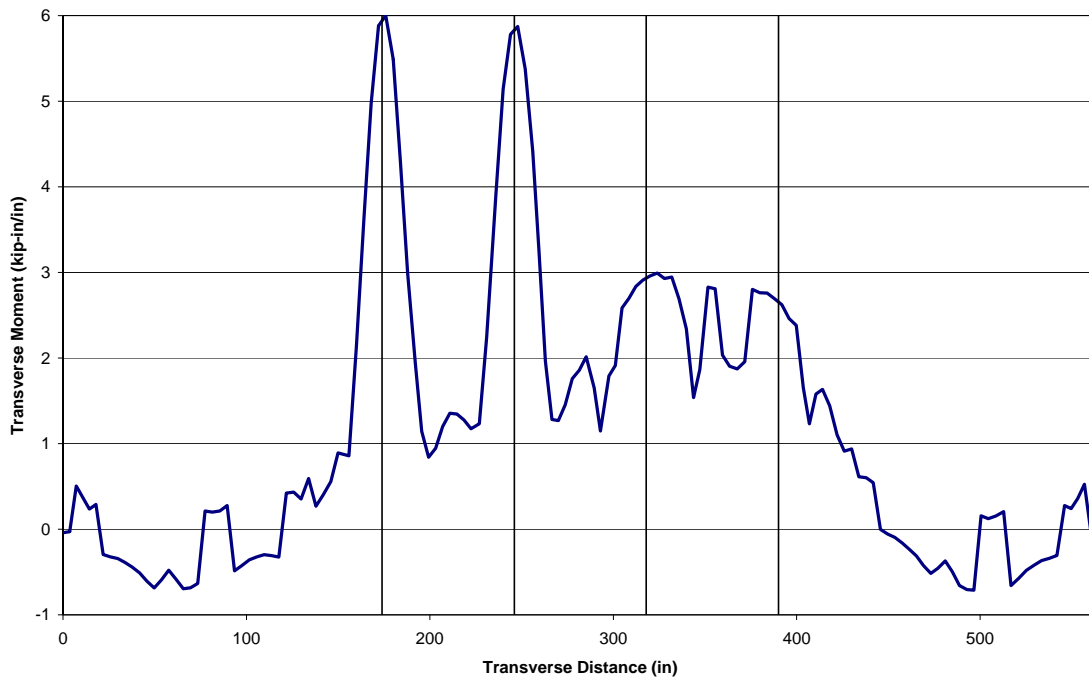
100' Span, 6' Girder Spacing: Longitudinal Moment v. Longitudinal Distance



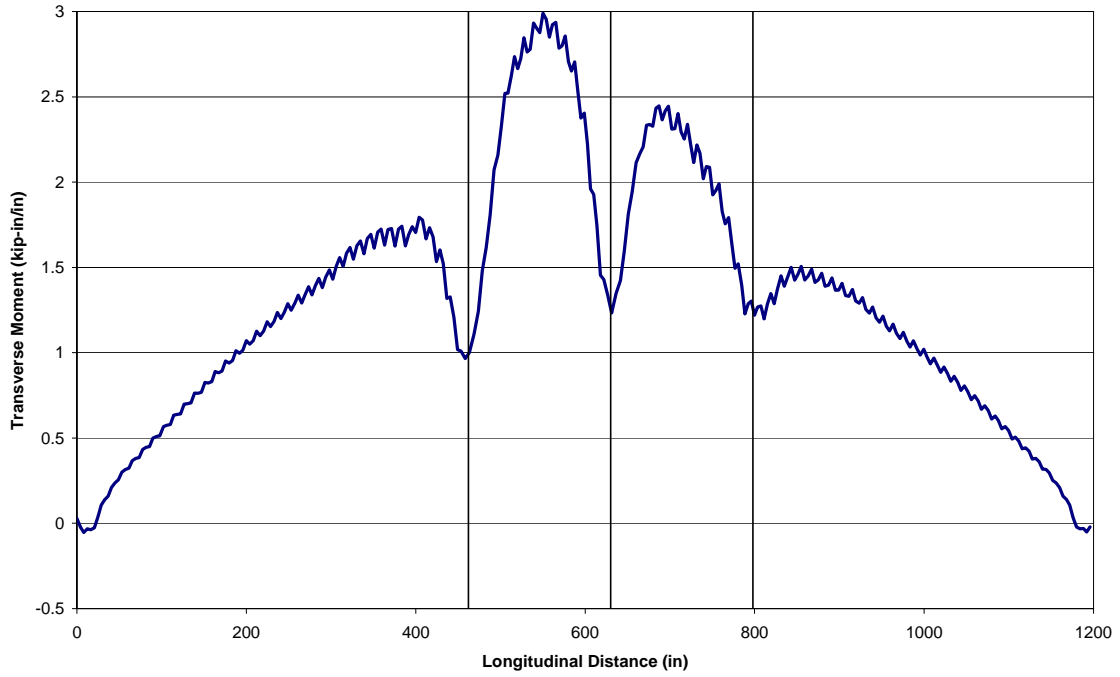
## Appendix IX. Bridge Case 8: FE Models Responses



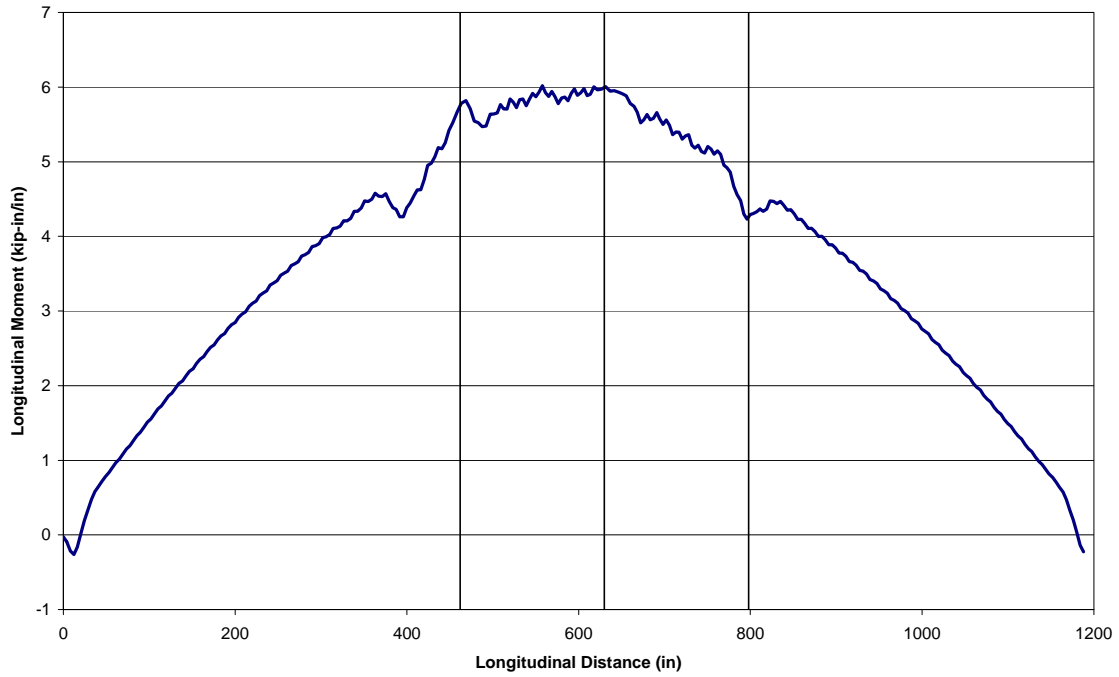
100' Span, 8' Girder Spacing, Two Diaphragms: Transverse Moment v. Transverse Distance



100' Span, 8' Girder Spacing, Two Diaphragms: Transverse Moment v. Longitudinal Distance

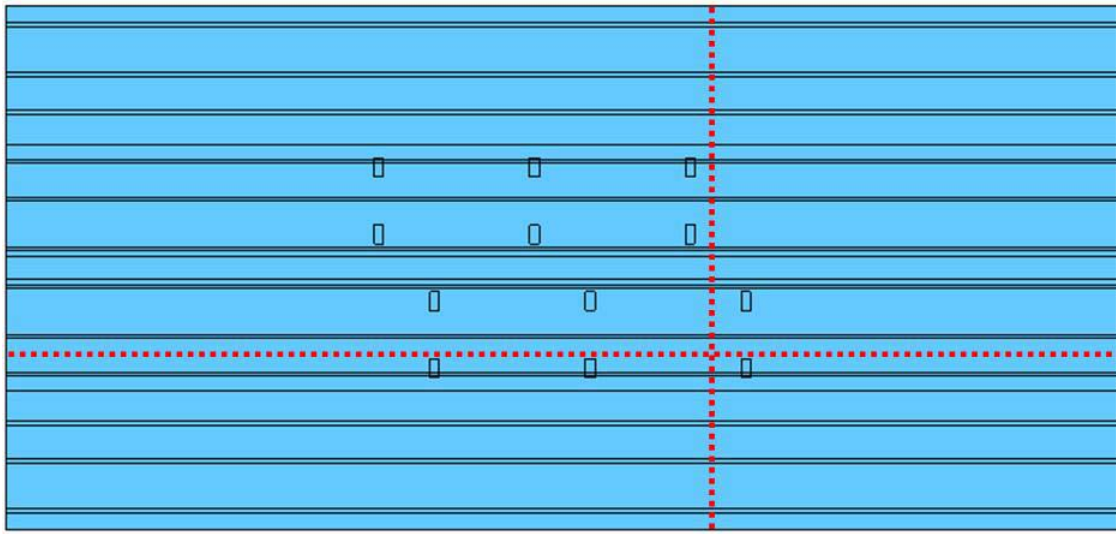


100' Span, 8' Girder Spacing, Two Diaphragms: Longitudinal Moment v. Longitudinal Distance

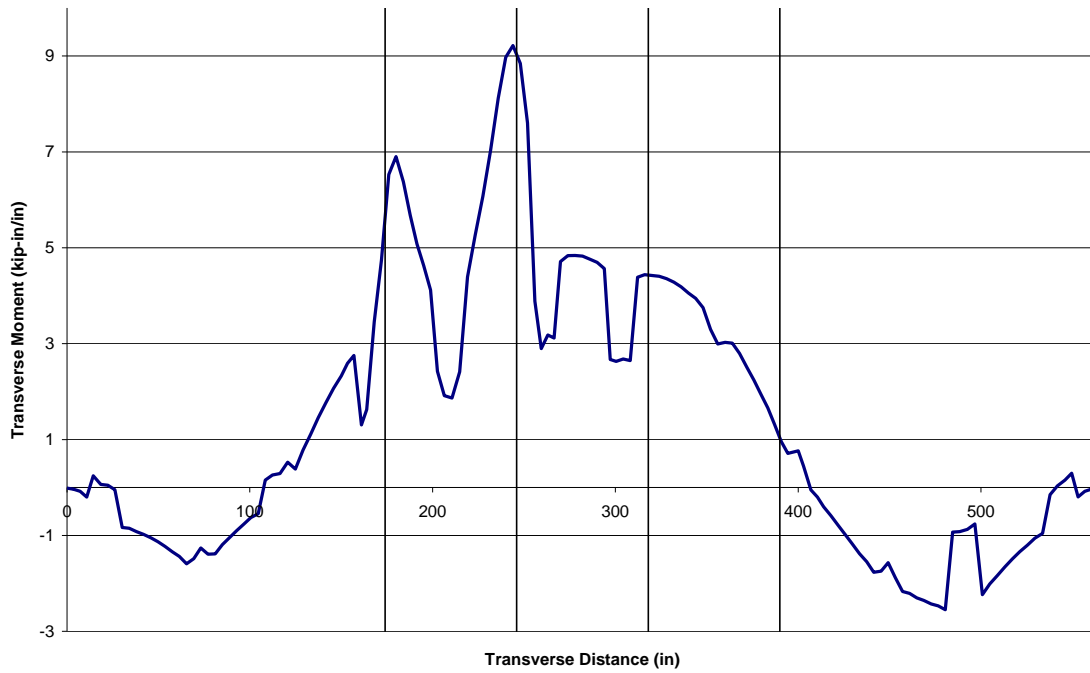




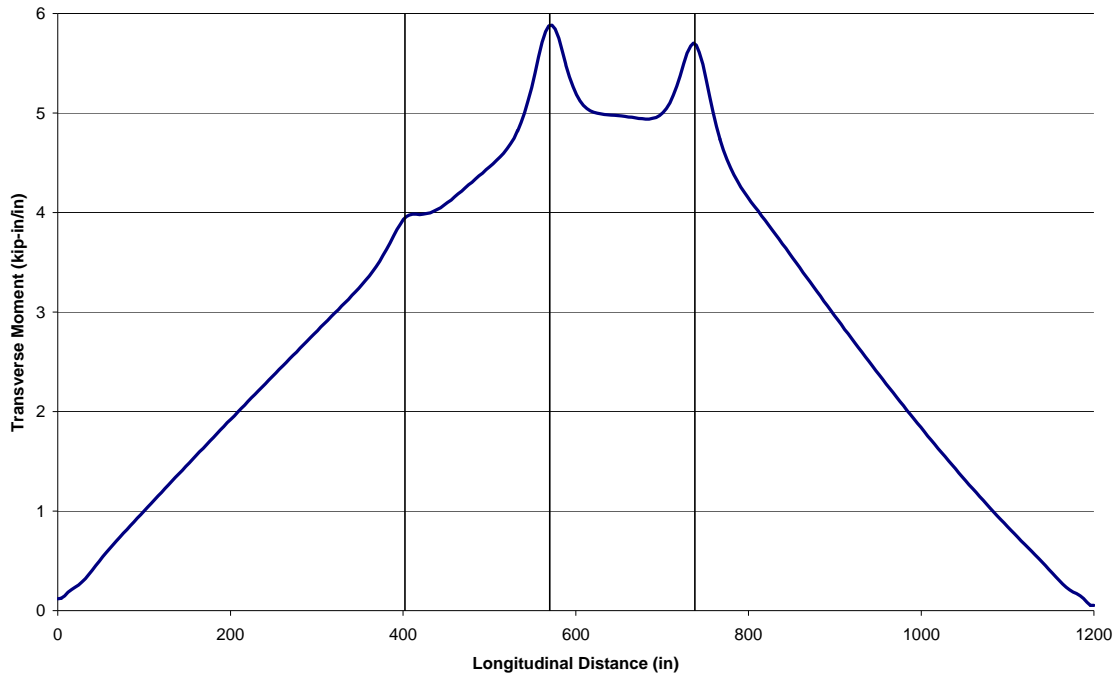
## Appendix X. Bridge Case 9: FE Models Responses



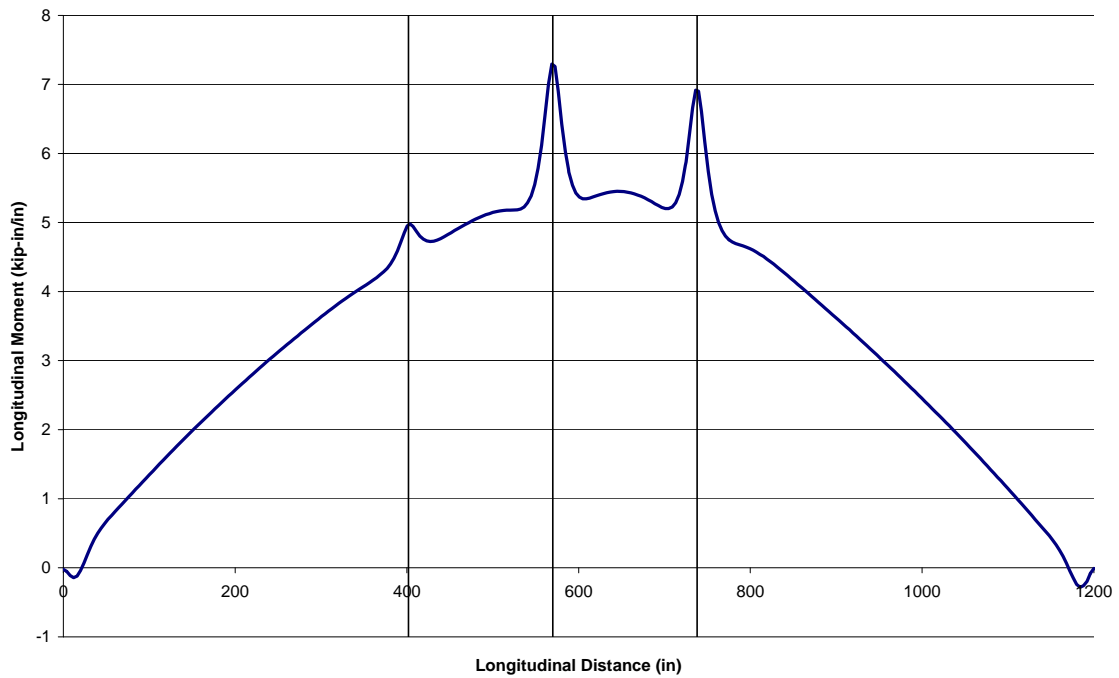
100' Span, 8' Girder Spacing: Transverse Moment v. Transverse Distance



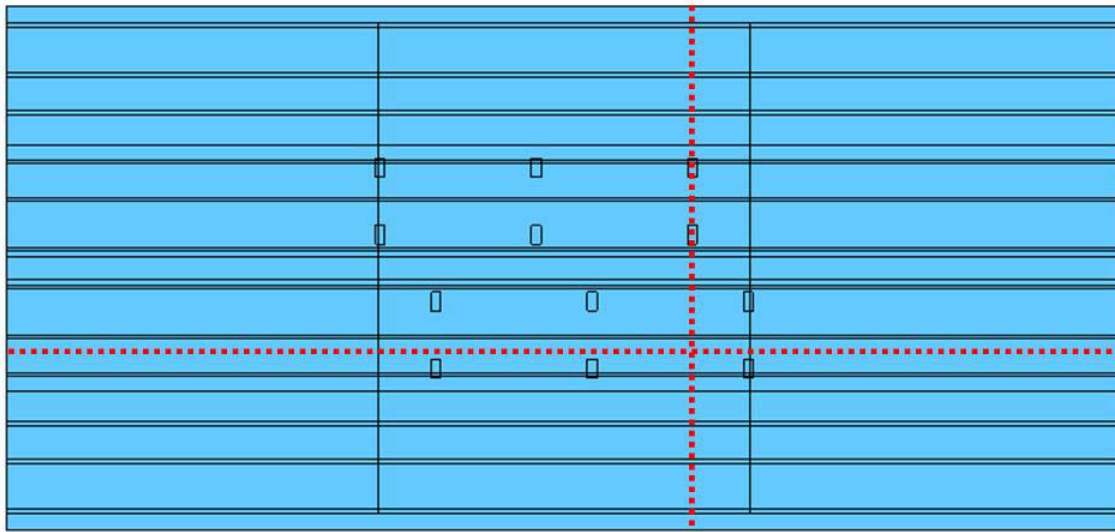
100' Span, 8' Girder Spacing: Transverse Moment v. Longitudinal Distance



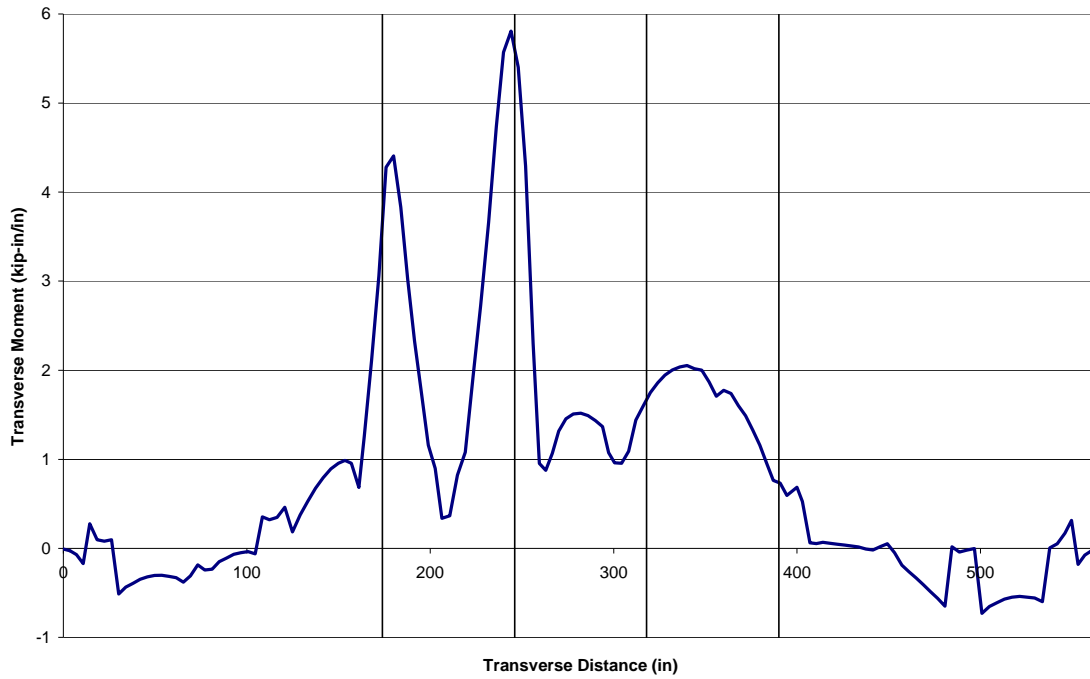
100' Span, 8' Girder Spacing: Longitudinal Moment v. Longitudinal Distance



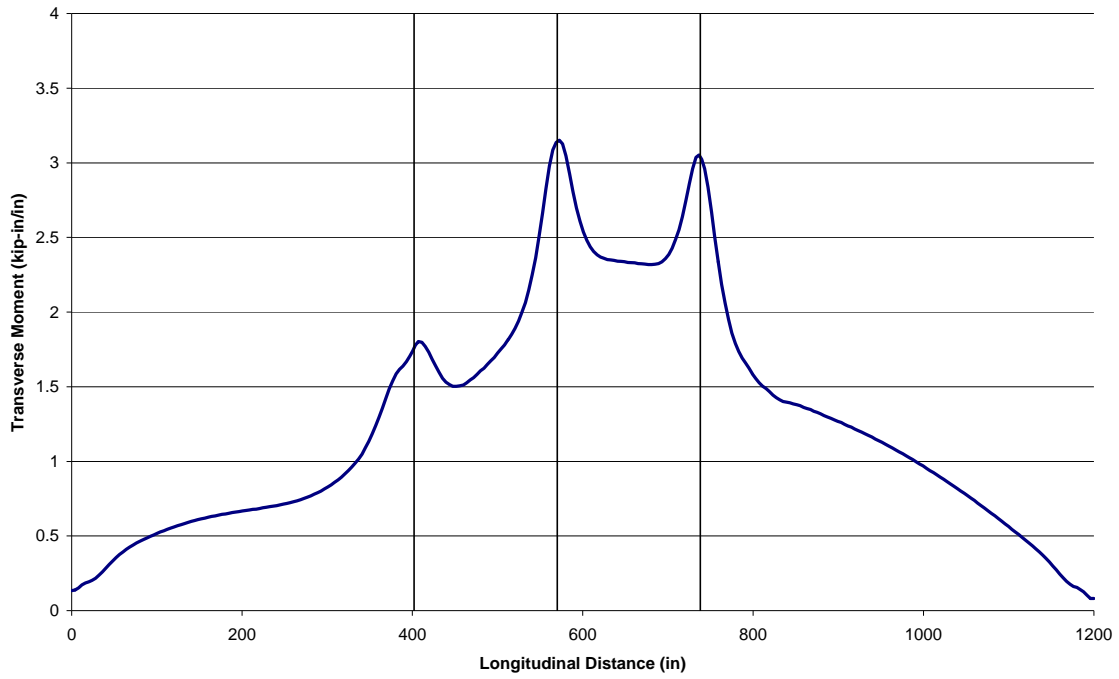
# Appendix XI. Bridge Case 10: FE Models Responses



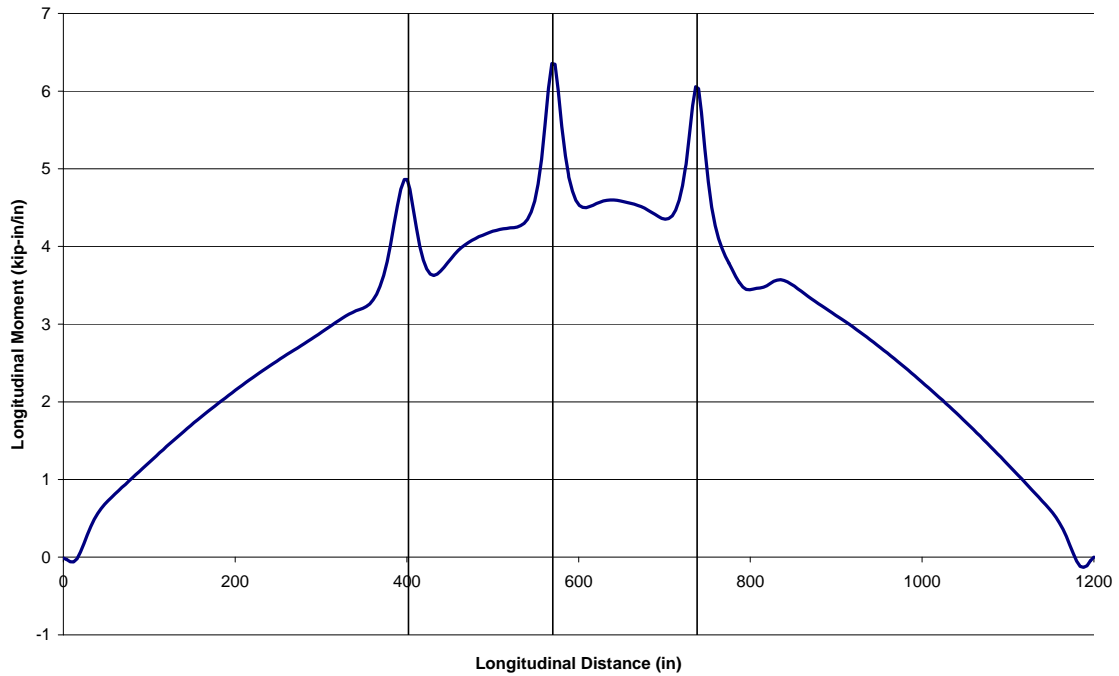
100' Span, 8' Girder Spacing, Two Diaphragms: Transverse Moment v. Transverse Distance



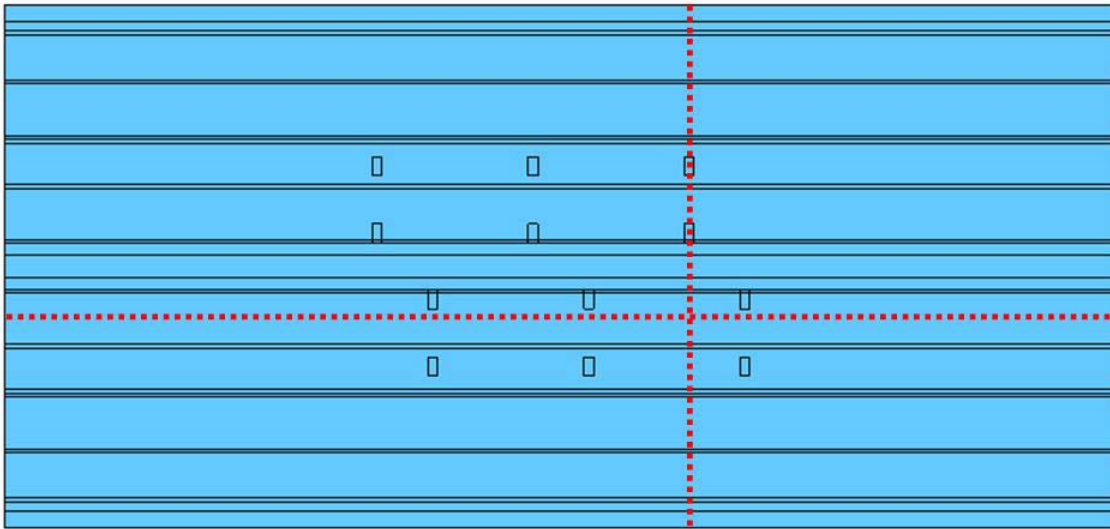
100' Span, 8' Girder Spacing, Two Diaphragms: Transverse Moment v. Longitudinal Distance



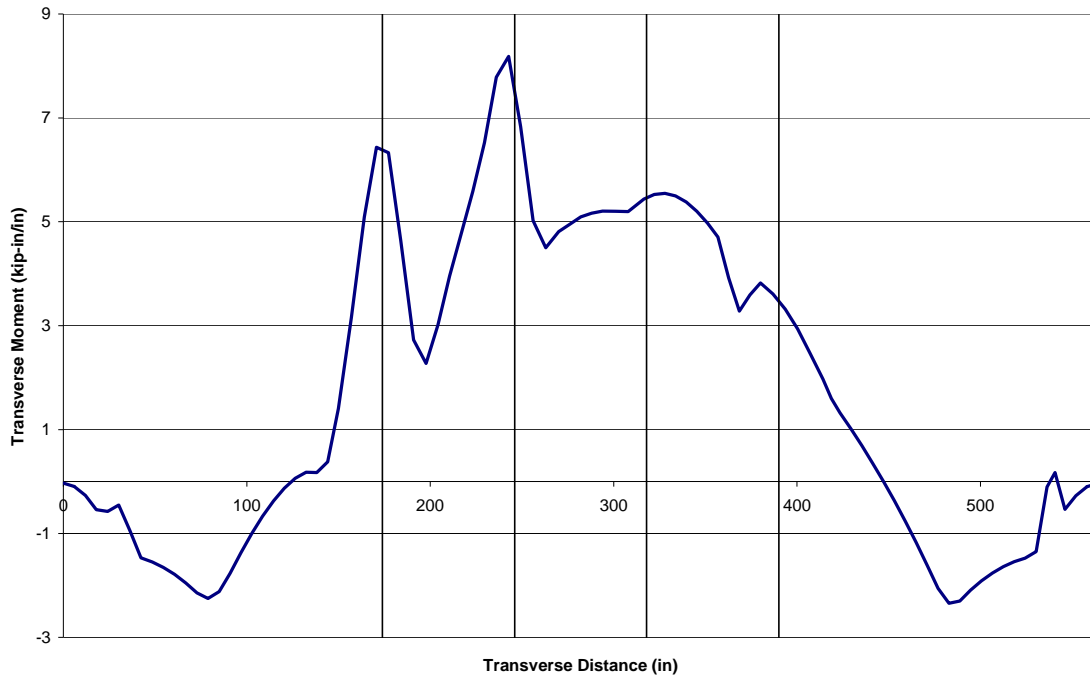
100' Span, 8' Girder Spacing, Two Diaphragms: Longitudinal Moment v. Longitudinal Distance



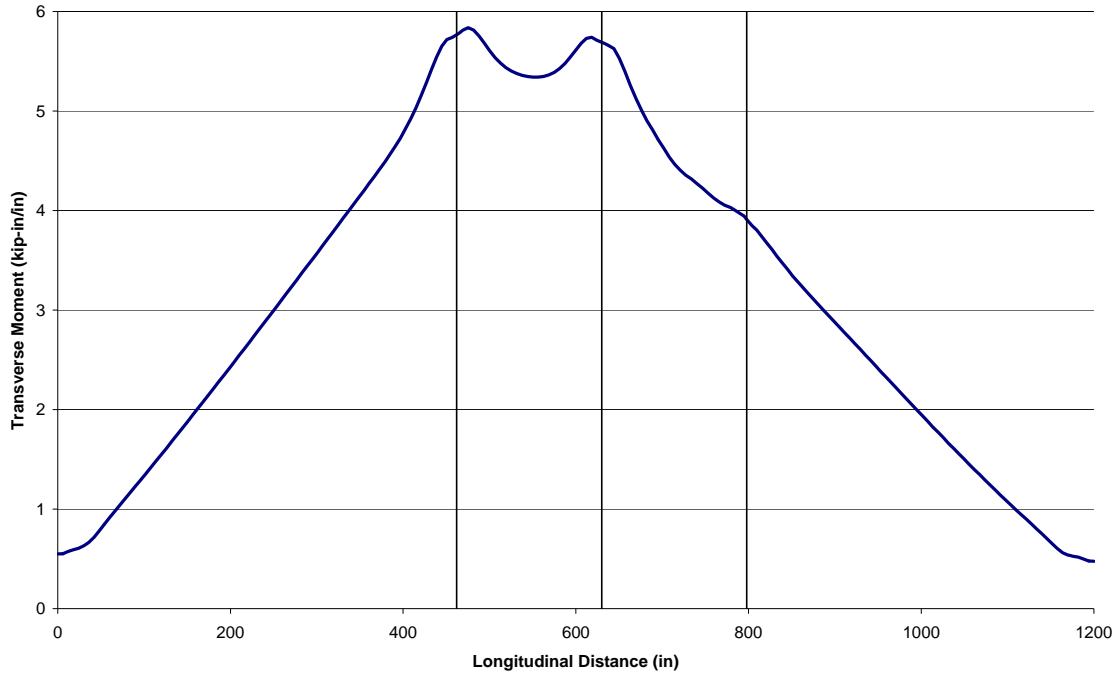
## Appendix XII. Bridge Case 11: FE Models Responses



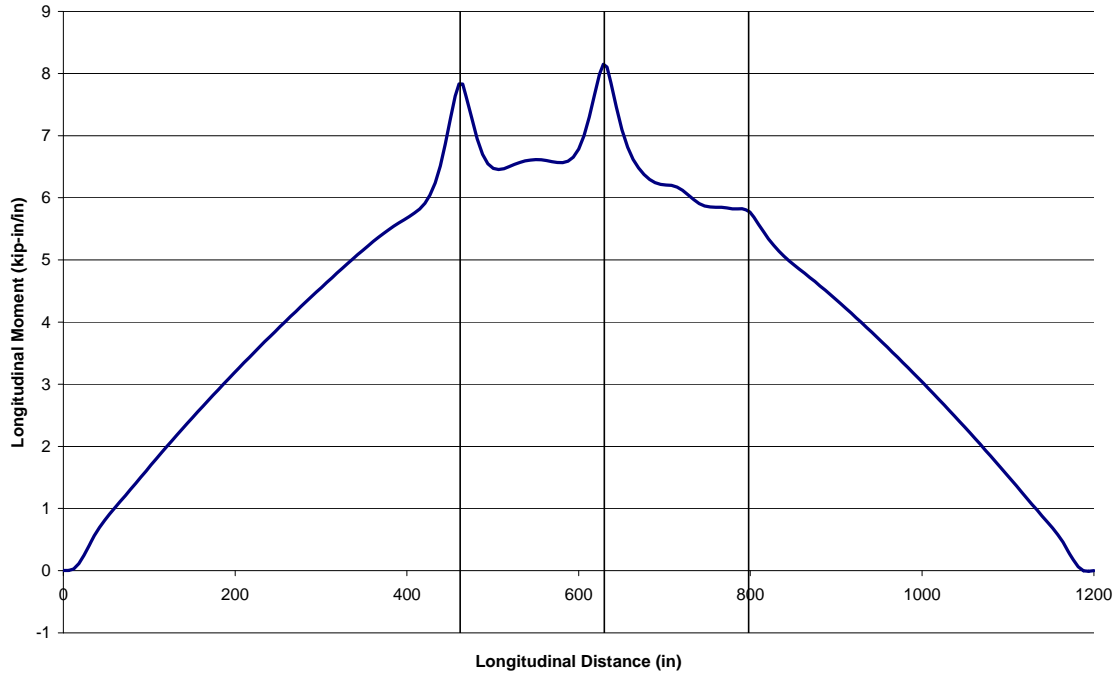
100' Span, 10' Girder Spacing: Transverse Moment v. Transverse Distance



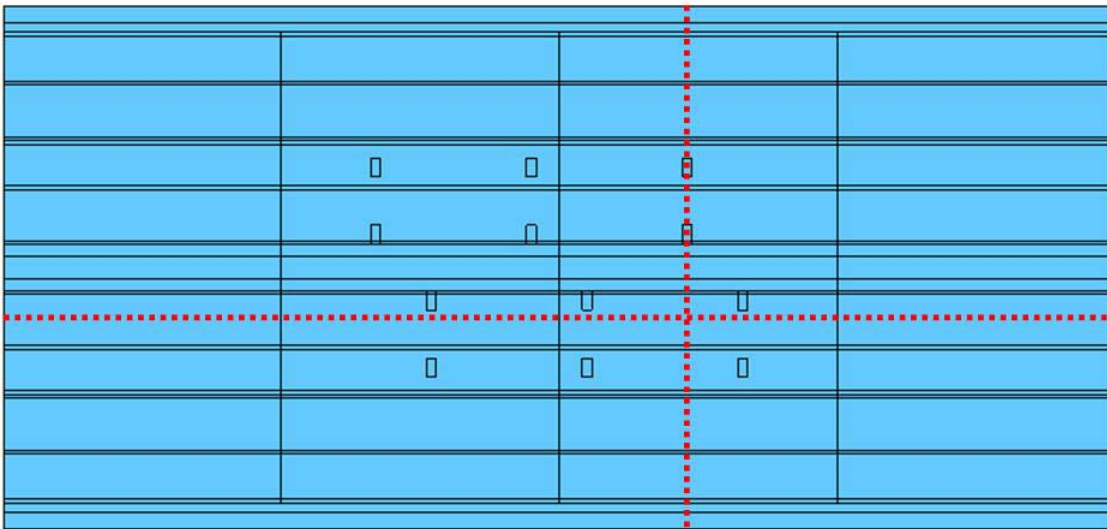
100' Span, 10' Girder Spacing: Transverse Moment v. Longitudinal Distance



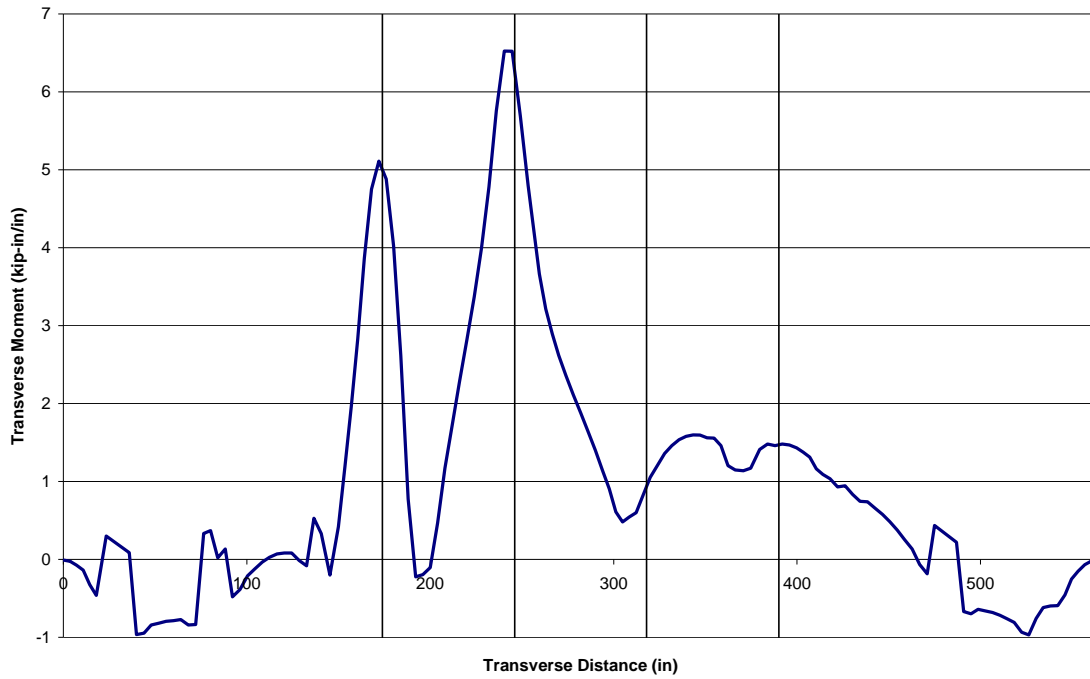
100' Span, 10' Girder Spacing: Longitudinal Moment v. Longitudinal Distance



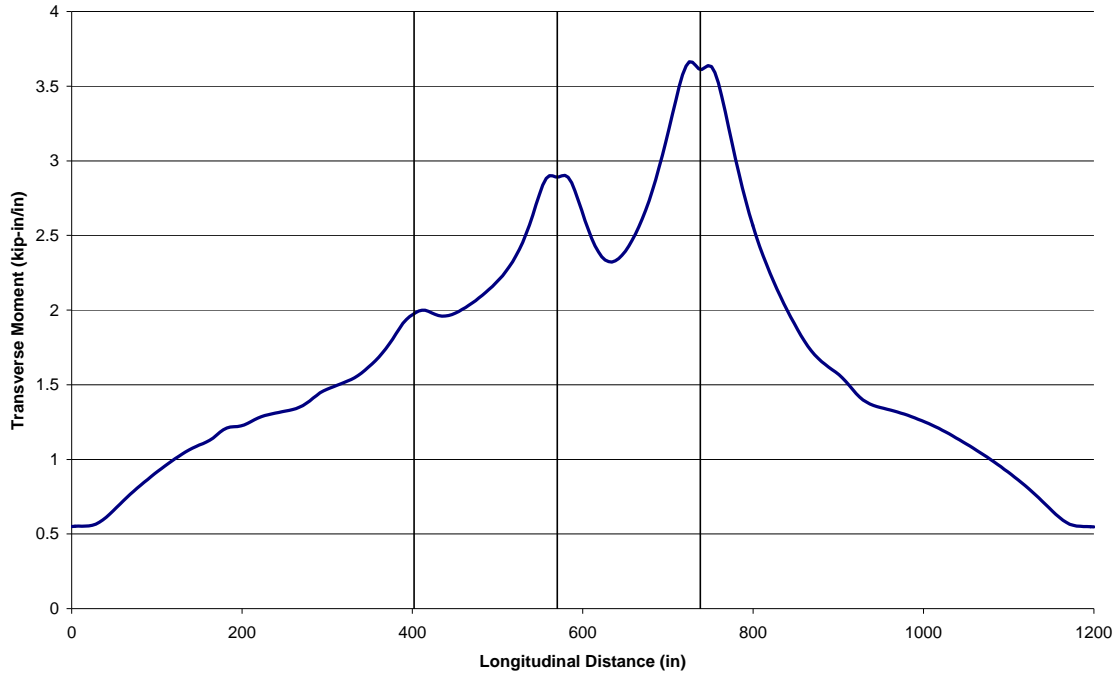
### Appendix XIII. Bridge Case 12: FE Models Responses



100' Span, 10' Girder Spacing, Three Diaphragms: Transverse Moment v. Transverse Distance



100' Span, 10' Girder Spacing, Three Diaphragms: Transverse Moment v. Longitudinal Distance



100' Span, 10' Girder Spacing, Three Diaphragms: Longitudinal Moment v. Longitudinal Distance

